Novel biomarkers in multiple sclerosis pathology with a focus on neuroprotection and myelin repair

Intakhar Ahmad

Thesis for the degree of Philosophiae Doctor (PhD)
University of Bergen, Norway
2024

UNIVERSITY OF BERGEN

Novel biomarkers in multiple sclerosis pathology with a focus on neuroprotection and myelin repair

Intakhar Ahmad

Thesis for the degree of Philosophiae Doctor (PhD)
at the University of Bergen

Date of defense: 16.01.2024

Year: 2024

Title: Novel biomarkers in multiple sclerosis pathology with a focus on neuroprotection and myelin repair

Name: Intakhar Ahmad

Print: Skipnes Kommunikasjon / University of Bergen

Scientific Environment

This research was conducted at the Norwegian Multiple Sclerosis (MS) Competence Centre, situated within the Department of Neurology at Haukeland University Hospital (Department of Clinical Medicine, University of Bergen). Additionally, the Proteomics unit at the University of Bergen (PROBE) was involved in the study. Animal experiments were carried out at the Laboratory Animal Facility Core, also part of the University of Bergen. The PhD fellowship was funded by both the University of Bergen and the Kristian Gerhard Jebsen Foundation.

Acknowledgements

Embarking on the challenging journey of a PhD has tested my perseverance and resilience, with moments of both breakthrough and breakdown. I am deeply grateful to acknowledge that this achievement is not a solitary endeavor but the result of a collective effort of many individuals, to whom I owe my heartfelt gratitude.

First and foremost, I express my sincerest appreciation to Professor Lars Bø, my supervisor from the Department of Neurology at Haukeland University Hospital. Throughout this journey, Professor Bø has been an invaluable mentor, imparting upon me the lesson of skepticism in scientific understanding and research rationalization. His guidance and dedicated time spent teaching me about multiple sclerosis (MS) pathology, particularly through our collaborative examination of human brain tissue slides, have been immensely valuable. Despite the initial challenges stemming from my different background, Professor Bø's unwavering support helped me overcome that obstacle.

In addition to Professor Bø, I extend my heartfelt appreciation to my co-supervisor, Dr. Stig Wergeland, also from the Department of Neurology at Haukeland University Hospital. Dr. Wergeland shared his expertise, taking time out of his busy schedule. Furthermore, I am grateful to Dr. Eystein Oveland, my other co-supervisor, whose enthusiasm and support were instrumental throughout this journey. I would also like to acknowledge Professor Kjell-Morten Myhr and Professor Frode Berven for their support during the period they co-supervised me before Dr. Wergeland and Dr. Oveland took over. Furthermore, I extend my sincere gratefulness to my colleagues, co-authors, friends, and well-wishers at my workplace, both past and present.

Finally, I would like to express my deepest gratitude to my family for their support, compassion, and patience. A special thanks go to my children, Labib and Aayrah. As they grow up, they may come to understand how they have shaped my philosophy on life. Undeniably, at the very essence of human desires lies the relentless pursuit of happiness—an intrinsic quest that transcends material worth, for its true value is immeasurable and cannot be confined by monetary means. I would also like to thank my mother, Rizia, and my wife, Farjana. Of course, a simple

'thank you' cannot fully capture the depth of my gratitude. I am aware that a kite needs to be anchored to soar, and my family has provided me with that anchor.

Intakhar Ahmad

Abstract

Multiple sclerosis (MS) is a demyelinating disease characterized by well-defined focal areas of tissue damage (lesions) in the central nervous system (CNS), leading to permanent disability in patients. Areas of myelin loss are the hallmark of MS pathology, along with inflammation, oligodendrocyte death, gliosis, and axonal loss. The current understanding of MS pathology primarily focuses on inflammatory processes in the CNS. However, available medications targeting inflammation are largely ineffective in some aspects of the disease, including chronic neurodegeneration and myelin repair.

Because of the complex and variable pathology of MS, a reductionistic approach has been taken in this study. We focused on two pathological mechanisms: neuroprotection and myelin repair. We used two complementary animal models of MS, the experimental autoimmune encephalomyelitis (EAE) model and the cuprizone (CPZ)-induced de-and remyelination model. Proteomic studies highlighted regulated protein molecules in the frontal cortex of the brain in two complementary MS mouse models. Both Legumain (LGMN) and complement component 1q (C1Q) showed significant upregulation in the cuprizone (CPZ) model, whereas hemopexin was notably upregulated in the experimental autoimmune encephalomyelitis (EAE) model. In the MS brain, we observed a correlation between legumain and increased lesion activity in white matter (WM). In grey matter (GM), a subset of cortical neurons demonstrated weak legumain immunopositivity. MS cases showed higher overall legumain immunopositivity in the cortex compared to the controls. Legumain could potentially be a valuable therapeutic target in MS, with existing inhibitors suggested for use in Parkinson's and Alzheimer's diseases (Paper I). In the proteomic study, ermin, an oligodendrocyte-specific protein, was down-regulated in the CPZ model of de-remyelination at the disease peak compared to controls. In our histopathological study in the CPZ model of de- and remyelination, the relative proportion of ermin+ cells compared to cells positive for the late-stage oligodendrocyte biomarker Nogo-A increased significantly at the onset of remyelination in the corpus callosum, the brain part containing the bundles of myelinated axons. The human orthologue of ermin protein had substantially higher immunopositivity in remyelinated parts of MS lesions, both in WM and GM lesions, and expressed in the

developmental stage of oligodendrocyte progenitors capable of myelination. Thus, a relatively higher proportion of ermin immunopositivity in oligodendrocytes compared to Nogo-A could indicate recent or ongoing remyelination (Paper II). Chitinase 3 Like 1 (CHI3L1), a secretory glycoprotein, is one of the most studied CSF biomarker candidates in MS. We found that the density of CHI3L1-positive neurons was found to be significantly higher in normal-appearing MS grey matter tissue compared to that of control subjects ($p = 0.014$). In MS white matter, CHI3L1 was detected in astrocytes located within lesion areas, as well as in perivascular normal-appearing areas and in phagocytic cells from the initial phases of lesion development. In the CPZ model, the density of CHI3L1-positive cells was strongly associated with microglial activation in the WM and choroid plexus inflammation. Compared to controls, CHI3L1-immunopositivity in WM was increased from an early phase of CPZ exposure. In the GM, CHI3L1 immunopositivity increased later in the CPZ exposure phase, particularly in the deep grey matter region. This observation implies a correlation between CHI3L1 and neuronal stress in MS as a response to inflammation, potentially leading to neuronal senescence (Paper III).

All three protein molecules, LGMN, ermin, and CHI3L1, are of sufficient potential importance to be explored/used as biomarkers and/or therapeutic targets in further clinical studies on neuroprotection and myelin repair in MS.

Abstract in Norwegian / sammendrag

Multippel sklerose (MS) er en sykdom som fører til skade på nervesystemet, kjennetegnet av definerte områder med vevsskade (lesjoner) i sentralnervesystemet (CNS). Dette resulterer i varig funksjonshemming hos pasienter. Tap av myelin, sammen med betennelse, død av oligodendrocytter, gliose og tap av aksoner, er sentrale elementer i MS-patologien. Den nåværende forståelsen av MS-patologien er hovedsakelig fokusert på inflammatoriske prosesser i CNS. Imidlertid er tilgjengelige medikamenter som retter seg mot betennelse, begrenset effektive når det gjelder kronisk nevrodegenerasjon og reparasjon av myelin.

I denne studien har vi tatt en reduksjonistisk tilnærming på grunn av den komplekse og varierte patologien til MS. Vi har fokusert på to patologiske mekanismer: nevrobeskyttelse og reparasjon av myelin. Vi har benyttet to komplementære dyremodeller for MS, nemlig den eksperimentelle autoimmune encefalomyelitt (EAE)-modellen og cuprizone (CPZ)-indusert modell for de- og remyelinisering. Proteomiske studier har identifisert regulerte proteinmolekyler i den frontale cortex i hjernen i begge musmodellene for MS. Både legumain (LGMN) og komplementkomponent 1q (C1Q) viste betydelig økt aktivitet i CPZ-modellen, mens hemopexin var markert økt i EAE-modellen. Vi observerte en sammenheng mellom legumain og økt lesjonsaktivitet i hvit substans (WM) i MS-hjernen. I grå substans (GM) viste en del kortikale nevroner svak legumain immunpositivitet. MS-tilfeller viste generelt høyere legumain immunpositivitet i cortex sammenlignet med kontrollgruppen. Legumain kan derfor potensielt være et verdifullt terapeutisk mål i MS, med eksisterende hemmere som allerede brukes i behandlingen av Parkinsons og Alzheimers sykdommer (Artikkel I).

I den proteomiske studien fant vi at ermin, et oligodendrocytt-spesifikt protein, var nedregulert i CPZ-modellen for de- og remyelinisering på sykdommens høydepunkt sammenlignet med kontroller. I vår histopatologiske studie i CPZ-modellen observerte vi at andelen av ermin-positive celler økte betydelig i begynnelsen av remyelinisering i corpus callosum, et område i hjernen som inneholder bunter av myeliniserte aksoner. Det humane tilsvaret til ermin-proteinet hadde betydelig høyere immunpositivitet i remyeliniserte deler av MS-lesjoner, både i WM- og GM-lesjoner, og ble uttrykt i utviklingsstadiet av oligodendrocyttprogenitorer som er i stand til å

produsere myelin. Derfor kan en relativt høyere andel av ermin-immunpositivitet i oligodendrocytter sammenlignet med Nogo-A indikere pågående eller nylig remyelinisering (Artikkel II).

Chitinase 3 Like 1 (CHI3L1), et sekretorisk glykoprotein, er en av de mest studerte biomarkørkandidatene for MS. Vi fant at tettheten av CHI3L1-positive nevroner var betydelig høyere i tilsynelatende normalt grå substansvev hos MS-pasienter sammenlignet med kontrollgruppen ($p = 0,014$). I MS-hvit substans ble CHI3L1 påvist i astrocytter i lesjonområder, så vel som i perivaskulære områder som så normale ut, og i fagocytiske celler i tidlige stadier av lesjonsutviklingen. I CPZ-modellen var tettheten av CHI3L1-positive celler sterkt assosiert med mikroglial aktivering i WM og betennelse i koroidplexus. Sammenlignet med kontroller økte CHI3L1-immunpositivitet i WM allerede i den tidlige fasen av CPZ-eksponering. I GM økte CHI3L1 immunpositivitet senere i CPZ-eksponeringsfasen, spesielt i de dype områdene av grå substans. Dette tyder på en sammenheng mellom CHI3L1 og nevronal belastning som respons på betennelse i MS, noe som potensielt kan føre til nevronal aldring (Artikkel III).

Alle tre proteinmolekylene, LGMN, ermin og CHI3L1, er av tilstrekkelig betydning til å bli utforsket og brukt som biomarkører og/eller terapeutiske mål i fremtidige kliniske studier av nevrobeskyttelse og reparasjon av myelin ved MS.

.

Abbreviations

AP	Action potential
APP	Amyloid precursor protein
BBB	Blood-brain barrier
bFGF	Basic fibroblast growth factor
BRBN-T	Neuropsychological Tests
C1Q	Complement component 1q
CC	Corpus callosum
CFA	complete Freund's adjuvant
CHI3L1	Chitinase-3-like protein 1
CIS	Clinically isolated syndrome
CNS	Central nerves system
CPZ	Cuprizone
CSF	Cerebrospinal fluid
CTL	Control
Ctx	Cortex
CXCL1	C-X-C Motif Chemokine Ligand 1
DGM	Deep grey matter
DMTs	Disease-modifying therapies
DNA	Deoxyribonucleic acid
EAE	Experimental autoimmune encephalomyelitis
EBV	Epstein-Barr virus
ECM	Extracellular matrix
EDSS	Expanded Disability Status Scale
ERMN	Ermin
GFAP	Glial fibrillary acidic protein
GM	Grey matter
GML	Gray matter lesion
HEMO	Hemopexin
Ig	Immunoglobulin
LC–MS	Liquid chromatography-mass spectrometry
LFB	Luxol fast blue
LGMN	Legumain
Mac-3	Lysosomal-associated membrane protein 2
MBP	Myelin basic protein
MOG	Myelin oligodendrocyte glycoprotein
MRI	Magnetic resonance imaging

MS	Multiple sclerosis
MSFC	Multiple Sclerosis Functional Composite
NAWM	Normal-appearing white matter
NfL	Neurofilament light chain
Ng	Neurogranin
NN	Healthy neurological controls
Nogo-A	Neurite outgrowth factor A
NPTX2	Neuronal pentraxin 2
NR1H3	Nuclear Receptor Subfamily 1 Group H Member 3
OCBs	Oligoclonal bands
OLG	Oligodendrocyte
OND	Another neurological disease
OPC	Oligodendrocyte progenitor cell
OS	Oxidative stress
PLP	Proteolipid protein
PNS	Peripheral nervous system
PP-MS	Primary progressive MS
PRM	Parallel reaction monitoring
PR-MS	Progressive-Relapsing MS
PTx	Pertussis toxin
PVL	Periventricular lesion
RNA	Ribonucleic acid
ROS	Reactive oxygen species
RR-MS	Relapsing-remitting multiple sclerosis
SC	Schwann cell
SP-MS	Secondary-Progressive MS
TG-2	Transglutaminase-2
TMT	Tandem mass tag
WES	Whole exome sequencing
WGS	Genome-wide association
WM	White matter
WML	White matter lesions

List of Articles

I. Oveland, E., **Ahmad, I**., Lereim, R.R. et al. Cuprizone and EAE mouse frontal cortex proteomics revealed proteins altered in multiple sclerosis. Sci Rep 11, 7174 (2021). https://doi.org/10.1038/s41598-021-86191-5

II. **Ahmad, I**., Wergeland, S., Oveland, E., and Bo, L. A higher proportion of ermin-immunopositive oligodendrocytes in areas of remyelination. PLOS ONE 16(8): e0256155 (2021). https://doi.org/10.1371/journal.pone.0256155

III. **Ahmad, I**., Wergeland, S., Oveland, E., and Bo, L. An association of Chitinase-3 like-protein-1 with neuronal deterioration in multiple sclerosis. (In the second round of peer review)

Contents

1. Introduction

1.1 Overview of Multiple Sclerosis (MS)

Myelination of the axon is a crucial evolutionary achievement in our intricate nervous systems (Weil et al., 2018). Myelin is targeted in several diseases, including multiple sclerosis (MS). MS is a multifocal demyelinating disorder of the central nervous system (CNS), likely to be caused by previous Epstein Barr virus (EBV) infection and known/unknown additional co-factors in a small minority of EBV-infected individuals (Bjornevik et al., 2022). MS is widely considered an autoimmune disease in which focal lymphocytic infiltration damages myelin and axon (Compston & Coles, 2008). It is among the most common causes of non-traumatic disability among young and middle-aged adults. MS usually manifests with a relapsing-remitting course in the third or fourth decade of a patient's life (Polman et al., 2011).

Histopathologically, MS is characterized by well-defined focal areas in the CNS parenchyma, with a breakdown of the blood-brain barrier (BBB), inflammation, myelin, and oligodendrocyte loss (demyelination), transection of axons, and neuronal loss. These processes cause impaired or absent nerve impulses, leading to acute and chronic progressive disability (Nathan & Scobell, 2012). Although there are treatment options to modify the course of the disease, there is currently no cure for MS. There is also a lack of reliable biomarkers that can help MS diagnosis in the early stages, predict the progression of the disease course of the disease early in the disease, or forecast treatment efficacy.

The earliest recorded mention of MS can be traced back to the 14th century during the time of the black death (F. Lublin, 2005). A complete description of the clinical and pathological features of MS was recorded during the latter half of the 19th century (1868) by Jean-Martin Charcot (Zalc, 2018). Although the pathophysiology of MS has been extensively investigated for more than a century, it remains poorly understood. Nevertheless, epidemiological data can provide us with some basic assumptions. The general view is that MS is particularly prevalent in white Caucasians of Nordic origin. The highest regional prevalence is in North America, 140 per hundred thousand, then in Europe, 108 per hundred thousand, and the lowest in East Asia and sub-Saharan

Africa, 2.2 and 2.1 respectively per hundred thousand (Leray et al., 2016). A comprehensive meta-regression analysis indicates a universal continuous increase in the prevalence and incidence of MS (Koch-Henriksen & Sørensen, 2010). Moreover, epidemiological data underline a female preponderance in MS incidence with a ratio of 2:1 (Tintoré & Arrambide, 2009). Remarkably, recent data show that the female prevalence of MS is increasing over time (Magyari, 2016).

1.1.1 Clinical and pathological variations

MS has a high heterogeneity and unpredictability in disease course among individuals. The US National Multiple Sclerosis Society (NMSS) Advisory Committee specified four MS clinical courses (subtypes): relapsing-remitting (RR), secondary progressive (SP), primary progressive (PP), and progressive relapsing (PR) (F. D. Lublin & Reingold, 1996). A further recommendation dropped the term PR-MS, as it is overlapped with other subtypes, but clinically isolated syndrome (CIS) was added in to recognise the first clinical presentation of the disease (F. D. Lublin et al., 2014). Classification of clinical courses is as follows:

- **Relapsing-Remitting MS (RR-MS)**: This is the most widespread clinical course of MS. Approximately 85% of MS patients have a disease course at disease onset, characterized by alternating episodes subacute clinical attack and gradual (often impartial) recovery, which is called RR-MS (Dutta & Trapp, 2014).
- **Secondary-Progressive MS (SP-MS)** PPMS is characterized by progressive worsening of symptoms with no relapses or remission from the disease onset. This form of MS is present in 10-20 % of the patients at disease onset, and the disease course has proved difficult to modify by medical treatment. Many immunomodulatory drugs found effective in RRMS sclerosis failed in PPMS trials (Plantone et al., 2016).
- **Primary-Progressive MS (PP-MS)**: PP-MS is characterized by progressive worsening of symptoms with no relapses or remission. This form of MS is relatively rare and more challenging. Many anti-inflammatory drugs found effective in RRMS sclerosis regularly failed in PPMS (Abdelhak et al., 2017).

- **Clinically isolated syndrome (CIS)**: The first manifestation of a clinical episode suggestive of MS, not filling the criteria for MS diagnosis. CIS often affects optic nerves, the brainstem, or the spinal cord (D. H. Miller et al., 2012).

The disease subtype can be static or changed over time. That means a patient with CIS could persist in the CIS state, progressing to RR-MS or may enter a progressive diseases stage (Hou et al., 2018).

MS could be completely asymptomatic, and autopsy studies reported that there were individuals without any known clinical history of MS but accumulated neuropathologic changes typical of MS (Siva, 2013). Moreover, some atypical forms of MS, such as Marburg's acute MS, Balò's concentric sclerosis, and Schilder's diffuse sclerosis, share some key features of MS pathology (Stadelmann & Brück, 2004).

Besides heterogeneity in clinical courses, researchers have found considerable heterogeneity in MS pathology as reflected in autopsy studies. There are substantial differences in lesion load, lesion activity, lesion location, degree of demyelination and remyelination between patients (C. Lucchinetti et al., 2000). A large cohort study (182 MS brain donors, 3188 tissue blocks containing 7562 MS lesions) was conducted in the Netherlands (Luchetti et al., 2018), confirming the heterogeneity of MS pathology. They found that in progressive MS, there is substantial inflammatory lesion activity at the point of death. Patients with more severe disease courses have a greater percentage of lesions with inflammatory areas and elevated brainstem lesion counts. A progressive disease course was associated with a lower proportion of remyelinated lesions than patients with a relapsing disease course. Males had a higher load of cortical grey matter lesions and a higher proportion of mixed active/inactive lesions than females studied in the cohort.

Besides, the formation of white matter lesions (WML) and grey matter lesions (GML) are strikingly different. Unlike WMLs, infiltrating immune cells are hardly present in GMLs (Bø et al., 2003b). Blood-brain barrier (BBB) disruption is not a critical event in the development of GMLs, and they lack gliosis (Van Horssen et al., 2007).

1.1.2 The complex interplay among genetics, epigenetics, environment, lifestyle, and microbiota

MS is primarily manifested in young adults. Family and twin studies have demonstrated the influence of genetics on the disease (Fagnani et al., 2015). Genome-wide association (GWA) studies have identified around 200 genes as risk factors for MS (Beecham et al., 2013). This implies that these genes may play a role, to varying degrees, in the overall susceptibility to developing MS. In this respect, genetic risk factors of MS can be inherited but not the disease.

Epigenetic mechanisms such as acetylation, methylation, and citrullination play an important role in the activation or inhibition of genes regulating the expression of pro-inflammatory and myelination factors in the CNS. Therefore, epigenetic factors also play a role in the risk of developing MS (Küçükali et al., 2015). A small non-coding RNA molecule called microRNA may also be associated with disease activity and duration (C. Chen et al., 2018). MicroRNAs (miRNAs), miR-155, and miR-223 have been confirmed to be upregulated in the EAE mice model of MS (J. Zhang et al., 2014).

Environmental and lifestyle factors also contribute to the MS risk. Among many candidates, inadequate vitamin D levels, infection with the Epstein-Barr virus (EBV) early in life, and cigarette smoking are important risk factors for MS (O'Gorman et al., 2012). Several studies indicated that EBV as an aetiological agent in MS. Although EBV is consistently detected in numerous cancers, more than 90% of adults worldwide have lifelong EBV infection (Soldan & Lieberman, 2022). The more an infectious agent circulates in its hosts, the more they get adapted within them (Hossain et al., 2008).

A research team analysed serum samples taken in alternate years from military personnel to investigate EBV's association with MS onset during active duty. MS risk increased 32-fold after EBV infection, not after infection with other viruses. Neurofilament light chain levels, indicative of nerve degeneration in MS, rose only post EBV infection. Thus, EBV appears to be the leading cause of MS (Bjornevik et al., 2022). At present, there is no effective method to prevent or treat EBV infection.

A growing body of evidence has shown that the gut microbiome profoundly affects the articulation and maintenance of the immune system and is involved in various disorders, including MS (Bhargava & Mowry, 2014). Studies using the EAE animal model showed that gut microbes could influence BBB permeability, astrocyte-associated pathogenicity, microglia activity, and myelin-related gene expressions (Chu et al., 2018). Moreover, environmental and lifestyle risk factors of MS can disturb the composition of the gut microbiota, adding an extra dimension to the relations of risk factors.

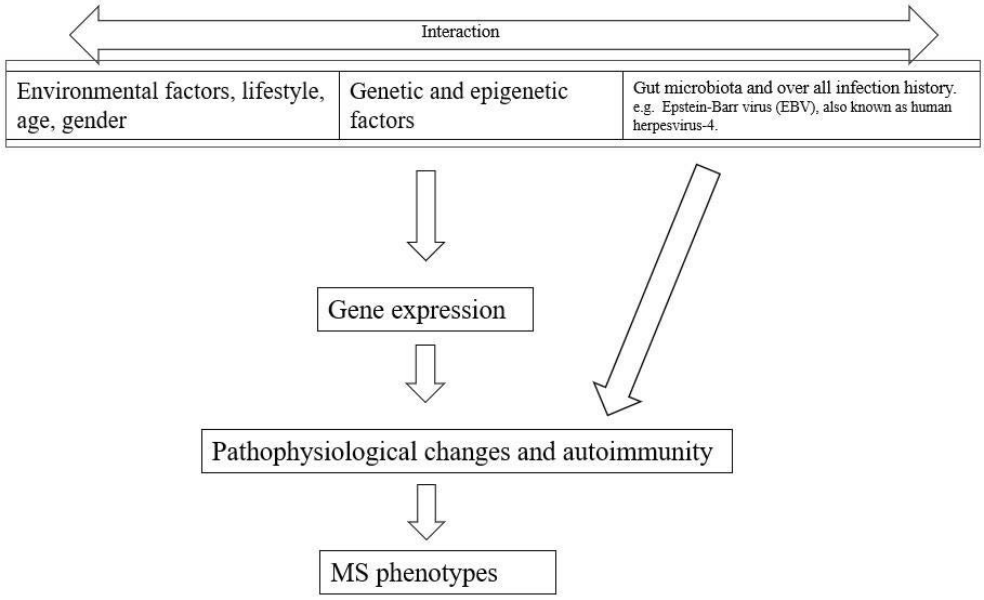

Figure 1: **MS susceptibility factors involve a complex interaction of various risk contributors.** Understanding MS pathogenesis necessitates network analysis of genetics, epigenetics, lifestyle, environmental factors, gut microbes, and infection history. For instance, EBV has been linked as a potential trigger or contributor to MS.

1.2 MS pathology: Outside-in and Inside-out model

MS could be viewed as a myelinopathy, oligodendropathy or axonopathy (Court & Coleman, 2012; Tsunoda & Fujinami, 2002). There are two models of the initiation of MS pathology – the "outside-in" vs "inside-out" model. MS has been described as an autoimmune disease that starts with alterations in the immune cells circulating in the body, which enter the brain and attack the myelin. MS displays some hallmark features of an autoimmune inflammatory disorder, including the breakdown of the BBB (Ortiz et al., 2014). Another school of thought states that primary damage to the axon and/or myelin/oligodendrocytes may prime the immune attack into the CNS.

A large collaborative study has unveiled over 200 genetic variations that impact the possibility of developing MS. Most of these genes relate to the immune system, indicating that MS most likely starts with immune system dysfunction (Beecham et al., 2013). Only recently, a genetic mutation in myelin proteolipid protein (PLP) has been identified in an MS case (Cloake et al., 2018). Alternatively, Oligodendrocytes, the myelin-forming cells of the CNS (OLGs) could be the primary target of inflammatory and immune attacks. These attacks could lead to the activation of apoptosis or necrosis pathways in OLGs and thus halt the production of myelin (Cudrici et al., 2006). Localized apoptosis of myelinating oligodendrocytes is sufficient to cause rapid demyelination, gliosis, and microglial response (Caprariello et al., 2012). Therefore, the primary pathology may begin with the immune system, targeting myelin (myelinopathy) or the oligodendrocytes (oligodendropathy). Thus the "Outside-in model" model defines a primary auto-immune response from the immune cells in peripheral blood (the outside) against the CNS (the inside) as the primary event of MS pathology.

Studies on grey matter lesions and axonal injury in normal-appearing white matter (NAWM) may challenge the first model (Trapp et al., 1998; Trapp & Nave, 2008). Accumulation of the axonal injury marker, amyloid precursor protein (APP), in active lesions and at the border of chronic active lesions suggested that an axonal injury could also be an early event in lesion formation (Ferguson et al., 1997). In addition, Theiler's murine encephalomyelitis virus

infection model of MS demonstrates that axonal injury leads to delayed oligodendrocyte apoptosis and precedes demyelination (Tsunoda & Fujinami, 2010).

Functional and/or structural defects of exons are termed “axonopathy”. Different stimuli can provoke axonal degeneration, including mechanical, metabolic, infectious, toxic, hereditary, and inflammatory stresses (Court & Coleman, 2012). The axonal cytoskeleton can be disrupted by reactive oxygen species (ROS), nitric oxide generation, intracellular Ca2+ surge, protease activation and some other abnormal mitochondrial metabolism (Di Meo et al., 2016). Thus, the axoplasmic transport mechanism is hampered by a gradual congregation of transport products. Eventually this leads to axonal swellings, breakage, and neuronal death (Patron et al., 2018). The reduced trophic support from the injured axon or degeneration of efferent fibres could trigger neurodegenerative pathways followed by acute inflammatory responses (Bjartmar et al., 2003).

Many aspects of cellular biology unite in keeping healthy axons. For example, axonal length involves cytoskeleton dynamics and appropriate transport machinery with correct topology and turnover. Axons also require a close alliance with myelinating glial cells (oligodendrocytes) to work as a mutually dependent functional units to sustain a healthy CNS. Therefore, MS could also be initiated by abnormality in the CNS, contributing to other secondary damages, including inflammation and myelin damage.

This "Inside-out model" of MS posits that the disease's primary cause lies in abnormalities within the central nervous system (CNS), which subsequently trigger immune responses outside the CNS, rather than vice versa (Compston & Coles, 2008). In contrast, the "Outside-in model" is based on evidence that autoreactive T-cells and B-cells specific for myelin antigens infiltrate the CNS (Sospedra & Martin, 2016).

Not necessarily only one of these hypotheses is true. Variations in pathological processes may be responsible for the observed heterogeneity in individual MS patients. Intriguingly, whether MS is a single disease or not has not been determined (Rolak, 2003).

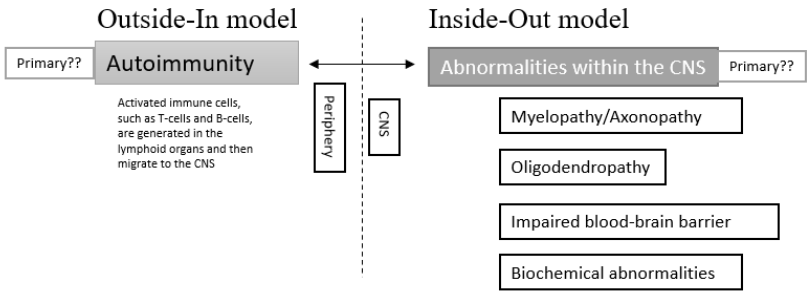

Figure 2: Hypotheses for MS pathology. Autoimmunity is the primary event, and myelin/axonal loss is a secondary event in the process of MS pathology (Outside-in model). Alternatively, abnormalities originating in oligodendrocytes and/or neurons could trigger autoimmune inflammatory demyelination through (Inside-out model).

1.3 Processes manifested in MS pathology

MS is characterized by the formation of demyelinated lesions anywhere in the central nervous system. Although the sequence of pathological events is not determined, it includes several processes; disruption of the blood-brain barrier, inflammation, demyelination, gliosis, oligodendrocyte loss, axonal/ neuronal loss, oxidative damage, remyelination and repair (Bielekova & Martin, 2004; Filippi et al., 2018; Ramagopalan et al., 2010).

1.3.1 Disruption of the blood-brain barrier (BBB)

The innermost part of the blood-brain barrier (BBB) is a complex organisation of cerebral endothelial cells united by tight junctions, pericytes and their basal lamina. These cells are surrounded and supported by astrocyte foot processes (Ortiz et al., 2014). The BBB plays a major role in controlling transport channels, facilitating the passage of oxygen and glucose. The BBB

stops the unwanted influx of cells and other biomolecules. Without the BBB, the 'interior milieu' of the central nervous system (CNS) would be overwhelmed by the influx of humoral neurotransmitters and blood elements that would upset normal CNS functions and lead to vascular/neural damage (Minagar & Alexander, 2003).

A pathological condition may activate lymphocytes in the peripheral infiltrate of the CNS and that may cross the BBB, initiate infiltrates perivascularly in the CNS, and disrupt the BBB by free radicals and proteases (Rosenberg, 2012). Consequently, the local immune response damages myelin and axons (Ortiz et al., 2014). The perivenous location of early MS lesions in patients without clinical MS suggests that BBB may be disrupted early in the lesion development (Rosenberg, 2012).

1.3.2 Inflammation

Inflammation is a biological response by components of the immune system to destructive stimuli, for instance, pathogens, damaged cells, toxins, and irradiation, to initiate the healing process (L. Chen et al., 2018). MS had been characterized as a chronic inflammatory disease from the earliest histopathological descriptions (Charcot, 1888). There is a consensus that autoimmunity is an important part of the pathogenesis of MS. Most therapies used or tested primarily target the inflammatory process (Hohlfeld & Wekerle, 2004). The specific element or elements that start this inflammation are unknown. Numerous immunological studies have been conducted on the animal model for MS, known as experimental autoimmune encephalomyelitis (EAE) (Constantinescu et al., 2011).

Though there is a significant lack of understanding of the differences between EAE and MS, depending on the EAE model, quite a few immunological pathways have been targeted to be involved in MS. The target includes both innate and adaptive immune responses. Adaptive peripheral immune response helps immune cell infiltration into the CNS in the early phase, while components of the innate immune reaction within the CNS may govern the progressive phase

(Hemmer et al., 2015). This feature is not only specific to neuroinflammatory diseases. It is also shared by other, not primarily autoimmune neurological diseases like Parkinson's Disease, which is considered primarily a neurodegenerative disease (Kannarkat et al., 2013).

1.3.3 Gliosis

Gliosis is a nonspecific common parenchymal reaction of the CNS to injury of the brain or spinal cord. Gliosis is a prominent feature of many CNS diseases, including MS. It is characterized by a dense fibrous network of non-neuronal cells (microglia, oligodendrocyte precursor cells, astrocytes, meningeal cells, and stem cells) in areas of injury (Fawcett & Asher, 1999). The process of gliosis involves a cascade of cellular and molecular events. Typically, the first response to injury is associated with reactivated microglia. Later, oligodendrocyte precursor cells are recruited to the injury site, and may contribute to healing or remyelination. The final constituent of this process is astrogliosis.

Activated microglia participate in the presentation of antigens and the production of cytokines, oxidative radicals, chemokines, and nitric oxide (Luo et al., 2017). The mechanisms by which the resident microglial cells of CNS get activated in MS are not entirely understood. Data suggest that microglia are sensitive to minor alterations in the local microenvironment, even ionic disbalance and other kinds of cellular stress (Kreutzberg, 1996). Primarily, microglia activation had been perceived as a temporary event (Streit et al., 1999). However, it was observed that the microglial response to damage could be long-lasting (Huh et al., 2003). Following injury and demyelination caused by activated microglia, neighbouring oligodendrocyte precursor cells rapidly travel to the injury site and differentiate into oligodendrocytes, and may remyelinate denuded axons (Miron et al., 2011). Scar formation by astrogliosis in the site of damage plays a critical role in limiting the spread of inflammatory cells into neighbouring healthy tissue (Bush et al., 1999). On the other hand, astrogliosis inhibits the migration of oligodendrocyte precursors and Schwann cells, which could restrain remyelination at the injury site (Fawcett & Asher, 1999).

1.3.4 Oligodendrocyte loss

Oligodendrocyte (OLG) death by apoptosis or necrosis causes oligodendrocyte loss in MS plaques. Oligodendrocytes are a target of inflammatory and immune attacks. Among many other factors, cytopathic changes in oligodendrocytes, such as abnormal nuclei, complement deposition and apoptosis of oligodendrocytes, have been suggested to be triggering factors of MS demyelination initiation (Prineas & Parratt, 2012).

Mitochondrial dysfunction plays a significant part in the process of apoptosis of OLGs (Rose et al., 2017). The signalling pathways that regulate apoptosis have been divided into intrinsic (non-receptor-mediated stimuli- endogenous) and extrinsic (receptor-mediated stimuli- exogenous) pathways. Apoptosis through the extrinsic pathway can be triggered by the activation of the death-signalling receptors leading to the activation of caspases, a well-known family of cysteine proteases in the modulation of programmed cell death (Lavrik et al., 2005). Studies on experimental allergic encephalomyelitis (EAE) in caspase-deficient mice showed that caspase-mediated death of OLGs are critical to the demyelination process (Hisahara et al., 2003).

Oligodendrocytes (OLGs) are sensitive to various cell death stimuli, for example cytotoxic cytokines, anti-myelin antibodies, nitric oxide, and oxidative stress (Hisahara et al., 2003). Areas of OLG loss are associated with the presence of enlarged microglia, early-stage macrophages, an open blood-brain barrier, and the presence of CD8+ T cells (Prineas & Parratt, 2012).

1.3.5 Axonal/ neuronal loss

Axon/neuronal degeneration or loss is a pathophysiological process of disruption and eventual death of axon/neurone. Axonal injury may slowly evolve into axonal/neuronal degeneration and loss. The process includes the build-up of axoplasmic organelles, disassembly of microtubules, and fragmentation of the axonal cytoskeleton (Y. Wang et al., 2018).

Axonal swelling and transection are not new observations in MS pathology. Even Jean-Martin Charcot (1825–93), one of the founders of modern neurology, was aware of axonal damage in MS (Kornek & Lassmann, 1999). Nerve fibres can be cut or lost not only at the site of inflammatory injury (acute axonal damage) but also distal to the injury, defined as Wallerian degeneration (Singh et al., 2017).

The axonal injury occurs early in the MS disease course and accumulates with disease progression (Tallantyre et al., 2009). In the white matter part of the MS brain, the largest extent of ongoing axonal loss is in active lesions. A lower but substantial loss is observed in chronic active/inactive lesions, even in normal-appearing white matter (Trapp et al., 1998). Ongoing axonal loss can also be detected in grey matter MS lesions (Peterson et al., 2001a).

The extent of axonal loss in MS white matter tracts varies widely. For example, 19 to 60 percent axonal loss was observed in several studies (DeLuca et al., 2004; Ganter et al., 1999; Lovas et al., 2000; Tallantyre et al., 2009). Intriguingly, small-diameter axons are more affected than larger ones (DeLuca et al., 2004). That means the flow rate of ions through the axon may influence axonal loss. In chronic lesions, axons are dystrophic and contain multiple swellings that disturb interaction with premyelinating oligodendrocytes (Chang et al., 2002). Thus, axonal pathologic processes may limit the remyelination of chronic MS lesions.

Cognitive dysfunction may be a clinical feature of axonal/neuronal abnormalities in MS. The early synaptic loss could initiate neuronal death and cognitive dysfunction (Friese, 2016). In MS lesions, the major synaptic vesicle protein p38 (synaptophysin) has been noticed to be declining along with neuronal and glial density (Wegner et al., 2006). In addition, my axons in chronic MS lesions cannot conduct impulses, because they are negative for Na+/K+ ATPase (Young et al., 2008).

Grey matter (GM) lesions are detected even at the earliest stages of MS. However, they are more frequent in the progressive form of MS. In MS patients, the study of grey matter lesions is difficult, due to the low sensitivity of MRI to grey matter demyelination (Pirko et al., 2007).

Therefore, biomarkers for molecular axonal/neuronal loss are crucial for understanding GM aspect of MS aetiology and pathogenesis.

1.3.6 Oxidative stress in MS

Oxidative stress (OS) is defined as the discrepancy between the production of reactive oxygen species (free radicals) and antioxidant encounters (Betteridge, 2000). The view of OS has been broadened with the discovery of reactive nitrogen and lipid species that can modulate physiological functions through redox cell signalling (Gutierrez et al., 2006). Free radicals are a regular by-product of aerobic cellular metabolism, especially in the mitochondrial matrix and cytosol (Cadenas & Davies, 2000). The in-built antioxidant system of the body neutralises them and prevents any damage due to free radical attacks to fatty acids, proteins and DNA (Gutierrez et al., 2006). Besides various functional deficiencies of our body's enzymatic or nonenzymatic endogenous reaction system, several other external factors contribute to oxidative stress. These factors include food habits, lifestyle, and environmental factors such as toxic chemicals and radiation (Lobo et al., 2010). Moreover, regular immune responses can temporarily trigger oxidative stress to develop a defence against pathogens (Muralidharan & Mandrekar, 2013).

Uncontrolled OS can accelerate the ageing process (Cadenas & Davies, 2000) and can contribute to the development of several disease conditions, including MS. In the acute phase of MS disease, OS plays a role in initiating inflammation; however, in the chronic phase, it may aid the neurodegenerative process. Redox signalling processes in MS are related to abnormal axonal bioenergetics, cerebral iron accumulation, mitochondrial dysfunction, and overall impaired oxidant/antioxidant balance (Adamczyk & Adamczyk-Sowa, 2016).

1.3.7 Remyelination

In MS and other demyelinating diseases, the myelin sheaths from axons are either partially or entirely stripped off. A spontaneous repair process occurs, by which new myelin sheaths are generated around axons, termed “remyelination” (Chari, 2007). The CNS is generally referred to as an organ with a limited capacity for regeneration; but enhancing regeneration of the myelin sheath is a major opportunity to possibly reverse neurological damage in MS.

Although all the players and mechanisms involved in remyelination are not entirely understood, axonal myelin is generated by wrappings of the plasma membrane of oligodendrocytes (OLGs) in the central nervous system (CNS) and Schwann Cells (SCs) in the peripheral nervous system (PNS). Myelination involves extensive plasma membrane rearrangements, suggesting that molecules that regulate membrane dynamics play prominent roles in remyelination (Gerber et al., 2019). Research data showed that even immunoregulatory (M2) microglia/macrophages may assist CNS remyelination by inducing oligodendrocyte differentiation (Miron et al., 2013).

Animal models have demonstrated that the remyelination event may start by the activation of oligodendrocyte progenitor cells (OPCs) (Cayre et al., 2021). Remyelination probably is initiated through inflammation-associated signalling factors. It is observed that OPCs can repopulate the site of inflammation to remyelinate (Foote & Blakemore, 2005). OPCs proliferate and differentiate into mature oligodendrocytes, able to remyelinate axons (Miron et al., 2011).

Remyelination can re-establish conduction properties to axons nearly to the normal level (Honmou et al., 1996). The new myelin sheaths have shorter internodes and uniformly distributed thinner myelin loops (Gledhill et al., 1973). Remyelination events can also be detected in MRI images by changes in magnetization transfer ratio within lesions (J. T. Chen et al., 2008).

1.4 Crosstalk of cells in myelination, de- remyelination and neuroprotection

Neurons and neuroglial cells (glial cells) are key cell types of the mammalian CNS. Glial cells primarily comprise microglia, astrocytes, or oligodendrocyte lineage cells (Jäkel & Dimou, 2017). For many decades, glial cells received less scientific interest because of an incomplete understanding of their physiology and their diverse role. However, it is becoming more evident that crosstalk between all CNS residents and infiltrating cells plays important roles in brain function, homeostasis, and disease development.

Myelination is a crucial feature of the mammalian brain and occurs relatively late in the temporal sequence of CNS development. It continues into young adulthood (Fields, 2008). Myelin is a whitish substance that gives the characteristic appearance of the nervous system's white matter. Myelin consists primarily of lipids, which provide its insulating properties, and proteins stabilise its structure (Butt, 2009). Myelin allows nerve impulses (action potential) to travel along the axon efficiently by increasing membrane resistance and decreasing capacitance. Myelinated portions of axons passively propagate action potentials (AP), which are regenerated by active, voltage-dependent Na+ and K+ ion-specific conductance at non-myelinated parts called “nodes of Ranvier” (Stiefel et al., 2013).

Oligodendrocytes are the myelin-forming cells in the CNS. Enormously large cell membrane extensions wrapped around the axon are called “myelin sheaths” (Raine, 1984). A study claims that myelination of the axons varies depending on the neuron type and the surrounding myelin-producing cells (Tomassy et al., 2014).

Oligodendrocytes are found throughout the grey and white matter in the CNS. The classic characteristics of oligodendrocytes are found only in the white matter part of the brain, where individual oligodendrocytes can myelinate 40–50 axons (Popovich et al., 2009). Unlike in white matter, oligodendrocytes function as satellite cells in grey matter. They do not physically interact with neurons but regulate the extracellular fluid (Baumann & Pham-Dinh, 2001).

Neuronal/axonal structure imposes vulnerability on itself. Axons need to be enormously long to maintain complex connectivity, making them vulnerable. Additionally, most of the neuron's cytoplasm is contained within the axon, and most of an axon's surface area (up to 99%) is covered with myelin (Bargmann & Marder, 2013). For this reason, axons are likely to acquire metabolic energy directly from oligodendroglia through their myelin sheaths. Oligodendrocytes can influence neuron survival by delivering lactate, pyruvate, and ketone bodies to the axon (Morrison et al., 2013).

Oligodendrocytes, astrocytes, and microglia have complex crosstalk during the developmental process of myelin. Quiescent astrocytes (not reactive) support myelin maintenance through trophic support. Oligodendrocytes connect with astrocytes through astrocyte-oligodendrocyte gap junctions (Orthmann-Murphy et al., 2008). Astrocytes transport metabolites to oligodendrocytes, such as glucose and presumably lactate (Morrison et al., 2013). Oligodendrocytes use the metabolites for their own metabolism and for transport to neurons. Quiescent astrocytes can help OPC migration and differentiation (Kıray et al., 2016). Microglia can modulate (encourage or prevent) OPC differentiation into mature myelinating oligodendrocytes by polarizing exogenous ligands (Domingues et al., 2016). In animal models of demyelination, it has been shown that microglia-derived transglutaminase-2 (TG2) signals to OPCs in the presence of the ECM protein laminin and TG2/laminin-dependent activation of ADGRG1 (a receptor involved in cell adhesion). This promotes OPC proliferation, and eventually enhance remyelination (Giera et al., 2018).

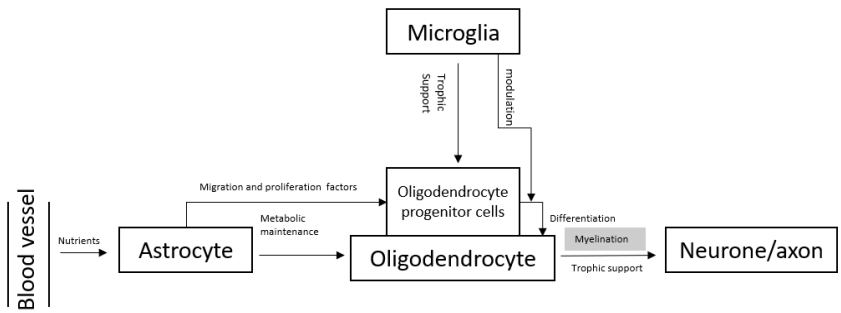

Figure 3: A simplified model of the crosstalk of oligodendrocytes and other CNS resident cells during myelin formation and maintenance. Both quiescent astrocytes and steady-state microglia may influence OPC differentiation into mature oligodendrocytes to perform myelination. Quiescent astrocytes give metabolic support to myelinating oligodendrocytes. Steady-state microglia might contribute to trophic support to OPCs. Furthermore, Quiescent astrocytes can influence the migration of OPCs to the site of preference.

In the process of myelin damage, resident and infiltrating cells could play essential roles. Autopsy studies demonstrated that MS lesions contain multiple infiltrating cells, including lymphocytes (T cells and B cells), monocytes, macrophages, and dendritic cells (Cheng et al., 2017). In addition, the CNS also contains non-parenchymal macrophages in the choroid plexus, perivascular space, and meninges. Non-parenchymal macrophages are getting attention in recent studies as promoters of neuroinflammation and degeneration (Prinz et al., 2011).

Little is known about the peripheral and central stimuli that initiate the infiltration of immune cells in the CNS. It is assumed that oligodendrocytes can be attacked by antibodies directed to myelin proteins, leading to oligodendrocyte death. Infiltrated B cells differentiate into plasma cells, that may make and release antibodies that attack myelin and recruit other immune cells (Genain et al., 1999). The role of B and T cells are multi-directional. B cells can present antigens to T cells to launch an immune attack. They also release chemical messengers to activate/deactivate and differentiate other immune cells. B and T cells may establish a permanent presence in CNS to continue the attack. Different differentiated forms of B and T cells also interact with resident microglia and astrocytes in a complex manner; some are activatory, and some are inhibitory, though the patterns are not entirely identified (Noseworthy et al., 2000; Reich et al., 2018). Oligodendrocytes are also vulnerable to inflammation, which may activate apoptotic or necrotic pathways in oligodendrocytes (Cudrici et al., 2006).

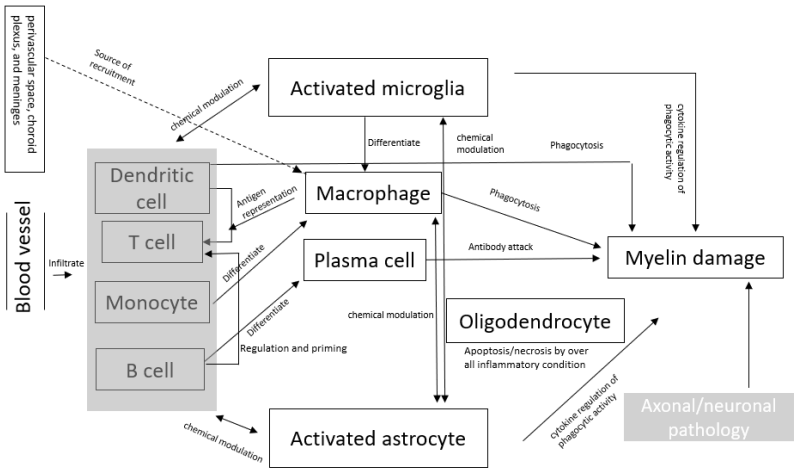

Figure 4: A simplified model of myelin injury/ demyelination. Autoreactive immune cells and demyelinating antibodies from the systemic circulation may enter the central nervous system by disrupting the blood-brain barrier. In the CNS, multidimensional interactions may contribute to the process of inflammatory activity and phagocytosis. Additionally, Axonal/neuronal pathology can also contribute to myelin damage.

Myelin damage can be restored spontaneously to some extent. OPCs may replicate and remyelinate the denuded axon (Chamberlain et al., 2016). The stimuli for remyelination may stem from the inflammation process; M2 microglia/ macrophage has already been recognized to initiate remyelination (Foote & Blakemore, 2005). Other remyelination triggering factors include axonal size, the presence of neuronal signal molecules and trophic support, e.g., the presence of ATP, K+, glutamate, GABA, and adhesion molecules (Felten et al., 2016). An individual oligodendrocyte can myelinate several axons simultaneously, and adjacent internodal parts are myelinated by different oligodendrocytes (Simons & Nave, 2016).

Oligodendrocytes are the myelinating/remyelinating cells in the CNS, but mature oligodendrocytes are not good at myelination/remyelination. It is thought that the denuded axon

can thus only be remyelinated by the generation of new oligodendrocytes from OPCs residing near the injury. Adult neural stem cells may also arrive from the subependymal zone of the CNS to aid the process (Gensert & Goldman, 1997; Salmond & Fineran, 2015). Mature oligodendrocytes may be physiologically incompetent to migrate to the site of interest, as it has been observed that mature oligodendrocytes have a limited migratory capacity (Simons & Nave, 2016). However, a recent study claims that even mature oligodendrocytes can participate in remyelination (Duncan et al., 2018). In addition, mature oligodendrocytes and their precursor cells provide growth factors for the proliferation and survival of immature oligodendrocytes, e.g., brain-derived neurotrophic factor (BDNF), Neurotrophin-3 and insulin-like growth factor-1 (IGF-1) (Y. Du & Dreyfus, 2002).

Besides restoration of axonal conduction properties, remyelination is likely to have a neuroprotective role. New myelin may act as a physical barrier to protect from harmful inflammatory molecules (Podbielska et al., 2013) and provide trophic support to axons. It is known that oligodendrocytes support axons metabolically with lactate for aerobic ATP production (Fünfschilling et al., 2012). Although remyelination can be very efficient and extensive in experimental models, especially in the EAE model (Franklin & Goldman, 2015), spontaneous regeneration in mammalian CNS is limited (Huebner & Strittmatter, 2009). In addition, remyelination is slower in the CNS than in the PNS (Ludwin, 1988).

It has been identified that remyelination is relatively frequent in early MS lesions (Goldschmidt et al., 2009). Eventually, this process becomes insufficient and stops in most lesions (Chari, 2007). The underlying cause of failure could be linked to the lack of sufficient OPC generation, limitation in OPC migration, a failure in differentiation and the presence of inhibitory factors (Stangel et al., 2017).

Spatial differences in CNS and the clinical course of MS also affect the degree of remyelination. For example, more remyelination is observed in the GM than in the WM (Chang et al., 2012) and in those with PP-MS than RR-MS (Strijbis et al., 2017). In general, the extent of remyelination is widely variable between MS cases and between lesions in the individual case.

Unfortunately, there is no reliable clinical or paraclinical molecular marker to investigate the extent of remyelination, as remyelination is an important therapeutic approach for repairing neurological damage and protecting from further injury.

In MS, axonal damage and neuronal loss occur from disease onset and lead to progressive and permanent neurological disability. However, unlike the inflammatory processes, the molecular mechanisms leading to neurodegeneration are poorly understood. Therefore, no established treatment at present specifically addresses neurodegeneration in MS (Rommer et al., 2019).

1.5 Biomarkers in MS

Biomarkers are indicators derived from biomolecular, radiographic, or physiologic characteristics. Biomarkers are distinct from direct measures of well-being (how a person feels, functions, or if he survives), known as “clinical outcome assessment”. Biomarkers are as indicators of one or several of the following.

- Pathogenic process
- Clinical manifestation
- Pharmacological response to a therapeutic intervention.

A classic definition is “A defining characteristic that is measured as an indicator of normal biological processes, pathogenic processes or responses to an exposure or intervention.”(Group, 2016). MS is indisputably a complex and highly variable disease; it is challenging to have an accurate early diagnosis or prognosis based on clinical information only. So far, magnetic resonance imaging (imaging marker) and cerebrospinal fluid biomarkers (molecular markers) are the principal sources of supportive indicators used clinically. Inflammation-related markers are investigated as early-stage markers in MS. On the other hand, markers for neuronal/axonal loss and gliosis are considered as markers for the progressive stages of the diseases (Teunissen et al., 2015).

A categorised overview of molecular biomarkers specific to distinctive pathological processes in MS.

BBB disruption

Biomarker name	Function/origin	Reference
Ninjurin-1	Cell surface adhesion molecule that contributes to leukocyte trafficking induced by nerve injury.	(Ahn et al., 2014)
ICAM-1	Intracellular adhesion molecule-1 (ICAM-1) helps inflammatory homing in EAE and MS.	(Mycko et al., 1998)
MCAM	Melanoma cell adhesion molecule to accumulate CD4+ lymphocytes in the CNS.	(Malpass, 2012)
Endothelin-1	Vasoconstrictive peptide released from reactive astrocytes and mediate the disruption of BBB permeability via endothelin ET(A)-receptor.	(Castellazzi et al., 2019; Narushima et al., 1999)
MMPs	Matrix Metalloproteinases (MMPs) contribute to a loss of the BBB integrity and infiltration of	(Mirshafiey et al., 2014)

Laminin 411 and 511	inflammatory immune cells to the CNS. Expressed in the CNS vasculature and increase T cell trafficking through BBB	(Alvarez et al., 2011)

Immunological Activation/Inflammation

Biomarker name	Function/origin	Reference
Antibody protein		
IgG OCB, IgM OCB	Oligoclonal bands (OCB) from CSF indicate inflammatory neurological condition.	(Freedman et al., 2005)
LFLC, KFLC	Inflammatory factors, Free light chains lambda (LFLC) and kappa (KFLC) have prognostic value in patients with CIS suggestive of MS and early MS.	(Voortman et al., 2017)
Measles/rubella/varicella-zoster and Epstein-Barr virus antibodies	Non-Self antigens from infectious agents, can disrupt the control of adaptive immunity resulting in severe inflammation in MS.	(Owens et al., 2011)
Anti MBP, Anti MOG	Myelin antigens (MBP, MOG protein) are important in the	(Egg et al., 2001)

	inflammation and demyelinating process in MS.	
Cytokines IL1, IL6, IL12,IL15,IL17, IL17F, IL21, IL23, TNF-alpha, IFNs, TGF-beta	Cytokines contribute to the trafficking of immune cells across the BBB, and the regulation of their transfer to lesion sites in MS.	(Palle et al., 2017)
Chemokines CXCR3, CXCL9, CXCL10, CCR1, CCL3, CCL4, CCL5, CCR2, CCL2, CCR5,CCL3,CCL4, CCL5,CXCL8,CXCL12,CXCL13,IP-10	Chemokines help to initiate information by trafficking immune cells across the BBB, and regulating their transfer to lesion sites in MS.	(Szczuciński & Losy, 2007)
Other proteins		
Osteopontin	Osteopontin is a proinflammatory molecule that may have diagnostic and prognostic value in MS.	(Agah et al., 2018)
Fetuin-A	An increase of Fetuin-A in CSF is described as a biomarker of disease activity in patients with a recent relapse.	(Harris et al., 2013)

αB-Crystalline	A stress-related protein expressed in activated astrocytes that play pivotal roles during inflammation.	(Ponath et al., 2018a)
ICAM-1, VCAM-1	Cell adhesion molecules, intercellular adhesion molecule 1 (ICAM-1) and vascular cell adhesion molecule 1 (VCAM-1) could play a dual role in inflammation and BBB homeostasis.	(Lécuyer et al., 2017)
Legumain	A cysteine protease, expressed by macrophages and reactive astrocytes, found in active lesions.	(Oveland et al., 2021)

Demyelination

Biomarker name	Function/origin	Reference
PLP, MBP	Loss of myelin basic protein (MBP) and proteolipid Protein (PLP) are indicative of demyelination in MS lesions	(Bø et al., 2003a)

Gliosis

Biomarker name	Function/origin	Reference
GFAP	Glial Fibrillary acidic protein (GFAP) is a good marker of astroglia cell activation (astrogliosis) following CNS injuries and neurodegeneration.	(Yang & Wang, 2015)
S100B	S100B is predominantly expressed in astrocytes after injury and serves as a marker for gliosis.	(Barateiro et al., 2016)

Oligodendrocyte loss

Biomarker name	Function/origin	Reference
Nogo-A	Nogo-A is expressed on mature oligodendrocytes, A marker of oligodendrocyte loss.	(Wergeland et al., 2011)

A2B5, O1, O4	Maturation stage-specific markers for OPCs	(Ma et al., 2009)

Axonal/ neuronal loss

Biomarker name	Function/origin	Reference
Neurofilaments (NFs)	NFs Constituent of microtubules. A major marker for axonal loss.	(Grevesse et al., 2015)
14-3-3 Protein, Tau	14-3-3 and tau proteins in CSF are markers of axonal pathology and predictors of disease progression.	(Colucci et al., 2004)
Ferritin	Iron-related proteins ferritin is an indicator of iron accumulation and neurodegeneration	(Hametner et al., 2013)

Remyelination

Biomarker name	Function/origin	Reference
Ermin	A potential remyelination marker specific to oligodendrocyte.	(Ahmad et al., 2021)
BDNF	Brain-Derived Neurotrophic Factor (BDNF) plays a role in remyelination.	(Patrikios et al., 2006)
PDGFαR	Platelet-derived growth factor-α receptor (PDGFαR) is a regulator of remyelination, stimulating the proliferation of OPCs	(Armstrong, 2007)

Oxidative stress

Biomarker name	Function/origin	Reference
Nitric Oxide (NO) Reactive Oxygen Species (ROS),	Redox processes in MS are associated with mitochondrial dysfunction and neurodegeneration.	(Adamczyk & Adamczyk-Sowa, 2016)
Lactate	Higher Lactate level in CSF relates to mitochondrial dysfunction and concomitant oxidative damage.	(Albanese et al., 2016)

Biomarkers in early pathology

Here we have a list of molecules which are most likely involved in early pathology in MS

Biomarker name	Function/origin	Reference
Kallikrein-6	A serine protease that is increased in active multiple MS lesions.	(Scarisbrick et al., 2012)
Plasminogen inhibitor	Plasminogen activator inhibitor-1, a serine-protease inhibitor, that can be detected in acute MS lesions.	(Gveric, 2001)
Vitronectin and integrin vitronectin receptor	These can be detected within dystrophic, demyelinated axons in active MS lesions	(Sobel et al., 1995)

1.6 Emerging biomarkers molecular markers in MS diagnosis and prognosis

CSF and serum are the two most common sources for biomarker exploration. A long list of potential biomolecules has been identified in these two sources. In that long list, CHI3L1, a chitin-binding glycoprotein, and NfL, a neuron-specific cytoskeletal protein, got significant scientific attention, because of a valuable diagnostic and prognostic potential (Biernacki et al., 2022).

CHI3L1 is a glial marker, with a more diverse cellular presence and function than that of NfL. CHI3L1 is a member of the mammalian chitinase-like protein family. In MS cases, it is expressed primarily by reactive astrocytes, present in active and chronic active MS lesions (Burman et al., 2016), and in some microglia/macrophages (Pranzatelli et al., 2017). CHI3L1 lacks

the enzymatic activity of chitinase. It is considered to play an important role in chronic inflammation and tissue remodelling following injury (Lee et al., 2011). In addition, it is a potential prognostic marker of the conversion of clinically isolated syndrome (CIS) to clinically definite MS (Comabella et al., 2010).

A higher cerebrospinal fluid CHI3L1 level is correlated with clinical and radiological disease activity in MS (Comabella et al., 2010). Furthermore, it can predict a worse disease prognosis (Canto et al., 2015). The plasma level of CHI3L1 is also related to MS disease activity (Hinsinger et al., 2015). However, higher levels of chitinase 3-like 1 are not specific to MS; the molecule plays a vital role in the pathogenesis of other diseases related to inflammation and cancer (Geng et al., 2018).

2. The rationale of the study

The pathological features of MS differ in WM and GM. WM is composed mainly of myelinated axons, oligodendrocytes, astrocytes, microglia, and blood vessels. The main pathological feature of MS in WM is the presence of inflammatory demyelinating lesions, which are characterized by focal inflammatory lesions, associated with of the phagocytosis of myelin sheaths axonal damage and gliosis (Trapp et al., 1998). The extent and location of WM lesions correlate with physical disability and cognitive impairment in MS patients (Filippi et al., 2018).

GM, on the other hand, contains mainly neuronal cell bodies, dendrites, synapses, in addition to the cell types present in WM. GM involvement in MS was initially thought to be limited to the later stages of the disease. However, recent studies have shown that GM damage occurs early in the course of MS and can even precede the appearance of WM lesions (Filippi et al., 2018). GM pathology in MS includes cortical and deep gray matter demyelination, neuronal loss, synaptic dysfunction and loss, and microglial activation(Frischer et al., 2009). GM damage has been linked to cognitive impairment, fatigue, depression, and physical disability in MS patients, even in the absence of WM lesions (Filippi et al., 2014).

Histopathologically, different involvement of WM and GM in MS has been attributed to their different physiological and immunological properties. WM has a higher water content, higher density of immune cells, and fewer blood-brain barrier (BBB) tight junctions, making it more vulnerable to inflammation and demyelination. GM, on the other hand, has a lower water content, higher density of immune cells, and more BBB tight junctions, making it more resistant to inflammation and demyelination (C. F. Lucchinetti et al., 2011).

Understanding the differential involvement of WM and GM in MS is crucial for the development of new biomarkers and therapeutic approaches to improve the clinical outcome of MS patients.

The diagnosis of MS presents its unique set of challenges. The 2010 McDonald criteria were widely used for the diagnosis of MS (Polman et al., 2011). The improvements in the 2017 McDonald criteria were mainly helpful for setting an early MS diagnosis. MRI may be sufficient to confirm the diagnosis if typical clinical signs and syndromes accompany it. Supplementary information is also obtained from the cerebrospinal fluid (McDonald et al., 2001). In MS diagnosis, it is important to differentiate it from other demyelinating diseases, such as neuromyelitis optica spectrum disorder (NMOSD) and acute disseminated encephalomyelitis (ADEM). Additionally, MS needs to be distinguished from some non-demyelinating disorders that can overlap with the signs and symptoms of MS, such as chronic small vessel disease and other inflammatory, granulomatous, infective, metabolic, and genetic causes (Brownlee et al., 2017).

A wrong assignment of an MS diagnosis on a patient is not unusual. A study shows that nearly 1 in 5 people (17% at Cedars-Sinai and 19% at UCLA) were misdiagnosed with MS with different disease conditions (Kaisey et al., 2019). However, the 2017 McDonald's criteria comprise some new recommendations to handle potential misdiagnoses.

Since there is no definitive diagnostic test or tests for MS, setting the diagnosis is largely based on excluding other diagnoses. Brain MRI, spinal fluid biomarkers, health history, vision tests, and clinical neurological status. Though MRI is a central diagnostic tool for MS detection, over-emphasis on a single criterion could easily lead to misdiagnosis (J. J. Chen et al., 2016). A wide range of factors like hypoxic-ischemic vasculopathy, small-vessel disease, other CNS inflammation, vasculitis, toxins, and infections may give MS-like lesions in MRI scans (Aliaga & Barkhof, 2014).

When it comes to MS treatment, there could be three approaches to cure MS; a) Prevent the initiation of MS, b) Stop the progression of MS c) Reverse neurological damages and restore function (Weiner, 2009). Unfortunately, no treatment for MS can successfully achieve one of the approaches. Until now, treatment typically focuses on preventing exacerbations and speed-up recovery from attacks by disease-modifying therapies (DMTs) and high dose corticosteroids,

respectively. In addition, symptomatic therapies manage MS symptoms like fatigue, spasticity and depression (Wingerchuk & Carter, 2014).

Nonetheless, significant progress has been made in the biological understanding and treatment of MS in the last few decades. DMTs are still the primary treatment option for people with MS. However, DMTs are commonly hampered by adverse side effects caused by immune suppression. Moreover, they are for mainly effective for RRMS, by delaying inflammatory/clinical exacerbations (Fogarty et al., 2016). Autologous hematopietic stem cell transplantation (HSCT) has come into the picture of MS intervention. Nevertheless, a few short-term investigations have documented their safety and beneficial outcomes (Burt et al., 2019). In this treatment method, patients may be their own donor, without the risk of rejection. Autologous bone marrow-derived mesenchymal stem cell transplantation is safer for malignant transformation (Bejargafshe et al., 2019). There is still a need for determining the role of HSCT vs. standard DMTs, by comparing long-term efficacy and side effect outcomes.

It is evident that MS is a multifaceted disease with complex pathogenesis (Banwell Brenda, Giovannoni Gavin, Hawkes Chris, 2014). Currently, there is no single biological mechanism to target, no definitive diagnostic marker, no curative treatment. The main reason behind this is likely to be the complexity of the disease processes, with different mechanisms contributing to a common end result. Therefore, investigating the pathogenesis of MS in different CNS tissue types/regions are important to identifying processes/markers essential for future therapies. The pathological process-specific high-throughput studies could help understanding the disease better than a hypothesis-driven approach.

Pathological process-specific biomarkers could be valuable in several ways. For example, to subcategorise MS based on pathology, identify clinical stage/subgroup, predict the onset and diseases course, aid in individualized treatment selection, improve the prognosis of the treatment and to evaluate novel therapeutics targeting a specific pathological process. From a broader perspective, searching for novel biomarkers could also challenge our perceived notion of MS. Unexpected targets could lead us to identify novel disease pathways or processes.

Despite the large number of studies proving an extensive list of candidate biomarkers in MS, only a few are presently used at the clinical or paraclinical level. The fact is, we have an enormous pile of candidate markers which is growing very fast with the aid of high throughput techniques. On the other hand, little progress has been made in relating novel biomarker candidates with disease activity and specific underlying processes. Moreover, the biology of these markers is largely unknown. In this circumstance, two distinct but interrelated approaches could be taken in MS biomarker research; an expedition for novel candidates and studies to better understand the biology of existing candidates.

Exploring potential biomarkers for the grey matter pathology and remyelination

One of the biggest challenges in therapeutic decision-making for MS is the effective stratification (personalisation) of treatment. A major objective in MS treatment is to arrest the disease as early as possible in the course of the disease. Disease-modifying therapies for MS should ideally be applied during the 'preclinical' or early clinical stage (before severe neuronal and/or axonal damage). This requires biomarker panels to identify early pathology, categorise disease stages and monitor disease progression. So far, there is no molecular biomarker for the early detection of MS pathology. Early-stage pathology in the grey matter pathology is overlooked in most studies, although grey matter damage in MS starts early in the disease process and may substantially affects the cognitive function of patients (Geurts & Barkhof, 2008). Detection of cortical grey matter lesions by standard T2-weighted MR imaging techniques has low sensitivity (Filippi & Rocca, 2010).

The two most established animal models of MS are experimental autoimmune encephalomyelitis (EAE), and cuprizone (CPZ) mediated intoxication, alongside a viral-mediated demyelination model, which has susceptibility issues, e.g., anti-inflammatory cytokines produced in TMEV infection can be protective to anti-viral immune responses and can cause myocarditis (Omura et al., 2018). The EAE model, which may represent RRMS, has been extensively used in MS research. The EAE model has provided a good number of target biomarkers, and a handful of

them has helped develop DMTs. Although the cuprizone model has a solid potential for adding novel biomarkers to the MS biomarker arsenal, it has been studied less extensively than the EAE model. The cuprizone model generally represents the chronic phases of MS, where currently we lack good candidate markers to study further for clinical or paraclinical usage.

Therapies are needed to enhance the repair (remyelination) in MS, particularly for the progressive forms of MS, where the current treatments are unsuccessful. High-throughput screenings have led us to identify potential potential/partial remyelination therapies such as clemastine, opicinumab, GNbAC1, ocrelizumab, simvastatin, biotin, and quetiapine (Kremer et al., 2019). Unfortunately, it is challenging to measure remyelination in lesions with the existing MRI techniques. Therefore, we need a reliable molecular marker to evaluate the extent of remyelination in lesions. Moreover, introducing a novel remyelination marker could significantly enhance our comprehension of the remyelination pathways.

Validation of established CSF biomarkers in CNS tissue

The CSF is a valuable source of biomarkers for CNS disease, due to its natural proximity to the CNS parenchyma. Proteomic studies have identified several protein biomarkers in the CSF of MS patients, compared with healthy controls and/or other neuronal diseases. CSF proteins are an indirect measure of markers in MS pathogenesis. On top of that, factors like circadian fluctuation can influence the measurement (Nilsson et al., 1992). Therefore, additional investigation is needed on the presence and distribution of these biomarkers in the CNS parenchyma. It can provide additional information related to involvement in lesion types/stages in different regions and tissue types.

The overall aim of this thesis is to identify pathological process-specific biomarkers in MS. Since the disease course is highly heterogeneous, personalisation of treatment would be more effective. Therefore, identifying clinically useful, pathological process-specific biomarkers could aid the personalised treatment strategy in MS.

3. Specific objectives

1. *To identify novel molecular biomarkers from experimental models; experimental autoimmune encephalomyelitis (EAE) and the cuprizone model and associate them with a specific pathological process in MS.* In this project, we aimed to identify novel molecular markers in the frontal cortex from animal models, and thereafter validate them in CSF and tissue.
2. *To identify and validate novel molecular biomarker candidates to address remyelination in MS patients.* In this project, we aimed to investigate an oligodendrocyte-specific potential molecular marker for remyelination named ermin; which had been identified by our proteomic study. The investigation had three parts. First, to find its cellular expression pattern during and after cuprizone exposure in the cuprizone mouse model, and thereafter its cellular distribution both in the remyelinated and non-remyelinated parts of human MS lesions, and the last part was to relate ermin expression with the maturation stages of oligodendrocyte progenitor cells (OPCs).
3. *To study the association of an established CSF marker for MS, Chitinase-3-like Protein 1, with different MS lesion types and lesion parts. Additionally, examine its spatio-temporal distribution in a de-remyelination model of MS.* CHI3L1 is one of the most established diagnostic and prognostic CSF molecular markers for MS. Intriguingly, this protein may be cytotoxic to neurons. However, no previous article had systematically associated this molecule with different tissue types in the CNS. Thus, CHI3L1 was a tempting candidate to study further in the human CNS sample and animal models, especially targeting grey matter. In this project, we aimed to investigate the cellular distribution of Chitinase-3-like Protein 1 in white and grey matter lesions, and its cellular distribution during and after cuprizone exposure in the cuprizone mouse model, both in the white and grey matter parts.

4. Methodological considerations

4.1 Selection of animal models

Humans are the only living organisms to develop MS (Bove, 2018). It is thus challenging to simulate this disease condition in an animal model, given that the etiology of that disease is unknown. Additionally, the physiology of the human brain is unique; for example, ion channel expression in neurons is different in rodents compared to that of humans (Kalmbach et al., 2018). Humans have larger neuron cells; thereby, those cells have a decreased surface-to-volume ratio exhibiting higher membrane ionic conductance compared to that of other mammalian species (Beaulieu-Laroche et al., 2021). The structural and molecular differences in the human brain may make humans susceptible to develop this myelin-related disease. Unlike other mammals, humans must maintain a large amount of metabolically costly myelin to support their neurological development. Considering these complex phenomena of human CNS, it is not easy to develop an animal model that could truly represent MS. However, several models have been developed in laboratory animals to mimic certain features of MS. Since human CNS tissue to a large extent may not be used for experimentation, the experimental models serve as valuable instruments for MS research. Even though no single model characterizes the pathophysiology of MS, each animal model has the strength to allow studying a single or several aspects of MS.

In terms of induction, the most studied animal models of MS are of three types; (1) the autoimmune-induced experimental encephalomyelitis (EAE); (2) toxin-induced models of demyelination, such as the cuprizone (CPZ), (3) viral induced models, mainly Theiler′s murine encephalomyelitis virus (TMEV) infection and substantial chronic demyelination (Procaccini et al., 2015).

However, from a more reductionist point of view, animal models can be divided into two categories; a) A model which attempts to replicate neuroinflammatory mechanisms in MS. Experimental autoimmune encephalomyelitis (EAE) falls in this category. b) A model that follows the crucial pathological feature, de- and remyelination. Toxin-induced rapid de/remyelination model is considered in this category.

In our proteomic study, we combined both the autoimmune encephalomyelitis and toxin-induced demyelination and remyelination models to cover both the immune-mediated and de- and remyelination events in MS pathology. A combination of differentially expressed proteins could show better translational value when investigated in CSF and tissue from MS patients.

4.1.1 The experimental autoimmune encephalomyelitis (EAE) model

Experimental autoimmune encephalomyelitis (EAE) is the most common and oldest experimental model for MS. EAE was not developed targeting MS. Instead, the model concentrated on the entire field of comparative and experimental inflammatory-demyelinating pathology, ranging from post-vaccinal complications to MS (Hurst, 1952). Relapsing-remitting disease is the most common clinical course of MS. It is widely believed in the MS research community that these occasional flare-ups are initiated by an aberrant autoimmune attack directed against proteins embedded in the myelin sheath. EAE is an excellent model of autoimmune inflammation in the brain, by introducing myelin destruction with perivascular infiltrates in the brain and spinal cords (Denic et al., 2011).

EAE models can vary depending on immunization and animal genotype. Generally, EAE is induced by subcutaneous injection of CNS homogenates or peptides of myelin proteins, as an emulsion that also contains an adjuvant, for higher immunogenic potential. EAE can also be induced by CD4+ T cell transfer from EAE donors to naive recipient mice, without adjuvant (Fletcher et al., 2010). The strength of the EAE model is the wide variety of species and transgenic strains, numerous encephalitogenic peptides, and a large array of induction protocols. This variability has been widely used to mimic the different disease manifestations of MS (Burrows et al., 2019).

Our study used the most extensively used EAE model, C57BL/6 mice, after immunization with the myelin peptide $MOG_{1–125}$. C57BL/6 mouse is the most common strain, and myelin oligodendrocyte glycoprotein (MOG) frequently acts as an immunogenic agent. It has been

demonstrated that $MOG_{35–55}$-immunized mice show increased severity of EAE in WT mice (C. Du & Sriram, 2002). In contrast to immunization with the short $MOG_{35–55}$ peptide, induction of EAE with $MOG_{1–125}$ involves B-cell recognition of the native MOG protein (Dang et al., 2015). In our study, the immunogenic epitope MOG_{1-125} was suspended in complete Freund's adjuvant (CFA) before immunization, and pertussis toxin (PTx) was injected intraperitoneally to provoke leakage of serum proteins (antibody) through the BBB.

In the classic scenario, immunization causes activation and expansion of peripheral antigen-specific T-cell response. Autoantigen-presenting dendritic cells (DCs) process the immunizing peptide and sensitize mainly CD4+ T cells in the periphery. Naïve antigen-specific cells encounter their myelin antigen entering the CNS and subsequently induce inflammation involving several cell types (Kuerten & Lehmann, 2011). The EAE models are extensively used to test therapies targeting the inflammation-component of MS. This was important to the development of an arsenal of disease-modifying treatments for relapsing forms of active MS, including interferon-β (IFN-β) glatiramer acetate, and natalizumab (Baecher-Allan et al., 2018).

Like most other animal models, EAE has several limitations. Current EAE models primarily show inflammation induced by CD4+ T-cells. However, pathological data indicate that CD8+ T-cells and B-lymphocytes may play an important role in MS inflammation and tissue damage (Lassmann & Bradl, 2017). MS lesions exhibit heterogeneity in the extent of inflammation in different lesions in the same MS patient (Lucchinetti et al., 2000), which is not observed in the EAE model. EAE is a good model for RR-MS, not for SP-MS or PP-MS.

Nevertheless, this well-characterized animal model, experimental autoimmune encephalomyelitis (EAE), generally comes first on the choice list to unravel the mechanisms of autoimmune inflammation in MS. In our study, EAE in C57BL/6 mice after immunization with $MOG_{1–125}$ was a good choice to study the differential abundance of CNS biomolecules in immune-mediated events (paper-I).

4.1.2 Toxin-induced model of demyelination and remyelination

MS is the most common demyelinating disorder of the human CNS. Multifocal demyelination is considered the hallmark of the disease (Popescu et al., 2013). The cuprizone model (CPZ model), lysolecithin model and ethidium bromide model can be used as toxic models of demyelination and remyelination in mice. Among them, the cuprizone model is much more widely used (Kipp et al., 2009). For example, this model has successfully been used to study the influence of dietary vitamin D supplements to reduce demyelination (Wergeland et al., 2011) and the efficacy of omega-3 treatment to boost remyelination (Siegert et al., 2017).

The cuprizone model presents heterogeneous pathologies of both focal and diffuse MS lesions (Y. Zhang et al., 2019). In this model, demyelination is induced by a massive depletion of oligodendrocytes bypassing myelin destruction by immune components (Blakemore, 1972). Thus, the cuprizone model serves as a reductionist approach to study crucial demyelination features in MS, primarily independent of inflammation (the CPZ model does exhibit secondary inflammation). Although cuprizone, a copper-chelating agent, was initially used to induce a copper deficiency in the animal model, it induced neurological impairment and demyelination instead (Carlton, 1966). Presumably, cuprizone induces global perturbations in cellular metabolism independent of its copper-chelating ability (Taraboletti et al., 2017).

In the CPZ model, it was observed that spontaneous remyelination follows demyelination after the removal of the cuprizone exposure. That is why the cuprizone model was established as a tool to study de- and remyelination in the superior cerebellar peduncle (Blakemore, 1973). This model got importance after a report demonstrated this as an easily inducible, localized, and predictable model (Hiremath et al., 1998). Currently, cuprizone treatment is the most frequently used toxin-induced MS model to study mechanisms of oligodendrocyte turnover, astrogliosis, and microgliosis besides de- and remyelination (Blakemore & Franklin, 2008).

Generally, young mice are used in the cuprizone model. However, mouse age, sex, strain, cuprizone concentration, or even additional drug can regulate the rate and susceptibility of demyelination and remyelination to fit the aim of the experiment. For example, CPZ treatment can

lead to more severe demyelination in juvenile and young mice than in middle-aged mice (H. Wang et al., 2013). Additional factors, for example, differences in the colonizing microbiota in mice from different vendors, can cause variations in results (Velazquez et al., 2019).

The CPZ model proves valuable and reliably replicable in investigating fundamental biology during de- and remyelination processes, irrespective of peripheral immune cells, in both white and grey matter. However, it does have certain limitations when it comes to accurately representing the efficacy of treatments targeting MS-related remyelination and disease outcomes, mainly due to the absence of suitable molecular markers. Furthermore, there is currently no consensus on the underlying induction mechanism and pathophysiology of the CPZ model. It is generally accepted that the pathology is caused by oligodendrocyte death with the perturbation of active metabolism carried out by microdontia (Praet et al., 2014). Oral administration of cuprizone induces a global insult, not only in the CNS but also in the entire body system. Morphological change in liver mitochondria (mega-mitochondria) is a good indication of this phenomenon (Suzuki, 1969). Furthermore, numerous physiological functions are linked to copper-containing enzymes such as hemocyanin, tyrosinase, and methane monooxygenase (Liu et al., 2016). The cuprizone model has never been examined concerning the enzyme functions affecting the outcome. This limitation can question the use of the cuprizone model to study behavioural, cognitive and motor function deficiencies in MS.

For our study, the cuprizone model fitted well with our reductionistic approach to investigate the differential abundance of CNS biomolecules in de and remyelination (paper I). Moreover, it shows regional heterogeneities in the demyelination pattern (Wergeland et al., 2012). According to Lucchinetti/Lassmann/Brück system, type II and IV grey matter lesions mimic cuprizone-induced demyelination associating oligodendrocyte loss (C. Lucchinetti et al., 2000). Therefore, the CPZ model is relevant to studying cortical pathology, and underlying regional pathology in MS. These points provide a strong basis to investigate our candidates of interest in the white, grey, and deep grey matter (mixed tissue) parts of the CPZ mouse model (paper II & III). Additionally, in this model, remyelination events are detectable as early as after three weeks

of ongoing CPZ exposure (Pfeifenbring et al., 2015). Hence, this is a standard model for remyelination in the early phase of CPZ exposure (paper II).

4.2 Human CSF samples

CSF is directly affected by diseases in the CNS. However, the CSF system can be influenced by other factors unrelated to CNS diseases, e.g., ageing, hypertension, atherosclerosis, and sleep deprivation (Benveniste et al., 2017). Human CSF has been used in our study to verify and quantify our candidate molecular markers identified in tissue proteomics. Our CSF samples were collected from 22 patients with RRMS. For comparison, we had 9 samples from subjects without neurological symptoms, 7 with other inflammatory neurological diseases, and 6 with other neurological disorders. All 22 MS patients were positive for oligoclonal bands (OCBs) that has diagnostic and prognostic relevance in MS (Brändle et al., 2016).

Clinical and demographic description of CSF samples at the time of lumbar puncture

Controls					Multiple sclerosis cases				
Diagnose at LP	EDSS	OCB status	Age (yrs)	Sex	Diagnose at LP	EDSS	OCB status	Age (yrs)	Sex
Non-neurological	N/A	Neg	74	F	RRMS	2	Pos	29	M
Non-neurological	N/A	Neg	25	F	RRMS	3	Pos	51	M
Non-neurological	N/A	Neg	36	M	RRMS	2	Pos	43	F
Non-neurological	N/A	Neg	28	M	RRMS	1.5	Pos	42	M
Non-neurological	N/A	Neg	79	M	RRMS	2	Pos	51	F
Non-neurological	N/A	Neg	63	M	RRMS	0	Pos	40	M
Non-neurological	N/A	Neg	86	F	RRMS	1.5	Pos	42	F
Non-neurological	N/A	Neg	39	F	RRMS	2	Pos	43	F
Non-neurological	N/A	Neg	68	M	RRMS	-	Pos	74	F
OIND	N/A	Neg	35	F	RRMS	2	Pos	35	F
OIND	N/A	Pos	32	M	RRMS	1.5	Pos	38	F
OIND	N/A	Pos	45	F	RRMS	3	Pos	35	F
OIND	N/A	Neg	63	F	RRMS	1.5	Pos	42	M
OIND	N/A	Neg	33	M	RRMS	1.5	Pos	29	F
OIND	N/A	Neg	35	M	RRMS	1	Pos	28	F
OIND	N/A	Neg	35	M	RRMS	1	Pos	33	F
OND	N/A	Neg	50	F	RRMS	1	Pos	29	F
OND	N/A	Neg	28	F	RRMS	2	Pos	32	F
OND	N/A	Neg	36	F	RRMS	1	Pos	37	F
OND	N/A	Neg	38	F	RRMS	1	Pos	35	F
OND	N/A	Neg	37	F	RRMS	0	Pos	28	F
OND	N/A	Neg	33	M	RRMS	1	Pos	41	F

LP=Lumbar puncture; EDSS=Expanded disability status scale; OCB=Oligoclonal bands; CSF=Cerebrospinal fluid; Pos= positive; Neg= Negative; - = information unavailable.

4.3 Human CNS sample material

Conducting research on post-mortem tissue is challenging. Unlike animal CNS tissue, several variables of human tissue collection cannot be controlled to maintain the highest quality of samples. Several molecular makers (RNA quality, protein quality) have been proposed recently to control tissue quality (Stan et al., 2006). Nevertheless, it has been observed that there is no significant difference between macromolecules extracted from older (over 11–12 years) formalin-fixed paraffin-embedded (FFPE) blocks in comparison to recent FFPE blocks (Kokkat et al., 2013).

The description and basic clinical features of autopsy material used in our studies are listed in the following table.

MS	Postmortem delay (hrs.)	MS Phenotype	Gender	Age at autopsy	Disease duration (years)	Cause of death
1	–	Progressive	M	34	13	Bronchopneumonia
2	28	Progressive	F	65	26	Congestive heart failure
4	–	–	M	43	–	–
5	8	Relapsing–remitting	F	52	20	Bronchopneumonia
7	24	Progressive	F	45	8	Acute pyelonephritis with sepsis
8	10	–	F	45	23	Bronchopneumonia
9	15	Progressive	M	55	36	Acute pyelonephritis with sepsis
10	70	Progressive	F	60	4	Bronchopneumonia
12	46	Progressive	M	67	42	Bronchopneumonia
13	13	–	M	50	20	Bronchopneumonia
14	29	Progressive	F	68	14	Cerebral hemorrhage
15	40	Progressive	M	83	–	Pseudomembranous colitis
16	29	Progressive	F	49	20	Bronchopneumonia
18	83	Progressive	F	62	28	Bronchopneumonia
19	31	–	M	52	8	Acute pyelonephritis
20	45	Progressive	M	43	7	Bronchopneumonia
21	27	Relapsing–remitting	F	21	4	Bronchopneumonia
23	24	–	F	56	26	Bronchopneumonia
25	50	–	M	46	12	Suicide
26	23	–	F	46	–	Hyperthermia
Control						
1			F	37		Epilepsy*
2			M	53		Diabetes mellitus
3			F	47		Heart disease (HSCRT)
4			M	40		Endocarditis
5			F	30		Lymphangioleiomyomatosis

- information unavailable

* The patient had no prior history of CNS disease, indicating that the seizure occurred without any identifiable preexisting structural or functional abnormalities in the brain, classifying it as cryptogenic epilepsy (histopathologically was not different from other controls).

4.4 Histopathology and lesion classification

Histopathological study of MS autopsy samples is still a gold standard for understanding the pathological processes of MS. Despite the recent advances, non-invasive MRI techniques cannot provide enough pathological specificity (Traboulsee & Li, 2006). Additionally, MS lesion pathology is strictly specific to human subjects (Lassmann & Bradl, 2017). To study MS pathology, it is essential to classify lesions correctly according to the research question.

From the perspective of lesion development, MS is the formation of focal demyelinated plaques that disperse into the CNS parenchyma, including white matter, grey matter, brain stem, spinal cord, and optic nerve (Reich et al., 2018). Although MS lesions can be developed anywhere in the CNS, some areas are highly susceptible to develop lesions. For example, the periventricular region (Adams et al., 1987). Other than the periventricular area, the corpus callosum (CC), subcortical region, brain stem, subcortical U-fibres, cervical spinal cord, and optic nerves are also common parts of CNS for lesion development (Ge, 2006).

Macroscopically, white matter plaques are distinctly identifiable scar tissue with a different colour and texture from the normal-appearing parts (Matthews et al., 2016). On the other hand, grey matter lesions are barely recognisable to the naked eye. With the help of a light microscope, lesions are characterized by varying degrees of demyelination, inflammation, axonal/neuronal degeneration, gliosis and remyelination (Filippi et al., 2012) and are studied upon staining different cell types with specific antibodies and dye. MS plaques largely vary in number, size, shape, topography, and cellular and molecular association. In addition, they have dynamic temporal changes (Kuhlmann et al., 2017). On that account, it is essential to have a standardised system to classify MS lesion types considering common features.

4.4.1 Classification of white matter lesions (WMLs)

Traditionally, MS was considered a white matter disease. Therefore, white matter lesion classification grabbed the initial attention. Among several classification systems, the Bö/Trapp system (Bö et al., 1994), the Vienna consensus system (Lassmann et al., 1998), the Lucchinetti/Lassmann/Brück system (C. Lucchinetti et al., 2000) and the van der Valk/De Groot modification (Van Der Valk & De Groot, 2000) are cited in the scientific literature.

Bö/Trapp classification system constructed a linear temporal sequence of lesion evolution depending on the inflammatory signature. This system staged MS lesions into three prime phases: active, chronic active, and inactive. On the other hand, Lucchinetti/Lassmann/Brück system classified lesions based on patterns of demyelination. They considered the topography and extension of plaques, oligodendrocyte destruction, the presence of immune cells and complement activation. The incorporation of several parameters made this classification system somewhat complicated in practice.

The Lucchinetti/Lassmann/Brück system differentiated pathological features of lesion development into four distinctive patterns. In short, the demyelination patterns are;Macrophage-associated (Pattern I), Antibody/complement-associated (Pattern II), and patterns III and IV are associated with possibly primary oligodendrocyte loss.

However, the latest literature on lesion classification proposes a simple and unifying classification of MS lesions which focuses on the staging of lesions. In addition to the previously recommended framework (Bö/Trapp classification), this update proposes to divide chronic active lesions into two groups, depending on ongoing demyelination (Kuhlmann et al., 2017).

On the basis of Bö/Trapp classification, we characterized WM lesions in the following types:

Active lesion: An active MS plaque is characterized by the presence of activated microglia/macrophages throughout the lesion. Typically, active lesions are small and perivascular. Alongside resident immune cells, perivascular inflammatory cells (lymphocytes, monocytes,

macrophages, and occasional plasma cells) encounter degenerating/missing myelin sheaths. Activated astrocytes (large hypertrophic) are prominent.

In early active lesions, degraded myelin protein in macrophages can be detected immunohistochemically. The presence of degraded product indicates a more precise timeline of the lesion stage. An in-vitro study has demonstrated that a larger protein molecule (e.g., PLP) can be detected immunohistochemically in macrophages within 1 to 2 days of lesion development. For a smaller molecule (e.g., MOG), the time frame could be just a day (Van Der Goes et al., 2005).

Chronic active lesion: The smouldering rim of activated/amoeboid microglia/macrophages at the lesion border characterises the chronic active lesions. The demyelination process can also be paused on the rim. The chronic inactive lesions appear relatively hypocellular but rich in fibrillary astrocytes. They show reduced axonal density and loss of mature oligodendrocytes. Different parts of a chronic active lesion can have varying degrees of inflammation and cellular orientation. The less inflamed area contains ramified/resting microglia. Lesions may have remyelinated parts on the boundary.

Inactive lesion: Inactive lesions are almost completely lacking macrophages/microglia. The entire lesion forms a scar with GFP-positive astrocytes having a small cytoplasm and elongated thin processes. These lesions have massive axonal loss leaving the centre completely demyelinated and hypocellular.

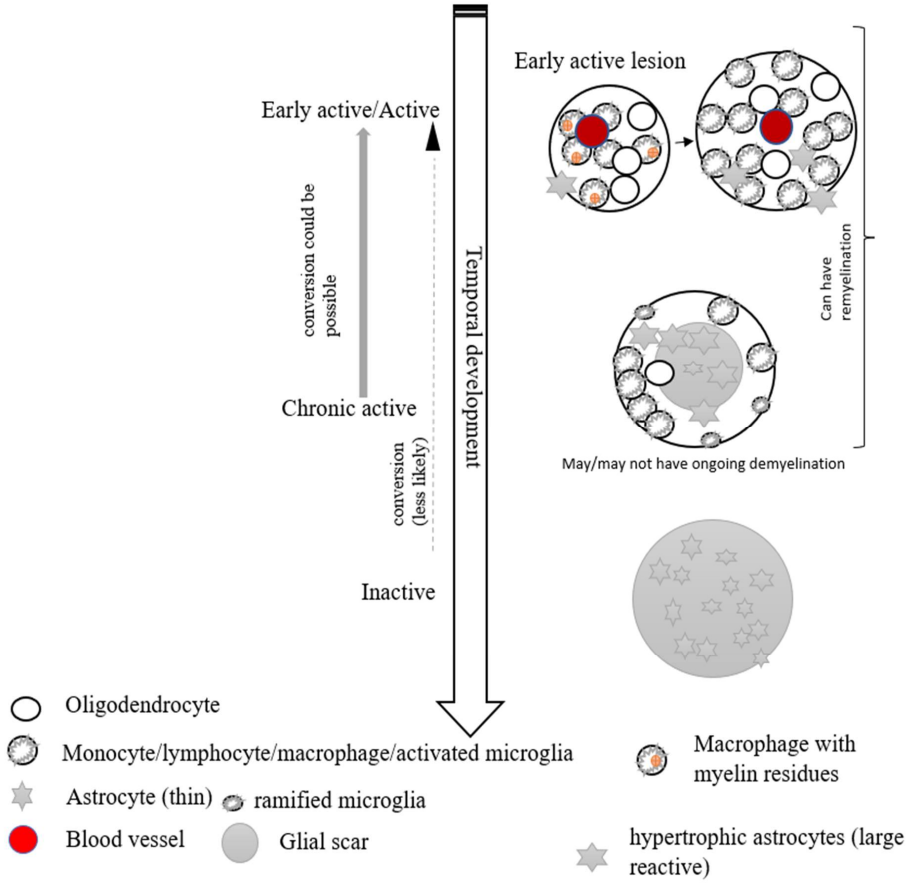

Figure 5: A simplified schematic summarizing the temporal classification of MS lesions. This diagram shows that the change is not unidirectional. Chronic active or inactive lesions might be infiltrated by a second attack of macrophages/microglia resulting in an active lesion formation. Lesions become hypocellular over the temporal progression, in terms of a load of immune cells, oligodendrocytes and active astrocytes, forming an astroglial scar (This schematic has been generated based on the concepts described in Kuhlmann et al., 2017).

Besides these three major temporal stages of lesions, normal-appearing white matter (NAWM) part, pre-active, and shadow plaques are important in MS white matter pathology. In recent times, a substantial accumulation of evidence suggests changes in normal-appearing white matter (NAWM) parts, independent of lesions. These changes associate endogenous inflammatory reactions throughout the brain parenchyma (Zeis et al., 2008). Near lesion tissue also has especial topographies. For example, reactive astrocytes are present on the margins of demyelinating and extend into adjacent normal-appearing white matter (NAWM) (Ponath et al., 2018b). Compelling evidence indicated that changes occur in the pre-active lesion area before the actual development of the active demyelinating lesion. It develops foci of activated microglia and leukocyte infiltrates (Van Der Valk & Amor, 2009). Additionally, remyelination is quite common in MS lesions, especially restricted to the lesion edge. Sometimes it even extends through the entire lesion area, which is designated as shadow plaque (Bruck et al., 2003).

For our studies, we used the Bö/Trapp classification system. In our sample material, we found very few early active white matter MS lesions (3 in number). Therefore, we combined the early lesion group with the chronic active lesion group and described them as an active lesion group.

4.4.2 Classification of grey matter lesions (GMLs)

Classical histochemical myelin stains like luxol fast blue (LFB) were not adequate for visualizing changes in GM myelin density; this might be one of the causes of considering MS a white matter disease in the first place. With the development of better antibody-dependent staining techniques, it became apparent that extensive cortical and deep grey matter pathology is present in MS. Gray matter demyelination can even exceed white matter demyelination in MS postmortem samples (Bø et al., 2003a). Multiple sclerosis functional composite (MSFC) analysis suggests GM atrophy is the best predictor of neurologic disability in MS patients (Rudick et al., 2009).

Myelin content is low in the cortex, when compared to white matter, and inflammation with perivascular infiltrates/monocytes is limited or absent in purely cortical lesions (Peterson et al., 2001b). That is why cortical lesions cannot be classified according to demyelinating activity or the pattern of inflammation. The initial classification system subdivided GM lesions into seven groups, which was proposed based on the relationship of lesions to the cerebral cortical venous supply (Kidd et al., 1999). This classification system was difficult with regular light microscopy and error-prone in practice. Later, a less complex classification based on the location within the layers of the cortex was proposed (Peterson et al., 2001a). This location-based classification system grouped GM lesions into three sets. However, this grouping did not include purely cortical lesions spanning the whole width of the cortex. The modification of this classification system thus added a fourth type (Bø et al., 2003b). For our studies, we classified GM lesions according to the system proposed by Bø and colleagues.

Type I: These lesions extend through grey matter (mostly deeper layers but can span through the entire cortical thickness) and adjacent white matter parts. They are called "leukocortical lesions" or "mixed GM-WM lesions". It is not clear whether the leukocortical lesions originate in the WM and spread to the GM, or vice versa or develop simultaneously in both (Maranzano et al., 2017). However, distinct parts have distinct pathology (Chang et al., 2012).

Type II: Cortical lesions that do not contact WM or with the pial surface of the brain. In general, they are small and perivascular, largely undetectable with regular MRI (1.5 to 3.0 Tesla magnet). This lesion type may indicate the involvement of perivascular inflammatory infiltrate in GM lesion development (Popescu et al., 2013).

Type III: These lesions extend inward from the pial surface of the brain. That is why they are named "subpial lesions". Demyelination is observed in subpial areas, usually confined within layers III or IV of the cortex and can be spanned over several gyri (Trapp et al., 2018). These are the most common type of GM lesions (Klaver et al., 2015). This type of lesion highlights the relationship between cortical demyelination and meningeal inflammation (Howell et al., 2011).

Type IV: These lesions are the least common type and extend through the entire width of the cortex without reaching into the underlying WM part. These lesions cover the largest surface area, typically involving multiple gyri, even the entire lobe. Interestingly, never touch the white matter part. Pattern IV lesions are infrequent and could be found in only 1% of MS brain samples (Popescu et al., 2013). This type of lesion challenges the classical concept of MS development as an inflammatory disease of white matter.

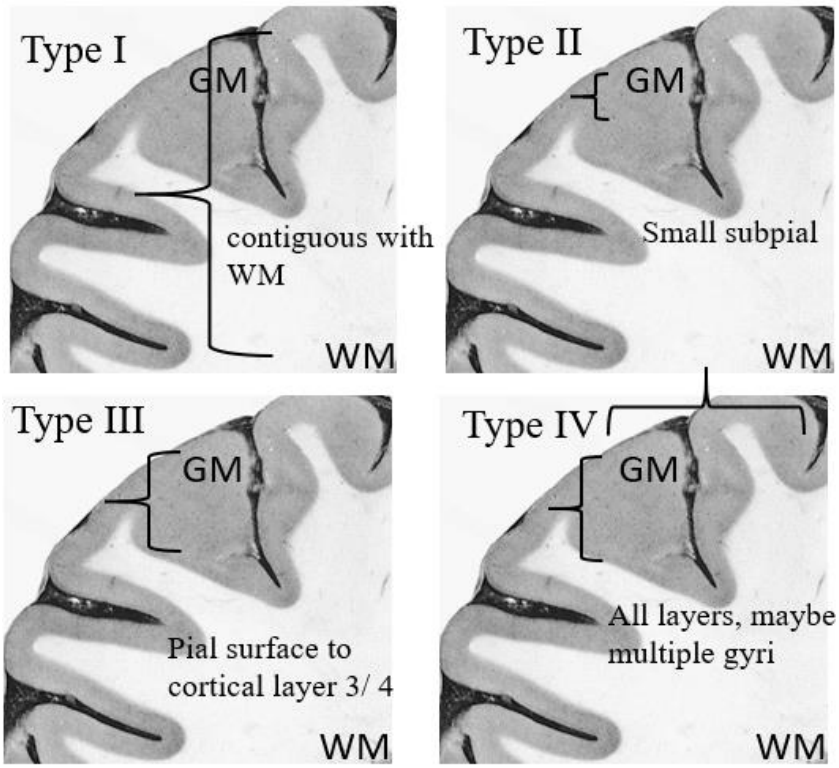

Figure 6: **Schematic of cortical MS lesions, categorized according to spatial demyelination.** Mixed GM-WM lesions are placed in type I. If lesions are purely cortical, they

are categorized into three groups; if they reach the cortical surface (Type III) or not (Type II), or if they span the entire width of the cortex (Type IV). WM= White matter

A new pathological subtype of MS termed “Myelocortical multiple sclerosis” was identified in 2018 (Trapp et al., 2018). In that study, this lesion type has been characterized by demyelination of the spinal cord and cerebral cortex but not of the cerebral white matter. Neuronal loss is greater in this type of cortical lesions than in typical GM lesions. In our study material, we did not find any lesion of that category.

4.5 Quantification of histopathology

4.5.1 Human brain samples

In our study, manual identification of lesions and their pathological stages were performed by three well-trained individual investigators depending on previously described criteria of lesion classification. Each lesion was assigned a unique identifying number. The measurement of immunopositive cells was semi-quantitative for paper 1 and quantitative cell density profiling was performed for papers II and III. The density of immunopositive cell profiles was counted by light microscopy (Zeiss Axio Imager A2, Wetzlar, Germany) using an ocular morphometric grid on randomly selected regions of interest (ROIs)

Inflammatory activity of a lesion on a PLP-immunostained section was determined by the HLA-DR immunostaining of the successive section of the same tissue Block. PLP and HLA-DR-stained sections were digitized using a Scanscope XT slide scanner (Aperio Technologies; Vista, CA) system with an Olympus UPLSAPO camera having 40× objective lens (Olympus, Southend-on-Sea, UK). Techniquip Model 21DC was used as light source (Techniquip, Pleasanton, California, USA), with a GE quartzline projector lamp, model EKE 21V 150W (General Electric, Fairfield, Connecticut, USA). Images were scanned with a final resolution of 0.247 μm per pixel. Files were saved in Aperio SVS file format. Files were viewed in Aperio Imagescope software V.11 (Aperio, Vista, California, USA).

4.5.2 Mouse brain samples

The lateral corpus callosum, medial corpus callosum, supplementary motor cortex and deep grey matter were analysed in mouse brain tissue. The density of immunopositive cell populations was determined by light microscopy (Zeiss® Axio Imager A2, Wetzlar, Germany), using an ocular morphometric grid. Immunopositive cell density count was made in an area of 0.0625 mm^2. For the corpus callosum area, lateral and medial counts were averaged to get an overall count for the corpus callosum. For counting purpose, we considered cells with a preserved nucleus and characteristic morphology of cell types of interest. To quantify myelin content, greyscale images of tissue sections stained with PLP were thresholded to eliminate low-intensity background staining. The myelin content was expressed as the percentage of positive pixels in each image of PLP-stained sections, using ImageJ software (U. S. National Institutes of Health; Bethesda 2009). During cell profile counting, all tissue slides, and images were blinded to analysts for experimental group allocation.

4.6 Mass spectrometry-based quantitative proteomics

In our study, we employed proteomics techniques to discover new biomarkers and pathways related to MS. The application of quantitative proteomics provides a comprehensive understanding of the protein landscape in MS pathology, allowing us to gain insights into the disease mechanisms and identify potential biomarkers (Sen et al., 2021). While genomics and RNA-level analysis offer valuable information on genetic and transcriptional aspects, studying proteins directly enables us to investigate functional outcomes and identify specific proteins that are regulated in the context of a particular pathological condition. Biomarker discovery is greatly facilitated by the promising advancements in proteomic methods, which are accompanied by a growing arsenal of tools for protein identification and quantification (Rifai et al., 2006).

Different variations of mass spectrometry-based proteomics frameworks have been applied to search for biomarkers in MS, focusing on MS models as well as human MS tissue and fluids.

In Paper I, mass spectrometry-based proteomics, using liquid chromatography-tandem mass spectrometry (LC-MS/MS), was applied for the quantitative determination of proteins in brain tissue homogenates from both the EAE and CPZ mice.

Mass spectrometry-based proteomics can be divided into two main principles depending on the approach of the study: top-down and bottom-up. In protein-centred top-down proteomics, intact proteins are explored by mass spectrometry to study post-translational modifications (PTMs) together with genetic variations, alternative splicing isoforms, and the function of protein complexes (Melby et al., 2021). On the other hand, in peptide-centred bottom-up proteomics, proteins are proteolytically digested into peptides prior to the mass spectrometric analysis to study the protein profile of biological specimens (Dupree et al., 2020).

In quantitative proteomics, the primary aim is to acquire information about a relative or absolute protein abundance in a complex mixture (Ong & Mann, 2005). A complex protein mixture is proteolytically digested, normally by trypsin, into peptides. The peptides are introduced by HPLC into a mass spectrometer. Consequently, ions are generated in an ionization source and peptide ions are separated due to their m/z (mass-to-charge) (MS1) and fragmented into fragment ions (MS2) in a collision cell before being analysed by a detector (Eng et al., 2011). Each peptide is identified by its fragments (fingerprint) by searching the data against a database with theoretical peptide masses, thus elucidating the peptide sequence and, subsequently, protein sequence (Steen & Mann, 2004).

In Paper I, both isotopic labelling and label-free quantitative proteomics were applied for achieving low number of missing values and better quantitative precision in the protein profile analysis.

4.6.1 Isotopic labelling proteomics quantitative proteomics

A higher accuracy of quantification is achieved for label-based methods (Megger et al., 2014). TMT-labelling approach is an example of such a strategy, and TMT workflows might yield 15-20% more identified proteins compared to the label-free method (Muntel et al., 2019). In the TMT isotopically labelled quantitative approach, each of the sample groups is chemically labelled *in vitro* with a unique tag variant, and then the samples are mixed. In the mass spectrometer, the specific "reporter ions" appear in the MS2 spectrum and report the respective intensities for a peptide in each of the differentially labelled samples (L. Zhang & Elias, 2017).

4.6.2 Label-free quantitative proteomics

One label-free proteomics approach aims to determine the relative abundance of proteins based on the peptide intensities in MS1 without isotopically labelling. Sample groups are then run individually on the mass spectrometer, and the approach relies on reproducible LC-MS/MS runs (Bantscheff et al., 2007). Since in the label-free approaches, samples are run separately, the run conditions, e.g., temperature, experimenter, and column condition, need to be controlled carefully. Label-free proteomics might present better proteome coverage (Megger et al., 2014) with lower missing values on protein level (<2%) (Muntel et al., 2019).

4.6.3 Targeted quantitative proteomics

In Paper I, targeted quantitative proteomics using internal isotopically labelled peptide standards was applied in attempts to verify regulation of specific proteins detected in the label-free and isotopically labelling approach. Knowing the exact amounts of internal standards allows for absolute quantification of the respective endogenous peptides' concentration using parallel reaction monitoring (PRM). In this way, the results will be comparable across studies. The peak signal for each peptide was determined by the Skyline algorithm (MacLean et al., 2010), and verified based on fragment pattern, elution profile and retention time and synthesized internal isotopic standards (IS).

4.6.4 Processing and analysis of mass-spectrometric data

The protein lists from the TMT-labelling and label-free experiments were fused, and the average quantification values were applied for the proteins detected in both experiments. In the pathway analysis, the proteins significantly altered with a fold change greater than 20% in both TMT and label-free were considered more significant than in one of the experiments.

MS/MS data files from mass spectrometry were searched against the UniProt protein database (https://www.uniprot.org) using SearchGUI (Vaudel et al., 2011) and PeptideShaker (Vaudel et al., 2015). The results were imported back into the Progenesis LC-MS software from Nonlinear Dynamics. The protein abundances reported from Progenesis were based on the sum of the normalized abundance of the identified unique peptides. Identified mouse proteins were converted to human orthologues using MADGene (Baron et al., 2011). Whenever the accession numbers not found by MADGene were done manually by the Basic Local Alignment Search Tool (BLAST) in UniProt with default settings. Finally, human orthologues were compared against the results in the CSF-PR database (Guldbrandsen et al., 2017).

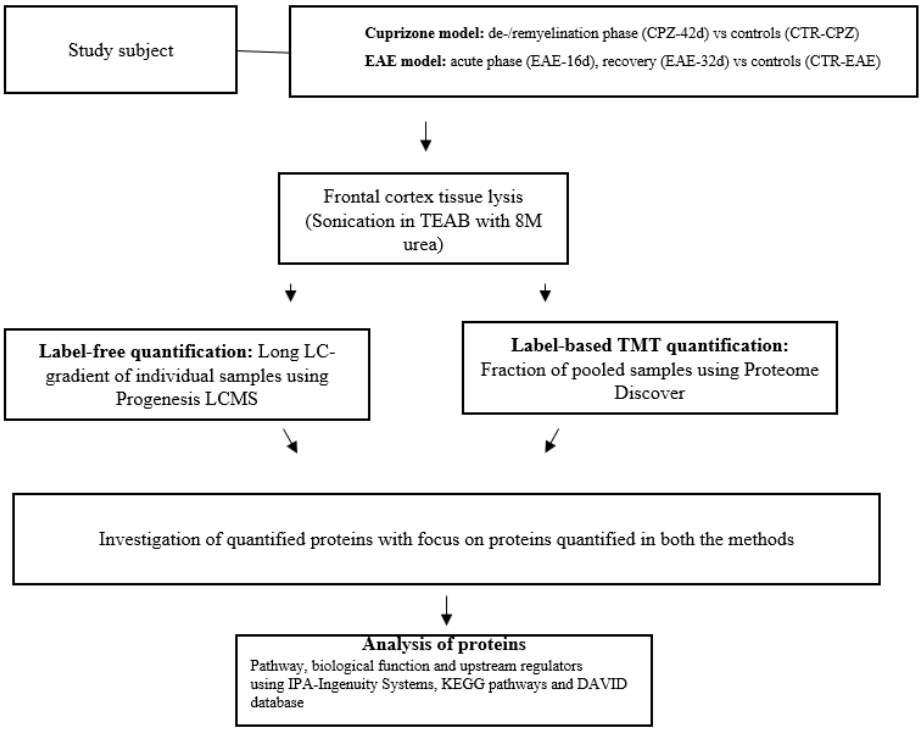

Figure 7: Study diagram combining label-free and label-based quantification. Frontal cortex tissue materials from mice were thawed on ice and homogenized in triethylammonium bicarbonate (TEAB) buffer containing 8 M urea. Proteins in tissue lysate were identified and quantified in combination of two methods, label-free and TMT label-based techniques. A quantification tool kit, Progenesis LC-MS was used for label-free quantification and Proteome Discoverer was used for label-based quantification. MS/MS data files from both methods were searched against the UniProt protein database for the mouse (Mus musculus). Identified mouse proteins were converted to human orthologues, and protein functions and pathway involvements were analysed using IPA® (QIAGEN), KEGG pathways (http://www.kegg.jp) and DAVID (https://david.ncifcrf.gov).

4.7 Ethical standards and regulations

The regional committee approved our research involving human brain tissue (permit ID: 2013–560). All studies were conducted per the ethical standards recommended by the regional committee. All autopsy tissue was obtained from the National MS biobank & registry at Haukeland University Hospital, Bergen, Norway. Written consent to the use of tissue for research had been given by the patient or by their close relatives. The patient's medical records and personal identity information were anonymized in the studies.

The Norwegian Animal Research Authority (Forsøksdyrutvalget) approved our animal research protocols. The acclimatization period of animals used in studies was one week. During the acclimatization, six mice were put together to reduce stress. To reduce distress and suffering, cages were provided with bedding and nesting material, and chewing implements. Cage maintenance and animal health monitoring were performed on a regular basis. Humane endpoints were defined prior to the study start based on clinical observation. All mice had ad libitum access to food and water. A need for analgesics was not expected in our studies. The experiment was conducted following the recommendations of the Federation of European Laboratory Animal Science Associations and the ARRIVE guidelines (du Sert et al., 2020).

5. Synopsis of papers

5.1 Paper I

In search of diagnostic and disease activity biomarkers in the cortex of MS patients, we have analysed the brain proteome in two experimental models for MS: the cuprizone model for toxic de- and remyelination, and the immune-mediated experimental autoimmune encephalomyelitis model using quantitative proteomics. Candidate proteins were analysed specifically in cerebrospinal fluid and autopsy tissue samples from MS patients. In total, 1871 proteins were quantified using TMT labelling and verified using label-free proteomics, revealing few similarities in protein regulation in the brain between the two disease models. One of the most promising candidate proteins, the lysosomal endopeptidase legumain, was identified by its prominent upregulation in the cuprizone model. The human orthologue of legumain was investigated in post-mortem MS brain tissues (n=19) by immunohistochemistry. Legumain was expressed significantly higher in the centre and at the edge of white matter active and chronic active lesions compared to inactive lesions. In cortical lesions, increased immunopositivity for legumain was observed, especially at the edges of type 1 neocortical lesions. Normal appearing white matter tissue parts and non-neurological disease control tissue had similar low legumain expression patterns. However, overall expression of legumain was higher in all grey matter compared to control grey matter tissue. In conclusion, the quantification of regulated proteins in the frontal cortex of cuprizone and EAE models of MS revealed distinct pathway and biological function signatures related to MS pathophysiology. These included processes such as myelinogenesis, lysosomal pathways, amino acid transport, acute phase signalling, and glutamate signalling. Additionally, elevated expression of LGMN in active and chronic active lesions in human white matter indicated its potential clinical utility in detecting ongoing inflammatory activity in MS.

5.2 Paper II

The limiting factors of remyelination in MS remains poorly understood, and there is no reliable clinical or paraclinical marker for remyelination. It has previously been shown in a mouse

model that an oligodendrocyte-specific protein called ermin (Erm) had higher RNA expression at the peak of myelin synthesis. In our high throughput proteomics study, Erm was significantly downregulated at the peak of demyelination (CPZ-42 days vs control) in the cuprizone model of de/remyelination. Consequently, we investigated Erm expression during de/remyelination, immunohistochemically in brain tissue of CPZ-exposed mice and further in MS brain tissue. The ermin-immunopositive (Erm+) cell population reduced gradually with CPZ exposure. There was an upward trend of Erm+ cell density at the beginning of the late phase of cuprizone exposure when spontaneous remyelination started. Moreover, at this stage, the ratio of the Erm+ cell population increased significantly concerning the NOGO-A+ cell population. Afterwards, in the extensive remyelination phase, two weeks after ending CPZ exposure, there was a widespread increase of the Erm+ cell density compared to the endpoint of CPZ exposure (CPZ-42days). In MS lesions with both the de- and remyelination areas, the numbers of Erm+ cells were significantly increased in the remyelinated areas compared to the non-remyelinated areas and normal-appearing areas both in white and grey matter. In remyelinated white matter areas, the NogoA+ cell population had significantly different densities than the Erm+ cell population. Double immunostaining showed that Erm+ cells were negative for early-stage oligodendrocyte progenitor cell (OPC) markers, O4 and O1, but a subpopulation of them was positive for a mature stage maker, Nogo-A. These data suggest that ermin is a late-stage marker of oligodendrocyte maturation. A relatively higher proportion of ermin immunopositivity in oligodendrocytes compared to Nogo-A may indicate recent or ongoing remyelination.

5.3 Paper III

Chitinase-3 like-protein-1 (CHI3L1) is a marker of inflammation associated with the conversion of clinically isolated syndrome to multiple sclerosis (MS). This protein is neurotoxic in primary cultured neurons. However, the presence and distribution of CHI3L1 in different lesion types and sub-types in MS brain tissue have not been studied extensively, particularly in grey matter (GM). In this study, the presence and distribution of CHI3L1+ cells were assessed in GM and WM lesions of MS, and the spatio-temporal dynamics of toxic/metabolic demyelination was

assessed in the cuprizone (CPZ) mouse model. Irrespective of tissue type, CHI3L1+ cells were frequently observed around blood vessels in the MS brain. Morphologically, astrocytes and microglia/macrophage were CHI3L1 positive. In the GM, CHI3L1+ lipofuscin aggregates in neurons were detected. CHI3L1+ neurone density in the MS cortex was elevated compared to controls ($p = 0.014$). In MS WM, CHI3L1+ phagocyting macrophages were detected in the early activity of lesion development. Comparably, in the CPZ model, from the first week, the density of CHI3L1+ cells increased most rapidly in the corpus callosum (CC), the WM area with the most inflammatory activation. Nevertheless, in the cortex, CHI3L1+ cell density started to increase in the later stage of the CPZ exposure phase compared to controls ($p<0.05$). Two weeks after the end of CPZ exposure, unlike in the cortex, a significant reduction in CHI3L1 density was observed in the CC compared to the end of the exposure phase ($p=0.002$). In DGM, CHI3L1+ cells appeared earlier in WM patches compared to in surrounding GM areas. CHI3Ll+ cell density correlated with that of microglia/macrophage activation marker Mac-3 in the CC throughout the experimental period ($r= 0.76$, $p<0.05$). These data not only confirm the association of CHI3L1 with inflammatory activation but also shows tissue-specific temporal variation. Additionally, the study suggests CHI3L1 as a marker of disease-related neuronal senescence in GM.

6. General discussion

In this research, our primary focus was on early-stage pathology in grey matter, neurodegeneration and remyelination. A key distinguishing feature of MS from other inflammatory diseases of the brain is its widespread cortical demyelination (Lassmann et al., 2007). Cortical demyelination is suggested to be a predictor of long-term severity and cognitive impairment in MS (Filippi & Rocca, 2010, 2019). Unlike WM lesions, purely cortical MS lesions contain little perivascular inflammation(Brück, 2005). Therefore, in animal models, we intended to search for regulated proteins distant from the site of major inflammation to mimic the cortical pathology of MS. It is known that there is a minor (mild microglial activity) or no inflammatory pathology in the frontal cortex of EAE mice (Lassmann & Bradl, 2017). On the other hand, in the CPZ de-and remyelination model, like MS pathology, the CPZ pathology has a global pattern in the CNS and displays a regional heterogeneity in respect to tissue types (Wergeland et al., 2012). Thus, combinatory study of the frontal cortex from both animal models can offer an approximation of the grey matter pathology that is observed in MS. In terms of time point, it is assumed that the highest number of proteins is regulated at the peak of the disease condition encompassing several ongoing pathological processes. In the CPZ model, the late demyelination phase overlaps with the partial remyelination process. Therefore, we compared the disease peak of the EAE and CPZ models versus controls. Additionally, we added the recovery phase of the EAE model, assuming a different set of ongoing pathological processes. In the validation process, the biomarker panel of interest was analysed immunohistochemically in brain tissues from MS autopsies and model animals.

6.1 Molecular alteration in the brain cortex in mouse models and its relevance to MS

In the frontal cortex, we observed different sets of proteins regulated in the CPZ and EAE mouse models. This result was expected from the known pathological differences between those models. Pathway analysis of regulated proteins indicated that the perturbed pathways involve myelinogenesis, lysosomal pathway, amino acid transport, acute phase signalling and glutamate

signalling. Since we analysed the part of the mouse brain away from apparent demyelination/inflammation, it is likely that in normal-appearing MS brain tissue, the pathways mentioned above may be impacted as a global CNS effect, apart from a lesion or near lesion pathology.

We analysed the tissue homogenate from the frontal hemisphere of the mouse brain, where gilia cells and neurons are in almost equal ratio, unlike the human brain, where there is a higher proportion of glial cells (Herculano-Houzel et al., 2006). It was expected that the pathology of the animal models would impact the brain proteome globally, irrespective of cell type. We did not observe differential regulation in neuronal proteins in the EAE or the CPZ model. On the other hand, there were regulated proteins in astrocytes, e.g., GFAP and VIME; in oligodendrocytes, e.g., MOG, MAG, MBP, CLD11, ERMIN and in microglia, e.g., LGMN and C1Q. This could have two reasons; glial cells could have protected neurons by providing physical and chemical support (Allen & Lyons, 2018) and/or neuronal cells could have some endurance mechanisms uncommon in glial cells (Kole et al., 2013). Glia cells protect and support neurons and help to repair injuries by detecting signals of neuronal damage, releasing cytokines, attracting immune cells, and interacting with them (Xu et al., 2020).

We have an open question, having a higher glial ratio in humans than rodents, why humans could have spontaneous MS and rodents do not? There might be an evolutionary divergence of human and mouse glial proteome related to neuropathological pathways. It has already been noticed from gene expression studies that there is a significant enrichment for known neurodegenerative process-related genes in human microglia (J. A. Miller et al., 2010) and enrichment of cognitive disease-associated genes in oligodendrocytes (Berto et al., 2019). Glial cells may thus be promising targets for MS treatment, either by inhibiting their pathological roles or by re-establishing lost homeostatic functions. Differentially regulated molecules in glia of MS models could be the starting point of target identification for possible intervention. Since we studied the cortex in our proteomic study, we found a list of differentially regulated proteins in the glial cells that are closely associated with neurones (Paper I).

6.2 An oligodendrocyte-centric view of MS etiopathogenesis and target for therapeutics

The most prevalent view of MS etiopathology is centred around myelin itself (myelinopathy). Alternatively, the primary target of MS could be the myelin-forming cell, the oligodendrocyte (oligodendrogliopathy) (Tsunoda & Fujinami, 2002). The crucial differentiating aspect of MS pathology from other inflammatory pathologies of the brain is its widespread cortical demyelination (Lassmann et al., 2007). A subgroup of MS patients may have a primary oligodendropathic disease because in a subset of MS lesions, it was found that the first signs of damage belonged to the periaxonal inner tongue, suggestive of dying oligodendrocytes (Lassmann et al., 1997; C. Lucchinetti et al., 2000). Understanding disease progression related to oligodendrocyte pathology and developing therapeutics targeting that pathology would benefit a subtype of MS patients.

From the viewpoint of morphology and bioenergetics, oligodendrocytes could be more sensitive to alteration and perturbation compared to other CNS cells. Oligodendrocytes in the CNS and Schwann cells in the PNS, generate an enormous amount of plasma membrane during the myelination process, making them particularly susceptible to disruptions to the secretory pathway, ER stress, and accumulation of unfolded or misfolded proteins (Lin & Popko, 2009). It is likely that multistep developmental processes and remarkably extended structure may make this cell type sensitive to even minor physiological changes. Thereby a small alternation of oligodendrocyte proteome could have a detrimental effect on myelination. For example, the oligodendrocyte-specific protein called ermin represents only 1% proteome found on myelin, making it a very low abundance protein (Jahn et al., 2013). However, ermin knockout mice show abnormal myelin architecture, splitting of myelin layers, and peeling of the myelin sheath from axons (S. Wang et al., 2020). A discrepancy in the formation of this protein molecule could have severe implications on oligodendrocyte vulnerability and myelination on axons in the CNS. Our study (paper II) supports the hypothesis that ermin is crucial for the early stages of myelin formation before myelin compaction. Further study on ermin could help us understand the cellular pathways involving critical factors of myelination.

6.3 MS pathology may have more neurodegeneration than anticipated for early stages.

In terms of common pathological mechanisms, neuroinflammatory and neurodegenerative diseases are even closer than expected. It is assumed that the primary triggers in different neurological diseases and disease subtypes may differ, while the subsequent pathology shares a significant number of common pathways. Therefore, common pathology could have some common clinical outcomes. For example, cognitive impairment, depression, fatigue, and even optic neuropathy seem to be routed in the degenerative mechanism shared by several CNS illnesses, though they may have variations in temporal activation. Thus, targeting common processes in CNS disorders may help to develop more common but selective pharmacological interventions.

Immunomodulatory therapies may be advantageous for primary neurodegenerative diseases because cellular abnormalities and destruction can result in secondary inflammation which enhances or mediates further neurodegeneration. For example, glatiramer acetate (GA), an immunomodulatory drug, may be effective for neuroprotection and cognitive preservation in Alzheimer's disease (Arnon & Aharoni, 2019). On the other hand, therapies countering neurodegeneration could be beneficial for primary inflammatory diseases. For example, legumain is one of the target enzymes for the treatment of Alzheimer's disease and Parkinson's disease to prevent neurodegenerative processes (Yu et al., 2020). Our study found that legumain could also be a drug target in MS pathology (Paper I).

Neurodegeneration in MS may begin early in the disease course, with silent clinical progression (Sandi et al., 2021) and sometimes can be confounded with the ageing process (paper III). Therefore, neurodegeneration did not get much attention for therapeutic intervention in MS, particularly in the early course of the disease. There are good treatment options against the inflammatory component of MS. Unfortunately, it lacks treatment opportunities targeting neuroprotection. Legumain and CHI3L1 showed good potential as treatment targets for treatment studies of neuroprotection.

6.4 Improvement of tools to study target drugs for remyelination

The classical view of the CPZ model is that it is an attractive animal model to study spontaneous remyelination after the CPZ exposure period. However, it is known that remyelination continues in parallel with the demyelination phase (Pfeifenbring et al., 2015), which did not get much interest in CPZ experiments. Studies on the initiation phase of remyelination are essential to understand remyelination biology, thereby finding drug targets to provoke the initiation of the spontaneous remyelination process. It has been observed that a relatively higher proportion of ermin immunopositivity in oligodendrocytes compared to Nogo-A indicates recent or ongoing remyelination (paper II). Potential drug targets for remyelination, e.g., quetiapine fumarate (Bi et al., 2012), could be revisited in the CPZ mouse model in relation to the early phases of the remyelination process.

From a broader perspective, results from our studies fall into a consensus that there is a significant pathological difference between white and grey matter parts in the MS brain. The same therapeutic intervention might act differently (if not inversely) in different parts of the brain. This issue needs to be addressed in the development of improved medications for MS. The cuprizone (CPZ) model can also be used to examine tissue-specific heterogeneity of remyelination (Paper-II).

6.5 Molecular biomarkers facilitating the classification of lesions in MS

The developmental stage of an MS-lesion cannot be entirely understood from the snapshot offered by immuno-histochemistry slides. Conventional immuno-histochemistry provides a 2D approximation of a 3D lesion at only one point in time. White matter lesions are principally classified based on temporal changes of inflammation and demyelination status (Van Der Valk & De Groot, 2000). On the other hand, grey matter lesions are classified based on the spatial distribution of lesions (Bø et al., 2003a). Temporal staging of white matter lesions depends on the assumption of the linear inflammatory model. Inflammatory processing in a lesion does not always

follow a linear progression. An inactive lesion can turn into an active one with a secondary influx of immune cells, which is apparent in MRI images (Campbell et al., 2012). Even different parts of a lesion could have a difference in the gradient of inflammatory activity.

There are some technical limitations in classifying lesions depending on a single feature or marker. For example, antigen epitopes can be masked by the tissue fixation process in traditional histochemistry technique, which can influence the identification of low-abundant molecules.

It can be concluded that an ideal classification system for MS lesions has not been developed yet. Consequently, lesion classification is subjected to the aim of different research projects. Whole slide image analysis may come in handy. Addressing morphological changes is easier to identify in high-resolution scanned images. Furthermore, a new imaging technique called imaging mass cytometry (IMC) can identify an array of cell types in a single sample to understand the interaction of cells in a lesion (Ramaglia et al., 2019). These new techniques would improve lesion classification with the help of novel cellular and extracellular matrix markers with respect to ongoing pathological events in a lesion. In our research, we have detected neuron and oligodendrocyte-specific biomarkers. These would be useful for recognising persistent pathological stages in an MS lesion and near-lesion areas to aid the lesion classification system.

7. Conclusion

In the course of this research endeavour, we have identified a cluster of proteins and pathways that may undergo alterations in the MS brain cortex. We proposed ermin as a promising molecular marker to track remyelination and investigated the involvement of CHI3L1 in MS pathology from a tissue perspective, specifically as a potential marker of MS-related neuronal senescence in the grey matter. Our findings suggest that neurodegeneration and inflammation may occur simultaneously, with a widespread distribution throughout the CNS parenchyma. The conclusions of our study resonate with previous research, underscoring tissue-specific variations in biomolecular expression and function within the MS-CNS, and these variations appear to be governed by the underlying pathophysiology. Therefore, it becomes crucial to acknowledge and address the pathological disparities between white and grey matter, with the aim of enhancing the detection of robust biomarkers and formulating more effective clinical interventions for MS. Furthermore, we accentuate a considerable drawback in relying exclusively on cerebrospinal fluid (CSF) analyses for biomarker discovery. This research also emphasized the cuprizone (CPZ) model, which proficiently encapsulates the tissue-specific heterogeneity, demyelination and remyelination, along with particular attributes of progressive MS.

8. Future perspectives

In the first paper, from animal model studies, we have identified a good number of potential molecular markers concerning cortical pathology in MS. Pathway analysis indicated some of their known biological roles in the CNS. None of them was comprehensively studied in different MS lesions and/or tissue types. Because of the scope of our study, our histopathological investigation was focused on legumain (LGMN). However, all the other candidates could be validated in the CNS tissue both in MS autopsy materials and animal models, especially in the grey matter part.

We have investigated the remyelination marker, ermin, in the MS brain tissue (Paper II). Ermin is detectable in the human CSF. To study the CSF level of ermin in different MS clinical subgroups and relate that with MRI data would be interesting to justify the importance of ermin as a remyelination marker in preclinical studies.

With respect to papers, I & III, LGMN and CHI3L1 could be treatment targets for neurodegenerative processes. It is essential to understand the cellular distribution pattern of those two protein molecules in different parts of the brain in different CNS diseases like Alzheimer's disease (AD) and Parkinson's disease (PD). This type of comparative study, especially in the grey matter part, could help to understand the likelihood of LGMN and CHI3L1 as drug targets for neuroprotection in general.

Studies on human MS and MS animal models suggest that a unique microenvironment in different tissue parts influences pathological processes (Pierson et al., 2012). A sizeable percentage of lesions are present outside the cerebrum (Nakashima et al., 1999); those regions did not get much attention for pathological classifications, biomarker identification and validation. All our candidate makers could be further studied in the cerebellum and the spinal cord tissue.

Since MS is a disease of unknown etiology and pathological heterogeneity, there might be hidden relations in identified biomarkers in high throughput studies that are beyond the scope of traditional statistical analyses with limited parameters. To encounter this problem, sophisticated clustering algorithms in the machine learning approach could be adopted. Precise clustering of

pathological processes involved in MS variants might answer critical questions regarding individual differences in MS pathology. Most importantly, collaborative multicentred and multicohort studies are needed instead of single-centred studies to understand MS pathology better.

9. References

Abdelhak, A., Weber, M. S., & Tumani, H. (2017). Primary progressive multiple sclerosis: Putting together the Puzzle. In *Frontiers in Neurology* (Vol. 8, Issue MAY). https://doi.org/10.3389/fneur.2017.00234

Adamczyk, B., & Adamczyk-Sowa, M. (2016). New Insights into the Role of Oxidative Stress Mechanisms in the Pathophysiology and Treatment of Multiple Sclerosis. In *Oxidative Medicine and Cellular Longevity* (Vol. 2016). https://doi.org/10.1155/2016/1973834

Adams, C. W. M., Abdullah, Y. H., Torres, E. M., & Poston, R. N. (1987). Periventricular lesions in multiple sclerosis: their perivenous origin and relationship to granular ependymitis. *Neuropathology and Applied Neurobiology*, *13*(2), 141–152. https://doi.org/10.1111/j.1365-2990.1987.tb00177.x

Agah, E., Zardoui, A., Saghazadeh, A., Ahmadi, M., Tafakhori, A., & Rezaei, N. (2018). Osteopontin (OPN) as a CSF and blood biomarker for multiple sclerosis: A systematic review and meta-analysis. In *PLoS ONE* (Vol. 13, Issue 1). https://doi.org/10.1371/journal.pone.0190252

Ahmad, I., Wergeland, S., Oveland, E., & Bø, L. (2021). A higher proportion of ermin-immunopositive oligodendrocytes in areas of remyelination. *PLOS ONE*, *16*(8), e0256155. https://doi.org/10.1371/journal.pone.0256155

Ahn, B. J., Le, H., Shin, M. W., Bae, S. J., Lee, E. J., Wee, H. J., Cha, J. H., Lee, H. J., Lee, H. S., Kim, J. H., Kim, C. Y., Seo, J. H., Lo, E. H., Jeon, S., Lee, M. N., Oh, G. T., Yin, G. N., Ryu, J. K., Suh, J. K., & Kim, K. W. (2014). Ninjurin1 deficiency Attenuates Susceptibility of Experimental Autoimmune Encephalomyelitis in mice.

Journal of Biological Chemistry, *289*(6), 3328–3338. https://doi.org/10.1074/jbc.M113.498212

Albanese, M., Zagaglia, S., Landi, D., Boffa, L., Nicoletti, C. G., Marciani, M. G., Mandolesi, G., Marfia, G. A., Buttari, F., Mori, F., & Centonze, D. (2016). Cerebrospinal fluid lactate is associated with multiple sclerosis disease progression. *Journal of Neuroinflammation*, *13*(1). https://doi.org/10.1186/s12974-016-0502-1

Aliaga, E. S., & Barkhof, F. (2014). MRI mimics of multiple sclerosis. In *Handbook of Clinical Neurology* (Vol. 122, pp. 291–316). https://doi.org/10.1016/B978-0-444-52001-2.00012-1

Allen, N. J., & Lyons, D. A. (2018). Glia as architects of central nervous system formation and function. In *Science* (Vol. 362, Issue 6411). https://doi.org/10.1126/science.aat0473

Alvarez, J. I., Cayrol, R., & Prat, A. (2011). Disruption of central nervous system barriers in multiple sclerosis. In *Biochimica et Biophysica Acta - Molecular Basis of Disease* (Vol. 1812, Issue 2, pp. 252–264). https://doi.org/10.1016/j.bbadis.2010.06.017

Armstrong, R. C. (2007). Growth factor regulation of remyleination: Behind the growing interest in endogenous cell repair of the CNS. In *Future Neurology* (Vol. 2, Issue 6, pp. 689–697). https://doi.org/10.2217/14796708.2.6.689

Arnon, R., & Aharoni, R. (2019). Glatiramer acetate: From bench to bed and back. *Israel Medical Association Journal*, *21*(3).

Baecher-Allan, C., Kaskow, B. J., & Weiner, H. L. (2018). Multiple Sclerosis: Mechanisms and Immunotherapy. In *Neuron* (Vol. 97, Issue 4, pp. 742–768). https://doi.org/10.1016/j.neuron.2018.01.021

Bantscheff, M., Schirle, M., Sweetman, G., Rick, J., & Kuster, B. (2007). Quantitative mass spectrometry in proteomics: A critical review. *Analytical and Bioanalytical Chemistry*, *389*(4), 1017–1031. https://doi.org/10.1007/s00216-007-1486-6

Banwell Brenda, Giovannoni Gavin, Hawkes Chris, L. F. (2014). Multiple Sclerosis is a multifaceted disease. *Multiple Sclerosis and Related Disorders*, *3*(5), 553–554.

Barateiro, A., Afonso, V., Santos, G., Cerqueira, J. J., Brites, D., van Horssen, J., & Fernandes, A. (2016). S100B as a Potential Biomarker and Therapeutic Target in Multiple Sclerosis. *Molecular Neurobiology*, *53*(6), 3976–3991. https://doi.org/10.1007/s12035-015-9336-6

Bargmann, C. I., & Marder, E. (2013). From the connectome to brain function. In *Nature Methods* (Vol. 10, Issue 6, pp. 483–490). https://doi.org/10.1038/nmeth.2451

Baron, D., Bihouee, A., Teusan, R., Dubois, E., Savagner, F., Steenman, M., Houlgatte, R., & Ramstein, G. (2011). MADGene: retrieval and processing of gene identifier lists for the analysis of heterogeneous microarray datasets. *Bioinformatics*, *27*(5), 725–726. https://doi.org/10.1093/bioinformatics/btq710

Baumann, N., & Pham-Dinh, D. (2001). Biology of oligodendrocyte and myelin in the mammalian central nervous system. In *Physiological Reviews* (Vol. 81, Issue 2, pp. 871–927). https://doi.org/10.1152/physrev.2001.81.2.871

Beaulieu-Laroche, L., Brown, N. J., Hansen, M., Toloza, E. H. S., Sharma, J., Williams, Z. M., Frosch, M. P., Cosgrove, G. R., Cash, S. S., & Harnett, M. T. (2021). Allometric rules for mammalian cortical layer 5 neuron biophysics. *Nature*, *600*(7888). https://doi.org/10.1038/s41586-021-04072-3

Beecham, A. H., Patsopoulos, N. A., Xifara, D. K., Davis, M. F., Kemppinen, A., Cotsapas, C., Shah, T. S., Spencer, C., Booth, D., Goris, A., Oturai, A., Saarela, J.,

Fontaine, B., Hemmer, B., Martin, C., Zipp, F., D'Alfonso, S., Martinelli-Boneschi, F., Taylor, B., … McCauley, J. L. (2013). Analysis of immune-related loci identifies 48 new susceptibility variants for multiple sclerosis. *Nature Genetics*, *45*(11), 1353–1362. https://doi.org/10.1038/ng.2770

Bejargafshe, M. J., Hedayati, M., Zahabiasli, S., Tahmasbpour, E., Rahmanzadeh, S., & Nejad-Moghaddam, A. (2019). Safety and efficacy of stem cell therapy for treatment of neural damage in patients with multiple sclerosis. In *Stem Cell Investigation* (Vol. 6). https://doi.org/10.21037/sci.2019.10.06

Benveniste, H., Lee, H., & Volkow, N. D. (2017). The Glymphatic Pathway: Waste Removal from the CNS via Cerebrospinal Fluid Transport. In *Neuroscientist* (Vol. 23, Issue 5). https://doi.org/10.1177/1073858417691030

Berto, S., Mendizabal, I., Usui, N., Toriumi, K., Chatterjee, P., Douglas, C., Tamminga, C. A., Preuss, T. M., Yi, S. V., & Konopka, G. (2019). Accelerated evolution of oligodendrocytes in the human brain. *Proceedings of the National Academy of Sciences of the United States of America*, *116*(48). https://doi.org/10.1073/pnas.1907982116

Betteridge, D. J. (2000). What is oxidative stress? *Metabolism: Clinical and Experimental*, *49*(2 Suppl 1), 3–8. https://doi.org/10.1016/s0026-0495(00)80077-3

Bhargava, P., & Mowry, E. M. (2014). Gut Microbiome and Multiple Sclerosis. In *Current Neurology and Neuroscience Reports* (Vol. 14, Issue 10). https://doi.org/10.1007/s11910-014-0492-2

Bi, X., Zhang, Y., Yan, B., Fang, S., He, J., Zhang, D., Zhang, Z., Kong, J., Tan, Q., & Li, X. M. (2012). Quetiapine prevents oligodendrocyte and myelin loss and promotes maturation of oligodendrocyte progenitors in the hippocampus of global cerebral

ischemia mice. *Journal of Neurochemistry*, *123*(1). https://doi.org/10.1111/j.1471-4159.2012.07883.x

Bielekova, B., & Martin, R. (2004). Development of biomarkers in multiple sclerosis. In *Brain* (Vol. 127, Issue 7, pp. 1463–1478). https://doi.org/10.1093/brain/awh176

Biernacki, T., Kokas, Z., Sandi, D., Füvesi, J., Fricska-Nagy, Z., Faragó, P., Kincses, T. Z., Klivényi, P., Bencsik, K., & Vécsei, L. (2022). Emerging Biomarkers of Multiple Sclerosis in the Blood and the CSF: A Focus on Neurofilaments and Therapeutic Considerations. *International Journal of Molecular Sciences*, *23*(6). https://doi.org/10.3390/ijms23063383

Bjartmar, C., Wujek, J. R., & Trapp, B. D. (2003). Axonal loss in the pathology of MS: Consequences for understanding the progressive phase of the disease. *Journal of the Neurological Sciences*, *206*(2), 165–171. https://doi.org/10.1016/S0022-510X(02)00069-2

Bjornevik, K., Cortese, M., Healy, B. C., Kuhle, J., Mina, M. J., Leng, Y., Elledge, S. J., Niebuhr, D. W., Scher, A. I., Munger, K. L., & Ascherio, A. (2022). Longitudinal analysis reveals high prevalence of Epstein-Barr virus associated with multiple sclerosis. *Science*, *375*(6578). https://doi.org/10.1126/science.abj8222

Blakemore, W. F. (1972). Observations on oligodendrocyte degeneration, the resolution of status spongiosus and remyelination in cuprizone intoxication in mice. *Journal of Neurocytology*, *1*(4), 413–426. https://doi.org/10.1007/BF01102943

Blakemore, W. F. (1973). Demyelination of the superior cerebellar peduncle in the mouse induced by cuprizone. *Journal of the Neurological Sciences*, *20*(1), 63–72. https://doi.org/10.1016/0022-510X(73)90118-4

Blakemore, W. F., & Franklin, R. J. M. (2008). Remyelination in experimental models of toxin-induced demyelination. In *Current Topics in Microbiology and Immunology* (Vol. 318, pp. 193–212). https://doi.org/10.1007/978-3-540-73677-6-8

Bö, L., Mörk, S., Kong, P. A., Nyland, H., Pardo, C. A., & Trapp, B. D. (1994). Detection of MHC class II-antigens on macrophages and microglia, but not on astrocytes and endothelia in active multiple sclerosis lesions. *Journal of Neuroimmunology*. https://doi.org/10.1016/0165-5728(94)90075-2

Bø, L., Vedeler, C. a, Nyland, H. I., Trapp, B. D., & Mørk, S. J. (2003a). Subpial demyelination in the cerebral cortex of multiple sclerosis patients. *Journal of Neuropathology and Experimental Neurology*, *62*(7), 723–732. https://doi.org/10.1093/jnen/62.7.723

Bø, L., Vedeler, C. A., Nyland, H., Trapp, B. D., & Mørk, S. J. (2003b). Intracortical multiple sclerosis lesions are not associated with increased lymphocyte infiltration. *Multiple Sclerosis*, *9*(4), 323–331. https://doi.org/10.1191/1352458503ms917oa

Bove, R. M. (2018). Why monkeys do not get multiple sclerosis (spontaneously): An evolutionary approach. In *Evolution, Medicine and Public Health* (Vol. 2018, Issue 1, pp. 43–59). https://doi.org/10.1093/emph/eoy002

Brändle, S. M., Obermeier, B., Senel, M., Bruder, J., Mentele, R., Khademi, M., Olsson, T., Tumani, H., Kristoferitsch, W., Lottspeich, F., Wekerle, H., Hohlfeld, R., & Dornmair, K. (2016). Distinct oligoclonal band antibodies in multiple sclerosis recognize ubiquitous self-proteins. *Proceedings of the National Academy of Sciences of the United States of America*, *113*(28). https://doi.org/10.1073/pnas.1522730113

Brownlee, W. J., Hardy, T. A., Fazekas, F., & Miller, D. H. (2017). Diagnosis of multiple sclerosis: progress and challenges. In *The Lancet* (Vol. 389, Issue 10076, pp. 1336–1346). https://doi.org/10.1016/S0140-6736(16)30959-X

Brück, W. (2005). Inflammatory demyelination is not central to the pathogenesis of multiple sclerosis. *Journal of Neurology*, *252*(SUPPL. 5). https://doi.org/10.1007/s00415-005-5003-6

Bruck, W., Kuhlmann, T., & Stadelmann, C. (2003). Remyelination in multiple sclerosis. *Journal of the Neurological Sciences*, *206*(2), 181–185. https://doi.org/10.1016/s0022-510x(02)00191-0

Burman, J., Raininko, R., Blennow, K., Zetterberg, H., Axelsson, M., & Malmeström, C. (2016). YKL-40 is a CSF biomarker of intrathecal inflammation in secondary progressive multiple sclerosis. *Journal of Neuroimmunology*, *292*, 52–57. https://doi.org/10.1016/j.jneuroim.2016.01.013

Burrows, D. J., McGown, A., Jain, S. A., De Felice, M., Ramesh, T. M., Sharrack, B., & Majid, A. (2019). Animal models of multiple sclerosis: From rodents to zebrafish. In *Multiple Sclerosis Journal* (Vol. 25, Issue 3, pp. 306–324). https://doi.org/10.1177/1352458518805246

Burt, R. K., Balabanov, R., Burman, J., Sharrack, B., Snowden, J. A., Oliveira, M. C., Fagius, J., Rose, J., Nelson, F., Barreira, A. A., Carlson, K., Han, X., Moraes, D., Morgan, A., Quigley, K., Yaung, K., Buckley, R., Alldredge, C., Clendenan, A., … Helenowski, I. B. (2019). Effect of Nonmyeloablative Hematopoietic Stem Cell Transplantation vs Continued Disease-Modifying Therapy on Disease Progression in Patients with Relapsing-Remitting Multiple Sclerosis: A Randomized Clinical Trial. *JAMA - Journal of the American Medical Association*, *321*(2). https://doi.org/10.1001/jama.2018.18743

Bush, T. G., Puvanachandra, N., Horner, C. H., Polito, A., Ostenfeld, T., Svendsen, C. N., Mucke, L., Johnson, M. H., & Sofroniew, M. V. (1999). Leukocyte infiltration, neuronal degeneration, and neurite outgrowth after ablation of scar-forming, reactive astrocytes in adult transgenic mice. *Neuron*, *23*(2), 297–308. https://doi.org/10.1016/S0896-6273(00)80781-3

Butt, A. M. (2009). Oligodendrocyte morphology. In *Encyclopedia of Neuroscience* (pp. 203–208). https://doi.org/10.1016/B978-008045046-9.01017-2

Cadenas, E., & Davies, K. J. A. (2000). Mitochondrial free radical generation, oxidative stress, and aging. *Free Radical Biology and Medicine*, *29*(3–4), 222–230. https://doi.org/10.1016/S0891-5849(00)00317-8

Campbell, Z., Sahm, D., Donohue, K., Jamison, J., Davis, M., Pellicano, C., Auh, S., Ohayon, J., Frank, J. A., Richert, N., & Bagnato, F. (2012). Characterizing contrast-enhancing and re-enhancing lesions in multiple sclerosis. *Neurology*, *78*(19), 1493–1499. https://doi.org/10.1212/WNL.0b013e3182553bd2

Canto, E., Tintore, M., Villar, L. M., Costa, C., Nurtdinov, R., Alvarez-Cermeno, J. C., Arrambide, G., Reverter, F., Deisenhammer, F., Hegen, H., Khademi, M., Olsson, T., Tumani, H., Rodriguez-Martin, E., Piehl, F., Bartos, A., Zimova, D., Kotoucova, J., Kuhle, J., … Comabella, M. (2015). Chitinase 3-like 1: Prognostic biomarker in clinically isolated syndromes. *Brain*, *138*(4), 918–931. https://doi.org/10.1093/brain/awv017

Caprariello, A. V., Mangla, S., Miller, R. H., & Selkirk, S. M. (2012). Apoptosis of oligodendrocytes in the central nervous system results in rapid focal demyelination. *Annals of Neurology*, *72*(3), 395–405. https://doi.org/10.1002/ana.23606

Carlton, W. W. (1966). Response of mice to the chelating agents sodium diethyldithiocarbamate, α-benzoinoxime, and biscyclohexanone oxaldihydrazone. *Toxicology and Applied Pharmacology*, *8*(3), 512–521. https://doi.org/10.1016/0041-008X(66)90062-7

Castellazzi, M., Lamberti, G., Resi, M. V., Baldi, E., Caniatti, L. M., Galante, G., Perri, P., & Pugliatti, M. (2019). Increased Levels of Endothelin-1 in Cerebrospinal Fluid Are a Marker of Poor Visual Recovery after Optic Neuritis in Multiple Sclerosis Patients. *Disease Markers*, *2019*, 9320791. https://doi.org/10.1155/2019/9320791

Cayre, M., Falque, M., Mercier, O., Magalon, K., & Durbec, P. (2021). Myelin Repair: From Animal Models to Humans. In *Frontiers in Cellular Neuroscience* (Vol. 15). https://doi.org/10.3389/fncel.2021.604865

Chamberlain, K. A., Nanescu, S. E., Psachoulia, K., & Huang, J. K. (2016). Oligodendrocyte regeneration: Its significance in myelin replacement and neuroprotection in multiple sclerosis. In *Neuropharmacology* (Vol. 110, pp. 633–643). https://doi.org/10.1016/j.neuropharm.2015.10.010

Chang, A., Staugaitis, S. M., Dutta, R., Batt, C. E., Easley, K. E., Chomyk, A. M., Yong, V. W., Fox, R. J., Kidd, G. J., & Trapp, B. D. (2012). Cortical remyelination: A new target for repair therapies in multiple sclerosis. *Annals of Neurology*, *72*(6), 918–926. https://doi.org/10.1002/ana.23693

Chang, A., Tourtellotte, W. W., Rudick, R., & Trapp, B. D. (2002). Premyelinating oligodendrocytes in chronic lesions of multiple sclerosis. *New England Journal of Medicine*, *346*(3), 165–173. https://doi.org/10.1056/NEJMoa010994

Charcot, J. M. (1888). Lecons sur les Maladies du Système Nerveux faites à la Salpêtrière. *Journal of Mental Science*, *34*(145), 113–116. https://doi.org/10.1192/s0368315x00231010

Chari, D. M. (2007). Remyelination In Multiple Sclerosis. In *International Review of Neurobiology* (Vol. 79, pp. 589–620). https://doi.org/10.1016/S0074-7742(07)79026-8

Chen, C., Zhou, Y., Wang, J., Yan, Y., Peng, L., & Qiu, W. (2018). Dysregulated microRNA involvement in multiple sclerosis by induction of T helper 17 cell differentiation. *Frontiers in Immunology*, *9*(JUN). https://doi.org/10.3389/fimmu.2018.01256

Chen, J. J., Carletti, F., Young, V., Mckean, D., & Quaghebeur, G. (2016). MRI differential diagnosis of suspected multiple sclerosis. In *Clinical Radiology* (Vol. 71, Issue 9, pp. 815–827). https://doi.org/10.1016/j.crad.2016.05.010

Chen, J. T., Collins, D. L., Atkins, H. L., Freedman, M. S., Arnold, D. L., Antel, J. P., Bar-Or, A., Bence-Bruckler, I., Duquette, P., Huebsch, L., Laneuville, P., Lapierre, Y., Messner, H., Pierre Sekaly, R., O'Connor, P., & Halpenny, M. (2008). Magnetization transfer ratio evolution with demyelination and remyelination in multiple sclerosis lesions. *Annals of Neurology*, *63*(2), 254–262. https://doi.org/10.1002/ana.21302

Chen, L., Deng, H., Cui, H., Fang, J., Zuo, Z., Deng, J., Li, Y., Wang, X., & Zhao, L. (2018). Inflammatory responses and inflammation-associated diseases in organs. In *Oncotarget* (Vol. 9, Issue 6, pp. 7204–7218). https://doi.org/10.18632/oncotarget.23208

Cheng, Y., Sun, L., Xie, Z., Fan, X., Cao, Q., Han, J., Zhu, J., & Jin, T. (2017). Diversity of immune cell types in multiple sclerosis and its animal model: Pathological and therapeutic implications. In *Journal of Neuroscience Research* (Vol. 95, Issue 10, pp. 1973–1983). https://doi.org/10.1002/jnr.24023

Chu, F., Shi, M., Lang, Y., Shen, D., Jin, T., Zhu, J., & Cui, L. (2018). Gut microbiota in multiple sclerosis and experimental autoimmune encephalomyelitis: current applications and future perspectives. In *Mediators of Inflammation* (Vol. 2018). https://doi.org/10.1155/2018/8168717

Cloake, N., Yan, J., Aminian, A., Pender, M., & Greer, J. (2018). PLP1 Mutations in Patients with Multiple Sclerosis: Identification of a New Mutation and Potential Pathogenicity of the Mutations. *Journal of Clinical Medicine*, *7*(10), 342. https://doi.org/10.3390/jcm7100342

Colucci, M., Roccatagliata, L., Capello, E., Narciso, E., Latronico, N., Tabaton, M., & Mancardi, G. L. (2004). The 14-3-3 protein in multiple sclerosis: A marker of disease severity. *Multiple Sclerosis*, *10*(5), 477–481. https://doi.org/10.1191/1352458504ms1089oa

Comabella, M., Fernández, M., Martin, R., Rivera-Vallvé, S., Borrás, E., Chiva, C., Juli, E., Rovira, A., Cantó, E., Alvarez-Cermeño, J. C., Villar, L. M., Tintoré, M., & Montalban, X. (2010). Cerebrospinal fluid chitinase 3-like 1 levels are associated with conversion to multiple sclerosis. *Brain*, *133*(4), 1082–1093. https://doi.org/10.1093/brain/awq035

Compston, A., & Coles, A. (2008). Multiple sclerosis. *Lancet*, *372*(9648), 1502–1517. https://doi.org/10.1016/S0140-6736(08)61620-7

Constantinescu, C. S., Farooqi, N., O'Brien, K., & Gran, B. (2011). Experimental autoimmune encephalomyelitis (EAE) as a model for multiple sclerosis (MS). In *British Journal of Pharmacology* (Vol. 164, Issue 4, pp. 1079–1106). https://doi.org/10.1111/j.1476-5381.2011.01302.x

Court, F. A., & Coleman, M. P. (2012). Mitochondria as a central sensor for axonal degenerative stimuli. In *Trends in Neurosciences* (Vol. 35, Issue 6, pp. 364–372). https://doi.org/10.1016/j.tins.2012.04.001

Cudrici, C., Niculescu, T., Niculescu, F., Shin, M. L., & Rus, H. (2006). Oligodendrocyte cell death in pathogenesis of multiple sclerosis: Protection of oligodendrocytes from apoptosis by complement. In *Journal of Rehabilitation Research and Development* (Vol. 43, Issue 1, pp. 123–132). https://doi.org/10.1682/JRRD.2004.08.0111

Dang, A. K., Jain, R. W., Craig, H. C., & Kerfoot, S. M. (2015). B cell recognition of myelin oligodendrocyte glycoprotein autoantigen depends on immunization with protein rather than short peptide, while B cell invasion of the CNS in autoimmunity does not. *Journal of Neuroimmunology*, *278*. https://doi.org/10.1016/j.jneuroim.2014.12.008

DeLuca, G. C., Ebers, G. C., & Esiri, M. M. (2004). Axonal loss in multiple sclerosis: A pathological survey of the corticospinal and sensory tracts. In *Brain* (Vol. 127, Issue 5, pp. 1009–1018). https://doi.org/10.1093/brain/awh118

Denic, A., Johnson, A. J., Bieber, A. J., Warrington, A. E., Rodriguez, M., & Pirko, I. (2011). The relevance of animal models in multiple sclerosis research. *Pathophysiology*, *18*(1), 21–29. https://doi.org/10.1016/j.pathophys.2010.04.004

Di Meo, S., Reed, T. T., Venditti, P., & Victor, V. M. (2016). Role of ROS and RNS Sources in Physiological and Pathological Conditions. In *Oxidative Medicine and Cellular Longevity* (Vol. 2016). https://doi.org/10.1155/2016/1245049

Domingues, H. S., Portugal, C. C., Socodato, R., & Relvas, J. B. (2016). Oligodendrocyte, astrocyte, and microglia crosstalk in myelin development, damage, and repair. In *Frontiers in Cell and Developmental Biology* (Vol. 4). https://doi.org/10.3389/fcell.2016.00071

Du, C., & Sriram, S. (2002). Increased Severity of Experimental Allergic Encephalomyelitis in lyn −/− Mice in the Absence of Elevated Proinflammatory Cytokine Response in the Central Nervous System . *The Journal of Immunology*, *168*(6). https://doi.org/10.4049/jimmunol.168.6.3105

du Sert, N. P., Hurst, V., Ahluwalia, A., Alam, S., Avey, M. T., Baker, M., Browne, W. J., Clark, A., Cuthill, I. C., Dirnagl, U., Emerson, M., Garner, P., Holgate, S. T., Howells, D. W., Karp, N. A., Lazic, S. E., Lidster, K., MacCallum, C. J., Macleod, M., … Würbel, H. (2020). The arrive guidelines 2.0: Updated guidelines for reporting animal research. *PLoS Biology*, *18*(7). https://doi.org/10.1371/journal.pbio.3000410

Du, Y., & Dreyfus, C. F. (2002). Oligodendrocytes as providers of growth factors. In *Journal of Neuroscience Research* (Vol. 68, Issue 6, pp. 647–654). https://doi.org/10.1002/jnr.10245

Duncan, I. D., Radcliff, A. B., Heidari, M., Kidd, G., August, B. K., & Wierenga, L. A. (2018). The adult oligodendrocyte can participate in remyelination. *Proceedings of the National Academy of Sciences of the United States of America*, *115*(50), E11807–E11816. https://doi.org/10.1073/pnas.1808064115

Dupree, E. J., Jayathirtha, M., Yorkey, H., Mihasan, M., Petre, B. A., & Darie, C. C. (2020). A critical review of bottom-up proteomics: The good, the bad, and the future of this field. In *Proteomes* (Vol. 8, Issue 3). https://doi.org/10.3390/proteomes8030014

Dutta, R., & Trapp, B. D. (2014). Relapsing and progressive forms of multiple sclerosis: Insights from pathology. In *Current Opinion in Neurology* (Vol. 27, Issue 3, pp. 271–278). https://doi.org/10.1097/WCO.0000000000000094

Egg, R., Reindl, M., Deisenhammer, F., Linington, C., & Berger, T. (2001). Anti-MOG and anti-MBP antibody subclasses in multiple sclerosis. *Multiple Sclerosis*, *7*(5), 285–289. https://doi.org/10.1191/135245801681137979

Eng, J. K., Searle, B. C., Clauser, K. R., & Tabb, D. L. (2011). A face in the crowd: Recognizing peptides through database search. In *Molecular and Cellular Proteomics* (Vol. 10, Issue 11). https://doi.org/10.1074/mcp.R111.009522

Fagnani, C., Neale, M. C., Nisticò, L., Stazi, M. A., Ricigliano, V. A., Buscarinu, M. C., Salvetti, M., & Ristori, G. (2015). Twin studies in multiple sclerosis: A meta-estimation of heritability and environmentality. *Multiple Sclerosis*, *21*(11), 1404–1413. https://doi.org/10.1177/1352458514564492

Fawcett, J. W., & Asher, R. A. (1999). The glial scar and central nervous system repair. In *Brain Research Bulletin* (Vol. 49, Issue 6, pp. 377–391). https://doi.org/10.1016/S0361-9230(99)00072-6

Felten, D., O'Banion, M. K., & Maida, M. (2016). Netter's Atlas of Neuroscience. In *Netter's Atlas of Neuroscience*. https://doi.org/10.1016/c2013-0-13970-0

Ferguson, B., Matyszak, M. K., Esiri, M. M., & Perry, V. H. (1997). Axonal damage in acute multiple sclerosis lesions. *Brain*, *120*(3), 393–399. https://doi.org/10.1093/brain/120.3.393

Fields, R. D. (2008). White matter in learning, cognition and psychiatric disorders. In *Trends in Neurosciences* (Vol. 31, Issue 7, pp. 361–370). https://doi.org/10.1016/j.tins.2008.04.001

Filippi, M., Bar-Or, A., Piehl, F., Preziosa, P., Solari, A., Vukusic, S., & Rocca, M. A. (2018). Multiple sclerosis. *Nature Reviews Disease Primers*, *4*(1), 43. https://doi.org/10.1038/s41572-018-0041-4

Filippi, M., Preziosa, P., & Rocca, M. A. (2014). Magnetic resonance outcome measures in multiple sclerosis trials: Time to rethink? In *Current Opinion in Neurology* (Vol. 27, Issue 3). https://doi.org/10.1097/WCO.0000000000000095

Filippi, M., & Rocca, M. A. (2010). MR imaging of gray matter involvement in multiple sclerosis: Implications for understanding disease pathophysiology and monitoring treatment efficacy. In *American Journal of Neuroradiology* (Vol. 31, Issue 7). https://doi.org/10.3174/ajnr.A1944

Filippi, M., & Rocca, M. A. (2019). Cortical lesions on 7-T MRI in multiple sclerosis: A window into pathogenetic mechanisms? In *Radiology* (Vol. 291, Issue 3). https://doi.org/10.1148/radiol.2019190398

Filippi, M., Rocca, M. A., Barkhof, F., Brück, W., Chen, J. T., Comi, G., DeLuca, G., De Stefano, N., Erickson, B. J., Evangelou, N., Fazekas, F., Geurts, J. J. G., Lucchinetti, C., Miller, D. H., Pelletier, D., Popescu, B. F. G., & Lassmann, H. (2012). Association between pathological and MRI findings in multiple sclerosis. In *The*

Lancet Neurology (Vol. 11, Issue 4, pp. 349–360). https://doi.org/10.1016/S1474-4422(12)70003-0

Fletcher, J. M., Lalor, S. J., Sweeney, C. M., Tubridy, N., & Mills, K. H. G. (2010). T cells in multiple sclerosis and experimental autoimmune encephalomyelitis. In *Clinical and Experimental Immunology* (Vol. 162, Issue 1). https://doi.org/10.1111/j.1365-2249.2010.04143.x

Fogarty, E., Schmitz, S., Tubridy, N., Walsh, C., & Barry, M. (2016). Comparative efficacy of disease-modifying therapies for patients with relapsing remitting multiple sclerosis: Systematic review and network meta-analysis. *Multiple Sclerosis and Related Disorders*, *9*, 23–30. https://doi.org/10.1016/j.msard.2016.06.001

Foote, A. K., & Blakemore, W. F. (2005). Inflammation stimulates remyelination in areas of chronic demyelination. *Brain*, *128*(3), 528–539. https://doi.org/10.1093/brain/awh417

Franklin, R. J. M., & Goldman, S. A. (2015). Glia disease and repair—Remyelination. *Cold Spring Harbor Perspectives in Biology*, *7*(7), 1–28. https://doi.org/10.1101/cshperspect.a020594

Freedman, M. S., Thompson, E. J., Deisenhammer, F., Giovannoni, G., Grimsley, G., Keir, G., Öhman, S., Racke, M. K., Sharief, M., Sindic, C. J. M., Sellebjerg, F., & Tourtellotte, W. W. (2005). Recommended standard of cerebrospinal fluid analysis in the diagnosis of multiple sclerosis: A consensus statement. In *Archives of Neurology* (Vol. 62, Issue 6, pp. 865–870). https://doi.org/10.1001/archneur.62.6.865

Friese, M. A. (2016). Widespread synaptic loss in multiple sclerosis. In *Brain* (Vol. 139, Issue 1, pp. 2–4). https://doi.org/10.1093/brain/awv349

Frischer, J. M., Bramow, S., Dal-Bianco, A., Lucchinetti, C. F., Rauschka, H., Schmidbauer, M., Laursen, H., Sorensen, P. S., & Lassmann, H. (2009). The relation between inflammation and neurodegeneration in multiple sclerosis brains. *Brain*, *132*(5). https://doi.org/10.1093/brain/awp070

Fünfschilling, U., Supplie, L. M., Mahad, D., Boretius, S., Saab, A. S., Edgar, J., Brinkmann, B. G., Kassmann, C. M., Tzvetanova, I. D., Möbius, W., Diaz, F., Meijer, D., Suter, U., Hamprecht, B., Sereda, M. W., Moraes, C. T., Frahm, J., Goebbels, S., & Nave, K. A. (2012). Glycolytic oligodendrocytes maintain myelin and long-term axonal integrity. *Nature*, *485*(7399), 517–521. https://doi.org/10.1038/nature11007

Ganter, P., Prince, C., & Esiri, M. M. (1999). Spinal cord axonal loss in multiple sclerosis: A post-mortem study. *Neuropathology and Applied Neurobiology*, *25*(6), 459–467. https://doi.org/10.1046/j.1365-2990.1999.00205.x

Ge, Y. (2006). Multiple sclerosis: The role of MR imaging. In *American Journal of Neuroradiology* (Vol. 27, Issue 6, pp. 1165–1176).

Genain, C. P., Cannella, B., Hauser, S. L., & Raine, C. S. (1999). Identification of autoantibodies associated with myelin damage in multiple sclerosis. *Nature Medicine*, *5*(2), 170–175. https://doi.org/10.1038/5532

Geng, B., Pan, J., Zhao, T., Ji, J., Zhang, C., Che, Y., Yang, J., Shi, H., Li, J., Zhou, H., Mu, X., Xu, C., Wang, C., Xu, Y., Liu, Z., Wen, H., & You, Q. (2018). Chitinase 3-like 1-CD44 interaction promotes metastasis and epithelial-to-mesenchymal transition through β-catenin/Erk/Akt signaling in gastric cancer. *Journal of Experimental and Clinical Cancer Research*, *37*(1). https://doi.org/10.1186/s13046-018-0876-2

Gensert, J. A. M., & Goldman, J. E. (1997). Endogenous progenitors remyelinate demyelinated axons in the adult CNS. *Neuron*, *19*(1), 197–203. https://doi.org/10.1016/S0896-6273(00)80359-1

Gerber, D., Ghidinelli, M., Tinelli, E., Somandin, C., Gerber, J., Pereira, J. A., Ommer, A., Figlia, G., Miehe, M., Nägeli, L. G., Suter, V., Tadini, V., Sidiropoulos, P. N., Wessig, C., Toyka, K. V., & Suter, U. (2019). Schwann cells, but not Oligodendrocytes, Depend Strictly on Dynamin 2 Function. *ELife*, *8*. https://doi.org/10.7554/eLife.42404

Geurts, J. J. G., & Barkhof, F. (2008). Grey matter pathology in multiple sclerosis. *The Lancet Neurology*, *7*(9), 841–851. https://doi.org/10.1016/S1474-4422(08)70191-1

Giera, S., Luo, R., Ying, Y., Ackerman, S. D., Jeong, S. J., Stoveken, H. M., Folts, C. J., Welsh, C. A., Tall, G. G., Stevens, B., Monk, K. R., & Piao, X. (2018). Microglial transglutaminase-2 drives myelination and myelin repair via GPR56/ADGRG1 in oligodendrocyte precursor cells. *ELife*, *7*. https://doi.org/10.7554/eLife.33385

Gledhill, R. F., Harrison, B. M., & McDonald, W. I. (1973). Demyelination and remyelination after acute spinal cord compression. *Experimental Neurology*, *38*(3), 472–487. https://doi.org/10.1016/0014-4886(73)90169-6

Goldschmidt, T., Antel, J., König, F. B., Brück, W., & Kuhlmann, T. (2009). Remyelination capacity of the MS brain decreases with disease chronicity. *Neurology*, *72*(22), 1914–1921. https://doi.org/10.1212/WNL.0b013e3181a8260a

Grevesse, T., Dabiri, B. E., Parker, K. K., & Gabriele, S. (2015). Opposite rheological properties of neuronal microcompartments predict axonal vulnerability in brain injury. *Scientific Reports*, *5*. https://doi.org/10.1038/srep09475

Group, F.-N. B. W. (2016). BEST (Biomarkers, EndpointS, and other Tools) Resource. In *BEST (Biomarkers, EndpointS, and other Tools) Resource*.

Guldbrandsen, A., Farag, Y., Kroksveen, A. C., Oveland, E., Lereim, R. R., Opsahl, J. A., Myhr, K. M., Berven, F. S., & Barsnes, H. (2017). CSF-PR 2.0: An interactive literature guide to quantitative cerebrospinal fluid mass spectrometry data from neurodegenerative disorders. *Molecular and Cellular Proteomics*, *16*(2), 300–309. https://doi.org/10.1074/mcp.O116.064477

Gutierrez, J., Ballinger, S. W., Darley-Usmar, V. M., & Landar, A. (2006). Free radicals, mitochondria, and oxidized lipids: The emerging role in signal transduction in vascular cells. In *Circulation Research* (Vol. 99, Issue 9, pp. 924–932). https://doi.org/10.1161/01.RES.0000248212.86638.e9

Gveric, D. (2001). Plasminogen activators in multiple sclerosis lesions: Implications for the inflammatory response and axonal damage. *Brain*, *124*(10), 1978–1988. https://doi.org/10.1093/brain/124.10.1978

Hametner, S., Wimmer, I., Haider, L., Pfeifenbring, S., Brück, W., & Lassmann, H. (2013). Iron and neurodegeneration in the multiple sclerosis brain. *Annals of Neurology*, *74*(6), 848–861. https://doi.org/10.1002/ana.23974

Harris, V. K., Donelan, N., Yan, Q. J., Clark, K., Touray, A., Rammal, M., & Sadiq, S. A. (2013). Cerebrospinal fluid fetuin-A is a biomarker of active multiple sclerosis. *Multiple Sclerosis Journal*, *19*(11), 1462–1472. https://doi.org/10.1177/1352458513477923

Hemmer, B., Kerschensteiner, M., & Korn, T. (2015). Role of the innate and adaptive immune responses in the course of multiple sclerosis. In *The Lancet Neurology* (Vol. 14, Issue 4, pp. 406–419). https://doi.org/10.1016/S1474-4422(14)70305-9

Herculano-Houzel, S., Mota, B., & Lent, R. (2006). Cellular scaling rules for rodent brains. *Proc Natl Acad Sci U S A*, *103*(32), 12138–12143. https://doi.org/10.1073/pnas.0604911103

Hinsinger, G., Galéotti, N., Nabholz, N., Urbach, S., Rigau, V., Demattei, C., Lehmann, S., Camu, W., Labauge, P., Castelnovo, G., Brassat, D., Loussouarn, D., Salou, M., Laplaud, D., Casez, O., Bockaert, J., Marin, P., & Thouvenot, E. (2015). Chitinase 3-like proteins as diagnostic and prognostic biomarkers of multiple sclerosis. *Multiple Sclerosis*, *21*(10), 1251–1261. https://doi.org/10.1177/1352458514561906

Hiremath, M. M., Saito, Y., Knapp, G. W., Ting, J. P. Y., Suzuki, K., & Matsushima, G. K. (1998). Microglial/macrophage accumulation during cuprizone-induced demyelination in C57BL/6 mice. *Journal of Neuroimmunology*, *92*(1–2), 38–49. https://doi.org/10.1016/S0165-5728(98)00168-4

Hisahara, S., Okano, H., & Miura, M. (2003). Caspase-mediated oligodendrocyte cell death in the pathogenesis of autoimmune demyelination. *Neuroscience Research*, *46*(4), 387–397. https://doi.org/10.1016/S0168-0102(03)00127-5

Hohlfeld, R., & Wekerle, H. (2004). Autoimmune concepts of multiple sclerosis as a basis for selective immunotherapy: From pipe dreams to (therapeutic) pipelines. *Proceedings of the National Academy of Sciences of the United States of America*, *101*(SUPPL. 2), 14599–14606. https://doi.org/10.1073/pnas.0404874101

Honmou, O., Felts, P. A., Waxman, S. G., & Kocsis, J. D. (1996). Restoration of normal conduction properties in demyelinated spinal cord axons in the adult rat by transplantation of exogenous Schwann cells. *Journal of Neuroscience*, *16*(10), 3199–3208. https://doi.org/10.1523/jneurosci.16-10-03199.1996

Hossain, M. A., Ahmad, M. I., & Karim, M. M. (2008). Bird Flu, the Hanging Pandemic Threat for Human - It's Risk Assessment and Containment. *Bangladesh Journal of Microbiology*, *25*(1), 1–8. https://doi.org/10.3329/bjm.v25i1.4847

Hou, Y., Jia, Y., & Hou, J. (2018). Natural Course of Clinically Isolated Syndrome: A Longitudinal Analysis Using a Markov Model. *Scientific Reports*, *8*(1). https://doi.org/10.1038/s41598-018-29206-y

Howell, O. W., Reeves, C. A., Nicholas, R., Carassiti, D., Radotra, B., Gentleman, S. M., Serafini, B., Aloisi, F., Roncaroli, F., Magliozzi, R., & Reynolds, R. (2011). Meningeal inflammation is widespread and linked to cortical pathology in multiple sclerosis. *Brain*, *134*(9), 2755–2771. https://doi.org/10.1093/brain/awr182

Huebner, E. A., & Strittmatter, S. M. (2009). Axon regeneration in the peripheral and central nervous systems. *Results and Problems in Cell Differentiation*, *48*, 339–351. https://doi.org/10.1007/400_2009_19

Huh, Y., Jung, J. W., Park, C., Ryu, J. R., Shin, C. Y., Kim, W. K., & Ryu, J. H. (2003). Microglial activation and tyrosine hydroxylase immunoreactivity in the substantia nigral region following transient focal ischemia in rats. *Neuroscience Letters*, *349*(1), 63–67. https://doi.org/10.1016/S0304-3940(03)00743-2

Hurst, E. W. (1952). Experimental demyelination in relation to human and animal disease. *The American Journal of Medicine*, *12*(5), 547–560. https://doi.org/10.1016/0002-9343(52)90235-0

Jahn, O., Tenzer, S., Bartsch, N., Patzig, J., & Werner, H. B. (2013). Myelin proteome analysis: Methods and implications for the myelin cytoskeleton. *Neuromethods*, *79*. https://doi.org/10.1007/978-1-62703-266-7_15

Jäkel, S., & Dimou, L. (2017). Glial cells and their function in the adult brain: A journey through the history of their ablation. In *Frontiers in Cellular Neuroscience* (Vol. 11). https://doi.org/10.3389/fncel.2017.00024

Kaisey, M., Solomon, A. J., Luu, M., Giesser, B. S., & Sicotte, N. L. (2019). Incidence of multiple sclerosis misdiagnosis in referrals to two academic centers. *Multiple Sclerosis and Related Disorders*, *30*, 51–56. https://doi.org/10.1016/j.msard.2019.01.048

Kalmbach, B. E., Buchin, A., Long, B., Close, J., Nandi, A., Miller, J. A., Bakken, T. E., Hodge, R. D., Chong, P., de Frates, R., Dai, K., Maltzer, Z., Nicovich, P. R., Keene, C. D., Silbergeld, D. L., Gwinn, R. P., Cobbs, C., Ko, A. L., Ojemann, J. G., … Ting, J. T. (2018). h-Channels Contribute to Divergent Intrinsic Membrane Properties of Supragranular Pyramidal Neurons in Human versus Mouse Cerebral Cortex. *Neuron*, *100*(5), 1194-1208.e5. https://doi.org/10.1016/j.neuron.2018.10.012

Kannarkat, G. T., Boss, J. M., & Tansey, M. G. (2013). The role of innate and adaptive immunity in Parkinson's disease. *Journal of Parkinson's Disease*, *3*(4), 493–514. https://doi.org/10.3233/JPD-130250

Kidd, D., Barkhof, F., McConnell, R., Algra, P. R., Allen, I. V, & Revesz, T. (1999). Cortical lesions in multiple sclerosis. *Brain : A Journal of Neurology*, *122 (Pt 1*, 17–26. https://doi.org/10.1093/brain/122.1.17

Kipp, M., Clarner, T., Dang, J., Copray, S., & Beyer, C. (2009). The cuprizone animal model: New insights into an old story. In *Acta Neuropathologica* (Vol. 118, Issue 6). https://doi.org/10.1007/s00401-009-0591-3

Kıray, H., Lindsay, S. L., Hosseinzadeh, S., & Barnett, S. C. (2016). The multifaceted role of astrocytes in regulating myelination. In *Experimental Neurology* (Vol. 283, pp. 541–549). https://doi.org/10.1016/j.expneurol.2016.03.009

Klaver, R., Popescu, V., Voorn, P., Galis-De Graaf, Y., Van Der Valk, P., De Vries, H. E., Schenk, G. J., & Geurts, J. J. G. (2015). Neuronal and Axonal Loss in Normal-Appearing Gray Matter and Subpial Lesions in Multiple Sclerosis. *Journal of Neuropathology and Experimental Neurology*, *74*(5), 453–458. https://doi.org/10.1097/NEN.0000000000000189

Koch-Henriksen, N., & Sørensen, P. S. (2010). The changing demographic pattern of multiple sclerosis epidemiology. In *The Lancet Neurology* (Vol. 9, Issue 5, pp. 520–532). https://doi.org/10.1016/S1474-4422(10)70064-8

Kokkat, T. J., Patel, M. S., McGarvey, D., Livolsi, V. A., & Baloch, Z. W. (2013). Archived formalin-fixed paraffin-embedded (FFPE) blocks: A valuable underexploited resource for extraction of DNA, RNA, and protein. *Biopreservation and Biobanking*, *11*(2). https://doi.org/10.1089/bio.2012.0052

Kole, A. J., Annis, R. P., & Deshmukh, M. (2013). Mature neurons: equipped for survival. In *Cell death & disease* (Vol. 4). https://doi.org/10.1038/cddis.2013.220

Kornek, B., & Lassmann, H. (1999). Axonal pathology in multiple sclerosis. A historical note. In *Brain Pathology* (Vol. 9, Issue 4, pp. 651–656). https://doi.org/10.1111/j.1750-3639.1999.tb00547.x

Kremer, D., Akkermann, R., Küry, P., & Dutta, R. (2019). Current advancements in promoting remyelination in multiple sclerosis. In *Multiple Sclerosis Journal* (Vol. 25, Issue 1). https://doi.org/10.1177/1352458518800827

Kreutzberg, G. W. (1996). Microglia: A sensor for pathological events in the CNS. In *Trends in Neurosciences* (Vol. 19, Issue 8, pp. 312–318). https://doi.org/10.1016/0166-2236(96)10049-7

Küçükali, C. İ., Kürtüncü, M., Çoban, A., Çebi, M., & Tüzün, E. (2015). Epigenetics of Multiple Sclerosis: An Updated Review. In *NeuroMolecular Medicine* (Vol. 17, Issue 2, pp. 83–96). https://doi.org/10.1007/s12017-014-8298-6

Kuerten, S., & Lehmann, P. V. (2011). The immune pathogenesis of experimental autoimmune encephalomyelitis: Lessons learned for multiple sclerosis? In *Journal of Interferon and Cytokine Research* (Vol. 31, Issue 12, pp. 907–916). https://doi.org/10.1089/jir.2011.0072

Kuhlmann, T., Ludwin, S., Prat, A., Antel, J., Brück, W., & Lassmann, H. (2017). An updated histological classification system for multiple sclerosis lesions. *Acta Neuropathologica*, *133*(1), 13–24. https://doi.org/10.1007/s00401-016-1653-y

Lassmann, H., Bartsch, U., Montag, D., & Schachner, M. (1997). Dying-back oligodendrogliopathy: A late sequel of myelin-associated glycoprotein deficiency. *GLIA*, *19*(2). https://doi.org/10.1002/(SICI)1098-1136(199702)19:2<104::AID-GLIA2>3.0.CO;2-0

Lassmann, H., & Bradl, M. (2017). Multiple sclerosis: experimental models and reality. In *Acta Neuropathologica* (Vol. 133, Issue 2, pp. 223–244). https://doi.org/10.1007/s00401-016-1631-4

Lassmann, H., Brück, W., & Lucchinetti, C. F. (2007). The immunopathology of multiple sclerosis: An overview. *Brain Pathology*, *17*(2), 210–218. https://doi.org/10.1111/j.1750-3639.2007.00064.x

Lassmann, H., Raine, C. S., Antel, J., & Prineas, J. W. (1998). Immunopathology of multiple sclerosis: Report on an international meeting held at the Institute of Neurology of the University of Vienna. *Journal of Neuroimmunology*, *86*(2), 213–217. https://doi.org/10.1016/S0165-5728(98)00031-9

Lavrik, I., Golks, A., & Krammer, P. H. (2005). Death receptor signaling. *Journal of Cell Science*, *118*(2), 265–267. https://doi.org/10.1242/jcs.01610

Lécuyer, M. A., Saint-Laurent, O., Bourbonnière, L., Larouche, S., Larochelle, C., Michel, L., Charabati, M., Abadier, M., Zandee, S., Jahromi, N. H., Gowing, E., Pittet, C., Lyck, R., Engelhardt, B., & Prat, A. (2017). Dual role of ALCAM in neuroinflammation and blood-brain barrier homeostasis. *Proceedings of the National Academy of Sciences of the United States of America*, *114*(4), E524–E533. https://doi.org/10.1073/pnas.1614336114

Lee, C. G., Da Silva, C. A., Dela Cruz, C. S., Ahangari, F., Ma, B., Kang, M.-J., He, C.-H., Takyar, S., & Elias, J. A. (2011). Role of Chitin and Chitinase/Chitinase-Like Proteins in Inflammation, Tissue Remodeling, and Injury. *Annual Review of Physiology*, *73*(1), 479–501. https://doi.org/10.1146/annurev-physiol-012110-142250

Leray, E., Moreau, T., Fromont, A., & Edan, G. (2016). Epidemiology of multiple sclerosis. *Revue Neurologique*, *172*(1), 3–13. https://doi.org/10.1016/j.neurol.2015.10.006

Lin, W., & Popko, B. (2009). Endoplasmic reticulum stress in disorders of myelinating cells. In *Nature Neuroscience* (Vol. 12, Issue 4). https://doi.org/10.1038/nn.2273

Liu, J. J., Diaz, D. E., Quist, D. A., & Karlin, K. D. (2016). Copper(I)-Dioxygen Adducts and Copper Enzyme Mechanisms. In *Israel Journal of Chemistry* (Vol. 56, Issues 9–10, pp. 738–755). https://doi.org/10.1002/ijch.201600025

Lobo, V., Patil, A., Phatak, A., & Chandra, N. (2010). Free radicals, antioxidants and functional foods: Impact on human health. In *Pharmacognosy Reviews* (Vol. 4, Issue 8, pp. 118–126). https://doi.org/10.4103/0973-7847.70902

Lovas, G., Szilágyi, N., Majtényi, K., Palkovits, M., & Komoly, S. (2000). Axonal changes in chronic demyelinated cervical spinal cord plaques. *Brain*, *123*(2), 308–317. https://doi.org/10.1093/brain/123.2.308

Lublin, F. (2005). History of modern multiple sclerosis therapy. *Journal of Neurology*, *252*(SUPPL. 3). https://doi.org/10.1007/s00415-005-2010-6

Lublin, F. D., & Reingold, S. C. (1996). Defining the clinical course of multiple sclerosis: Results of an international survey. In *Neurology* (Vol. 46, Issue 4, pp. 907–911). https://doi.org/10.1212/WNL.46.4.907

Lublin, F. D., Reingold, S. C., Cohen, J. A., Cutter, G. R., Sørensen, P. S., Thompson, A. J., Wolinsky, J. S., Balcer, L. J., Banwell, B., Barkhof, F., Bebo, B., Calabresi, P. A., Clanet, M., Comi, G., Fox, R. J., Freedman, M. S., Goodman, A. D., Inglese, M., Kappos, L., … Polman, C. H. (2014). Defining the clinical course of multiple sclerosis: The 2013 revisions. In *Neurology* (Vol. 83, Issue 3, pp. 278–286). https://doi.org/10.1212/WNL.0000000000000560

Lucchinetti, C., Brück, W., Parisi, J., Scheithauer, B., Rodriguez, M., & Lassmann, H. (2000). Heterogeneity of multiple sclerosis lesions: Implications for the pathogenesis of demyelination. *Annals of Neurology*, *47*(6), 707–717. https://doi.org/10.1002/1531-8249(200006)47:6<707::AID-ANA3>3.0.CO;2-Q

Lucchinetti, C. F., Popescu, B. F. G., Bunyan, R. F., Moll, N. M., Roemer, S. F., Lassmann, H., Brück, W., Parisi, J. E., Scheithauer, B. W., Giannini, C., Weigand, S. D., Mandrekar, J., & Ransohoff, R. M. (2011). Inflammatory Cortical Demyelination in Early Multiple Sclerosis. *New England Journal of Medicine*, *365*(23). https://doi.org/10.1056/nejmoa1100648

Luchetti, S., Fransen, N. L., van Eden, C. G., Ramaglia, V., Mason, M., & Huitinga, I. (2018). Progressive multiple sclerosis patients show substantial lesion activity that correlates with clinical disease severity and sex: a retrospective autopsy cohort analysis. *Acta Neuropathologica*, *135*(4), 511–528. https://doi.org/10.1007/s00401-018-1818-y

Ludwin, S. K. (1988). Remyelination in the central nervous system and the peripheral nervous system. *Advances in Neurology*, *47*, 215–254.

Luo, C., Jian, C., Liao, Y., Huang, Q., Wu, Y., Liu, X., Zou, D., & Wu, Y. (2017). The role of microglia in multiple sclerosis. In *Neuropsychiatric Disease and Treatment* (Vol. 13, pp. 1661–1667). https://doi.org/10.2147/NDT.S140634

Ma, Z., Cao, Q., Zhang, L., Hu, J., Howard, R. M., Lu, P., Whittemore, S. R., & Xu, X. M. (2009). Oligodendrocyte precursor cells differentially expressing Nogo-A but not MAG are more permissive to neurite outgrowth than mature oligodendrocytes. *Experimental Neurology*, *217*(1), 184–196. https://doi.org/10.1016/j.expneurol.2009.02.006

MacLean, B., Tomazela, D. M., Shulman, N., Chambers, M., Finney, G. L., Frewen, B., Kern, R., Tabb, D. L., Liebler, D. C., & MacCoss, M. J. (2010). Skyline: An open source document editor for creating and analyzing targeted proteomics experiments. *Bioinformatics*, *26*(7). https://doi.org/10.1093/bioinformatics/btq054

Magyari, M. (2016). Gender differences in multiple sclerosis epidemiology and treatment response. *Danish Medical Journal*, *63*(3).

Malpass, K. (2012). Disease mechanisms in MS: Cell adhesion molecule MCAM on pathogenic T cells-a green light for CNS entry in multiple sclerosis. In *Nature Reviews Neurology* (Vol. 8, Issue 11, p. 592). https://doi.org/10.1038/nrneurol.2012.204

Maranzano, J., Rudko, D. A., Nakamura, K., Cook, S., Cadavid, Di., Wolansky, L., Arnold, D. L., & Narayanan, S. (2017). MRI evidence of acute inflammation in leukocortical lesions of patients with early multiple sclerosis. *Neurology*, *89*(7), 714–721. https://doi.org/10.1212/WNL.0000000000004227

Matthews, P. M., Roncaroli, F., Waldman, A., Sormani, M. P., De Stefano, N., Giovannoni, G., & Reynolds, R. (2016). A practical review of the neuropathology and neuroimaging of multiple sclerosis. In *Practical Neurology* (Vol. 16, Issue 4, pp. 279–287). https://doi.org/10.1136/practneurol-2016-001381

McDonald, W. I., Compston, A., Edan, G., Goodkin, D., Hartung, H. P., Lublin, F. D., McFarland, H. F., Paty, D. W., Polman, C. H., Reingold, S. C., Sandberg-Wollheim, M., Sibley, W., Thompson, A., Van Den Noort, S., Weinshenker, B. Y., & Wolinsky, J. S. (2001). Recommended diagnostic criteria for multiple sclerosis: Guidelines from the International Panel on the Diagnosis of Multiple Sclerosis. *Annals of Neurology*, *50*(1), 121–127. https://doi.org/10.1002/ana.1032

Megger, D. A., Pott, L. L., Ahrens, M., Padden, J., Bracht, T., Kuhlmann, K., Eisenacher, M., Meyer, H. E., & Sitek, B. (2014). Comparison of label-free and label-based strategies for proteome analysis of hepatoma cell lines. *Biochimica et Biophysica Acta - Proteins and Proteomics*, *1844*(5). https://doi.org/10.1016/j.bbapap.2013.07.017

Melby, J. A., Roberts, D. S., Larson, E. J., Brown, K. A., Bayne, E. F., Jin, S., & Ge, Y. (2021). Novel Strategies to Address the Challenges in Top-Down Proteomics. In *Journal of the American Society for Mass Spectrometry* (Vol. 32, Issue 6). https://doi.org/10.1021/jasms.1c00099

Miller, D. H., Chard, D. T., & Ciccarelli, O. (2012). Clinically isolated syndromes. In *The Lancet Neurology* (Vol. 11, Issue 2, pp. 157–169). https://doi.org/10.1016/S1474-4422(11)70274-5

Miller, J. A., Horvath, S., & Geschwind, D. H. (2010). Divergence of human and mouse brain transcriptome highlights Alzheimer disease pathways. *Proceedings of the National Academy of Sciences of the United States of America*, *107*(28). https://doi.org/10.1073/pnas.0914257107

Minagar, A., & Alexander, J. S. (2003). Blood-brain barrier disruption in multiple sclerosis. In *Multiple Sclerosis* (Vol. 9, Issue 6, pp. 540–549). https://doi.org/10.1191/1352458503ms965oa

Miron, V. E., Boyd, A., Zhao, J. W., Yuen, T. J., Ruckh, J. M., Shadrach, J. L., Van Wijngaarden, P., Wagers, A. J., Williams, A., Franklin, R. J. M., & Ffrench-Constant, C. (2013). M2 microglia and macrophages drive oligodendrocyte differentiation during CNS remyelination. *Nature Neuroscience*, *16*(9), 1211–1218. https://doi.org/10.1038/nn.3469

Miron, V. E., Kuhlmann, T., & Antel Jack P., J. P. (2011). Cells of the oligodendroglial lineage, myelination, and remyelination. In *Biochimica et Biophysica Acta - Molecular Basis of Disease* (Vol. 1812, Issue 2, pp. 184–193). https://doi.org/10.1016/j.bbadis.2010.09.010

Mirshafiey, A., Asghari, B., Ghalamfarsa, G., Jadidi-Niaragh, F., & Azizi, G. (2014). The significance of matrix metalloproteinases in the immunopathogenesis and treatment of multiple sclerosis. In *Sultan Qaboos University Medical Journal* (Vol. 14, Issue 1). https://doi.org/10.12816/0003332

Morrison, B. M., Lee, Y., & Rothstein, J. D. (2013). Oligodendroglia: Metabolic supporters of axons. In *Trends in Cell Biology* (Vol. 23, Issue 12, pp. 644–651). https://doi.org/10.1016/j.tcb.2013.07.007

Muntel, J., Kirkpatrick, J., Bruderer, R., Huang, T., Vitek, O., Ori, A., & Reiter, L. (2019). Comparison of Protein Quantification in a Complex Background by DIA and TMT Workflows with Fixed Instrument Time. *Journal of Proteome Research*, *18*(3). https://doi.org/10.1021/acs.jproteome.8b00898

Muralidharan, S., & Mandrekar, P. (2013). Cellular stress response and innate immune signaling: integrating pathways in host defense and inflammation. *Journal of Leukocyte Biology*, *94*(6), 1167–1184. https://doi.org/10.1189/jlb.0313153

Mycko, M. P., Kwinkowski, M., Tronczynska, E., Szymanska, B., & Selmaj, K. W. (1998). Multiple sclerosis: The increased frequency of the ICAM-1 exon 6 gene point mutation genetic type K469. *Annals of Neurology*, *44*(1), 70–75. https://doi.org/10.1002/ana.410440113

Nakashima, I., Fujihara, K., Okita, N., Takase, S., & Itoyama, Y. (1999). Clinical and MRI study of brain stem and cerebellar involvement in Japanese patients with multiple sclerosis. *Journal of Neurology Neurosurgery and Psychiatry*, *67*(2), 153–157. https://doi.org/10.1136/jnnp.67.2.153

Narushima, I., Kita, T., Kubo, K., Yonetani, Y., Momochi, C., Yoshikawa, I., Shimada, K., & Nakashima, T. (1999). Contribution of endothelin-1 to disruption of blood-

brain barrier permeability in dogs. *Naunyn-Schmiedeberg's Archives of Pharmacology*, *360*(6), 639–645. https://doi.org/10.1007/s002109900137

Nathan, A. J., & Scobell, A. (2012). How China sees America. In *Foreign Affairs* (Vol. 91, Issue 5). https://doi.org/10.1017/CBO9781107415324.004

Nilsson, C., Stahlberg, F., Thomsen, C., Henriksen, O., Herning, M., & Owman, C. (1992). Circadian variation in human cerebrospinal fluid production measured by magnetic resonance imaging. *American Journal of Physiology - Regulatory Integrative and Comparative Physiology*, *262*(1 31-1). https://doi.org/10.1152/ajpregu.1992.262.1.r20

Noseworthy, J. H., Lucchinetti, C., Rodriguez, M., & Weinshenker, B. G. (2000). Multiple sclerosis. *The New England Journal of Medicine*, *343*(13), 938–952. https://doi.org/10.1056/NEJM200009283431307

O'Gorman, C., Lucas, R., & Taylor, B. (2012). Environmental risk factors for multiple sclerosis: A review with a focus on molecular mechanisms. In *International Journal of Molecular Sciences* (Vol. 13, Issue 9, pp. 11718–11752). https://doi.org/10.3390/ijms130911718

Omura, S., Kawai, E., Sato, F., Martinez, N. E., Minagar, A., Al-Kofahi, M., Yun, J. W., Cvek, U., Trutschl, M., Alexander, J. S., & Tsunoda, I. (2018). Theiler's Virus-Mediated Immunopathology in the CNS and Heart: Roles of Organ-Specific Cytokine and Lymphatic Responses. *Frontiers in Immunology*, *9*. https://doi.org/10.3389/fimmu.2018.02870

Ong, S. E., & Mann, M. (2005). Mass Spectrometry–Based Proteomics Turns Quantitative. *Nature Chemical Biology*, *1*(5), 252–262. https://doi.org/10.1038/nchembio736

Orthmann-Murphy, J. L., Abrams, C. K., & Scherer, S. S. (2008). Gap junctions couple astrocytes and oligodendrocytes. In *Journal of Molecular Neuroscience* (Vol. 35, Issue 1, pp. 101–116). https://doi.org/10.1007/s12031-007-9027-5

Ortiz, G. G., Pacheco-Moisés, F. P., Macías-Islas, M. Á., Flores-Alvarado, L. J., Mireles-Ramírez, M. A., González-Renovato, E. D., Hernández-Navarro, V. E., Sánchez-López, A. L., & Alatorre-Jiménez, M. A. (2014). Role of the Blood-Brain Barrier in Multiple Sclerosis. In *Archives of Medical Research* (Vol. 45, Issue 8, pp. 687–697). https://doi.org/10.1016/j.arcmed.2014.11.013

Oveland, E., Ahmad, I., Lereim, R. R., Kroksveen, A. C., Barsnes, H., Guldbrandsen, A., Myhr, K. M., Bø, L., Berven, F. S., & Wergeland, S. (2021). Cuprizone and EAE mouse frontal cortex proteomics revealed proteins altered in multiple sclerosis. *Scientific Reports*, *11*(1). https://doi.org/10.1038/s41598-021-86191-5

Owens, G. P., Gilden, D., Burgoon, M. P., Yu, X., & Bennett, J. L. (2011). Viruses and multiple sclerosis. *Neuroscientist*, *17*(6), 659–676. https://doi.org/10.1177/1073858410386615

Palle, P., Monaghan, K. L., Milne, S. M., & Wan, E. C. K. (2017). Cytokine Signaling in Multiple Sclerosis and Its Therapeutic Applications. *Medical Sciences*, *5*(4), 23. https://doi.org/10.3390/medsci5040023

Patrikios, P., Stadelmann, C., Kutzelnigg, A., Rauschka, H., Schmidbauer, M., Laursen, H., Sorensen, P. S., Brück, W., Lucchinetti, C., & Lassmann, H. (2006). Remyelination is extensive in a subset of multiple sclerosis patients. *Brain*, *129*(12), 3165–3172. https://doi.org/10.1093/brain/awl217

Patron, M., Sprenger, H. G., & Langer, T. (2018). M-AAA proteases, mitochondrial calcium homeostasis and neurodegeneration. In *Cell Research* (Vol. 28, Issue 3, pp. 296–306). https://doi.org/10.1038/cr.2018.17

Peterson, J. W., Bö, L., Mörk, S., Chang, A., & Trapp, B. D. (2001a). Transected neurites, apoptotic neurons, and reduced inflammation in cortical multiple sclerosis lesions. *Annals of Neurology*. https://doi.org/10.1002/ana.1123

Peterson, J. W., Bö, L., Mörk, S., Chang, A., & Trapp, B. D. (2001b). Transected neurites, apoptotic neurons, and reduced inflammation in cortical multiple sclerosis lesions. *Annals of Neurology*, *50*(3). https://doi.org/10.1002/ana.1123

Pfeifenbring, S., Nessler, S., Wegner, C., Stadelmann, C., & Brück, W. (2015). Remyelination After Cuprizone-Induced Demyelination Is Accelerated in Juvenile Mice. *Journal of Neuropathology and Experimental Neurology*, *74*(8), 756–766. https://doi.org/10.1097/NEN.0000000000000214

Pierson, E., Simmons, S. B., Castelli, L., & Goverman, J. M. (2012). Mechanisms regulating regional localization of inflammation during CNS autoimmunity. *Immunological Reviews*, *248*(1), 205–215. https://doi.org/10.1111/j.1600-065X.2012.01126.x

Pirko, I., Lucchinetti, C. F., Sriram, S., & Bakshi, R. (2007). Gray matter involvement in multiple sclerosis. In *Neurology* (Vol. 68, Issue 9, pp. 634–642). https://doi.org/10.1212/01.wnl.0000250267.85698.7a

Plantone, D., De Angelis, F., Doshi, A., & Chataway, J. (2016). Secondary Progressive Multiple Sclerosis: Definition and Measurement. In *CNS Drugs* (Vol. 30, Issue 6, pp. 517–526). https://doi.org/10.1007/s40263-016-0340-9

Podbielska, M., Banik, N. L., Kurowska, E., & Hogan, E. L. (2013). Myelin recovery in multiple sclerosis: The challenge of remyelination. In *Brain Sciences* (Vol. 3, Issue 3, pp. 1282–1324). https://doi.org/10.3390/brainsci3031282

Polman, C. H., Reingold, S. C., Banwell, B., Clanet, M., Cohen, J. A., Filippi, M., Fujihara, K., Havrdova, E., Hutchinson, M., Kappos, L., Lublin, F. D., Montalban, X., O'Connor, P., Sandberg-Wollheim, M., Thompson, A. J., Waubant, E., Weinshenker, B., & Wolinsky, J. S. (2011). Diagnostic criteria for multiple sclerosis: 2010 Revisions to the McDonald criteria. *Annals of Neurology*, *69*(2), 292–302. https://doi.org/10.1002/ana.22366

Ponath, G., Park, C., & Pitt, D. (2018a). The role of astrocytes in multiple sclerosis. In *Frontiers in Immunology* (Vol. 9, Issue FEB). https://doi.org/10.3389/fimmu.2018.00217

Ponath, G., Park, C., & Pitt, D. (2018b). The role of astrocytes in multiple sclerosis. In *Frontiers in Immunology*. https://doi.org/10.3389/fimmu.2018.00217

Popescu, B. F. G., Pirko, I., & Lucchinetti, C. F. (2013). Pathology of multiple sclerosis: Where do we stand? In *CONTINUUM Lifelong Learning in Neurology* (Vol. 19, Issue 4, pp. 901–921). https://doi.org/10.1212/01.CON.0000433291.23091.65

Popovich, P.G., Jakeman, L.B. and McTigue, D.M. (2009). Glial Responses to Injury. pp.853–859. https://doi.org/10.1016/b978-008045046-9.00018-8.

Praet, J., Guglielmetti, C., Berneman, Z., Van der Linden, A., & Ponsaerts, P. (2014). Cellular and molecular neuropathology of the cuprizone mouse model: Clinical relevance for multiple sclerosis. In *Neuroscience and Biobehavioral Reviews* (Vol. 47, pp. 485–505). https://doi.org/10.1016/j.neubiorev.2014.10.004

Pranzatelli, M. R., Tate, E. D., & McGee, N. R. (2017). Microglial/macrophage markers CHI3L1, sCD14, and sCD163 in CSF and serum of pediatric inflammatory and non-inflammatory neurological disorders: A case-control study and reference ranges. *Journal of the Neurological Sciences*, *381*, 285–290. https://doi.org/10.1016/j.jns.2017.09.006

Prineas, J. W., & Parratt, J. D. E. (2012). Oligodendrocytes and the early multiple sclerosis lesion. In *Annals of Neurology* (Vol. 72, Issue 1, pp. 18–31). https://doi.org/10.1002/ana.23634

Prinz, M., Priller, J., Sisodia, S. S., & Ransohoff, R. M. (2011). Heterogeneity of CNS myeloid cells and their roles in neurodegeneration. In *Nature Neuroscience* (Vol. 14, Issue 10, pp. 1227–1235). https://doi.org/10.1038/nn.2923

Procaccini, C., De Rosa, V., Pucino, V., Formisano, L., & Matarese, G. (2015). Animal models of Multiple Sclerosis. In *European Journal of Pharmacology* (Vol. 759). https://doi.org/10.1016/j.ejphar.2015.03.042

Raine, C. S. (1984). Morphology of Myelin and Myelination. In *Myelin* (pp. 1–50). https://doi.org/10.1007/978-1-4757-1830-0_1

Ramaglia, V., Sheikh-Mohamed, S., Legg, K., Park, C., Rojas, O. L., Zandee, S., Fu, F., Ornatsky, O., Swanson, E. C., Pitt, D., Prat, A., McKee, T. D., & Gommerman, J. L. (2019). Multiplexed imaging of immune cells in staged multiple sclerosis lesions by mass cytometry. *ELife*, *8*. https://doi.org/10.7554/eLife.48051

Ramagopalan, S. V., Dobson, R., Meier, U. C., & Giovannoni, G. (2010). Multiple sclerosis: risk factors, prodromes, and potential causal pathways. In *The Lancet Neurology* (Vol. 9, Issue 7, pp. 727–739). https://doi.org/10.1016/S1474-4422(10)70094-6

Reich, D. S., Lucchinetti, C. F., & Calabresi, P. A. (2018). Multiple Sclerosis. *The New England Journal of Medicine*, *378*(2), 169–180. https://doi.org/10.1056/NEJMra1401483

Rifai, N., Gillette, M. A., & Carr, S. A. (2006). Protein biomarker discovery and validation: The long and uncertain path to clinical utility. In *Nature Biotechnology* (Vol. 24, Issue 8). https://doi.org/10.1038/nbt1235

Rolak, L. A. (2003). Multiple sclerosis: it's not the disease you thought it was. In *Clinical medicine & research* (Vol. 1, Issue 1, pp. 57–60). https://doi.org/10.3121/cmr.1.1.57

Rommer, P. S., Milo, R., Han, M. H., Satyanarayan, S., Sellner, J., Hauer, L., Illes, Z., Warnke, C., Laurent, S., Weber, M. S., Zhang, Y., & Stuve, O. (2019). Immunological aspects of approved MS therapeutics. In *Frontiers in Immunology* (Vol. 10, Issue JULY). https://doi.org/10.3389/fimmu.2019.01564

Rose, J., Brian, C., Woods, J., Pappa, A., Panayiotidis, M. I., Powers, R., & Franco, R. (2017). Mitochondrial dysfunction in glial cells: Implications for neuronal homeostasis and survival. *Toxicology*, *391*, 109–115. https://doi.org/10.1016/j.tox.2017.06.011

Rosenberg, G. A. (2012). Neurological diseases in relation to the blood-brain barrier. In *Journal of Cerebral Blood Flow and Metabolism* (Vol. 32, Issue 7, pp. 1139–1151). https://doi.org/10.1038/jcbfm.2011.197

Rudick, R. A., Lee, J. C., Nakamura, K., & Fisher, E. (2009). Gray matter atrophy correlates with MS disability progression measured with MSFC but not EDSS. *Journal of the Neurological Sciences*, *282*(1–2), 106–111. https://doi.org/10.1016/j.jns.2008.11.018

Salmond, G. P. C., & Fineran, P. C. (2015). A century of the phage: Past, present and future. In *Nature Reviews Microbiology* (Vol. 13, Issue 12, pp. 777–786). https://doi.org/10.1038/nrmicro3564

Sandi, D., Fricska-Nagy, Z., Bencsik, K., & Vécsei, L. (2021). Neurodegeneration in multiple sclerosis: Symptoms of silent progression, biomarkers and neuroprotective therapy—kynurenines are important players. In *Molecules* (Vol. 26, Issue 11). https://doi.org/10.3390/molecules26113423

Scarisbrick, I. A., Yoon, H., Panos, M., Larson, N., Blaber, S. I., Blaber, M., & Rodriguez, M. (2012). Kallikrein 6 regulates early CNS demyelination in a viral model of multiple sclerosis. *Brain Pathology*, *22*(5), 709–722. https://doi.org/10.1111/j.1750-3639.2012.00577.x

Sen, M. K., Almuslehi, M. S. M., Shortland, P. J., Mahns, D. A., & Coorssen, J. R. (2021). Proteomics of multiple sclerosis: Inherent issues in defining the pathoetiology and identifying (early) biomarkers. In *International Journal of Molecular Sciences* (Vol. 22, Issue 14). https://doi.org/10.3390/ijms22147377

Siegert, E., Paul, F., Rothe, M., & Weylandt, K. H. (2017). The effect of omega-3 fatty acids on central nervous system remyelination in fat-1 mice. *BMC Neuroscience*, *18*(1). https://doi.org/10.1186/s12868-016-0312-5

Simons, M., & Nave, K. A. (2016). Oligodendrocytes: Myelination and axonal support. In *Cold Spring Harbor Perspectives in Biology* (Vol. 8, Issue 1). https://doi.org/10.1101/cshperspect.a020479

Singh, S., Dallenga, T., Winkler, A., Roemer, S., Maruschak, B., Siebert, H., Brück, W., & Stadelmann, C. (2017). Relationship of acute axonal damage, Wallerian

degeneration, and clinical disability in multiple sclerosis. *Journal of Neuroinflammation*, *14*(1). https://doi.org/10.1186/s12974-017-0831-8

Siva, A. (2013). Asymptomatic MS. *Clinical Neurology and Neurosurgery*, *115*(SUPPL.1), S1. https://doi.org/10.1016/j.clineuro.2013.09.012

Sobel, R. A., Chen, M., Maeda, A., & Hinojoza, J. R. (1995). Vitronectin and integrin vitronectin receptor localization in multiple sclerosis lesions. *Journal of Neuropathology and Experimental Neurology*, *54*(2), 202–213. https://doi.org/10.1097/00005072-199503000-00007

Soldan, S. S., & Lieberman, P. M. (2022). Epstein–Barr virus and multiple sclerosis. *Nature Reviews Microbiology*. https://doi.org/10.1038/s41579-022-00770-5

Sospedra, M., & Martin, R. (2016). Immunology of Multiple Sclerosis. *Seminars in Neurology*, *36*(2), 115–127. https://doi.org/10.1055/s-0036-1579739

Stadelmann, C., & Brück, W. (2004). Lessons from the neuropathology of atypical forms of multiple sclerosis. *Neurological Sciences*, *25*(SUPPL. 4). https://doi.org/10.1007/s10072-004-0333-1

Stan, A. D., Ghose, S., Gao, X. M., Roberts, R. C., Lewis-Amezcua, K., Hatanpaa, K. J., & Tamminga, C. A. (2006). Human postmortem tissue: What quality markers matter? *Brain Research*, *1123*(1). https://doi.org/10.1016/j.brainres.2006.09.025

Stangel, M., Kuhlmann, T., Matthews, P. M., & Kilpatrick, T. J. (2017). Achievements and obstacles of remyelinating therapies in multiple sclerosis. In *Nature Reviews Neurology* (Vol. 13, Issue 12, pp. 742–754). https://doi.org/10.1038/nrneurol.2017.139

Steen, H., & Mann, M. (2004). The ABC's (and XYZ's) of peptide sequencing. In *Nature Reviews Molecular Cell Biology* (Vol. 5, Issue 9, pp. 699–711). https://doi.org/10.1038/nrm1468

Stiefel, K. M., Torben-Nielsen, B., & Coggan, J. S. (2013). Proposed evolutionary changes in the role of myelin. *Frontiers in Neuroscience*, *7 NOV*. https://doi.org/10.3389/fnins.2013.00202

Streit, W. J., Walter, S. A., & Pennell, N. A. (1999). Reactive microgliosis. In *Progress in Neurobiology* (Vol. 57, Issue 6, pp. 563–581). https://doi.org/10.1016/S0301-0082(98)00069-0

Strijbis, E. M. M., Kooi, E. J., van der Valk, P., & Geurts, J. J. G. (2017). Cortical remyelination is heterogeneous in multiple sclerosis. *Journal of Neuropathology and Experimental Neurology*, *76*(5), 390–401. https://doi.org/10.1093/jnen/nlx023

Suzuki, K. (1969). Giant hepatic mitochondria: Production in mice fed with cuprizone. *Science*, *163*(3862), 81–82. https://doi.org/10.1126/science.163.3862.81

Szczuciński, A., & Losy, J. (2007). Chemokines and chemokine receptors in multiple sclerosis. Potential targets for new therapies. In *Acta Neurologica Scandinavica* (Vol. 115, Issue 3, pp. 137–146). https://doi.org/10.1111/j.1600-0404.2006.00749.x

Tallantyre, E. C., Bø, L., Al-Rawashdeh, O., Owens, T., Polman, C. H., Lowe, J., & Evangelou, N. (2009). Greater loss of axons in primary progressive multiple sclerosis plaques compared to secondary progressive disease. *Brain*, *132*(5), 1190–1199. https://doi.org/10.1093/brain/awp106

Taraboletti, A., Walker, T., Avila, R., Huang, H., Caporoso, J., Manandhar, E., Leeper, T. C., Modarelli, D. A., Medicetty, S., & Shriver, L. P. (2017). Cuprizone Intoxication Induces Cell Intrinsic Alterations in Oligodendrocyte Metabolism Independent of

Copper Chelation. *Biochemistry*, *56*(10). https://doi.org/10.1021/acs.biochem.6b01072

Teunissen, C. E., Malekzadeh, A., Leurs, C., Bridel, C., & Killestein, J. (2015). Body fluid biomarkers for multiple sclerosis - The long road to clinical application. In *Nature Reviews Neurology* (Vol. 11, Issue 10, pp. 585–596). https://doi.org/10.1038/nrneurol.2015.173

Tintoré, M., & Arrambide, G. (2009). Early onset multiple sclerosis: The role of gender. *Journal of the Neurological Sciences*, *286*(1–2), 31–34. https://doi.org/10.1016/j.jns.2009.07.016

Tomassy, G. S., Berger, D. R., Chen, H. H., Kasthuri, N., Hayworth, K. J., Vercelli, A., Seung, H. S., Lichtman, J. W., & Arlotta, P. (2014). Distinct profiles of myelin distribution along single axons of pyramidal neurons in the neocortex. In *Science* (Vol. 344, Issue 6181, pp. 319–324). https://doi.org/10.1126/science.1249766

Torkildsen, Ø., Wergeland, S., Bakke, S., Beiske, A. G., Bjerve, K. S., Hovdal, H., Midgard, R., Lilleås, F., Pedersen, T., Bjørnarå, B., Dalene, F., Kleveland, G., Schepel, J., Olsen, I. C., & Myhr, K. M. (2012). ω-3 fatty acid treatment in multiple sclerosis (OFAMS study): A randomized, double-blind, placebo-controlled trial. *Archives of Neurology*, *69*(8), 1044–1051. https://doi.org/10.1001/archneurol.2012.283

Traboulsee, A. L., & Li, D. K. B. (2006). The role of MRI in the diagnosis of multiple sclerosis. *Advances in Neurology*, *98*, 125–146.

Trapp, B. D., & Nave, K.-A. (2008). Multiple sclerosis: an immune or neurodegenerative disorder? *Annual Review of Neuroscience*, *31*, 247–269. https://doi.org/10.1146/annurev.neuro.30.051606.094313

Trapp, B. D., Peterson, J., Ransohoff, R. M., Rudick, R., Mörk, S., & Bö, L. (1998). Axonal transection in the lesions of multiple sclerosis. *New England Journal of Medicine*, *338*(5), 278–285. https://doi.org/10.1056/NEJM199801293380502

Trapp, B. D., Vignos, M., Dudman, J., Chang, A., Fisher, E., Staugaitis, S. M., Battapady, H., Mork, S., Ontaneda, D., Jones, S. E., Fox, R. J., Chen, J., Nakamura, K., & Rudick, R. A. (2018). Cortical neuronal densities and cerebral white matter demyelination in multiple sclerosis: a retrospective study. *The Lancet Neurology*, *17*(10), 870–884. https://doi.org/10.1016/S1474-4422(18)30245-X

Tsunoda, I., & Fujinami, R. S. (2002). Inside-out versus outside-in models for virus induced demyelination: Axonal damage triggering demyelination. In *Springer Seminars in Immunopathology* (Vol. 24, Issue 2, pp. 105–125). https://doi.org/10.1007/s00281-002-0105-z

Tsunoda, I., & Fujinami, R. S. (2010). Neuropathogenesis of theiler's murine encephalomyelitis virus infection, an animal model for multiple sclerosis. In *Journal of Neuroimmune Pharmacology* (Vol. 5, Issue 3, pp. 355–369). https://doi.org/10.1007/s11481-009-9179-x

Van Der Goes, A., Boorsma, W., Hoekstra, K., Montagne, L., De Groot, C. J. A., & Dijkstra, C. D. (2005). Determination of the sequential degradation of myelin proteins by macrophages. *Journal of Neuroimmunology*, *161*(1–2), 12–20. https://doi.org/10.1016/j.jneuroim.2004.12.010

Van Der Valk, P., & Amor, S. (2009). Preactive lesions in multiple sclerosis. In *Current Opinion in Neurology* (Vol. 22, Issue 3, pp. 207–213). https://doi.org/10.1097/WCO.0b013e32832b4c76

Van Der Valk, P., & De Groot, C. J. A. (2000). Staging of multiple sclerosis (MS) lesions: Pathology of the time frame of MS. In *Neuropathology and Applied Neurobiology* (Vol. 26, Issue 1, pp. 2–10). https://doi.org/10.1046/j.1365-2990.2000.00217.x

Van Horssen, J., Brink, B. P., De Vries, H. E., Van Der Valk, P., & Bø, L. (2007). The blood-brain barrier in cortical multiple sclerosis lesions. *Journal of Neuropathology and Experimental Neurology*, *66*(4), 321–328. https://doi.org/10.1097/nen.0b013e318040b2de

Vaudel, M., Barsnes, H., Berven, F. S., Sickmann, A., & Martens, L. (2011). SearchGUI: An open-source graphical user interface for simultaneous OMSSA and X!Tandem searches. *Proteomics*, *11*(5), 996–999. https://doi.org/10.1002/pmic.201000595

Vaudel, M., Burkhart, J. M., Zahedi, R. P., Oveland, E., Berven, F. S., Sickmann, A., Martens, L., & Barsnes, H. (2015). PeptideShaker enables reanalysis of MS-derived proteomics data sets: To the editor. In *Nature Biotechnology* (Vol. 33, Issue 1). https://doi.org/10.1038/nbt.3109

Velazquez, E. M., Nguyen, H., Heasley, K. T., Saechao, C. H., Gil, L. M., Rogers, A. W. L., Miller, B. M., Rolston, M. R., Lopez, C. A., Litvak, Y., Liou, M. J., Faber, F., Bronner, D. N., Tiffany, C. R., Byndloss, M. X., Byndloss, A. J., & Bäumler, A. J. (2019). Endogenous Enterobacteriaceae underlie variation in susceptibility to Salmonella infection. *Nature Microbiology*, *4*(6). https://doi.org/10.1038/s41564-019-0407-8

Voortman, M. M., Stojakovic, T., Pirpamer, L., Jehna, M., Langkammer, C., Scharnagl, H., Reindl, M., Ropele, S., Seifert-Held, T., Archelos, J. J., Fuchs, S., Enzinger, C., Fazekas, F., & Khalil, M. (2017). Prognostic value of free light chains lambda and

kappa in early multiple sclerosis. *Multiple Sclerosis*, *23*(11), 1496–1505. https://doi.org/10.1177/1352458516681503

Wang, H., Li, C., Wang, H., Mei, F., Liu, Z., Shen, H. Y., & Xiao, L. (2013). Cuprizone-induced demyelination in mice: Age-related vulnerability and exploratory behavior deficit. *Neuroscience Bulletin*, *29*(2), 251–259. https://doi.org/10.1007/s12264-013-1323-1

Wang, S., Wang, T., Liu, T., Xie, R. G., Zhao, X. H., Wang, L., Yang, Q., Jia, L. T., & Han, J. (2020). Ermin is a p116RIP-interacting protein promoting oligodendroglial differentiation and myelin maintenance. *GLIA*, *68*(11). https://doi.org/10.1002/glia.23838

Wang, Y., Song, M., & Song, F. (2018). Neuronal autophagy and axon degeneration. In *Cellular and Molecular Life Sciences* (Vol. 75, Issue 13, pp. 2389–2406). https://doi.org/10.1007/s00018-018-2812-1

Wegner, C., Esiri, M. M., Chance, S. A., Palace, J., & Matthews, P. M. (2006). Neocortical neuronal, synaptic, and glial loss in multiple sclerosis. *Neurology*, *67*(6), 960–967. https://doi.org/10.1212/01.wnl.0000237551.26858.39

Weil, M. T., Heibeck, S., Töpperwien, M., Tom Dieck, S., Ruhwedel, T., Salditt, T., Rodicio, M. C., Morgan, J. R., Nave, K. A., Möbius, W., & Werner, H. B. (2018). Axonal ensheathment in the nervous system of lamprey: Implications for the evolution of myelinating glia. *Journal of Neuroscience*, *38*(29), 6586–6596. https://doi.org/10.1523/JNEUROSCI.1034-18.2018

Weiner, H. L. (2009). The challenge of multiple sclerosis: How do we cure a chronic heterogeneous disease? In *Annals of Neurology* (Vol. 65, Issue 3, pp. 239–248). https://doi.org/10.1002/ana.21640

Weinstock-Guttman, B., Baier, M., Park, Y., Feichter, J., Lee-Kwen, P., Gallagher, E., Venkatraman, J., Meksawan, K., Deinehert, S., Pendergast, D., Awad, A. B., Ramanathan, M., Munschauer, F., & Rudick, R. (2005). Low fat dietary intervention with ω-3 fatty acid supplementation in multiple sclerosis patients. *Prostaglandins Leukotrienes and Essential Fatty Acids*, *73*(5), 397–404. https://doi.org/10.1016/j.plefa.2005.05.024

Wergeland, S., Torkildsen, Ø., Myhr, K. M., Aksnes, L., Mørk, S. J., & Bø, L. (2011). Dietary vitamin D3 supplements reduce demyelination in the cuprizone model. *PLoS ONE*, *6*(10). https://doi.org/10.1371/journal.pone.0026262

Wergeland, S., Torkildsen, Ø., Myhr, K. M., Mørk, S. J., & Bø, L. (2012). The cuprizone model: Regional heterogeneity of pathology. *APMIS*, *120*(8), 648–657. https://doi.org/10.1111/j.1600-0463.2012.02882.x

Wingerchuk, D. M., & Carter, J. L. (2014). Multiple sclerosis: Current and emerging disease-modifying therapies and treatment strategies. In *Mayo Clinic Proceedings* (Vol. 89, Issue 2, pp. 225–240). https://doi.org/10.1016/j.mayocp.2013.11.002

Xu, S., Lu, J., Shao, A., Zhang, J. H., & Zhang, J. (2020). Glial Cells: Role of the Immune Response in Ischemic Stroke. In *Frontiers in Immunology* (Vol. 11). https://doi.org/10.3389/fimmu.2020.00294

Yang, Z., & Wang, K. K. W. (2015). Glial fibrillary acidic protein: From intermediate filament assembly and gliosis to neurobiomarker. In *Trends in Neurosciences* (Vol. 38, Issue 6, pp. 364–374). https://doi.org/10.1016/j.tins.2015.04.003

Young, E. A., Fowler, C. D., Kidd, G. J., Chang, A., Rudick, R., Fisher, E., & Trapp, B. D. (2008). Imaging correlates of decreased axonal Na+/K+ ATPase in chronic

multiple sclerosis lesions. *Annals of Neurology*, *63*(4), 428–435. https://doi.org/10.1002/ana.21381

Yu, T., Wan, F., Liu, C., Zhang, X., Liu, Z., Zhang, J., Xiong, J., Wang, T., & Zhang, Z. (2020). Asparagine endopeptidase inhibitor protects against fenpropathrin-induced neurodegeneration via suppressing α-synuclein aggregation and neuroinflammation. *European Journal of Pharmacology*, *888*. https://doi.org/10.1016/j.ejphar.2020.173586

Zalc, B. (2018). One hundred and fifty years ago Charcot reported multiple sclerosis as a new neurological disease. *Brain*, *141*(12). https://doi.org/10.1093/brain/awy287

Zeis, T., Graumann, U., Reynolds, R., & Schaeren-Wiemers, N. (2008). Normal-appearing white matter in multiple sclerosis is in a subtle balance between inflammation and neuroprotection. *Brain*, *131*(1), 288–303. https://doi.org/10.1093/brain/awm291

Zhang, J., Cheng, Y., Cui, W., Li, M., Li, B., & Guo, L. (2014). MicroRNA-155 modulates Th1 and Th17 cell differentiation and is associated with multiple sclerosis and experimental autoimmune encephalomyelitis. *Journal of Neuroimmunology*, *266*(1–2), 56–63. https://doi.org/10.1016/j.jneuroim.2013.09.019

Zhang, L., & Elias, J. E. (2017). Relative protein quantification using tandem mass tag mass spectrometry. In *Methods in Molecular Biology* (Vol. 1550, pp. 185–198). https://doi.org/10.1007/978-1-4939-6747-6_14

Zhang, Y., Cai, L., Fan, K., Fan, B., Li, N., Gao, W., Yang, X., & Ma, J. (2019). The Spatial and Temporal Characters of Demyelination and Remyelination in the Cuprizone Animal Model. *Anatomical Record*, *302*(11). https://doi.org/10.1002/ar.24216

Paper-1

scientific reports

Check for updates

OPEN

Cuprizone and EAE mouse frontal cortex proteomics revealed proteins altered in multiple sclerosis

Eystein Oveland[1], Intakhar Ahmad[2,3], Ragnhild Reehorst Lereim[1,2], Ann Cathrine Kroksveen[1,2], Harald Barsnes[1,4], Astrid Guldbrandsen[1,3,5], Kjell-Morten Myhr[2,6], Lars Bø[2,3,6], Frode S. Berven[1,3,7] & Stig Wergeland[3,6,7]✉

Two pathophysiological different experimental models for multiple sclerosis were analyzed in parallel using quantitative proteomics in attempts to discover protein alterations applicable as diagnostic-, prognostic-, or treatment targets in human disease. The cuprizone model reflects de- and remyelination in multiple sclerosis, and the experimental autoimmune encephalomyelitis (EAE, MOG1-125) immune-mediated events. The frontal cortex, peripheral to severely inflicted areas in the CNS, was dissected and analyzed. The frontal cortex had previously not been characterized by proteomics at different disease stages, and novel protein alterations involved in protecting healthy tissue and assisting repair of inflicted areas might be discovered. Using TMT-labelling and mass spectrometry, 1871 of the proteins quantified overlapped between the two experimental models, and the fold change compared to controls was verified using label-free proteomics. Few similarities in frontal cortex between the two disease models were observed when regulated proteins and signaling pathways were compared. Legumain and C1Q complement proteins were among the most upregulated proteins in cuprizone and hemopexin in the EAE model. Immunohistochemistry showed that legumain expression in post-mortem multiple sclerosis brain tissue (n = 19) was significantly higher in the center and at the edge of white matter active and chronic active lesions. Legumain was associated with increased lesion activity and might be valuable as a drug target using specific inhibitors as already suggested for Parkinson's and Alzheimer's disease. Cerebrospinal fluid levels of legumain, C1q and hemopexin were not significantly different between multiple sclerosis patients, other neurological diseases, or healthy controls.

Abbreviations

CNS	Central nervous system
CPZ	Cuprizone
CTR	Control
EAE	Experimental autoimmune encephalomyelitis
EDSS	Expanded disability status scale
GFAP	Glial fibrillary acidic protein
HE	Hematoxylin–eosin
HLA-DR	Human leukocyte antigen-DR
HPLC	High-pressure liquid chromatography
IPA	Ingenuity pathway analysis
LC–MS	Liquid chromatography–mass spectrometry

[1]Proteomics Unit, Department of Biomedicine, University of Bergen (PROBE), Bergen, Norway. [2]Department of Clinical Medicine, University of Bergen, Bergen, Norway. [3]Department of Neurology, Norwegian Multiple Sclerosis Competence Centre, Haukeland University Hospital, Jonas Lies vei 65, 5021 Bergen, Norway. [4]Department of Clinical Science, University of Bergen, Bergen, Norway. [5]Computational Biology Unit, Department of Informatics, University of Bergen, Bergen, Norway. [6]Neuro-SysMed, Department of Neurology, Haukeland University Hospital, Bergen, Norway. [7]These authors jointly supervised this work: Frode S. Berven and Stig Wergeland. ✉email: stig.wergeland@helse-bergen.no

LFB	Luxol fast blue
LGMN	Legumain
Mac-3	Lysosomal-associated membrane protein 2
MHC	Major histocompatibility complex
NOGO-A	Neurite outgrowth inhibitor protein A
OND	Other neurological disease
PLP	Proteolipid protein
PRM	Parallel reaction monitoring
RT	Room temperature
Ser	Serine
SPSS	Statistical package for social sciences
STAT	Signal transducer and activator of transcription
TCEP	Tris(2-carboxyethyl)phosphine
TEAB	Tetraethylammonium bromide
Thr	Threonine
TMT	Tandem mass tag
Tyr	Tyrosine

Multiple sclerosis (MS) is a chronic immune-mediated neurological disorder characterized by chronic inflammatory demyelination, oligodendrocyte depletion, axonal loss and astrocytosis, leading to sclerotic plaques in the CNS[1]. Successful treatment relies on early diagnosis and intervention with immunomodulatory or immunosuppressive therapy. To individualize and improve treatment, better clinical methods to stratify multiple sclerosis patients into those likely to have a rapid disease progression and those with a more benign disease course are needed. Several proteomics studies on biomarkers for multiple sclerosis in body fluids have shown promising results but have not yet met the validation criteria required for clinical implementation[2,3].

Biomarkers have been searched for in experimental disease models that reflect different MS pathophysiological mechanisms, such as the cuprizone (CPZ) model for de- and remyelination, and the T-cell mediated experimental autoimmune encephalomyelitis (EAE). Proteomics experiments have demonstrated upregulation of GFAP and downregulation of myelin proteins in CPZ c57Bl mouse brain tissue[4]. Differentially expressed proteins discovered in EAE, such as GFAP, have shown translational value when investigated in CSF from multiple sclerosis patients[5]. In contrast to MOG35-55, the full-length MOG1-125 has been shown to also induce B-cell responses. This may be of importance as B-cell depletion is among the most effective therapies in MS[6–8]. The mouse brain proteome during EAE MOG1-125 investigated in the presented study has not previously been characterized by proteomics.

Proteomic investigation of both models in parallel might identify key proteins or pathways involved in MS pathophysiology, that could be validated in brain tissue and CSF from MS patients.

Material and methods

Mice. Female C57Bl/6 mice obtained from Tacomic (Tornbjerg, Denmark) with a mean weight of 20.4 g ± 1.1 g were used for the experiment. The mice were housed six together in Macrolon IVC-II cages (Scanbur, Karlslunde) in standard laboratory conditions; light/dark cycles of 12/12 h, cage temperature of 22.3 ± 1 °C, relative humidity of 54 ± 5% and 75 air changes per hour. Cage maintenance was performed once weekly, and the animals were weighed twice a week by the same technician. The experiment was conducted in strict accordance with the Federation of European Laboratory Animal Science Associations recommendations, and the protocol was approved by the Norwegian Animal Research Authority (permits #2009-1767 and #2010-3814).

Cuprizone. Demyelination was induced in eight-week-old female mice by adding CPZ (bis-cyclohexanoneoxaldihydrazone, Sigma-Aldrich, St. Louis, MO) 0.2% (w/w) to milled mouse chow for six weeks (CPZ, N = 5). The mice had ad libitum access to chow and tap water during the whole experimental period. 10 mice were randomly assigned to either CPZ exposure (N = 5) or controls (N = 5). After six weeks of CPZ exposure (CPZ-42d) the disease severity was assessed by histopathological and immunohistochemical quantification of myelin loss in the corpus callosum in mouse brain (Supplementary Fig. 1), as previously described[9].

Experimental autoimmune encephalomyelitis. EAE was induced in eight-week-old female mice with recombinant human MOG (rh-MOG), 1–125 from Hooke Labs, Lawrence, MA) emulsified in complete Freund's adjuvant, injected subcutaneously at Day 0 (day of immunization). In addition, 200 ng of Pertussis toxin (Sigma-Aldrich) was injected intra-peritoneally at Day 0 and at post-immunization (p.i.) Day 2. The mice were sacrificed at the disease maximum (p.i. day 16 = EAE-16d, N = 6) and in the chronic phase (p.i. day 32 = EAE-32d, N = 12). Healthy control mice (N = 5) were sacrificed at p.i. day 32 (Supplementary Fig. 1).

Dissection of mouse brains. The brain was excised from the mice post-mortem. The frontal cortex of the right hemisphere anterior to bregma + 1.0 mm was collected by dissection and immediately stored at − 80 °C until further processing for proteomics analyses. The remaining part of the brain was prepared for immunohistochemistry.

Immunohistochemistry of mouse brain tissue. The mouse brains were post-fixed in 4% formalin for at least 7 days, then paraffin embedded. All analyses were performed on 5 µm sections ± 1 mm from the bregma.

Case #	# of tissue blocks	Post mortem delay (hrs)	MS Phenotype	Gender	Age at autopsy	Disease duration (years)	Cause of death
1	2	–	Progressive	M	34	13	Bronchopneumonia
2	1	28	Progressive	F	65	26	Congestive heart failure
4	5	–	–	M	43	–	–
5	1	8	Relapsing–remitting	F	52	20	Bronchopneumonia
7	1	24	Progressive	F	45	8	Acute pyelonephritis with sepsis
8	4	10	–	F	45	23	Bronchopneumonia
9	2	15	Progressive	M	55	36	Acute pyelonephritis with sepsis
10	2	70	Progressive	F	60	4	Bronchopneumonia
12	1	46	Progressive	M	67	42	Bronchopneumonia
13	1	13	–	M	50	20	Bronchopneumonia
14	1	29	Progressive	F	68	14	Cerebral haemorrhage
15	2	40	Progressive	M	83	–	Pseudomembraneous colitis
16	2	29	Progressive	F	49	20	Bronchopneumoina
18	3	83	Progressive	F	62	28	Bronchopneumonia
19	2	31	–	M	52	8	Acute pyelonephritis
20	3	45	Progressive	M	43	7	Bronchopneumonia
21	2	27	Relapsing–remitting	F	21	4	Bronchopneumonia
23	3	24	–	F	56	26	Bronchopneumonia
25	1	50	–	M	46	12	Suicide
26	2	23	–	F	46	–	Hyperthermia

Table 1. Clinical and demographic case description of brain autopsy cases. – Information not available.

The sections were stained for myelin with Luxol Fast Blue (LFB) and with hematoxylin and eosin (HE). For immunohistochemistry, sections were incubated with primary antibodies for myelin (proteolipid protein, PLP), mature oligodendrocytes (neurite outgrowth inhibitor protein A, NOGO-A) and activated microglia and macrophages (Mac-3), as described previously[10]. For each antibody, omission of the primary antibody served as negative control. Normal brain tissue from the healthy controls served as positive controls. Antibody specifications are available in Supplementary Information.

Tissue homogenization and protein extraction. The brain tissue from frontal cortex part of the right hemisphere was thawed on ice in a 4 °C room. In triethylammonium-bicarbonate buffer containing urea, protease-, Tyr-phosphatase-, and Ser/Thr phosphatase inhibitors, the tissue was homogenized by pulse-sonication (for details, see supplementary methods). The protein concentration was measured using the BCA Protein Assay Kit in a 96 well plate (Pierce, Thermo Scientific), and the yield was approximately 1.3 mg protein per 50 mg tissue.

TMT-labelling and protein quantification. Equal amounts of protein (urea/TEAB lysate) from the individual frontal cortex samples representing the same condition were pooled to give 100 µg protein for each condition. The samples were prepared, trypsinised and TMT-labelled as outlined in the manual for the TMT-sixplex Isobaric Label Reagent Set (ThermoFisher), except that the TCEP reduction was done at RT. The peptides from the whole trypsinised samples were labelled with the TMT reagents as follows: CTR-CPZ (pool of N = 5) = TMT130, CTR-EAE (pool of N = 6) = TMT127, CPZ-42d (pool of N = 5) = TMT126, EAE-16d (pool of N = 6) = TMT128 and EAE-32d (pool of N = 6) = TMT129. The TMT labelled samples were then combined 1:1:1:1:1 into a single tube (500 µg) and dried using a vacuum concentrator (Eppendorf).

The TMT-labelled tryptic peptides were fractionated in 60 fractions using mixed-mode HPLC chromatography (Supplementary Information). Mixed-mode fractions 1–3 were pooled and fractions 7–9 were pooled,

Controls					Multiple sclerosis cases				
Diagnose at LP	EDSS	OCB status	Age (years)	Sex	Diagnose at LP	EDSS	OCB status	Age (years)	Sex
Non-neurological	N/A	Neg	74	F	RRMS	2	Pos	29	M
Non-neurological	N/A	Neg	25	F	RRMS	3	Pos	51	M
Non-neurological	N/A	Neg	36	M	RRMS	2	Pos	43	F
Non-neurological	N/A	Neg	28	M	RRMS	1.5	Pos	42	M
Non-neurological	N/A	Neg	79	M	RRMS	2	Pos	51	F
Non-neurological	N/A	Neg	63	M	RRMS	0	Pos	40	M
Non-neurological	N/A	Neg	86	F	RRMS	1.5	Pos	42	F
Non-neurological	N/A	Neg	39	F	RRMS	2	Pos	43	F
Non-neurological	N/A	Neg	68	M	RRMS	–	Pos	74	F
OIND	N/A	Neg	35	F	RRMS	2	Pos	35	F
OIND	N/A	Pos	32	M	RRMS	1.5	Pos	38	F
OIND	N/A	Pos	45	F	RRMS	3	Pos	35	F
OIND	N/A	Neg	63	F	RRMS	1.5	Pos	42	M
OIND	N/A	Neg	33	M	RRMS	1.5	Pos	29	F
OIND	N/A	Neg	35	M	RRMS	1	Pos	28	F
OIND	N/A	Neg	35	M	RRMS	1	Pos	33	F
OND	N/A	Neg	50	F	RRMS	1	Pos	29	F
OND	N/A	Neg	28	F	RRMS	2	Pos	32	F
OND	N/A	Neg	36	F	RRMS	1	Pos	37	F
OND	N/A	Neg	38	F	RRMS	1	Pos	35	F
OND	N/A	Neg	37	F	RRMS	0	Pos	28	F
OND	N/A	Neg	33	M	RRMS	1	Pos	41	F

Table 2. Clinical and demographic case description of CSF sample cases at time of lumbar puncture. *LP* lumbar puncture, *EDSS* expanded disability status scale, *OCB* oligoclonal bands, *CSF* cerebrospinal fluid. – information unavailable.

while fractions 4 to 6 containing excessive TMT reagents were excluded, resulting in a total of 53 fractions plus the unfractionated sample. The samples (0.5 µg) were subjected to LC–MS using 120 min runs with a biphasic acetonitrile gradient on a 50 cm nanoViper column (Dionex) using an Ultimate NCS-3500RS (Dionex) coupled to an LTQ-Orbitrap Velos Pro (Thermo Scientific) (Supplementary Information).

Proteome Discoverer v1.4.1.14 (Thermo Scientific) was used for identification and quantification of the TMT data. The TMT protein quantification values were then exported to Microsoft Excel and normalized within each condition (each TMT label) by $\log_2$-transformation of all values and subtracting the condition median. The protein quantification value (transformed to anti-log) for each protein in CPZ and EAE was divided by the respective protein quantification value in the control, control 42 days was used for the CPZ animals and control 32 days for EAE animals. The z-scores for all the protein ratios in each condition were calculated using a Gaussian probability function, and the p-values corrected using Benjamini–Hochberg as previously described[11] (Supplemental Data 1).

Label-free protein quantification. The individual mouse brain frontal cortex lysates from EAE-16d (N = 6), EAE-32d (N = 12), CTR-EAE (N = 5), CPZ (N = 5) and CTR-CPZ (N = 5) were trypsinised using an in-house standardized in-solution digestion protocol. The peptide samples (2.5 µg) were subjected to LC–MS on an LTQ-Orbitrap Velos Pro (Supplementary Methods).

Progenesis LC–MS v2.6 (Nonlinear Dynamics Ltd, Newcastle, UK) was used in combination with SearchGUI v1.8.9[12] and PeptideShaker v0.17.3[13] for label-free quantification, identification and comparison of the LC–MS proteomics data (Supplementary Methods). Progenesis LC–MS was used to calculate statistically significant up- and downregulated proteins for the label-free data based on ANOVA (p-value) with correction for multiple hypotheses testing (q-value) (Supplemental Data 2). Proteins were considered significantly regulated when the ratios over CTR were ≥ 2 and ≤ 0.7 with $p < 0.05$ and low q-values; $q < 0.05$ for CPZ-42d/CTR, $q < 0.051$ for EAE-16d/CTR and $q < 0.11$ for EAE-32d/CTR. The CTR (n = 11) was represented by values from the controls for both the CPZ (42 days, n = 6) and EAE (32 days, n = 5) experiments.

Immunohistochemistry of human brain tissue. A total of 49 brain tissue blocks from 26 multiple sclerosis autopsy cases were obtained from the Multiple Sclerosis Biobank at the Department of Pathology, Haukeland University Hospital, Bergen. All research involving human brain tissue were conducted in accordance with the ethical standards of the regional committee for medical research ethics of Western Norway. The clinical data from the patients are summarized in Table 1. The study was approved by the regional committee for medical research ethics of Western Norway (#2013-560). Five micron thick paraffin-embedded sections were deparaffinized in xylene and rehydrated in serial aqueous dilutions of ethanol, before heat-induced epitope retrieval at pH 6.2 (Diva Decloaker antigen retrieval solution, Biocare Medical, CA, USA). To ensure optimal

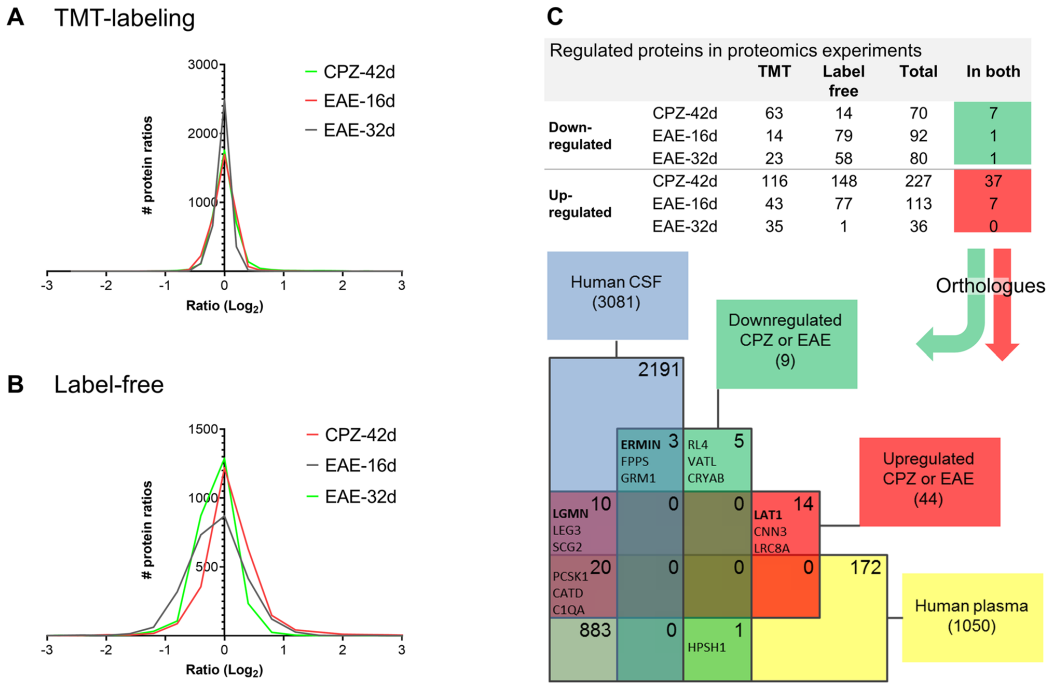

Figure 1. Proteins quantified in EAE and CPZ frontal cortex and human orthologues in CSF and plasma. (**A**) Frequency distribution of all normalized $\log_2$ ratios for proteins quantified using TMT-labeling in frontal cortex in CPZ-42d, EAE-16d and EAE-32d divided by the respective controls. The TMT data was normalized using the $\log_2$ minus the condition median value. The relative numbers of proteins in the ratio bins were automatically determined by GraphPad and presented as continuous lines. (**B**) Frequency distribution of all normalized $\log_2$ ratios for proteins quantified using label-free in frontal cortex in CPZ-42d, EAE-16d and EAE-32d divided by the respective controls. The label-free data was normalized using the default algorithm in Progenesis LC–MS. The relative numbers of proteins in the ratio bins were automatically determined by GraphPad and presented as continuous lines. Slight shifts/shoulders in the frequency distribution plots are due to that the label-free protein quantification is based on the sum of the quantified peptide features with proteins ID's assigned and the peptides being unique for the protein. The normalization was performed on all peptides. The log2 protein ratios are thus based on a selection of the peptide features from the LC–MS runs. (**C**) Number of significantly regulated proteins in the conditions CPZ-42d, EAE-16d and EAE-32d relative to respective controls using TMT-labelling and label-free proteomics. The numbers of proteins regulated in both methods are shown, downregulated squared in green and upregulated in red. The human orthologues of the proteins regulated in both TMT and label-free were compared to the CSF and plasma proteins in the CSF-PR database[21]. The Venn diagram shows how many protein accession numbers that were shared by the respective proteomes, and some of the most relevant regulated proteins.

consistency, immunohistochemistry on all sections was performed at the same time. Primary antibodies were: anti-Legumain (LGMN), anti-PLP, anti-HLA-DR. The tissue sections were counterstained with hematoxylin and visualized by 3,3′-Diaminobenzidine (EnVision, DAKO, Glostrup, Denmark). EnVision G|2 Doublestain System (Dako), Rabbit/Mouse (DAB + / Permanent Red) was used for double staining for LGMN/HLA-DR and LGMN/GFAP to determine cellular specificity of LGMN immunopositivity.

Digitalization of stained section and characterization of multiple sclerosis lesions. PLP, HLA and LGMN stained sections were digitized in NDPI file format using a Scanscope XT slide scanner (Aperio Technologies; Vista, CA) at a resolution of 0.247 µm per pixel. White matter and cortical lesions were identified and classified by three individual investigators, according to the Bø / Trapp system[14,15].

Quantification of LGMN levels in brain tissue. Immunopositivity for LGMN was scored on a semi quantitative scale, based on density and stain intensity compared to LGMN immunopositivity in non-lesioned, similar tissue within the same section. Each MS-lesion was scored in the lesion center, at the lesion edge, and immediately perilesionally, avoiding other proximate lesions, as evaluated on PLP- and HLA-DR stained sections: "no difference" (0), "minor increase" (+1), "minor decrease" (− 1), "extensive increase" (+2) and "signifi-

		TMT-labeling									Label-free							
				CPZ-42d		EAE-16d		EAE-32d			CPZ-42d		EAE-16d		EAE-32d			
Accession	Protein	P	S	FC	q	FC	q	FC	q	P	FC	q	FC	q	FC	q	hCSF	hP
(A) Upregulated in CPZ-42d																		
P14106	C1QB	5	19	5.3	***	0.8		0.8		2	19.4	*'	1.5		1.3		Y	Y
Q02105	C1QC	6	14	5.3	***	0.8		0.8		3	9.1	*'	1.2		1.3		Y	Y
O89017	LGMN	6	11	4.0	***	0.7		0.7		1	64.9	*	1.9		1.3		Y	
P98086	C1QA	6	20	3.8	***	0.9		0.9		4	6.8	*'	1.1		1.1		Y	Y
P16110	LEG3	5	5	3.7	***	1.1		0.8		2	338.7	*'	2.3		1.1		Y	
Q99L04	DHRS1	15	42	3.7	***	0.8		0.8		3	4.0	*'	0.9		0.9			
P24452	CAPG	6	9	3.4	***	0.9		0.9		1	4.7	*'	1.2		1.0		Y	
P20152	VIME	30	540	3.1	***	1.2		1.1		22	7.7	*'	1.6		1.2		Y	Y
P20060	HEXB	18	48	2.9	***	1.0		1.0		6	5.0	*'	1.6		1.2		Y	Y
P03995	GFAP	38	658	2.6	***	1.3		1.1		18	7.2	*'	1.5		1.0		Y	
P11835	ITB2	5	5	2.6	***	0.8		0.8		1	8.2	*'	0.5		0.7		Y	
Q9Z127	LAT1	3	7	2.4	***	0.5	***	0.6	***	1	4.5	*'	0.5		0.6			
P26041	MOES	20	46	2.3	***	1.1		1.0		4	2.6	*'	0.9		0.9		Y	Y
O35639	ANXA3	15	25	2.2	***	1.0		1.0		1	5.9	*'	1.4		1.3		Y	
P18242	CATD	16	119	2.2	***	1.0		0.9		10	2.8	*'	1.3		1.0		Y	Y
Q9DAW9	CNN3	8	22	2.1	***	1.0		1.0		4	4.0	*'	1.2		1.0			
Q9D379	HYEP	8	11	2.0	***	0.8		0.8		2	2.9	*'	0.6		0.7			
P10605	CATB	9	57	1.9	***	0.9		1.0		7	3.4	*'	1.0		0.9		Y	Y
Q8BTM8	FLNA	30	40	1.9	***	0.8		0.9		2	1.5	*'	1.4		1.0		Y	Y
P60824	CIRBP	4	17	1.9	***	1.0		1.0		1	4.8	*'	1.2		1.1			
Q9DCJ9	NPL	7	11	1.8	***	1.0		1.0		1	19.8	*'	1.4		0.7			
Q9WVA4	TAGL2	11	38	1.8	***	1.1		1.0		3	2.9	*'	1.2		0.9		Y	Y
P09055	ITB1	4	5	1.7	***	0.9		0.8		1	2.8	*	0.4		0.6		Y	Y
P10852	4F2	20	107	1.6	**	0.8		0.8		12	1.9	*'	0.8		0.8		Y	Y
Q80WG5	LRC8A	4	4	1.6	**	0.8		0.8		1	2.1	*'	0.8		0.7	§		
P16045	LEG1	6	25	1.6	**	0.9		0.9		2	3.1	*'	1.0		1.0		Y	
P61620	S61A1	2	4	1.6	**	0.8		0.8		1	2.5	*	0.4	*	0.6			
Q9CQI6	COTL1	13	138	1.5	*'	1.0		1.0		5	2.1	*'	0.9		0.9		Y	
P16675	PPGB	3	4	1.5	*'	0.9		1.0		1	3.2	*'	0.9		1.0		Y	Y
P07356	ANXA2	11	20	1.5	*	1.0		1.0		3	2.7	*'	0.7		0.7		Y	Y
Q9DCD0	6PGD	15	27	1.5	*	0.9		0.9		5	1.7	*	0.8		0.8		Y	Y
Q9Z110	P5CS	14	22	1.5	*	0.9		1.0		2	2.9	*'	0.8		0.9			
O89086	RBM3	5	19	1.5	*	1.0		1.0		1	5.0	*'	1.3		1.1			
P51880	FABP7	4	20	1.5	*	0.9		1.4	***	6	2.9	*'	1.1		1.9		Y	
Q8CGC7	SYEP	29	34	1.4	*	0.8		0.8		3	2.1	*'	0.6		0.7			
P08030	APT	6	11	1.4	*	1.1		1.0		1	2.2	*	1.1		1.0			
Q8VDD5	MYH9	47	94	1.4	*	0.9		0.9		8	1.8	*'	0.8		0.8		Y	Y
(B) Downregulated in CPZ-42d																		
Q5EBJ4	ERMIN	7	21	0.5	***	1.3		1.1		3	0.5	*'	0.9		0.8		Y	
P47911	RL6	13	25	0.5	***	1.3		1.0		1	0.5	*'	0.9		0.8			
P23927	CRYAB	6	67	0.6	***	1.2		1.0		4	0.5	*	1.2		1.0			
Q9D8E6	RL4	13	29	0.7	*'	1.1		1.0		1	0.5	*	0.6		0.8			
Q61699	HS105	36	78	0.7	*	1.0		1.0		12	0.6	*'	0.9		0.9			Y
Q920E5	FPPS	9	14	0.7	*	1.0		1.0		2	0.6	*	0.7		0.8		Y	
P14148	RL7	6	10	0.7	*	0.9		0.9		1	0.6	*	0.7		0.8			
(C) Upregulated in EAE-16d																		
Q91X72	HEMO	15	28	0.9		1.8	***	1.2		3	0.9		3.3	*	1.5		Y	Y
P07758	A1AT1	4	8	1.0		1.7	***	1.2		1	0.9		4.4	*	1.8		Y	Y
Q9QXV0	PCSK1	8	102	1.2		1.5	**	1.1		4	2.1		2.2	*	1.1		Y	Y
Q8K019	BCLF1	7	7	1.1		1.4	*'	1.4	***	1	1.3		1.4	*	1.2			
Q03517	SCG2	28	160	1.1		1.4	*	1.1		10	1.5		2.6	*	1.5		Y	
P22005	PENK	7	35	1.1		1.4	*	1.2		1	0.7		6.0	*	2.6		Y	Y
Q9JJF0	NP1L5	5	10	0.9		1.4	*	1.1		1	1.4		2.2	*	1.0			

Continued

		TMT-labeling									Label-free							
				CPZ-42d		EAE-16d		EAE-32d			CPZ-42d		EAE-16d		EAE-32d			
Accession	Protein	P	S	FC	q	FC	q	FC	q	P	FC	q	FC	q	FC	q	hCSF	hP
Mouse																		
(D) Downregulated in EAE-32d																		
P97772	GRM1	4	4	1.1		0.7		0.7	*	2.0	1.8		0.5		0.5	§	Y	

Table 3. Significantly regulated proteins in both TMT-labeling and label-free. (A) Proteins upregulated in CPZ-42d in both TMT and label-free. (B) Proteins downregulated in CPZ-42d in both TMT and label-free. (C) Proteins upregulated in EAE-16d in both TMT and label-free. (D) Protein downregulated in EAE-32d in both TMT and label-free. For all tables: quantified proteins, number of unique peptides (P) and spectra (S) with fold change relative to respective controls (FC) are shown for CPZ-42d, EAE-16d and EAE-32d. The p-values for the regulated proteins were corrected for multiple hypothesis testing to control false discovery rates, resulting in adjusted p-values (q-values). The q-values are denoted in the table as follows: §, $q < 0.1$; *, $q < 0.05$; *' $q < 0.01$; **, $q < 0.005$, *** $q < 0.0005$. For the TMT-data, the z-scores for all the protein ratios in each condition were calculated using a Gaussian probability function, and the p-values corrected using Benjamini–Hochberg (q-values), as previously described[11]. For the label-free data Progenesis LC–MS was used to calculate statistically up- and downregulated proteins based on ANOVA (p-value) with correction for multiple hypotheses testing based on FDR (q-value). Consistent regulation in all individuals in CPZ-42d allowed a stringent limit for the corrected p-value from multiple hypothesis testing ($q < 0.05$), a moderate in in EAE-16d ($q < 0.051$) and a higher limit in EAE-32d ($q \leq 0.1$). Human orthologues present in human cerebrospinal fluid (hCSF) and plasma (hP) according to the CSF-PR database[21] are indicated with yes (Y = yes).

cant decrease" (− 2). Two observers evaluated all slides independently (SW and IA) and disputes were resolved by a third observer (LB). In the same area, HLA-DR-stained sections were scored from 0 to 2 for degree of microglia and macrophage reactivity: "no signs of reactive cells, only sparse ramified microglia" (0); "Signs of reactive microglia and macrophages" (1), "Presence of amoeboid, phagocytosing microglia and macrophages" (2). Correlations between LGMN immunopositivity and multiple sclerosis lesion types, and relation to degree of microglia and macrophage activation was analyzed in SPSS 24.0 in a multinomial mixed model to account for dependency in the data, with random intercept for cases and blocks.

Human CSF samples. CSF was collected from patients that underwent diagnostic lumbar puncture at the Department of Neurology, Haukeland University Hospital, Bergen, Norway, according to the recommended consensus protocol for CSF collection and biobanking[16]. The study was approved by the regional committee for medical research ethics of Western Norway, all patients provided written informed consent, and all research involving human CSF samples were conducted in accordance with the ethical standards of the regional committee for medical research ethics of Western Norway. The included patients were 22 with RRMS, 9 without neurological symptoms, 7 with other inflammatory neurological diseases, 6 with other neurological diseases. The clinical characteristics of the cases are summarized in Table 2.

Parallel reaction monitoring to quantify LGMN, C1Q and HEMO in CSF. The concentration of the candidate protein LGMN, C1Q and HEMO in CSF from multiple sclerosis (MS), other neurological disease (OND) controls and healthy controls (NN) were determined using parallel reaction monitoring (PRM) both in absolute and relative terms.

The absolute amounts of these proteins were measured. All CSF samples were in-solution digested as previously described. About 1.5 µg CSF digested protein were injected for Legumain and C1q and about 0.2 µg for Hemopexin. Relative PRM was assisted by stable isotope-labeled internal standard (SIS) peptides (MS vs OND). The unique LGMN peptide DYTGEDVTPQNFLAVLR (a.a. 101–117), HEMO NFPSPVDAAFR and C1Q FQSVFTVTR were chosen to cover the protein sequence toward both termini (Supplementary Data 3, Supplementary Information).

Proteomics data post-processing and availability. Perseus v1.4.1.3[17] was used to generate the unsupervised clustering heatmap with dendrograms of z-score normalized data using the default settings. GraphPad Prism 6 (GraphPad Prism Software) was used for the statistical analyses and graphics and Venn diagrams were created using Venny (http://bioinfogp.cnb.csic.es/tools/venny/index.html). Ingenuity Pathway Analysis (IPA, Ingenuity Systems, http://www.ingenuity.com) was used for pathway and function analyses. DAVID[18] was used to investigate the regulated proteins in KEGG pathways[19]. MADGENE[20] was used to convert the mouse accession numbers to human orthologues for comparison against the results in CSF-PR[21]. Additional information on the tools used can be found in Supplementary Information.

The mouse discovery proteomics TMT and label-free data have been deposited to the ProteomeXchange Consortium[22] via the PRIDE partner repository[23] with the dataset identifier PXD002318. An overview of the raw data files and the analyzed data are available (Supplementary Data 1–2).

Figure 2. Clustering and pathway analyses of proteins quantified in EAE and CPZ. The protein ratios relative to respective controls for EAE-16d, EAE-32d and CPZ-42d from TMT and label-free were combined prior to analyses in Perseus and IPA. (**A**) Unsupervised hierarchical clustering of the TMT and label-free protein ratio list (Perseus). (**B,C**) The significance level of regulation (IPA "p-value") was set to 0.005 if the protein was significantly regulated with more than 1.2-fold in both TMT and label-free experiments and 0.05 if only in one experiment. Predicted activated upstream regulators, such as STAT3 and STAT4, are illustrated as networks together with associated proteins from our uploaded dataset EAE-16d (**B**) and CPZ-42d (**C**). Predicted network in IPA for CPZ-42d "Hematological disease, Immunological disease, Inflammatory disease" involving ISG15 (upregulated in CPZ-42d, in EAE-16d and EAE-32d only in TMT), SERPINA3 (upregulated in CPZ-42d only in TMT), and LGMN (highly upregulated in CPZ-42d) (**D**). The average $\log_2$ ratio and the "IPA p-value" from the combined TMT and label-free protein list are shown for each protein node. The proteins significantly altered with a fold change higher than 20% in both TMT and label-free were considered more significant (IPA p-value 0.005) than the proteins regulated in only one of the experiments (IPA p-value 0.05). The IPA prediction legend is shown as an insert in (**B**). *EC* extracellular space, *PM* plasma membrane, *CP* cytoplasm, *N* nucleus.

Results

The proteomic analysis uncovered differentially regulated proteins in the frontal cortex part of EAE and CPZ mice of which human orthologues were investigated as disease markers for multiple sclerosis.

Proteins regulated in CPZ and EAE frontal cortex and human orthologues in CSF. The cuprizone mice were sacrificed at the demyelination/re-myelination stage (CPZ-42d), and the EAE mice at the disease peak (EAE-16d) and at the recovery phase (EAE-32d) (Supplementary Fig. 1). The number of proteins (unique protein accession numbers and protein groups) quantified in CPZ and EAE mouse brains with respective controls was 3664 in the TMT-labelling experiment (Supplementary Data 1) and 2582 in the label-free experiment (Supplementary Data 2), a total of 4375 proteins. The distributions of protein ratios of CPZ-42d, EAE-16d or EAE-32d relative to control are presented in Fig. 1A,B.

The proteins significantly regulated in the TMT experiment and verified as regulated in the label-free experiment were considered to be the most certain changes (Table 3). Of these, the proteins with human orthologues previously detected in human CSF and/or plasma were identified using the CSF-PR database[21] (Fig. 1C, Table 3). These protein candidates were considered especially interesting as prognostic- and diagnostic markers.

In CPZ-42d several significantly regulated proteins, of which human orthologues were found using CSF-PR, were associated with inflammation and protease activity (upregulation of LGMN, LEG1, LEG3), migration and integrin signaling (upregulation of ITB1, ITB2, FABP7), microglia/macrophage signaling (upregulation of C1Q, CAPG, HEXB), astrocytosis (upregulation of GFAP, VIME) and demyelination (downregulation of ERMN) (Table 3A,B). ERMN, involved in myelinogenesis and oligodendroglia maturation[24], was the most downregulated protein in CPZ-42d and the human orthologue was found in CSF-PR.

The proteins regulated in EAE-16d indicate that the processes of inflammation, microglia activation, astrocytosis and demyelination were less prominent compared to CPZ-42d, and even less in EAE-32d than in EAE-16d. In EAE-16d the acute phase associated proteins HEMO and A1AT1 and the granin family proteins PCSK1 and SCG2 were significantly increased (Table 3C). In addition, proteins involved in glutamate homeostasis were regulated in EAE-16d (upregulation of PENK), and in EAE-32d (downregulation of GRM1) (Table 3D).

Pathway analyses of the quantified proteins. The data from the TMT experiment and the label-free experiment were combined and analyzed by unsupervised clustering. As expected, the EAE-16d and EAE-32d datasets appeared more similar to each other than to CPZ-42d (Fig. 2A). The combined data were analyzed using Ingenuity Pathway Analysis (IPA), and upstream regulators were predicted based on the protein regulations in EAE-16d and CPZ-42d (Fig. 2B,C). An activation of STAT3 (upregulated in CPZ-42d in TMT) and of STAT4 (not detected in our datasets) were predicted from both the EAE-16d and the CPZ-42d datasets (Fig. 2B,C), and activation of ISG15 was common for both STATs. ISG15 was upregulated in CPZ-42d, in EAE-16d and EAE-32d but only in TMT. The STATs have previously been discussed as possible treatment targets in multiple sclerosis[25]. The predicted networks with the highest scores in IPA are presented in Supplementary Fig. 2.

Investigation of regulated proteins in multiple sclerosis. One of the most upregulated proteins in CPZ-32d was legumain (LGMN), and the human orthologue has previously been detected in human CSF (CSF-PR). LGMN was one of the 19 regulated proteins that contributed to significant overrepresentation of the lysosomal KEGG pathway (FDR = 7×10^{-7}) when all regulated proteins were analyzed in DAVID[18]. In the lysosomes, LGMN is involved in processing proteins for MHC class II antigen presentation[26], a biological function relevant to multiple sclerosis pathology. ISG15 in the predicted STATs networks (Fig. 2B,C) has been reported to have protein interaction with LGMN[27] as illustrated in one of the predicted networks for CPZ-42D (Fig. 2D). LGMN has previously been shown to be expressed on macrophages in active demyelinating white matter lesions[28], and was further investigated in this study in both white and grey matter using IHC, and in human CSF using PRM.

C1Q proteins, important in complement activation in multiple sclerosis have previously been investigated in multiple sclerosis using IHC[29], and were among the most upregulated proteins in CPZ-42d. C1Q proteins were investigated using parallel reaction monitoring (PRM) in CSF from multiple sclerosis patients.

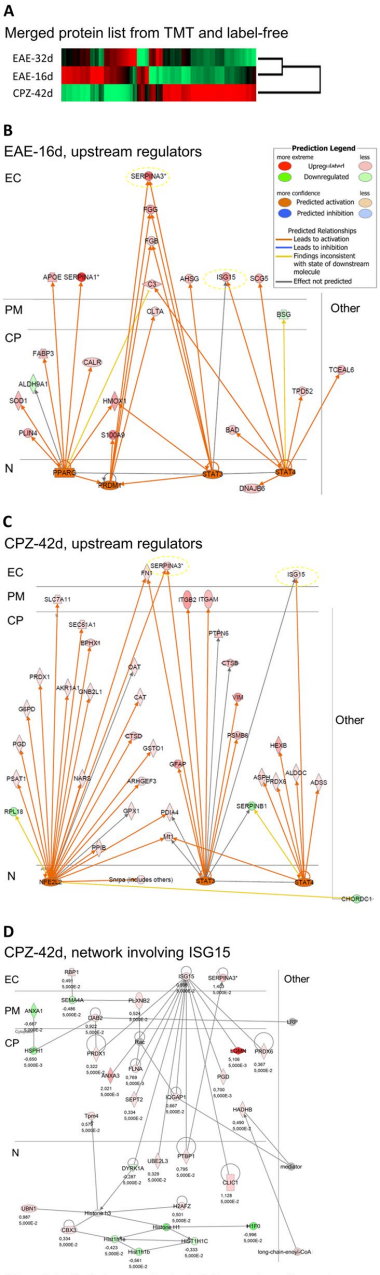

"Hematological-, immunological-, inflammatory disease"

	White matter lesions							Cortical lesions							
	Active		Chronic active		Inactive			Type 1		Type 2		Type 3		Type 4	
Lesion sublocation	M	SD	M	SD	M	SD		M	SD	M	SD	M	SD	M	SD
Center	1.6	0.7	0.8	0.9	0.0	0.9		0.6	1.0	-0.1	0.3	0.0	0.8	0.3	0.5
Edge	1.5	0.5	1.1	0.7	0.4	0.8		0.7	1.0	0.3	0.5	0.1	0.8	0.1	0.4
Perilesionally	0.3	0.5	0.3	0.6	0.0	0.3		0.1	0.7	0.2	0.4	0.0	0.7	0.0	0.0

Table 4. LGMN scores in human brain tissue samples. *M* mean, *SD* standard deviation, Type 1 leucocortical, Type 2 subpial, Type 3 intracortical, Type 4 throughout cortex.

	N	%	Center			Edge			Peri-lesion		
			B	95%CI	p	B	95%CI	p	B	95%CI	p
White matter lesions											
LR χ^2			$F_{df\,2} = 23.5$, $p < 0.001$			$F_{df\,2} = 14.9$, $p = 0.001$			$F_{df\,2,48} = 8.8$, $p = 0.001$		
Active	8	13.3%	4.00	[2.22,6.22]	**<0.001**	2.70	[1.17,4.46]	**0.001**	1.60	[−0.53,3.87]	0.129
Chronic active	17	28.3%	1.60	[0.45,2.86]	**0.008**	1.60	[0.41,2.91]	**0.011**	1.50	[−0.29,3.64]	0.108
Chronic inactive*	35	58.3%	0*	–	–	0*	–	–	0*	–	–
Gray matter lesions											
LR χ2			$F_{df\,3} = 7.6$, $p = 0.056$			$F_{df\,3} = 3.7$, $p = 0.154$			$F_{df\,3} = 1.6$, $p = 0.662$		
Type 1—leucocortical	11	17.7%	1.29	[−0.86,3.56]	0.248	1.74	[−0.45,4.05]	0.126	0.00	[−3.26,3.26]	<1
Type 2—intracortical	16	25.8%	-1.47	[−3.42,0.41]	0.129	0.52	[−1.35,2.45]	0.593	1.39	[−1.21,4.31]	0.322
Type 3—subpial	28	45.2%	-0.90	[−2.56,0.75]	0.283	-0.01	[−1.67,1.72]	0.990	0.38	[−2.06,3.02]	0.770
Type 4—throughout cortex*	7	11.3%	0*	–	–	0*	–	–	0*	–	–
HLA-DR											
LR χ^2			$F_{df\,2} = 35.7$, $p < 0.001$			$F_{df\,2} = 41.7$, $p < 0.001$			$F_{df\,2} = 8.0$, $p = 0.018$		
Inactive	74	66.1%	0*	–	–	0*	–	–	0*	–	–
Reactive	29	25.9%	2.28	[1.35,3.28]	**<0.001**	2.64	[1.67,3.7]	**<0.001**	1.39	[0.07,2.83]	0.064
Active, amoeboid	9	8.0%	3.27	[1.83,4.8]	**<0.001**	3.22	[1.82,4.71]	**<0.001**	2.18	[0.43,3.91]	**0.009**

Table 5. Multinominal linear regression analyses of LGMN score by lesion type and HLA-DR. *B* coefficient, *CI* confidence interval, * reference category, *LR χ2* loglinear chi square, *Df* degrees of freedom. Significant p-values after sequential Bonferroni correction indicated in bold typeface.

HEMO, the most upregulated protein in EAE (Table 3C, Supplementary Fig. 2B), has previously been suggested as affected candidates from proteomics of CSF from rats with EAE[30] and was upregulated in plasma of pediatric multiple sclerosis patients[31]. HEMO was investigated further in human CSF using PRM.

Legumain expression in multiple sclerosis lesions. LGMN levels were investigated in human brain tissue autopsy samples using IHC, and expression means and precision estimates in white matter and cortical lesions are given in Table 4. LGMN immunopositivity was significantly increased in the lesion center and at the lesion edge of active and chronic active white matter lesions compared to inactive lesions (Table 5, Fig. 3). There was no significant difference of LGMN immunopositivity in cortical lesions, compared to normal-appearing gray matter. There was a significant association between LGMN immunoreactivity in white matter MS lesion areas and density of HLA-DR immunopositive cells infiltration, where increased LGMN expression in the lesion center and edge were associated with the presence of HLA-DR positive cells with the morphology of foamy macrophages/activated microglia (Table 5, Fig. 3). Double labelling for HLA-DR / LGMN, and GFAP / LGMN showed predominantly colocalization of LGMN with HLA-DR-immunopositive, and not GFAP- immunopositive cells (astrocytes) (Fig. 4). A subpopulation of cortical neurons was weakly legumain immunopositive. This was not observed in controls, but the available tissue did not allow for comparison of neurons from the same anatomical area and layers. Brain autopsy samples from three control cases without known neurological diseases were available for PLP, HLA-DR and LGMN staining, and by visual comparison, the overall LGMN expression was higher in the cortex of multiple sclerosis cases compared to the controls (Fig. 5).

Quantification of upregulated proteins in CSF from multiple sclerosis patients. In order to investigate whether the levels of LGMN, C1Q (upregulated in CPZ) and HEMO (upregulated in EAE16d) were significantly affected in CSF samples from multiple sclerosis patients (Table 2), a targeted LC–MS/MS PRM

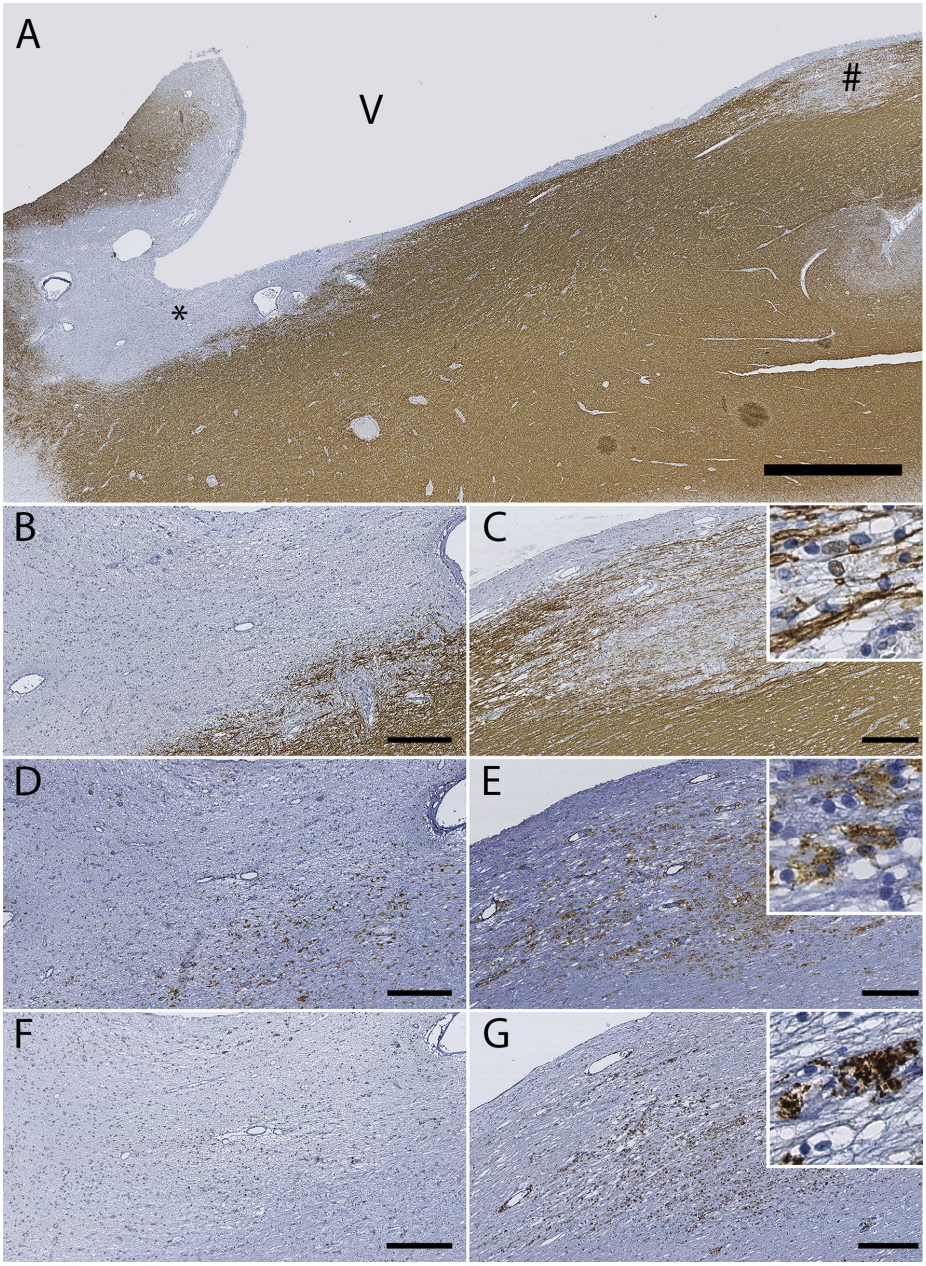

Figure 3. Expression of LGMN in white matter lesions. (**A**) Myelin (PLP) immunostained section with an active lesion (# in **A**, images **C,E,G**) and an inactive lesion (* in **A**, images **B,D,F**). Scale bar 2 mm. (**B,C**) Myelin (PLP) immunostaining of lesions indicated in **(A)** at higher magnification. Scale bar 300 µm. Insert in **(C)** shows intracellular PLP-positive myelin debris, suggesting an early active lesion with ongoing demyelination. (**D,E**) HLA-DR immunostaining of lesions indicated in **(A)**. Scale bar 300 µm. Insert in **(E)** shows activated HLA-DR positive cells. (**F,G**) LGMN immunostaining of the lesions indicated in **(A)**. Scale bar 300 µm. In **(G)**, increased LGMN expression is seen throughout the active lesion, while in the chronic inactive lesion **(F)**, there is reduced LGMN expression, due to general hypocellularity and absence of HLA-DR positive cells. Insert in **(G)** shows a representative image of LGMN immunostaining in a pattern compatible with cytoplasmic lysosomes.

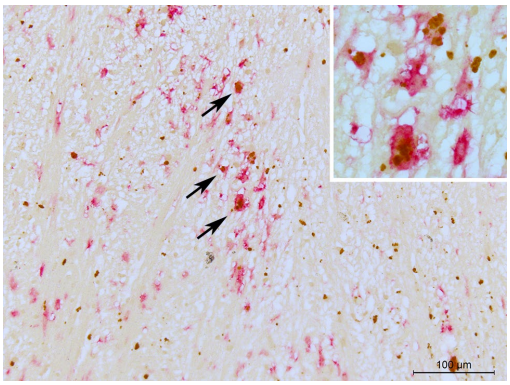

Figure 4. Double staining of lesion for identification of LGMN positive cells. (LGMN (DAB, brown) in HLA-DR (Alkaline phosphatase, reddish pink) positive cells (arrows), ×20 magnification and insert at ×63 magnification.

assay for quantification was developed. The protein levels for the three candidates were not significantly different between relapsing–remitting multiple sclerosis patients (n = 22) and OIND (n = 7) OND (n = 6) or healthy controls (n = 9) as illustrated in Supplementary Data 3. These results demonstrate that LGMN, C1Q and HEMO did not show potential as a diagnostic- or prognostic marker in the samples investigated.

Discussion

A high number of identified and regulated proteins in the brains of mice subjected to either EAE or CPZ exposure allowed for an extensive comparison of the brain proteomes in these two models. Several differences, both at single-protein and protein network levels were found. Proteome comparison between CPZ-42d and controls indicate that pathways annotated to inflammation, migration and integrin signaling, microglia/macrophage activation, astrocytosis and demyelination were affected during CPZ de-/remyelination. These events were less prominent in the brains of EAE mice at the disease peak (EAE-16d), and even less at the recovery phase (EAE-32d). Acute phase associated proteins, granins and glutamate homeostasis proteins were significantly altered in EAE-16d, and the latter were also altered in EAE-32d. Although inflammation and T-cell infiltration predominantly occurs in the spinal cord in the EAE model[32] pathological changes also occur in the brain [33,34]. In the latter studies, the areas outside the inflammatory foci revealed regulation of proteins potentially involved in neurodegenerative processes rather than regulation of proteins in general inflammatory processes. This supports the fact that we did not observe many proteins involved in inflammation in the EAE mouse brains.

LGMN was highly upregulated in CPZ-42d (Table 3A) and associated with protein networks known to be affected by multiple sclerosis (Fig. 2). LGMN is a lysosomal multifunctional protein that can exert situation dependent endopeptidase, carboxypeptidase and ligase activity[26]. LGMN has been shown to bind to ISG15 as illustrated in the predicted ISG15 network (Fig. 2D), and might thus be a target substrate for ISGylation to regulate LGMN activity. ISGylation is the conjugation of ISG15 to target substrates with the help of an enzymatic cascade, suggested to play a role as an endogenous neuroprotective mechanism[35]. Expression of ISG15 and its conjugation is most likely the by-product of IFN 1 response. ISG15 acts as a chemotactic factor, and the secreted form can induce natural killer cell proliferation.

In addition to LGMN, four other lysosomal proteases were upregulated in CPZ-42d, the cathepsins CATB, CATD, CATS and CATZ, and the lysosomal pathway was overrepresented in this dataset according to the DAVID analysis. An increased activity of cathepsins might contribute to increased multiple sclerosis disease activity[36]. LGMN has previously been suggested to play a role in antigen presentation in multiple sclerosis[37].

The increased LGMN expression in HLA-DR (MHC-II) immunopositive cells indicate an association with inflammatory activity in the MS-lesion[38]. Although we were not able to confirm increased immunopositivity for LGMN in neurons in normal-appearing cortex of MS patients due to limitations within the tissue samples, translocation of LGMN from the lysosomes to cytosol has been observed in other pathological conditions such as Alzheimer's disease[39,40] and colorectal cancer[41,42]. In microscopically normal appearing multiple sclerosis brain tissue, the LGMN gene, among other genes related to proteolytic processing, is hypo-methylated and more extensively transcribed compared to controls without neurological disease[43].

The network "Cellular assembly and organization, Neurological disease, Organismal development" was predicted with a high score for EAE-16d in IPA (Supplementary Fig. 2B) and involved the acute phase proteins HEMO (hemopexin, gene: HPX), A1AT (alpha-1-antitrypsin 1–1, gene: SERPINA1) and CO3 (complement 3, gene: C3). HEMO and A1AT1 were highly upregulated in EAE-16d (Table 3C) and have previously been suggested as affected candidates from proteomics of CSF from rats with EAE[30]. HEMO has also been observed to

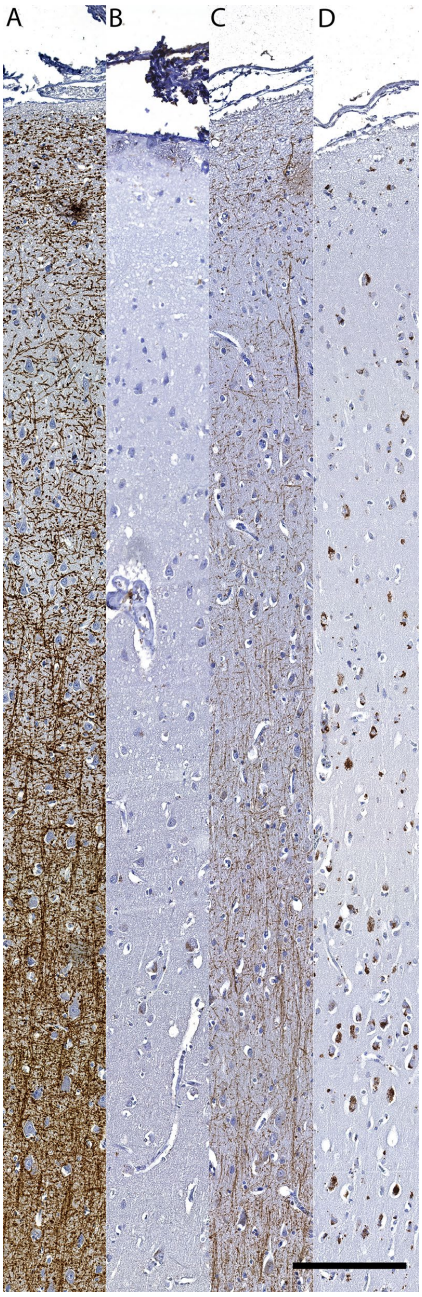

Figure 5. Increased LGMN expression in multiple sclerosis normal appearing cerebral cortex. LGMN (**A,B**) and myelin (**C,D**) immunostaining of cortex from a multiple sclerosis case (**B,D**) and control (**A,C**). Throughout all cortical layers there is reduced myelin content, and an increase in LGMN immunopositivity. Scale bar 200 μm.

be upregulated in plasma of pediatric multiple sclerosis patients[31], however, the protein was not significantly regulated in CSF in our PRM study.

When looking at other serpin family members in our dataset, we found that SPA3K, ANT3 and AIAT2 also were upregulated in EAE-16d suggesting a role in multiple sclerosis pathophysiology for several of the serpin family members. SPA3N (Alpha-1-antichymotrypsin), a verified candidate biomarker in CSF for secondary progressive multiple sclerosis[44] was upregulated in CPZ42d (only found in TMT). In contrast to EAE-16d, where only upregulation of CO3 was observed, complement C1Q subunits A, B and C were highly upregulated in CPZ-42d (Table 3A). This observation is in accordance with the high degree of demyelination and microglia activity seen in CPZ-42d (Supplementary Fig. 1C). In multiple sclerosis, activation of the classical complement pathway has been shown to occur especially in reactive astrocytes adjacent to clusters of microglia with opsonized myelin and damaged axons[29].

An increase of immunoglobulin IGKC was observed in both EAE-16d and EAE-32d but not in CPZ-42d and an increase has been reported to occur in CSF from multiple sclerosis patients[45]. The increase in EAE, and not the CPZ model, could be due to the involvement of T-cell infiltration in EAE.

In our frontal cortex proteomics approach, we observed that most of the proteins regulated in CPZ were not regulated in EAE and vice versa. As we were analyzing brain tissue form the frontal hemisphere, we would expect to characterize proteins from both glia cells and neurons given that the glia to neuron ratio in this tissue is suggested to be approximately 1:1[46]. However, in EAE and CPZ mice the numbers of certain glia cells and neurons are likely to have been altered [10,47] thereby affecting the global brain proteomes investigated. We did not observe differential regulation in neuronal markers in EAE or CPZ, however an increased number of astrocyte protein markers (increased GFAP and VIME) and a decreased level of oligodendrocyte protein markers (MOG, MAG, MBP, CLD11 and ERMIN) was observed in CPZ-42d with only tendencies in EAE-16d and EAE-32d. ERMIN, which was significantly downregulated in CPZ-42d (Table 3B) is an oligodendrocyte specific cytoskeleton-related protein involved in myelination in humans[48]. ERMIN has not previously been associated with multiple sclerosis and the regulation of this protein should thus be investigated further during phases of de- and remyelination in patients.

In CPZ-42d we observed upregulated macrophage/microglia markers ITAM (CD11B) and HEXB[49] indicating an increase in the number of these cell types; this was not observed in EAE. Furthermore, the galectins LEG3 (LGALS3) and LEG1 (LGALS1) were upregulated in CPZ-42d (fold change 3.7 and 1.6, respectively), and associated with the "Tissue development" network in IPA (Supplementary Fig. 2C). In cuprizone mice, it has been demonstrated that LEG3 is expressed in microglial cells, where one of its roles is to facilitate the onset of remyelination[50]. These findings are in accordance with our previous observations of astrocytosis, increased macrophage/microglia and loss of oligodendrocytes in the CPZ model[10]. In EAE, lesions are predominantly observed in the spinal cord[32], however, pathological changes have also been seen in brain tissue remote from inflammatory areas[33,34], as demonstrated in this study. Thus, protein regulations we observed in EAE might be pathological events in areas adjacent to inflammatory lesions, which may potentially reflect changes at an early stage prior to lesion formation, being involved in protecting healthy tissue and assisting repair of inflicted areas.

Conclusion

Based on the regulation of proteins quantified in the frontal cortex different pathway- and biological function signatures could be assigned to cuprizone and EAE models of multiple sclerosis. Differences in processes relevant to multiple sclerosis pathophysiology were indicated, such as myelinogenesis, lysosomal pathways, amino acid transport, acute phase signaling and glutamate signaling. Elevated expression of LGMN in human white matter active and chronic active lesions was associated with activated MHC class II positive microglia and macrophages, which could have clinical applicability in detecting ongoing inflammatory activity in multiple sclerosis if a corresponding association could be verified in serum or CSF of MS patients. The proteins LGMN, HEMO and C1Q were not significantly altered in CSF from multiple sclerosis patients investigated. Even if the number of patients in each category is small, this suggests that measurements of those proteins in CSF will have limited value in separating the examined groups.

Received: 30 September 2020; Accepted: 19 February 2021
Published online: 30 March 2021

References

1. Compston, A. & Coles, A. Multiple sclerosis. *Lancet* **372**, 1502–1517 (2008).
2. Singh, V., Tripathi, A. & Dutta, R. Proteomic approaches to decipher mechanisms underlying pathogenesis in multiple sclerosis patients. *Proteomics* **19**, 1800335. https://doi.org/10.1002/pmic.201800335 (2019).
3. Teunissen, C. E., Malekzadeh, A., Leurs, C., Bridel, C. & Killestein, J. Body fluid biomarkers for multiple sclerosis—The long road to clinical application. *Nat. Rev. Neurol.* **11**, 585–596. https://doi.org/10.1038/nrneurol.2015.173 (2015).
4. Werner, S. R. *et al.* Proteomic analysis of demyelinated and remyelinating brain tissue following dietary cuprizone administration. *J. Mol. Neurosci. (MN)* **42**, 210–225. https://doi.org/10.1007/s12031-010-9354-9 (2010).
5. Linker, R. A. *et al.* Proteome profiling in murine models of multiple sclerosis: Identification of stage specific markers and culprits for tissue damage. *PLoS ONE* **4**, e7624. https://doi.org/10.1371/journal.pone.0007624 (2009).
6. Hauser, S. L. *et al.* Ocrelizumab versus Interferon Beta-1a in relapsing multiple sclerosis. *N. Engl. J. Med.* https://doi.org/10.1056/NEJMoa1601277 (2016).
7. Lyons, J. A., Ramsbottom, M. J. & Cross, A. H. Critical role of antigen-specific antibody in experimental autoimmune encephalomyelitis induced by recombinant myelin oligodendrocyte glycoprotein. *Eur. J. Immunol.* **32**, 1905–1913. https://doi.org/10.1002/1521-4141(200207)32:7%3c1905::AID-IMMU1905%3e3.0.CO;2-L (2002).

8. Mony, J. T., Khorooshi, R. & Owens, T. MOG extracellular domain (p1–125) triggers elevated frequency of CXCR3+ CD4+ Th1 cells in the CNS of mice and induces greater incidence of severe EAE. *Mult. Scler.* **20**, 1312–1321. https://doi.org/10.1177/1352458514524086 (2014).
9. Wergeland, S. *et al.* Dietary vitamin D3 supplement reduces demyelination in the cuprizone model. *Neurology* **76**, A387–A387 (2011).
10. Wergeland, S., Torkildsen, Ø., Myhr, K. M., Mørk, S. J. & Bø, L. The cuprizone model: Regional heterogeneity of pathology. *APMIS* **120**, 648–657. https://doi.org/10.1111/j.1600-0463.2012.02882.x (2012).
11. Oveland, E. *et al.* Proteomic evaluation of inflammatory proteins in rat spleen interstitial fluid and lymph during LPS-induced systemic inflammation reveals increased levels of ADAMST1. *J. Proteome Res.* **11**, 5338–5349. https://doi.org/10.1021/pr3005666 (2012).
12. Vaudel, M., Barsnes, H., Berven, F. S., Sickmann, A. & Martens, L. SearchGUI: An open-source graphical user interface for simultaneous OMSSA and X!Tandem searches. *Proteomics* **11**, 996–999. https://doi.org/10.1002/pmic.201000595 (2011).
13. Vaudel, M. *et al.* PeptideShaker enables reanalysis of MS-derived proteomics data sets. *Nat. Biotechnol.* **33**, 22–24. https://doi.org/10.1038/nbt.3109 (2015).
14. Bø, L. *et al.* Detection of MHC class II-antigens on macrophages and microglia, but not on astrocytes and endothelia in active multiple sclerosis lesions. *J. Neuroimmunol.* **51**, 135–146 (1994).
15. Bø, L., Vedeler, C. A., Nyland, H. I., Trapp, B. D. & Mørk, S. J. Subpial demyelination in the cerebral cortex of multiple sclerosis patients. *J. Neuropathol. Exp. Neurol.* **62**, 723–732 (2003).
16. Teunissen, C. E. *et al.* A consensus protocol for the standardization of cerebrospinal fluid collection and biobanking. *Neurology* **73**, 1914–1922. https://doi.org/10.1212/WNL.0b013e3181c47cc2 (2009).
17. Cox, J. & Mann, M. 1D and 2D annotation enrichment: A statistical method integrating quantitative proteomics with complementary high-throughput data. *BMC Bioinform.* **13 Suppl 16**, S12, https://doi.org/10.1186/1471-2105-13-S16-S12 (2012).
18. Huang, D. W. *et al.* DAVID bioinformatics resources: Expanded annotation database and novel algorithms to better extract biology from large gene lists. *Nucleic Acids Res.* **35**, W169-175. https://doi.org/10.1093/nar/gkm415 (2007).
19. Kanehisa, M., Goto, S., Sato, Y., Furumichi, M. & Tanabe, M. KEGG for integration and interpretation of large-scale molecular data sets. *Nucleic Acids Res.* **40**, D109-114. https://doi.org/10.1093/nar/gkr988 (2012).
20. Baron, D. *et al.* MADGene: Retrieval and processing of gene identifier lists for the analysis of heterogeneous microarray datasets. *Bioinformatics* **27**, 725–726. https://doi.org/10.1093/bioinformatics/btq710 (2011).
21. Guldbrandsen, A. *et al.* In-depth characterization of the cerebrospinal fluid (CSF) proteome displayed through the CSF proteome resource (CSF-PR). *Mol. Cell. Proteom. (MCP)* **13**, 3152–3163. https://doi.org/10.1074/mcp.M114.038554 (2014).
22. Vizcaino, J. A. *et al.* ProteomeXchange provides globally coordinated proteomics data submission and dissemination. *Nat. Biotechnol.* **32**, 223–226. https://doi.org/10.1038/nbt.2839 (2014).
23. Vizcaino, J. A. *et al.* The PRoteomics IDEntifications (PRIDE) database and associated tools: Status in 2013. *Nucleic Acids Res.* **41**, D1063-1069. https://doi.org/10.1093/nar/gks1262 (2013).
24. Brockschnieder, D., Sabanay, H., Riethmacher, D. & Peles, E. Ermin, a myelinating oligodendrocyte-specific protein that regulates cell morphology. *J. Neurosci.* **26**, 757–762. https://doi.org/10.1523/JNEUROSCI.4317-05.2006 (2006).
25. Benveniste, E. N., Liu, Y., McFarland, B. C. & Qin, H. Involvement of the janus kinase/signal transducer and activator of transcription signaling pathway in multiple sclerosis and the animal model of experimental autoimmune encephalomyelitis. *J. Interferon Cytokine Res.* **34**, 577–588. https://doi.org/10.1089/jir.2014.0012 (2014).
26. Dall, E. & Brandstetter, H. Structure and function of legumain in health and disease. *Biochimie* **122**, 126–150. https://doi.org/10.1016/j.biochi.2015.09.022 (2016).
27. Zhao, C., Denison, C., Huibregtse, J. M., Gygi, S. & Krug, R. M. Human ISG15 conjugation targets both IFN-induced and constitutively expressed proteins functioning in diverse cellular pathways. *Proc. Natl. Acad. Sci. U.S.A.* **102**, 10200–10205. https://doi.org/10.1073/pnas.0504754102 (2005).
28. Satoh, J.-I., Asahina, N., Kitano, S. & Kino, Y. Legumain is expressed on macrophages in active demyelinating lesions of multiple sclerosis. *Clin. Exp. Neuroimmunol.* **6**, 304–305. https://doi.org/10.1111/cen3.12208 (2015).
29. Ingram, G. *et al.* Complement activation in multiple sclerosis plaques: An immunohistochemical analysis. *Acta Neuropathol. Commun.* **2**, 53. https://doi.org/10.1186/2051-5960-2-53 (2014).
30. Rosenling, T. *et al.* Profiling and identification of cerebrospinal fluid proteins in a rat EAE model of multiple sclerosis. *J. Proteome Res.* **11**, 2048–2060. https://doi.org/10.1021/pr201244t (2012).
31. Rithidech, K. N. *et al.* Protein expression profiles in pediatric multiple sclerosis: Potential biomarkers. *Mult. Scler.* **15**, 455–464. https://doi.org/10.1177/1352458508100047 (2009).
32. Simmons, S. B., Pierson, E. R., Lee, S. Y. & Goverman, J. M. Modeling the heterogeneity of multiple sclerosis in animals. *Trends Immunol.* **34**, 410–422. https://doi.org/10.1016/j.it.2013.04.006 (2013).
33. Zeis, T., Kinter, J., Herrero-Herranz, E., Weissert, R. & Schaeren-Wiemers, N. Gene expression analysis of normal appearing brain tissue in an animal model for multiple sclerosis revealed grey matter alterations, but only minor white matter changes. *J. Neuroimmunol.* **205**, 10–19. https://doi.org/10.1016/j.jneuroim.2008.09.009 (2008).
34. Castegna, A. *et al.* Oxidative stress and reduced glutamine synthetase activity in the absence of inflammation in the cortex of mice with experimental allergic encephalomyelitis. *Neuroscience* **185**, 97–105. https://doi.org/10.1016/j.neuroscience.2011.04.041 (2011).
35. Jeon, Y. J., Yoo, H. M. & Chung, C. H. ISG15 and immune diseases. *Biochim. Biophys. Acta* **485–496**, 2010. https://doi.org/10.1016/j.bbadis.2010.02.006 (1802).
36. Haves-Zburof, D. *et al.* Cathepsins and their endogenous inhibitors cystatins: Expression and modulation in multiple sclerosis. *J. Cell Mol. Med.* **15**, 2421–2429. https://doi.org/10.1111/j.1582-4934.2010.01229.x (2011).
37. Manoury, B. *et al.* Destructive processing by asparagine endopeptidase limits presentation of a dominant T cell epitope in MBP. *Nat. Immunol.* **3**, 169–174. https://doi.org/10.1038/ni754 (2002).
38. Solberg, R. *et al.* Legumain expression, activity and secretion are increased during monocyte-to-macrophage differentiation and inhibited by atorvastatin. *Biol. Chem.* **396**, 71–80. https://doi.org/10.1515/hsz-2014-0172 (2015).
39. Zhang, Z. *et al.* Cleavage of tau by asparagine endopeptidase mediates the neurofibrillary pathology in Alzheimer's disease. *Nat. Med.* **20**, 1254–1262. https://doi.org/10.1038/nm.3700 (2014).
40. Basurto-Islas, G., Grundke-Iqbal, I., Tung, Y. C., Liu, F. & Iqbal, K. Activation of asparaginyl endopeptidase leads to Tau hyperphosphorylation in Alzheimer disease. *J. Biol. Chem.* **288**, 17495–17507. https://doi.org/10.1074/jbc.M112.446070 (2013).
41. Haugen, M. H. *et al.* Nuclear legumain activity in colorectal cancer. *PLoS ONE* **8**, e52980. https://doi.org/10.1371/journal.pone.0052980 (2013).
42. Haugen, M. H. *et al.* High expression of the cysteine proteinase legumain in colorectal cancer—Implications for therapeutic targeting. *Eur. J. Cancer* **51**, 9–17. https://doi.org/10.1016/j.ejca.2014.10.020 (2015).
43. Huynh, J. L. *et al.* Epigenome-wide differences in pathology-free regions of multiple sclerosis-affected brains. *Nat. Neurosci.* **17**, 121–130. https://doi.org/10.1038/nn.3588 (2014).
44. Kroksveen, A. C. *et al.* Cerebrospinal fluid proteomics in multiple sclerosis. *Biochim. Biophys. Acta* **746–756**, 2015. https://doi.org/10.1016/j.bbapap.2014.12.013 (1854).
45. Kroksveen, A. C. *et al.* Cerebrospinal fluid proteome comparison between multiple sclerosis patients and controls. *Acta Neurol. Scand. Suppl.* 90–96, https://doi.org/10.1111/ane.12029 (2012).

46. Herculano-Houzel, S., Mota, B. & Lent, R. Cellular scaling rules for rodent brains. *Proc. Natl. Acad. Sci. U.S.A.* **103**, 12138–12143. https://doi.org/10.1073/pnas.0604911103 (2006).
47. Duffy, S. S., Lees, J. G. & Moalem-Taylor, G. The contribution of immune and glial cell types in experimental autoimmune encephalomyelitis and multiple sclerosis. *Mult. Scler. Int.* **2014**, 285245. https://doi.org/10.1155/2014/285245 (2014).
48. Wang, T. *et al.* Human Ermin (hErmin), a new oligodendrocyte-specific cytoskeletal protein related to epileptic seizure. *Brain Res.* **1367**, 77–84. https://doi.org/10.1016/j.brainres.2010.10.003 (2011).
49. Butovsky, O. *et al.* Identification of a unique TGF-beta-dependent molecular and functional signature in microglia. *Nat. Neurosci.* **17**, 131–143. https://doi.org/10.1038/nn.3599 (2014).
50. Hoyos, H. C. *et al.* Galectin-3 controls the response of microglial cells to limit cuprizone-induced demyelination. *Neurobiol. Dis.* **62**, 441–455. https://doi.org/10.1016/j.nbd.2013.10.023 (2014).

Author contributions

E.O., F.S.B., I.A., K.M.M., L.B. and S.W. conceptualized and designed the study and experiments. E.O., F.S.B. and S.W. wrote the manuscript. I.A., L.B. and S.W. performed E.A.E. and cuprizone experiments and immunohistochemistry including scoring and statistical analysis. E.O., R.R.L., A.C.K., H.B., A.G., F.S.B. designed and conducted the proteomic analyses including PRM analysis of human CSF, and interpreted results. I.A., S.W. and L.B. collected samples and analyzed human MS tissue samples. All authors reviewed the manuscript. EO Prepared Figs. 1, 2 and S2, the graphical abstract, Table 3 and supplementary data 1–3. IA and SW prepared Figs. 3–5, Figure S1. S.W. prepared Tables 1, 4 and 5. F.S.B. and A.G. prepared Table 2. E.O., F.S.B., I.A. and S.W. wrote supplementary methods.

Funding

This work received financial support from the Kristian Gerhard Jebsen foundation for Multiple Sclerosis research. H.B. was supported by the Research Council of Norway. KMM, LB and SW are funded by the Research Council of Norway (project no. 288164).

Competing interests

The authors declare no competing interests.

Additional information

Supplementary Information The online version contains supplementary material available at https://doi.org/10.1038/s41598-021-86191-5.

Correspondence and requests for materials should be addressed to S.W.

Reprints and permissions information is available at www.nature.com/reprints.

Publisher's note Springer Nature remains neutral with regard to jurisdictional claims in published maps and institutional affiliations.

Supplementary Figure S1.

A

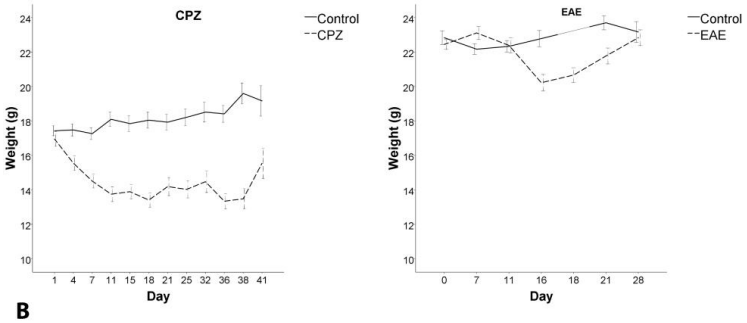

B

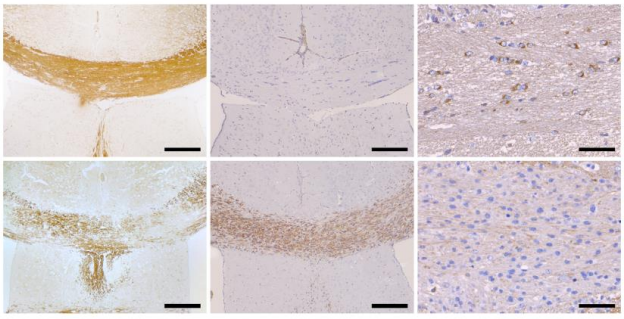

C

	Myelin (PLP)		Microglia (mac-3)		Oligodendrocytes (NOGO-A)	
	IR (%, mean)	SD	Cells/mm^2 (mean)	SD	Cells/mm^2 (mean)	SD
CTR	89.1	7.5	22.4	14.3	988.8	137.6
CPZ	56.7	16.5	4320	765.7	96	92.6

D

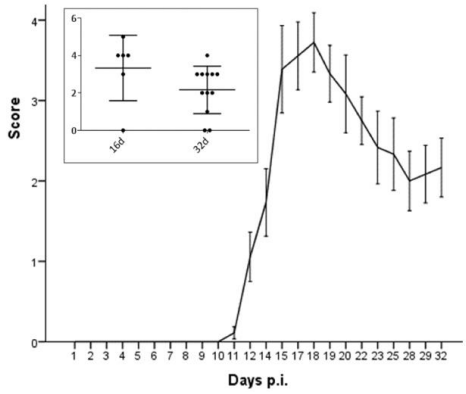

Supplementary Figure S2.

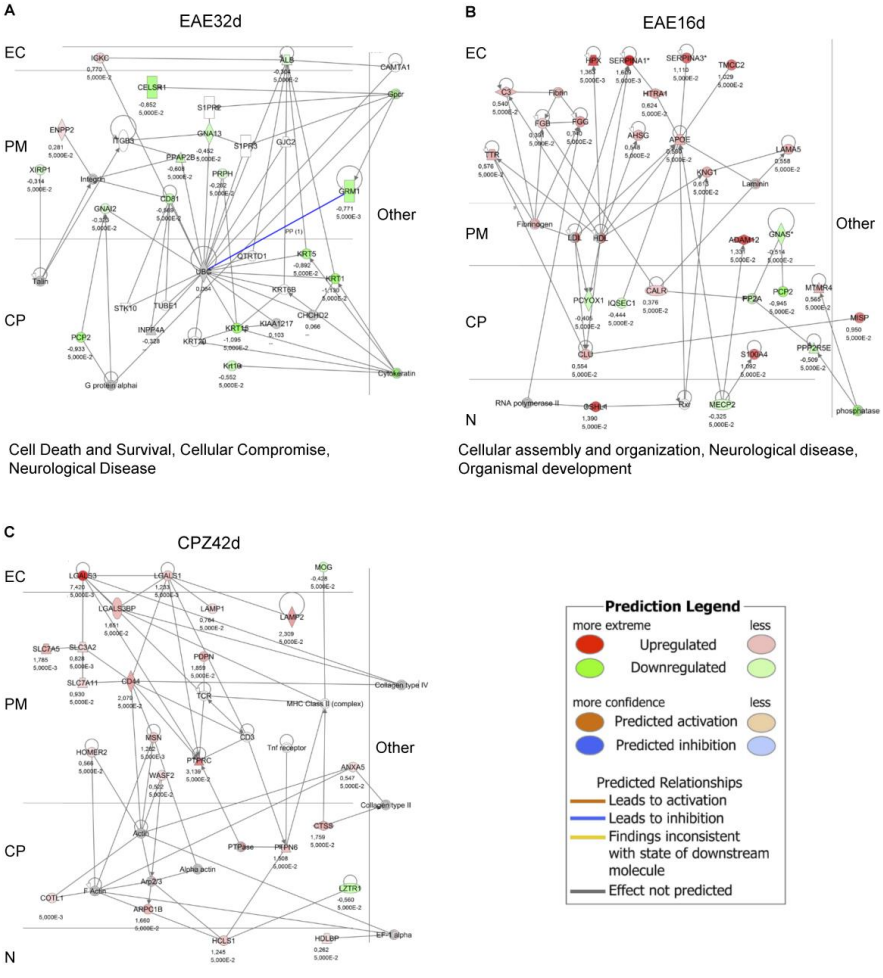

Cell Death and Survival, Cellular Compromise, Neurological Disease

Cellular assembly and organization, Neurological disease, Organismal development

Tissue Development, Cell-To-Cell Signaling and Interaction, Cellular Function and Maintenance

Supplementary methods

Cuprizone and EAE mouse frontal cortex proteomics revealed proteins altered in multiple sclerosis

Eystein Oveland[1], Intakhar Ahmad[2,3], Ragnhild Reehorst Lereim[1,2], Ann Cathrine Kroksveen[1,2], Harald Barsnes[1,4], Astrid Guldbrandsen[1,2,3], Kjell-Morten Myhr[2,6], Lars Bø[2,3,6], Frode S. Berven[1,3*], Stig Wergeland [3,5,6*§]

[1] Proteomics Unit at the University of Bergen (PROBE), Department of Biomedicine, University of Bergen, Norway.

[2] Department of Clinical Medicine, University of Bergen, Norway.

[3] Norwegian Multiple Sclerosis Competence Centre, Department of Neurology, Haukeland University Hospital, Bergen, Norway.

[4] Department of Clinical Science, University of Bergen, Norway.

[5] The Norwegian Multiple Sclerosis Registry and Biobank, Department of Neurology, Haukeland University Hospital, Bergen, Norway.

[6] Neuro-SysMed, Department of Neurology, Haukeland University Hospital, Bergen, Norway.

[*]Co-senior authors

Immunohistochemistry

Specification of antibodies and staining protocols

Antibody	Provider	Reactivity	Dilution	Antigen retrieval	Incubation
Proteolipid protein (PLP)	Serotec	Mouse	1:1000		ON @ 4 °C
Neurite outgrowth inhibitor protein A (NOGO-A)	Chemicon	Mouse	1:1000		1h @ RT
Mac-3	BD Biosciences	Mouse	1:200		ON @ 4 °C
Legumain (LGMN)	Sigma-Aldrich	Human	1:200	DIVA	2hrs @ RT
PLP	Abcam	Human	1:1000	DIVA	ON @ 4 °C
HLA-DR	DAKO (Agilent)	Human	1:20	DIVA	2hrs @ RT
GFAP	DAKO (Agilent)	Human	1:50	DIVA	2hrs @ RT
O1	Thermo Fisher Scientific Inc.	Human	1:50	DIVA	2hrs @ RT
O4	MyBioSource	Human	1:50	DIVA	2hrs @ RT
ON: Overnight, RT: Room temperature					

Digitalization of stained sections

PLP, HLA and LGMN stained sections were digitized using a Scanscope XT slide scanner (Aperio Technologies; Vista, CA) using an Olympus UPLSAPO 40× objective (Olympus, Southend-on-Sea, UK) and Techniquip Model 21DC Light source (Techniquip, Pleasanton, California, USA), with a GE quartzline projector lamp model EKE 21 V 150 W (General Electric, Fairfield, Connecticut, USA). Images were scanned with a final resolution of 0.247 µm

per pixel. The virtual slides were saved using the Aperio NDPI file format. Virtual slides were viewed in Aperio Imagescope software V.12 (Aperio, Vista, California, USA).

Experimental autoimmune encephalomyelitis

25 µg recombinant human MOG (rh-MOG, MOG1-125 from Hooke Labs, Lawrence, MA) was emulsified in Freund's adjuvant with 1mg/ml M. tuberculosis H37RA (Sigma-Aldrich) to a total volume of 0.1ml and injected subcutaneously at Day 0 (day of immunization). In addition, 200 ng of Pertussis toxin (Sigma-Aldrich) was injected intra-peritoneally at Day 0 and at post-immunization (p.i.) Day 2. The EAE clinical disease activity was scored from 0-8 (0: Healthy, 1: Tail weakness, 2: Tail paralysis, 3: Mild hind leg paresis, 4: Severe hind leg paresis, 5: Paralysis of one hind leg, 6: Complete paralysis of both hind legs, 7: Tetraparalysis, 8: Death) (Supplementary Fig. 1).

Tissue homogenization and protein extraction

The brain tissue was thawed on ice and immediately added 200 µl 50 mM triethylammonium bicarbonate (TEAB) buffer containing 8 M urea, 30 µl/ml complete mini protease inhibitor cocktail (Roche), 1 mM heat-activated sodium vanadate (Tyr phosphatase inhibition) and 10 mM NaF (Ser/Thr-phosphatase inhibition). The tissue was then homogenized by sonication (High Intensity Ultrasonic Processor 50 W, Sonics & Materials Inc.). The sample was left on ice for 30 min, centrifuged at 16.000g for 20 min, and the supernatant was transferred to a fresh tube and stored at -80ºC until LC-MS/MS analyses.

TMT-labeling and protein quantification

Mixed mode fractionation of the TMT-labeled peptides sample

The TMT-labeled tryptic peptides were fractionated in 60 fractions using mixed-mode HPLC chromatography. The dried TMT-labeled peptides (TMT-mix) were reconstituted in 400 µl buffer A (20 mM ammonium formate, 3% acetonitrile (ACN)). 100 µl of the sample was loaded onto a Sielc Promix column (MP-10.250.0530, 1.0 × 250 mm, 5 µm, 300Å, Sielc Technologies) using an Agilent 1260 LC system with Chemstation Rev. B0.4.0 (Agilent Technologies) using 85% A for 10 min at a flow rate of 50 µl/min. The peptides were eluted using a gradient of 15% - 60% buffer B (2 mM ammonium formate, 80% ACN, pH 3.0) over 35 min, 60%-100% B over 10 min and held constant for 5 min. The sample was fractionated into 60 fractions in a 96-well plate, one fraction (approximately 58.5 µl) was collected every 1.16 min until 70 min. The plate was frozen in -80ºC and peptides lyophilized in a vacuum concentrator (Centrivap with a Cold trap, Labconco) at 30ºC. The peptide powder was reconstituted in 10 µl 0.1% FA and transferred to HPLC-tubes.

Orbitrap LC-MS of TMT-labeled mixed mode fractions

Approximately 0.5 µg of TMT-labeled peptides were loaded and desalted on a pre-column (Acclaim PepMap 100, 2cm x 75µm i.d. nanoViper column, packed with 3 µm C18 beads, Thermo Scientific). The flow rate was 5 µl/min for 6 min with an isocratic flow of 0.1 % FA with 2% ACN using an Ultimate NCS-3500RS (Dionex). Peptide separation and elution were accomplished on an analytical column (Acclaim PepMap 100, 15 cm x 75 µm i.d. nanoViper column, packed with 2 µm C18 beads) using a biphasic ACN gradient from two nanoflow UPLC pumps (flow rate of 280 nl/min). Solvent A was 0.1% FA with 2% ACN and solvent B 0.1% FA

with 90% ACN. The HPLC gradient was generated by mixing solvent A with the following percentage of solvent B: 5% from 0 to 5 min, up to 8% from 5 to 6 min, up to 20% from 6 to 60 min, up to 35% from 60 to 90 min, up to 90% from 90 to 100 min, held at 90% from 100 to 105 min, down to 5% from 105 to 108 min, and held at 5% until 120 min.

The eluting peptides were ionized in the electrospray and analyzed by the LTQ-Orbitrap Velos Pro (Thermo Scientific). The mass spectrometer was operated in the DDA-mode (data-dependent-acquisition) to automatically switch between one survey full scan MS (FTMS) and 14 MS/MS acquisitions (ITMS). The instrument control was through Tune 2.7 and Xcalibur 2.2. The FTMS scans (from 300 to 2000 m/z) were acquired for 110 min in the Orbitrap with a resolution R = 60000 at 400 m/z (after accumulation to a target value of 1E6 in the linear ion trap with maximum allowed ion accumulation time of 500 ms).

The 7 most intense eluting peptides above an ion threshold value of 1000 counts and charge states 2 or higher, were sequentially isolated in a back-to-back analysis of same-precursors using two different fragmentation techniques, (i) CID (Collision-Induced Dissociation) and (ii) HCD (Higher-Energy Collision Dissociation).

(i) Ions were isolated to a target value of 1E4 at a maximum ion accumulation time of 200 ms, and fragmented in the high-pressure linear ion trap by low-energy CID with normalized collision energy of 35% and wideband-activation enabled. The maximum allowed accumulation time for CID was 200 ms, isolation width maintained at 2 Da, activation q = 0.25, and activation time of 10 ms. Fragments were detected in the low-pressure ion trap at normal scan rate, and recorded with the secondary electron multipliers.

(ii) Ions were isolated in the high-pressure linear ion trap to a target value of 5E5 at a maximum allowed accumulation time of 1000 ms, and isolation width maintained at 3 Da. Fragmentation in the HCD cell was performed with a normalized collision energy of 40%, and activation time of 0.1 ms. Fragments were detected in the Orbitrap at a resolution of 7500 with first mass fixed at 90 m/z.

Two MS/MS spectra of a precursor mass were allowed before dynamic exclusion for 20 s. Lock-mass internal calibration was not enabled.

Analysis of the TMT LC-MS data using Proteome Discoverer

Proteome Discoverer version 1.4.1.14 (Thermo Scientific) was used for quantification and identification of the TMT data. MS Amanda and SEQUEST were used as search engines and the Swissprot database *Mus musculus* (with canonical sequence data in FASTA version 27.03.14) was used. The enzyme was set to trypsin and the max missed cleavages to 2. The precursor mass tolerance was 10 ppm with accepted precursor charges from +2 to +7, and the fragment mass tolerance was 0.05 Da. Carbamidomethyl of C, TMT6plex on K and TMT6plex on any N-terminus were set to fixed modifications. Oxidation of M was set to variable modification. The perculator was used with target FDR strict 0.01 and relaxed 0.05. The method “Most Confident Centroid” without Quan Value Corrections (recommended in the PD v1.4 manual) and an integration tolerance of 1000 ppm were used for quantification of the TMT peaks in the HCD spectra.

Label-free protein quantification

Protein digestion and peptide clean-up

Based on the protein measurements a volume corresponding to 10 µg of protein was denatured by adding 20 µl of Urea solution (8M urea/20 mM methylamine). The sample was then added 20 µl of Trypsination buffer (50 mM Tris HCl pH 8.0/1 mM $CaCl_2$) and shaken at RT for 5 min at 300 rpm in an Eppendorf mixer (Eppendorf, Hamburg, Germany).

Proteins were reduced by adding 4 µl of fresh 100 mM DTT to the tube and incubated for 1 hour at RT. The proteins were then alkylated by adding 5 µl of fresh 200 mM iodoacetamide and incubating for 1 h at RT in the dark. A volume of 0.8 µl 100 mM DTT was added and the sample incubated for 10 min.

A volume of 110 µl of Trypsination buffer was added to reduce the urea concentration to 1 M. Trypsin from a vial (Trypsin porcine, Promega art. No. V 5111) dissolved in 50 mM acetic acid was added to obtain a trypsin:protein ratio of 1:50 (w/w). The sample was incubated in an Eppendorf shaker at 300 rpm for 16h at 37ºC. After 16 h the trypsination was stopped by adding 15 µl of 10 % formic acid (FA).

The tryptic peptide mixture was desalted and concentrated using Oasis HLB uElution Plate 30 um (Part no 186001828BA, Waters). The eluted peptides were frozen in -80ºC and lyophilized in a vacuum concentrator (Centrivap with a Cold trap, Labconco) set to 30ºC. The peptides were reconstituted in 1 µl 100% FA and diluted to 0.5 µg/µl and 5% FA by adding 19 µl H_2O.

Orbitrap LC-MS of label-free samples

Tryptic peptides (2.5 µg) were separated during a biphasic acetonitrile (ACN) gradient from two nanoflow UPLC pumps (flow rate of 280 nl/min) on a 50 cm analytical column (Dionex #164570, Acclaim PepMap100 nanoViper column, 75 µm i.d. × 50 cm, packed with 3 µm C18 beads). Solvent A was 0.1% FA (vol/vol) with 2% ACN and solvent B was 0.1% FA (vol/vol) with 90% ACN (vol/vol). The gradient composition was solvent A for 5 minutes, then from 5 to 8% solvent B over 0.5 min, then 8% B for 4.5 min, then 8 to 25% B over 100 min, then 25 to 45% B over 60 min, then 45 to 90% B over 10 min, then 90% B for 10 min, followed by 90 to 5% B over 3 min, and finally 5% solvent B for 27 min. The gradient time (from 5 to 90% solution B) and the acquisition time for MS data were 180 min, and the whole HPLC run was 220 min.

The peptide samples (2.5 µg) were subjected to LC-MS analysis using 220 min runs with a biphasic acetonitrile gradient and a 50 cm nanoViper column using an Ultimate NCS-3500RS HPLC coupled to an LTQ-Orbitrap Velos Pro. The eluting peptides were ionized in the electrospray and analyzed by an LTQ-Orbitrap Velos Pro. The mass spectrometer was operated in the DDA-mode (data-dependent-acquisition) to automatically switch between full scan MS and MS/MS acquisition. Instrument control was through Tune 2.7 and Xcalibur 2.2. Survey full scan MS spectra (from 300 to 2000 m/z) were acquired for 180 min in the Orbitrap with a resolution R = 60000 at 400 m/z (after accumulation to a target value of 1E6 in the linear ion trap with maximum allowed ion accumulation time of 500 ms). The 7 most intense eluting peptides above a ion threshold value of 1000 counts, and charge states 2 or higher, were sequentially isolated to a target value of 1E4 and fragmented in the high-pressure linear ion trap by low-energy CID (collision-induced-dissociation) with normalized collision energy of 40% and

wideband-activation enabled. The maximum allowed accumulation time for CID was 200 ms, the isolation width maintained at 2 Da, activation q = 0.25, and activation time of 10 ms. The resulting fragment ions were scanned out in the low-pressure ion trap at normal scan rate, and recorded with the secondary electron multipliers. One MS/MS spectrum of a precursor mass was allowed before dynamic exclusion for 20 s. Lock-mass internal calibration was not enabled.

Analysis of the label-free LC-MS data using Progenesis LC-MS

Progenesis LC-MS® v2.6 (Nonlinear Dynamics Ltd) was used for LF quantification and comparison of LC-MS proteomics data based on the volume, m/z and retention time of the MS^1 features (peptides). In Progenesis, the LC-MS runs were automatically aligned, and only features with charges between +2 to +7 and containing associated MS/MS spectra were accepted for export as an mgf file for identification. The mgf file was searched against the UniProt database *Mus musculus* (SwissProt with canonical sequence data in FASTA version September 2012) using SearchGUI v1.8.9 (Vaudel *et al.*, 2011) . The search criteria were: trypsin as the protease with one miss-cleavages accepted, fixed carbamidomethylation on cystein, variable oxidation on methionine, precursor mass tolerance of 10 ppm, fragment mass tolerance of 0.7 and X!Tandem (version Cyclone) as the search engine. The search result and associated spectra were combined and assigned to proteins in PeptideShaker v0.17.3 (Vaudel *et al.*, 2015) at 1% FDR. The results were exported from PeptideShaker as validated PSMs in a Phenyx format, and imported back into Progenesis. The protein abundances reported from Progenesis were based on the sum of the normalized abundance of the identified unique peptides.

Parallel reaction monitoring (PRM) targeted quantification

Protein concentration in the CSF pools was measured by the BCA (Pierce), following the manufacturers protocol. All CSF samples were in-solution digested as previously described (4). About 1.5 µg CSF digested protein were injected for Legumain and C1q and about 0.2 ug for Hemopexin.

Preparation and spike-in of synthetic peptides

All isotopic labelled peptides (IS peptides), C-terminally modified with 13C and 15N isotope arginine or lysine, used as internal standards were purchased from JPT Peptide Technologies with the highest quality (>95% purity) quality. The amount of spike-in per ug of CSF digested protein was 3 fmol for LGMN, 100 for HEMO and 14 fmol for C1Q . 2+ versions of the peptides were monitored.

PRM mass spectrometry

The separation of peptides was performed by an Ultimate™ 3000 RSLCnano System (Thermo Fisher Scientific™) with an Acclaim PepMap™ 100 trap column (diameter width at 75 µm x 2 cm nanoviper C18 column, with particle size 3 µm and length at 100 A) and 5 µL 0.1 % TFA solution. Peptides were separated on an analytical column PepMapTM RSLC C18 ES802 (diameter width 75 µm x 25 cm length, particle size at 2 µm) For the 90 minute method, the LC gradient was a combination of 95 % solvent A (0.1 % FA) and 5 % solvent B (100 % ACN, 0.1 % FA) with a flow rate of 250 µl/min. The column gradient for peptide elution went from 0-5.5 min with 5 % solvent B, then an increase at 5.5– 7 min to 7 % of solvent B, 7 – 50 min increase to 22 % B, 50 – 65 min increase to 35 % B and 65 – 70 min increase to 80 % B. At 70 – 77 min solvent B was kept constant at 80% B, from 77-80 min decreased to 5 % B and held at 5 % solvent B from 80 – 90 min.

For the 40 minute method, the LC gradient was a combination of 95 % solvent A (0.1 % FA) and 5 % solvent B (100 % ACN, 0.1 % FA) with a flow rate of 250 µl/min. The column gradient for peptide elution went from 0-5.5 min with 5 % solvent B, then an increase at 5.5 – 7 min to 7 % of solvent B, 7 – 16.5 min increase to 25 % B, 16.5 – 22.2 min increase to 40 % B and 22.2 – 22.6 min increase to 80 % B. At 22.6 – 29.2 min solvent B was kept constant at 80% B, from 29.2-31 min decreased to 5 % B and held at 5 % solvent B from 31 – 40 min.

The mass spectrometry method duration was 90 min (for LGMN and C1q) and 40 min (for HEMO). The Q-Exactive HF mass spectrometer controlled through Q Exactive HF Tune 2.4 and Xcalibur 3.0 was operated in PRM scheduled mode with on full scan MS1 between every 12th PRM MS2 scan. The target peptides on the inclusion list were sequentially isolated for higher-energy collision dissociation (HCD) fragmentation and MS2 acquisition resolution was 60 000, automatic gain control (AGC) target of 2e5, isolation window 0.7m/z, CE 28 and a maximum injection time (IT) of 120 ms (118 ms for the 90 min method). Lock-mass (445.12003 m/z) internal calibration was used.

Skyline analysis

Skyline (29) settings were overall kept at default. Notably, structural modifications were specified with carbamidomethyl (C) and isotope modification “label: 13C(6) 15N(2) (C-term K)” and label: “13C(6) 15N(4) (C-term R)”.

The peak signal for each peptide was determined by the Skyline peak picking algorithm, and manually verified or re-integrated based on the fragment pattern of the peptide, elution profile and simultaneous retention time of the endogenous and the IS peptide. The three fragments with the highest intensity, low interference, and mass error less than 10 ppm was selected for quantitation. The area under the curve, excluding background, were summed to give one peak area value for each peptide.

Furthermore, the endogenous peak area was divided by the peak area of the heavy internal standard peptide to generate a ratio to standard used for calculating the amount of endogenous peptide in each sample in fmol/ug. An unpaired two tailed student's t-test was used to compare disease groups and a p-value of ≤ 0.05 would indicate significant difference.

Post-processing of proteomics data and availability

Perseus v1.4.1.3 was used to generate the unsupervised clustering heatmap with dendrograms of z-score normalized data using the default settings. GraphPad Prism 6 (GraphPad Prism Software) was used for the statistical analyses and graphics and Venn diagrams were created using Venny (http://bioinfogp.cnb.csic.es/tools/venny/index.html).

Ingenuity Pathway Analysis (IPA, Ingenuity Systems, http://www.ingenuity.com) was used for pathway and function analyses. The protein lists from the TMT-labelling and label-free experiments were combined and the average of the quantification values were used for the proteins detected in both experiments. In the IPA analysis, the proteins significantly altered with a fold change higher than 20% in both TMT and label-free were considered more significant (IPA P-value 0.005) than the proteins significantly regulated in only one of the experiments (IPA p-value 0.05). The relationships were set to "experimentally observed direct interactions". IPA reported the likelihood that proteins were associated with a pathway or upstream regulator ($p<0.05$ = significant) and the predicted direction of the change ($z \leq 2$ = decreased; $z \geq 2$ = increased). DAVID [24] was used to investigate the regulated proteins in KEGG pathways [25].

MADGENE [26] was used to convert the mouse accession numbers to human orthologues for comparison against the results in CSF-PR [14]. The Basic Local Alignment Search Tool (BLAST) in UniProt was used with default settings for the accession numbers not found by MADGENE.

References

Vaudel M, Barsnes H, Berven FS, Sickmann A, Martens L. SearchGUI: An open-source graphical user interface for simultaneous OMSSA and X!Tandem searches. Proteomics 2011; 11: 996-9.

Vaudel M, Burkhart JM, Zahedi RP, Oveland E, Berven FS, Sickmann A, et al. PeptideShaker enables reanalysis of MS-derived proteomics data sets. Nat Biotechnol 2015; 33: 22-4.

Supplementary material

Supplementary File 1: Supplementary Figure 1. EAE and CPZ mice disease course and histopathology.

The average weight of the (**A)** CPZ mice and (**B**) EAE mice were lower than for the respective controls as previously reported (Wergeland *et al.*, 2011). (**C**) For CPZ mice (sacrificed at day 42) we observed demyelination (luxol fast blue, Anti-PLP), increased number of activated microglia cells (anti-Mac3) and a loss of oligodendrocytes (anti-NOGO-A) in accordance with previous results (Wergeland *et al.*, 2012a). (**D**) The clinical score of the EAE mice at different time points after peritoneal injection of rhMOG1-125, the scoring of the mice sacrificed after 16d (EAE-16d, disease peak) and after 32d (EAE-32d, partial recovery) are shown (insert); the respective control animals had a clinical score of zero. Error bars represent +/- 1 SD.

Supplementary File 2: Supplementary Figure 2. Predicted protein networks and diseases from EAE and CPZ proteomics data.

The protein ratios relative to respective controls for EAE-16d, EAE-32d and CPZ-42d from TMT and label-free were combined prior to analyses in IPA. The significance level of regulation (IPA "p-value") was set to 0.005 if the protein was significantly regulated with more than 1.2-fold in both TMT and label-free experiments and 0.05 if in only one experiment. The average $\log_2$ ratio and the IPA "p-value" from the combined TMT and label-free protein list are shown for each protein node. Networks predicted with high score in IPA are shown for (**A**) EAE-32d, (**B**) EAE-16d and (**C**) CPZ-42d.

Supplementary File 3. Supplementary methods.

Supplementary File 4. Supplementary Data 1. All proteins quantified using TMT including label free if found.

https://static-content.springer.com/esm/art%3A10.1038%2Fs41598-021-86191-5/MediaObjects/41598_2021_86191_MOESM4_ESM.xlsx

Supplementary File 5. Supplementary Data 2. All proteins quantified using label-free proteomics.

https://static-content.springer.com/esm/art%3A10.1038%2Fs41598-021-86191-5/MediaObjects/41598_2021_86191_MOESM5_ESM.xlsx

Supplementary File 6. Supplementary Data 3. PRM quantification of LGMN, C1Q and HEMO in human CSF.

https://static-content.springer.com/esm/art%3A10.1038%2Fs41598-021-86191-5/MediaObjects/41598_2021_86191_MOESM6_ESM.xlsx

Paper-2

PLOS ONE

RESEARCH ARTICLE

A higher proportion of ermin-immunopositive oligodendrocytes in areas of remyelination

Intakhar Ahmad[1,2], **Stig Wergeland**[2], **Eystein Oveland**[3], **Lars Bø**[1,2]*

1 Department of Clinical Medicine, University of Bergen, Bergen, Norway, **2** Department of Neurology, Norwegian Multiple Sclerosis Competence Centre, Haukeland University Hospital, Bergen, Norway, **3** Department of Biomedicine, Proteomics Unit at the University of Bergen (PROBE), University of Bergen, Bergen, Norway

* lars.bo@helse-bergen.no

OPEN ACCESS

Citation: Ahmad I, Wergeland S, Oveland E, Bø L (2021) A higher proportion of ermin-immunopositive oligodendrocytes in areas of remyelination. PLoS ONE 16(8): e0256155. https://doi.org/10.1371/journal.pone.0256155

Editor: Catherine Faivre-Sarrailh, Aix Marseille University, FRANCE

Received: March 24, 2021

Accepted: August 1, 2021

Published: August 26, 2021

Peer Review History: PLOS recognizes the benefits of transparency in the peer review process; therefore, we enable the publication of all of the content of peer review and author responses alongside final, published articles. The editorial history of this article is available here: https://doi.org/10.1371/journal.pone.0256155

Data Availability Statement: The authors of the study have not received any additional clinical information on the deceased for the Norwegian MS Registry and and Tissue Bank, and do thus not have any additional medical information available.

Abstract

Incomplete remyelination is frequent in multiple sclerosis (MS)-lesions, but there is no established marker for recent remyelination. We investigated the role of the oligodendrocyte/myelin protein ermin in de- and remyelination in the cuprizone (CPZ) mouse model, and in MS. The density of ermin+ oligodendrocytes in the brain was significantly decreased after one week of CPZ exposure ($p < 0.02$). The relative proportion of ermin+ cells compared to cells positive for the late-stage oligodendrocyte marker Nogo-A increased at the onset of remyelination in the corpus callosum ($p < 0.02$). The density of ermin-positive cells increased in the corpus callosum during the CPZ-phase of extensive remyelination ($p < 0.0001$). In MS, the density of ermin+ cells was higher in remyelinated lesion areas compared to non-remyelinated areas both in white- ($p < 0.0001$) and grey matter ($p < 0.0001$) and compared to normal-appearing white matter ($p < 0.001$). Ermin immunopositive cells in MS-lesions were not immunopositive for the early-stage oligodendrocyte markers O4 and O1, but a subpopulation was immunopositive for Nogo-A. The data suggest a relatively higher proportion of ermin immunopositivity in oligodendrocytes compared to Nogo-A indicates recent or ongoing remyelination.

Introduction

Multiple sclerosis (MS) is a chronic inflammatory demyelinating disease of the central nervous system (CNS) [1] and is a common cause of acquired neurologic disability in young adults [2]. In MS, there are multifocal areas, lesions of demyelination, inflammation, blood-brain-barrier breakdown, axonal and oligodendrocyte loss in the CNS [3]. There is frequent remyelination in MS lesions, starting at the early stages of lesion formation. Remyelination may include the recruitment of oligodendrocyte precursor cells (OPCs) and their differentiation into mature oligodendrocytes, which may extend processes to and enwrap demyelinated axons. The spirally enwrapped processes are then compacted to myelin. Remyelinated parts of an MS lesion are identified microscopically as areas with myelin staining being thinner and less organized, having uniformly thin myelin sheaths compared to the axon diameter [4, 5]. Typically, the

Raw cell count data are supplied in an supplementary data file.

Funding: The authors received no specific funding for this work.

Competing interests: The authors have declared that no competing interests exist.

remyelinated areas are found at the edge of a lesion, and the majority of lesions are incompletely remyelinated. The proportion of new MS-lesions in which remyelination occurs decreases over time [6].

Enhancing remyelination is an objective of many MS treatment trials, as this may confer neuroprotection, and less chronic disease progression [7]. There is a need for identifying sensitive and specific laboratory and radiological biomarkers for remyelination, both for use in clinical trials, and for a better understanding of the mechanisms of remyelination in MS. Currently, a reliable clinical or paraclinical biomarker for remyelination is not available [8].

In the cuprizone mouse model, oral administration of cuprizone (CPZ) continuously for five weeks results in oligodendrocyte loss, microglial activation, extensive demyelination and gliosis [9]. Remyelination occurs both during and after ending CPZ exposure, resulting in almost complete remyelination a few weeks after cuprizone exposure is ended [10, 11]. An increase in density of oligodendrocyte precursor cells is evident one week after starting CPZ exposure, and remyelination is detectable as early as after three weeks of ongoing CPZ exposure [10]. The CPZ model is considered appropriate for studying the remyelination process in MS, since several pathophysiological aspects of de- and remyelination are similar [12].

Ermin, also known as juxtanodin, is an oligodendrocyte-specific protein, known to be concentrated at the tip of F-actin-rich processes in the cytoskeleton synthesis [13–17]. Ectopic expression of ermin induced the formation of oligodendrocyte protrusions [13]. Ermin has been shown to be localized to the outer cytoplasmic lip of the myelin sheath, and the paranodal loops [13–16]. Ermin is a minor myelin protein, representing less than 1% of the total protein content [18]. Ermin knockout mice exhibits an aberrant myelin architecture in aged mice, with the splitting of myelin layers and display an increased sensitivity to cuprizone demyelination [19]. It is suggested that ermin may play a crucial role in myelin formation, in wrapping of axons and/or myelin compaction [13].

The objective of this study was to study whether the relative density of ermin-immunopositivie oligodendrocytes may be a marker of ongoing remyelination. We studied the extent and distribution of ermin immunopositivity during de-and remyelination in the cuprizone model and corroborated the findings by studying de- and remyelinated areas in MS-brain. The results indicate that the relative proportion of ermin-expressing oligodendrocytes, compared to the mature oligodendrocyte marker Nogo-A, may serve as a marker of remyelination in the CNS.

Materials and methods

The study was approved by the Regional committee for medical research ethics of Western Norway (permit ID: 2013–560). The autopsy tissue was obtained from the National MS biobank & registry, the use of tissue for MS-research has been approved by the Regional committee for medical research ethics for Western Norway (Permit No. 046.03) The Norwegian Animal Research Authority approved the protocol. Consent to the use of tissue for research had earlier been given by the deceased, or in writing by their next of kin. It then had to have been made likely that this was in line with the wish of the deceased. The patients and/or the next of kin to the patients included had provided written consent to have data from the patients medical records used in research. The medical records of the patients included were anonymized

Mice

Female c57Bl/6 mice (total n = 54) were acquired from Taconic (Ejby, Denmark) at the age of 7 weeks. The mean weight was 18.5 g (range 15.9–21.1). The mice were caged in Macrolon IVC-II cages (Scanbur, Karlslunde) in standard laboratory conditions; light/dark cycles of 12/

12 hours. The acclimatization period was one week. During the acclimatization and the experimental period, 6 mice were put together per cage; cage maintenance and animal health monitoring was performed twice daily by veterinary nurses at the laboratory animal facility at Haukeland University Hospital. Humane endpoints were defined prior to study start. Animals observed with reduced activity level and no food or water intake for > 12 hours, with weight loss >20% or absolute weight below 14 grams would be euthanized. The mice had ad libitum access to food (maintenance diet from Scanbur, Denmark) and water. To reduce suffering and distress, cages were provided with bedding and nesting material, shelters and chewing implements. Pain, and thus need for analgesics, due to experimental conditions or procedures were not expected in this study. The experiment was conducted following the recommendations of the Federation of European Laboratory Animal Science Associations, the ARRIVE guidelines (S1 Appendix), and the Norwegian Animal Research Authority approved the protocol.

Cuprizone administration

Mice were randomized at the age of 8 weeks into eight groups of six mice each and exposed to 0.2% (w/w) cuprizone (bis-cyclohexanone-oxaldihydrazone, Sigma-Aldrich, St. Louis, MO) added to the ordinary maintenance diet for up to 6 weeks. The control group was assigned to regular food and water. For immunohistological examination, the control group was sacrificed at week 8. Mice were sacrificed weekly during CPZ exposure, as a set group of 6 mice, and one group was sacrificed two weeks after stopping CPZ exposure (Week 8). One mouse died after three weeks of cuprizone exposure, not fulfilling the humane endpoint criteria prior to death.

Mouse brain histopathology

Mice were euthanized by CO_2. The brains were perfused by intracardial injection of 4% paraformaldehyde, before they were removed and post-fixed in 4% neutral buffered formalin (NBF) for seven days; then embedded in paraffin. All analyses were performed on 5 μm coronal sections at the bregma. For immunohistochemistry, the sections were dewaxed using xylene and rehydrated in serial aqueous dilutions of ethanol before antigen retrieval in the Diva Decloaker antigen retrieval solution (DV2004LX, Biocare Medical, CA, USA) at pH 6.2; 120˚C; 15 psi for 15 minutes. The sections were incubated with primary antibodies for myelin proteolipid protein, PLP (1:1000; Mouse monoclonal; Serotec; overnight at 4˚C), for mature oligodendrocytes, neurite outgrowth inhibitor A, Nogo-A (1:1000, Rabbit polyclonal; Chemicon; 1 hour at room temperature) and ermin (1:200; Mouse monoclonal; Merck Millipore; 2 hours at room temperature). The sections were then blocked with peroxidase blocking solution (Dako, Glostrup) and visualized with EnVision+ System (Dako, Glostrup) following the manufacturer's guideline (EnVision Systems: EnVision+ Dual Link, Single Reagents; HRP. Rabbit/Mouse). The tissue sections were counterstained with hematoxylin. The sections were dehydrated before mounting permanently in dibutylphthalate polystyrene xylene (DPX). For each antibody, the omission of the primary antibody served as a negative control. Normal brain tissue from the healthy controls served as a positive control. For all antibodies used, specific immunoreactivity has previously been identified in normal brain tissue. Information on immunopositivity in normal brain tissue has been published by the producers.

Human brain histopathology

Autopsy tissue from 26 MS autopsy cases were available for characterization of lesion type, and examined for remyelinated areas. In these, remyelinated areas were identified in tissue from 11 cases. The de-and re-myelinated MS lesion areas were selected for further study, along with brain tissue from 5 non-neurological disease controls (Table 1). The material was

Table 1. Clinical and demographic description of MS brain autopsies and control cases.

Case ID	Lesion type (Number)	Ermin+ cell counts (Remyelinated/non-Remyelinated area)	MS Phenotype	Gender	Age	Disease duration	Cause of death
1	Cr-WM (1) T1-GM (1)	41/19	Progressive	M	34	13	Bronchopneumonia
		7/4					
2	In-WM (1)	18/13	Progressive	F	65	26	Congestive heart failure
	T1-GM (1)	6/3					
	T3-GM (1)	4/3					
3	In-WM (1)	36/29	NA	M	43	NA	NA
	Ac-WM (1)	18/11					
	T3-GM (3)	8/5,9/3,7/4					
4	In-WM (1)	14/10	Progressive	M	55	36	Acute pyelonephritis with sepsis
5	In-WM (1)	17/10	Progressive	F	68	14	Cerebral haemorrhage
6	In-WM (1)	26/15	Progressive	M	83	NA	Pseudomembraneous colitis
	Ac-WM (1)	39/22					
7	T1-GM (1)	5/2	Progressive	F	62	28	Bronchopneumonia
	T3-GM (2)	3/1,4/1					
8	Cr-WM (1)	19/10	NA	M	52	8	Acute pyelonephritis
	T1-GM (1)	6/2					
9	Cr-WM (3)	13/8,22/15,24/16	Progressive	M	43	7	Bronchopneumonia
	T4-GM (1)	5/1					
	T2-GM (1)	3/3					
10	In-WM (2)	28/19,21/16	NA	F	56	26	Bronchopneumonia
	T4-GM (2)	6/3,4/1					
11	T3-GM (1)	6/2	NA	F	46	NA	Hyperthermia
Control							
1				F	37		Epilepsy
2				M	53		Diabetes mellitus
3				F	47		Heart disease (HSCRT)
4				M	40		Endocarditis
5				F	30		Lymphangioleiomyomatosis

NA = Information not available, WM = White matter, GM = Gray matter, Ac = Active, Cr = Chronic active In = Inactive, T1 = Type 1, T3 = Type 3, T4 = Type 4.

https://doi.org/10.1371/journal.pone.0256155.t001

obtained from the Norwegian MS Biobank (Department of Pathology, Haukeland University Hospital, Bergen, Norway). Information on the brain region studied was unfortunately not available for many of the tissue blocks studied. Pairwise comparisons were made within the individual tissue blocks, in order to correct for possible regional differences. White- and grey matter lesions, subclassified into de- and remyelinated areas, were identified by three individual investigators, in consensus. Remyelinated areas were identified by a pattern of PLP immunostaining with less dense, less organized and thinner myelin sheaths [4, 5]. All MS-lesions containing both de-and remyelinated areas was studied. In total, 14 white matter and 15 grey matter lesion areas were investigated (Table 1).

Sections from paraffin-embedded human brain autopsy tissue (5μm) were immunohistochemically stained for myelin proteolipid protein, PLP (1:1000, Rabbit polyclonal, Abcam; overnight at 4˚C), HLA-DR (1:20, Mouse monoclonal, Dako; hours at room temperature). Nogo-A (1:200, Rabbit polyclonal, Bio-Rad; hours at room temperature) and ermin (1:200, Rabbit polyclonal, Sigma-Aldrich; hours at room temperature). Processing of paraffin-

embedded tissue section for immunohistochemistry was the same as for mouse tissue sections. (PLP and HLA- DR isotype immunostainings were used to identify and classify MS lesions.

Double-labelling immunohistochemistry was performed using the EnVision™ G|2 Double stain System with two peroxidase steps, according to the manufacturer's recommended protocols (http://www.agilent.com). Tissue sections were incubated for 2 hours at room temperature with the primary antibodies followed by 30 minutes with the appropriate peroxidase-labelled secondary antibodies. Double stainings were performed for ermin (1:200, Rabbit polyclonal, Sigma-Aldrich) together with three stage-specific oligodendrocyte (OL) maturation markers: O4, O1 and Nogo-A [20, 21]. O4 (1:50, Mouse monoclonal, MyBioSource); O1 (1:50, Mouse monoclonal, Thermo Fisher Scientific Inc.) and Nogo-A (1:200, Rabbit polyclonal, Bio-Rad Laboratories). Secondary antibodies were visualized by 3,3′-Diaminobenzidine (DAB) and by reddish Alkaline Phosphatase (AP).

Assessment of the ermin and Nogo-A positive cell population and PLP positive areas in the mouse brain

In mouse brain tissue, the density of immunopositive cell populations (ermin immunopositive and Nogo-A immunopositive cells) was determined by light microscopy (Zeiss® Axio Imager A2, Wetzlar, Germany) using an ocular morphometric grid. Observed areas were lateral corpus callosum, medial corpus callosum, supplementary motor cortex and deep grey matter in order to characterize possible regional or tissue-specific differences in immunopositivity for ermin and/or Nogo-A. Immunopositive cells were identified by brown (DAB) staining along with blue (hematoxylin) nuclear stain. Immunopositive cell density count was made in an area of 0.0625 mm^2. For the corpus callosum area, lateral and medial counts were averaged. Only cells with a preserved nucleus and oligodendrocyte morphology were counted. To quantify myelin content, greyscale images of tissue sections stained with PLP were thresholded, avoiding low-intensity background staining. The myelin content was expressed as the percentage of positive pixels in each PLP-stained image within the threshold values, using image processing and analysis in ImageJ (U. S. National Institutes of Health; Bethesda 2009). All sections and images were blinded with respect to group allocation for all assessors.

Assessment of ermin+ and Nogo-A+ cell density in the human brain

Regions of interest (ROI) for counting were systematically randomized using grids. Grid-wise reference landmarks were utilized for identifying identical areas on ermin, Nogo-A and PLP immunostained tissue slides. To avoid regional bias, the comparisons were made between non-remyelinated and myelinated grey- or white matter areas having a similar spatial orientation (i.e. similar distance from the lesion edge/centre and similar tissue morphology) within the same tissue block. Ermin+ and Nogo-A+ cell densities were the nearest whole number of the average of three randomly selected areas (0.0625 mm^2 / area). For relatively smaller lesions, a single count was made since three randomly selected areas could not fit inside remyelinated regions.

Statistical analysis

Mean (M) and Standard Deviation (SD) were used to express the variability in the spatio-temporal change of ermin and Nogo-A positive cell densities in CPZ model. To investigate possible differences of density of ermin and Nogo-A immunopositive cells at each sampling point, paired sample t-test was performed. Ermin+ and Nogo-A+ cell densities were measured at each sampling point; in controls and after 1, 2, 3, 4, 5 and 6 weeks of cuprizone (CPZ) exposure along with 2 weeks after the end of CPZ exposure (week 8). The ratios of the density of ermin

+ to Nogo-A+ cells were calculated for each animal for each sampling point and averaged per group. Differences of the ratio occurring at two sequential time points during the cuprizone disease course were analyzed applying the Mann-Whitney U test. For MS, Paired sample t-test was used to compare ermin+ cell density of two different parts of the same lesion. Paired sample t-test was also carried out to examine the differences in density between ermin+ and Nogo-A+ cells both in the de- and remyelinated areas of the same lesions. Independent-group t test was carried out to investigate the difference of ermin+ and Nogo-A+ cell density in MS tissue compared to that in healthy control samples. In the cuprizone samples, the sample size was less than 10, and the Shapiro-Wilk test was used to ensure the normality of data sets. Otherwise, histogram and boxplot were used to obtain an indication. A sample size of 6 mice per experimental group detects an effect size d = 0.82 with respect to the difference in NOGO-A- and Ermin-positive cell density, given power 1-β = 0.80 and error probability $\alpha = 0.05$. Statistical analyses were performed using GraphPad Prism 6.0 (GraphPad Software, Inc., San Diego, CA). Differences were considered significant at $p < 0.05$. The correlation of the ratio of the density of ermin+ vs. Nogo-A+ cells in demyelinated and remyelinated MS-lesion areas with patient age and disease duration was calculated using the Pearson correlation coefficient.

Results

Ermin and Nogo-A immunopositivity and change of myelin content during and after cuprizone exposure

Myelin sheaths and the cytoplasm of cells with the morphology of oligodendrocytes were immunopositive for ermin (Fig 1), while for Nogo-A, immunopositivity was strong for oligodendrocytes, but weaker for myelin and the pattern of Nogo-A immunopositivity in the cuprizone mice was consistent with what has been reported previously [22].

Cuprizone exposure led to progressive demyelination and oligodendrocyte loss (Fig 2). White matter was represented by the corpus callosum, and by white matter tracts within deep grey matter (Fig 1). The density of PLP-immunopositive myelin sheaths decreased from week 2 to week 6 in corpus callosum and deep grey matter but, in the cerebral cortex, myelin loss was rapid and nearly complete after 1 week of cuprizone exposure (Fig 2A and 2B). Two weeks after cuprizone exposure was stopped (week 8), there was significant ($p < 0.05$) remyelination in the corpus callosum and deep grey matter, but not in the cerebral cortex (Fig 2A and 2B).

The density of Ermin+ cells with oligodendrocyte morphology decreased from the beginning of CPZ exposure (Fig 2C–2E and Table 2). Already at week 3, the density of Ermin+ oligodendrocytes was significantly lower in all regions studied, compared to controls (Fig 2C–2E) ($p<0.001$). During the period of remyelination, two weeks after withdrawal of CPZ exposure, the density of ermin+ oligodendrocytes was significantly increased in the corpus callosum (Fig 2C–2E and Table 2) ($p< 0.0001$).

The ratio of ermin-to-Nogo-A immunopositive cells in the controls were 1.17, 1.07 and 3.02 in the corpus callosum, the deep grey matter and the cortex, respectively. After three weeks of CPZ exposure, the ratio peaked in the corpus callosum and the deep grey matter, at 22.53 and 4.02, respectively. At this point, the density of ermin+ cells was significantly higher than that of Nogo-A+ cells in the corpus callosum and in the cortex ($p < 0.02$, Table 2). The sequential change of ratios of the density of ermin+ versus Nogo-A positive cells at week 3 was significant in the corpus callosum ($p < 0.02$). For the other areas, the density of ermin+ cells was so low at week 3 (Fig 2) that ermin+/Nogo-A+ ratios could not be determined, having some null values in the denominator. After week 3, the ratio gradually decreased throughout the cuprizone exposure phase in all areas observed (Table 2).

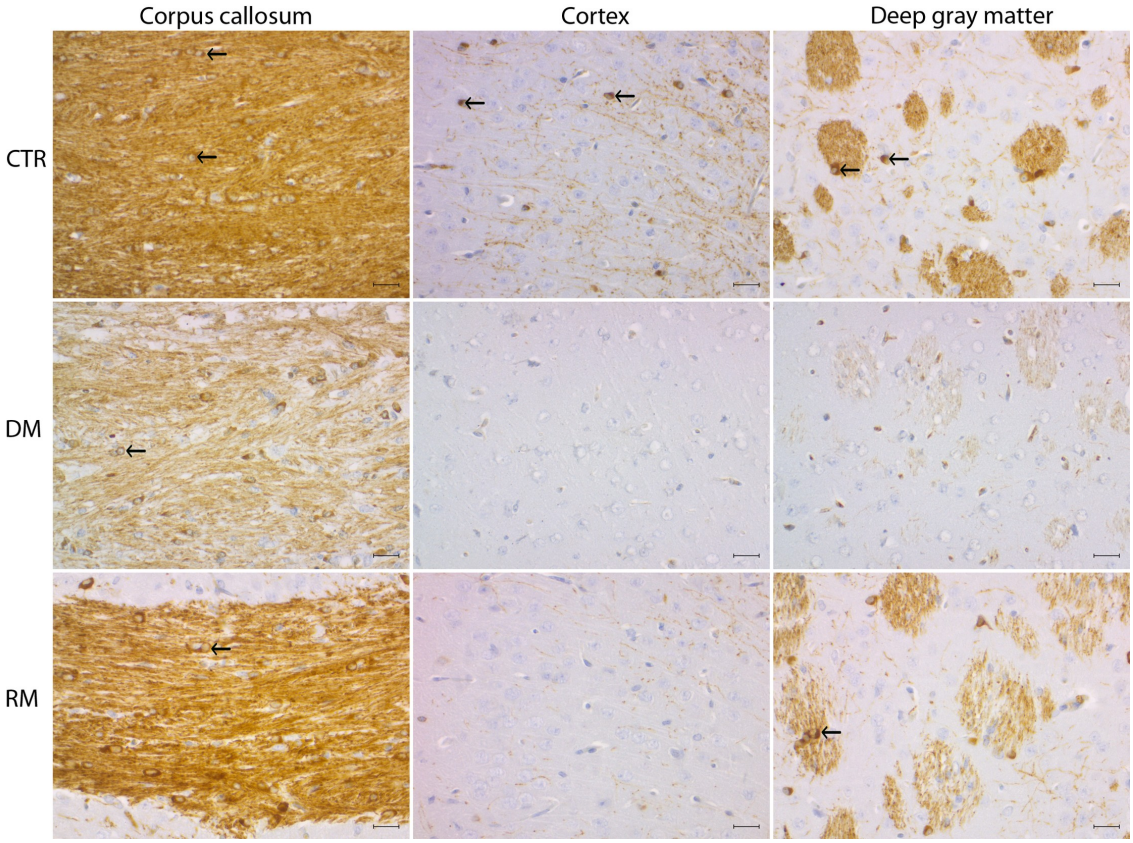

Fig 1. Immunopositivity for ermin during de- and remyelination in the cuprizone model. Tissue sections single labelled for ermin. First column: Corpus callosum (white matter), middle column: Cerebral cortex, last column: deep gray matter. Top row: Controls- CTR (week 8), middle row: 6 weeks of CPZ exposure (Demyelination-DM), last row: 2 weeks after the ending of CPZ exposure (Remyelination-RM). Black arrows: Cells with the morphology of oligodendrocytes, immunopositive for ermin. Myelin tracts and cells with the morphology of oligodendrocytes are immunopositive for ermin. There is extensive demyelination after 6 weeks of cuprizone exposure. At this time point, demyelination is more extensive in pure gray matter parts than in interspersed white matter in deep gray matter. Scale bar = 50 μm.

https://doi.org/10.1371/journal.pone.0256155.g001

Ermin and Nogo-A immunopositivity in MS

Adjacent tissue sections from the same MS tissue blocks were immunostained for PLP, ermin and Nogo-A. PLP immunostaining was used to define the lesion areas and the subregions of remyelination. Remyelinated areas had less dense myelin, the myelin was less organized, and myelin sheaths were thinner than in adjacent normal-appearing white- or grey matter (Figs 3A and 4A). Myelin was strongly immunopositive for ermin (Fig 5E), more weakly immunopositive for Nogo-A (Fig 5F), while cells with an oligodendrocyte morphology (both in the white and grey matter areas) were strongly immunopositive for both markers (Fig 5E and 5F). The density of ermin+ cells was significantly higher in remyelinated white matter MS lesion areas than in non-remyelinated lesion areas ($p < 0.0001$), or normal-appearing white matter ($p < 0.001$) (Fig 3B–3E). Ermin+ cell density was also increased in remyelinated grey matter

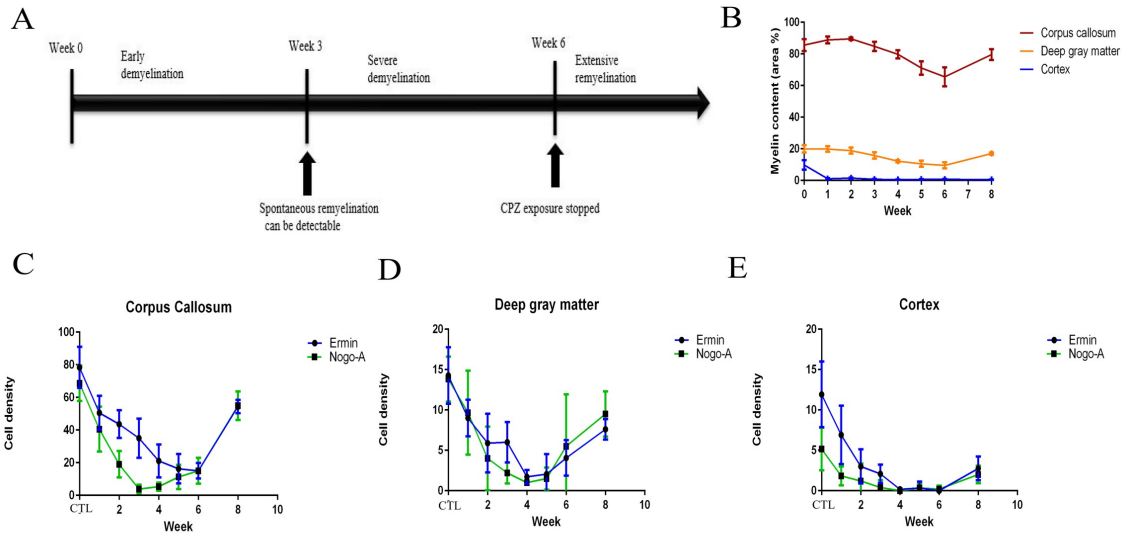

Fig 2. Temporal dynamics of ermin and Nogo-A immunopositive cell density and myelin content over the course of de- and remyelination in the cuprizone mouse model. (A) Schematic diagram of the course of demyelination/remyelination in the cuprizone mouse model (B) Temporal change of myelin content, measured by immunohistochemistry for proteolipid protein (PLP) (mean, SEM). (C-E) Temporal change of ermin and Nogo-A- immunopositive cell density (mean, SEM) in the corpus callosum (C), deep gray matter (D), cortex (E) from week 1 to week 8. CTL: Controls. Cuprizone exposure led to progressive demyelination and oligodendrocyte loss. The density of Nogo-A+ cells fell more rapidly than the density of ermin+ cells during the first 3 weeks (C-E). Two weeks after cuprizone exposure was stopped (week 8) remyelination was evident in corpus callosum and deep gray matter, but not in cerebral cortex (B).

https://doi.org/10.1371/journal.pone.0256155.g002

lesion areas compared to non-remyelinated grey matter lesion areas ($p < 0.0001$), but was lower compared to normal-appearing grey matter ($p < 0.01$, Fig 4B–4E). For Nogo-A cell densities, a significantly higher cell density was observed in remyelinated WM compared to NAWM ($p < 0.01$), but not in remyelinated GM compared to NAGM (S1 Fig). Ermin+ or Nogo-A+ cell density in normal-appearing parts of white-and grey matter in MS was not significantly different from Ermin- or Nogo-A immunopositive cell density in white-and grey matter in healthy controls. The density of cells immunopositive for ermin was significantly lower in WM/GM MS-lesions compared to NAWM/NAGM ($p<0.05$). The density of cells immunopositive for Nogo-A was significantly lower in WM/GM lesions compared to NAWM/NAGM ($p<0.05$). There was no significant correlation of the density of ermin+- or Nogo-A+ cells in remyelinated areas in WM/GM with patient age (R-value Ermin -0.383/-0.58 Nogo-A -0.202/-0.021). In remyelinated lesion areas, the density of ermin+ cells was significantly higher than Nogo-A+ oligodendrocytes in white matter ($p < 0.0001$), but not in grey matter ($p = 0.24$) (Fig 5A–5F).

Oligodendrocyte differentiation stage of ermin+ cells

MS tissue sections were double-stained for ermin and markers for stages of oligodendrocyte maturation; Nogo-A, O1 and O4. Ermin immunoreactivity was confined to only a minor subpopulation of Nogo-A+ cells with an oligodendrocyte morphology and *vice versa* (Fig 5G) and

Table 2. Sequential change of ermin and Nogo-A positive cell density and their ratios.

	Week 1–6: Weeks of cuprizone exposure Week 3: Onset of remyelination															
	Control		1		2		3 (Rem)		4		5		6		8 (AE)	
	M	SD	M	SD	M	SD	M	SD	M	SD	M	SD	M	SD	M	SD
Corpus callosum																
Ermin	78.4	12.6	50.6	10.4	43.6	8.5	35	12	21.2	10.1	16.3	9.1	15	4.8	52.8	4.8
Nogo-A	68.7	10.9	40.5	13.8	19	8.2	3.9	2.6	5.4	2.5	11.3	7.4	15.1	7.9	54.9	8.8
Ermin: Nogo-A	1.2		1.6		**2.7** [a,b]		**22.5** [a,b]		4.8 [a]		1.7		1.3		1	
Cortex																
Ermin	11.9	4.1	6.9	3.6	3	2.1	2.1	1.1	0.2	0.3	0.3	0.8	0	0	2.8	1.5
Nogo-A	5.2	2.6	1.8	1.2	1.2	2.2	0.4	0.9	0	0	0.3	0.5	0.2	0.4	2	1.1
Ermin: Nogo-A	3.0 [a]		3.3 [a*]		0.3*		1.7 [a*]		NaN		1*		NaN		1.7	
Deep gray matter																
Ermin	14.3	3.5	9	2.3	5.9	3.6	6	2.5	1.7	0.9	2.1	2.5	4.1	2.2	7.6	1.3
Nogo-A	13.8	2.8	9.7	5.2	4	3.9	2.2	1.3	1	0	1.5	1.4	5.5	6.4	9.5	2.8
Ermin: Nogo-A	1.1		1.2		1.3*		4.0		1.7		1.7*		1.1*		0.9	

Ermin+ and Nogo-A+ cell densities were measured at each sampling point; in controls, after 1, 2, 3, 4, 5 and 6 weeks of cuprizone (CPZ) exposure and 2 weeks after the end of CPZ exposure (week 8). Positive cell counts are provided as mean number per 0.0625 mm2 (SD). The ratios of ermin+ cells compared to Nogo-A+ cells were calculated for each animal for a sampling point and averaged (M). Paired sample t-test was performed to analyze ermin:Nogo-A ratio. The change in ratio (each sampling point compared to the preceding sampling point) was analyzed by Mann-Whitney U test.

a: denotes an ermin:Nogo-A ratio significantly ($p<0.05$) different by paired sample t-test.

b: denotes a significant ($p<0.05$) change in ermin:Nogo-A ratio compared to preceding sampling point by Mann-Whitney U test.

*: denotes the presence of zero values (0) for some Nogo-A cell counts (in the deep gray matter and the cortex, Nogo-A+ cell densities were very low during cuprizone (CPZ) exposure), Nogo-A cell counts being a denominator, this excluded such areas from the calculation. **NaN:** denotes groups for which the number of sampling regions with computable ratios was too low to compute a mean ratio. **Rem**: Remyelination has been found to occur from this time point. **AE**: 2 weeks after stopping CPZ exposure

https://doi.org/10.1371/journal.pone.0256155.t002

ermin protein expression was not detected in O1 and O4 positive oligodendrocyte cells, O1 and O4 are markers of oligodendrocyte progenitor cells (Fig 5H and 5I).

Discussion

The data of this study indicate that a high relative proportion of ermin immunopositivity in white matter oligodendrocytes is associated with remyelination. Ermin immunopositivity was localized to oligodendrocytes and myelin, both in white- and grey matter parts of the mouse and human CNS. The observed specificity of ermin immunopositivity for oligodendrocytes and myelin in the CNS is consistent with what has been found previously, in both humans and in mice [13]. A higher relative density of oligodendrocytes immunopositive for ermin was found in the cerebral cortex in the 8-week old mice. This may be due to differences in the time course of myelination of the cerebral cortex compared to the corpus callosum [23].

In the cuprizone model, remyelination starts after 3 weeks of cuprizone exposure [10], and is accelerated after the exposure is ended [11]. We observed a gradual decrease of ermin+ cell density in all the observed brain areas (corpus callosum, cerebral cortex and deep grey matter), during the first 4–5 weeks of CPZ exposure. After that, the density of ermin+ cells was stable during exposure and then increased after the exposure was stopped. This pattern differed from the density of Nogo-A+ oligodendrocytes, where the density of Nogo-A+ cells fell more rapidly during the first 3 weeks; then stabilized during continued exposure and later increased. Nogo-

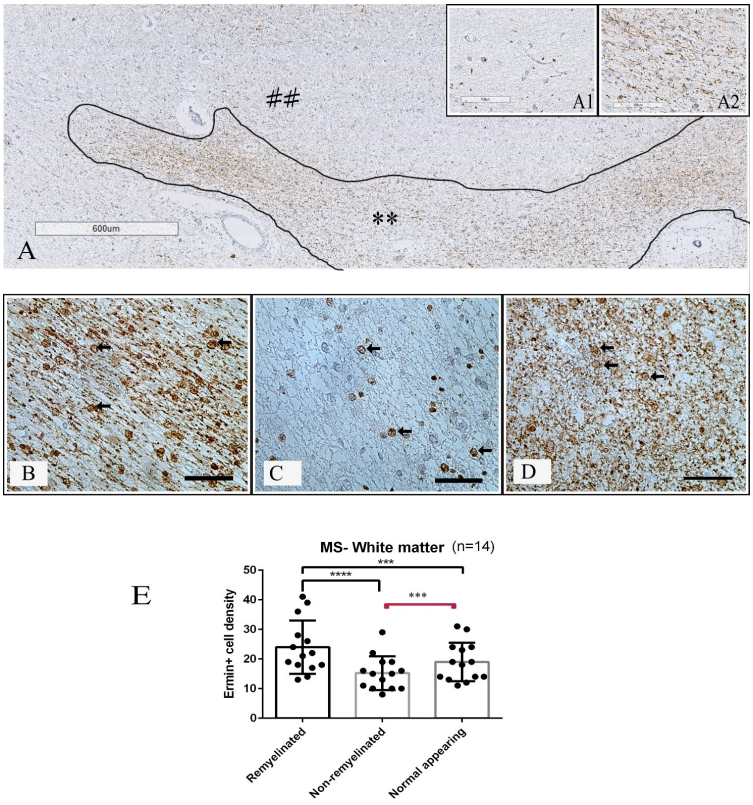

Fig 3. Ermin positive cell density in MS white matter lesions. (A) Myelin proteolipid protein (PLP) stained tissue section (** represents remyelinated white matter area and demyelinated white matter area is represented by ##); insertion A1 shows a demyelinated area with no remyelination, and insertion (A2) shows a partly remyelinated area. (B-D) Single-labelling immunohistochemistry for ermin in remyelinated (B) and non-remyelinated (C) lesion areas, and in normal-appearing (D) white matter tissue from MS brain. Immunopositive cells have the morphology of oligodendrocytes (arrows). (E) Density of ermin+ cells in remyelinated, non-remyelinated and normal-appearing regions in white matter. Scale bar = 50 μm, ****: $p < 0.00001$, ***: $p < 0.0001$.

https://doi.org/10.1371/journal.pone.0256155.g003

A is a marker of mature oligodendrocytes in both the adult mouse and human CNS [20]. The known function of Ermin and Nogo-A differs. Ermin concentrates at the tip of F-actin-rich processes in the cytoskeleton synthesis in oligodendrocytes [14]. Ermin is likely to have a role in cytoskeleton synthesis, important for the extension and wrapping of oligodendrocyte processes around axons during myelination [13, 14]. The expression of Nogo-A may increase during myelin compaction, to trigger the collapse of F-actin in oligodendrocyte processes, a role functionally similar to Nogo-A expression in neuronal growth cones [24–27]. This may explain why the changes in ermin+- and Nogo-A+ cell populations did not completely overlap during the time course of de-and remyelination in the cuprizone model, with a relative increase in density of ermin-immuopositive cells occurring during the onset of the remyelination process.

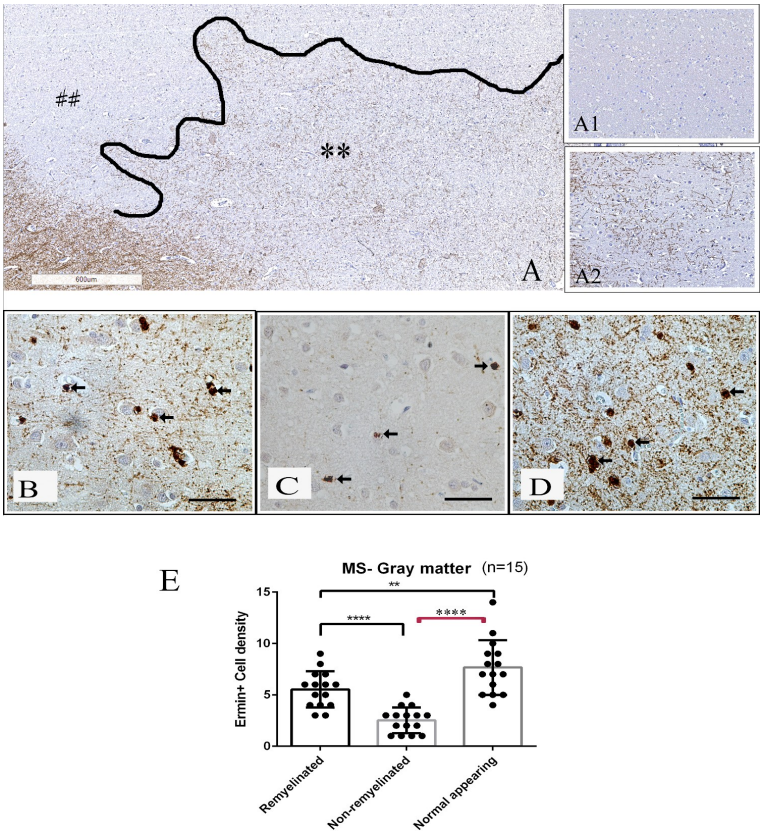

Fig 4. Ermin positive cell density in MS gray matter lesions. (A) Myelin proteolipid protein (PLP) stained tissue section (** represents remyelinated area, demyelinated area is represented by ##); the insertion A1 shows an area of complete demyelination in gray matter. The insertion A2 shows partial remyelination. (B–D) Single-label immunohistochemistry for ermin in regions of remyelinated (B), non-remyelinated (C) and normal-appearing (D) gray matter tissue from MS brain, immunopositive cells are marked with arrows. (E) The graph presents ermin+ cell density profile in remyelinated, non-remyelinated and normal-appearing regions in gray matter. Ermin+ cell density was increased in remyelinated gray matter lesion areas compared to non-remyelinated gray matter lesion areas ($p < 0.0001$), but was lower compared to normal-appearing gray matter ($p < 0.01$). Scale bar = 50 μm, ****: $p < 0.00001$, **: $p < 0.001$.

https://doi.org/10.1371/journal.pone.0256155.g004

In a subset of oligodendrocytes, ermin- and Nogo-A immunopositivity colocalized. Ermin + cells were negative for O4, a marker for immature oligodendrocyte precursor cells and for O1, a marker for an intermediate stage of oligodendrocyte differentiation [28]. This supports ermin expression to be a marker for oligodendrocytes at a later stage of differentiation.

The increased proportion of ermin+ oligodendrocytes compared to Nogo-A+ cells in areas of remyelination may be due to an increased density of not fully mature oligodendrocytes, but it could also be partly due to a disproportionate loss of mature oligodendrocytes in these areas, as remyelination in MS and in CPZ occurs simultaneously with myelin and oligodendrocyte loss [10].

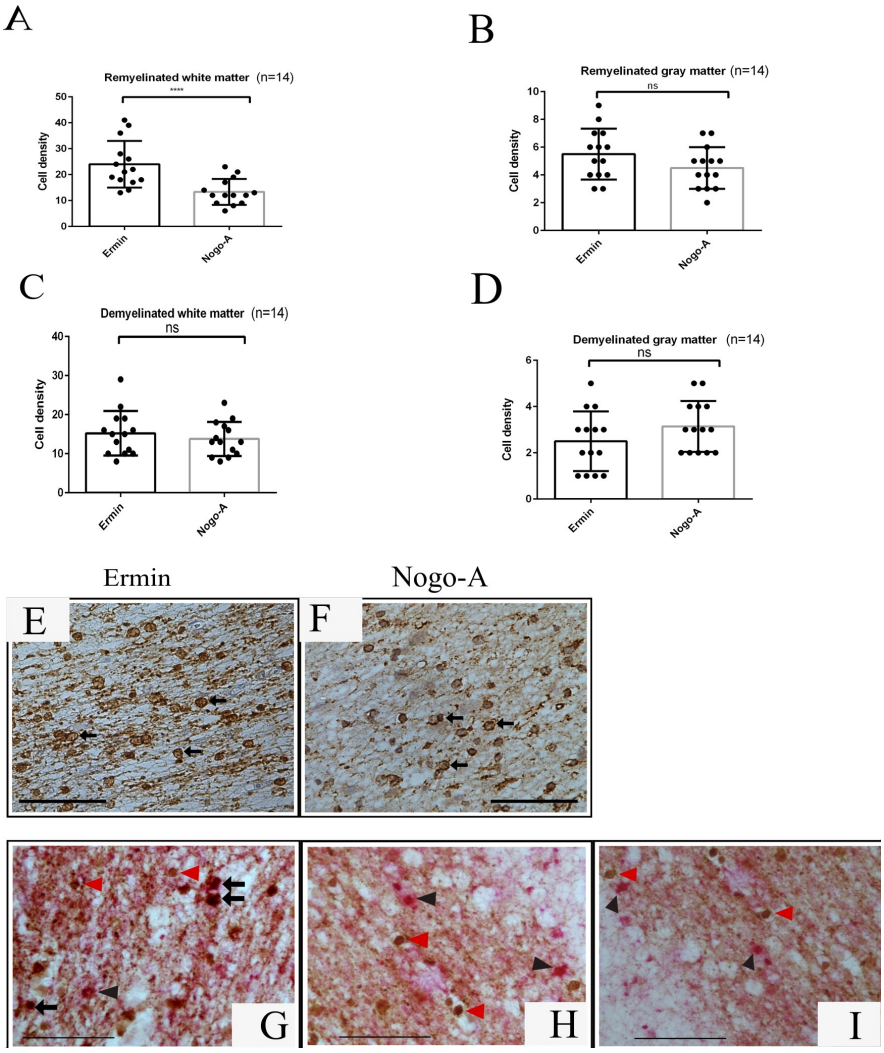

Fig 5. Comparison of ermin and Nogo-A expression in de- and remyelinated MS lesion areas. Density of ermin+ and Nogo-A + cells in remyelinated white matter (A) and gray matter (B) MS lesion areas, and demyelinated white matter (C) and gray matter (D) MS lesion areas. A remyelinated white matter MS lesion area single-label immunostained for ermin (E) and Nogo-A (F). White matter remyelinated MS lesion areas double-label immunostained for ermin (DAB, brown) (G-I) and Nogo-A (AP, red-pink) (G), O1 (AP, red-pink) (H), and O4 (AP, red-pink) (I). Arrows: Double-immunopositive cells. Red arrowhead: Cells immunopositve for ermin, Black arrowhead: Nogo-A (A); O1 (H) and O4 (I). A small proportion of oligodendrocytes were double immunopositive for ermin and Nogo-A (G, arrows). Ermin+ cells were not immunopositve for O1 or O4. Scale bar = 50 μm, ****: $p < 0.00001$, ns: Nonsignificant ($p > 0.05$).

https://doi.org/10.1371/journal.pone.0256155.g005

The relative loss of myelin was more rapid and extensive in CPZ grey matter than in white matter tracts, consistent with what has been described previously [22]. This was evident in the cerebral cortex and in deep grey matter, where demyelination was extensive in pure grey matter parts during cuprizone exposure, but not in interspersed white matter fibre tracts after 6 weeks of cuprizone exposure. Less differentiated oligodendrocytes may be more sensitive to metabolic injury than more mature cells [29]. This difference in the time course of toxic demyelination in grey-and white matter may thus be due to possible differences in the stage of differentiation of oligodendrocytes in grey and white matter in mice at age 8–14 weeks, compared to earlier time points.

Although the density of ermin+—and Nogo-A+ -oligodendrocytes increased both in white- and grey matter areas after ending cuprizone exposure, remyelination was not detected in cerebral cortex. After the end of CPZ exposure remyelination in the cerebral cortex has previously been found to occur at a slower rate than in white matter [10]. This difference may be due to location-dependent differences in oligodendrocyte phenotype, but may also be due to other factors, such as a difference in the extent of inflammation [30, 31].

The level of ermin expression in the CNS may be correlated with ermin levels in CSF and/or in blood. A recent study has reported downregulation of the ermin gene (mRNA) in blood from RRMS patients [32]. The possible correlation of the level of ermin expression in CSF and/or blood with the extent of remyelination needs to be investigated further.

The interpretation of the data presented in this study has several important limitations.

The density of ermin-immunopositive cells was not studied in relation to markers of lesion age and inflammatory activity, as there is no consensus on markers of lesion age and activity in MS grey matter lesions. The human material was mainly composed of patients with late stages of multiple sclerosis. Mechanisms of remyelination may differ in early vs. late stages of the disease. In the cuprizone model, the expression pattern of ermin was compared to Nogo-A only, because data on the function of ermin and Nogo-A indicate these proteins may be markers of adjacent stages in myelin formation. The antibodies used as markers for oligodendrocytes/oligodendrocyte precursors may have differences in sensitivity, however, this is not likely to explain the changes observed in the proportion of ermin-to Nogo-A immunopositive cells during the period of de-and remyelination in the cuprizone mice. Additional studies on other oligodendrocyte maturation markers would help to characterize the ermin+-cell population further, including the timing of ermin expression during remyelination. Ermin expression pattern may differ in different brain regions, but the spatial brain location of all MS-brain autopsy tissue studied could not be accurately determined. Only lesions containing myelinated and non-remyelinated parts were studied, in order to avoid confounding due to regional differences. Distinguishing remyelination from active demyelination is a challenge to both this and previous studies of post-mortem tissue. Areas of remyelination in chronic MS has been found to be characterized by focal or lesion border areas of thin, irregular myelin sheaths. In these areas, few microglia and macrophages are generally found, making it unlikely to represent active demyelination in initial lesions [4–7]. Very similar criteria for light microscopy has been confirmed by electron microscopy [33].

Conclusion

Several lines of evidence indicate that remyelination may confer neuroprotection, with axonal preservation in multiple sclerosis lesions [7]. Better knowledge of the mechanisms of remyelination in MS may provide therapeutic targets to enhance remyelination, and provide long term neuroprotection. The findings of this study suggest that remyelination is associated with a relative increase in the density of ermin-positive oligodendrocytes. The data strengthen the

hypothesis that ermin expression may be important for the early stages of myelin formation, prior to myelin compaction.

Supporting information

S1 Fig. Nogo-A+ cell density in white matter **(A)** and gray matter **(B)** in MS-brain. Remyelinated, non-remyelinated and normal-appearing areas are compared. ns: Nonsignificant ($p > 0.05$).
(TIF)

S1 Appendix. The ARRIVE guidelines checklist.
(PDF)

Author Contributions

Conceptualization: Stig Wergeland, Eystein Oveland, Lars Bø.

Data curation: Intakhar Ahmad, Eystein Oveland, Lars Bø.

Formal analysis: Intakhar Ahmad, Lars Bø.

Investigation: Intakhar Ahmad, Stig Wergeland, Eystein Oveland, Lars Bø.

Methodology: Intakhar Ahmad, Stig Wergeland, Eystein Oveland, Lars Bø.

Project administration: Stig Wergeland, Eystein Oveland, Lars Bø.

Resources: Eystein Oveland.

Supervision: Stig Wergeland, Eystein Oveland, Lars Bø.

Validation: Stig Wergeland, Eystein Oveland, Lars Bø.

Writing – original draft: Intakhar Ahmad, Stig Wergeland, Eystein Oveland, Lars Bø.

Writing – review & editing: Intakhar Ahmad, Stig Wergeland, Eystein Oveland, Lars Bø.

References

1. Thompson AJ, Baranzini SE, Geurts J, Hemmer B, Ciccarelli O. Multiple sclerosis. Lancet (London, England). England; 2018; 391: 1622–1636. https://doi.org/10.1016/S0140-6736(18)30481-1
2. Dobson R, Giovannoni G. Multiple sclerosis—a review. Eur J Neurol. England; 2019; 26: 27–40. https://doi.org/10.1111/ene.13819 PMID: 30300457
3. Baecher-Allan C, Kaskow BJ, Weiner HL. Multiple Sclerosis: Mechanisms and Immunotherapy. Neuron. 2018. pp. 742–768. https://doi.org/10.1016/j.neuron.2018.01.021 PMID: 29470968
4. Schultz V, van der Meer F, Wrzos C, Scheidt U, Bahn E, Stadelmann C, et al. Acutely damaged axons are remyelinated in multiple sclerosis and experimental models of demyelination. Glia. 2017; 65: 1350–1360. https://doi.org/10.1002/glia.23167 PMID: 28560740
5. Patrikios P, Stadelmann C, Kutzelnigg A, Rauschka H, Schmidbauer M, Laursen H, et al. Remyelination is extensive in a subset of multiple sclerosis patients. Brain. 2006; 129: 3165–3172. https://doi.org/10.1093/brain/awl217 PMID: 16921173
6. Goldschmidt T, Antel J, König FB, Brück W, Kuhlmann T. Remyelination capacity of the MS brain decreases with disease chronicity. Neurology. 2009; 72: 1914–1921. https://doi.org/10.1212/WNL.0b013e3181a8260a PMID: 19487649
7. Lubetzki C, Zalc B, Williams A, Stadelmann C, Stankoff B. Remyelination in multiple sclerosis: from basic science to clinical translation. The Lancet Neurology. 2020. https://doi.org/10.1016/S1474-4422(20)30140-X PMID: 32702337
8. Cunniffe N, Coles A. Promoting remyelination in multiple sclerosis. Journal of Neurology. Springer Berlin Heidelberg; 2019. https://doi.org/10.1007/s00415-019-09421-x PMID: 31190170

9. Blakemore WF, Franklin RJM. Remyelination in experimental models of toxin-induced demyelination. Current Topics in Microbiology and Immunology. 2008. pp. 193–212. https://doi.org/10.1007/978-3-540-73677-6_8 PMID: 18219819

10. Pfeifenbring S, Nessler S, Wegner C, Stadelmann C, Brück W. Remyelination After Cuprizone-Induced Demyelination Is Accelerated in Juvenile Mice. J Neuropathol Exp Neurol. 2015; 74: 756–766. https://doi.org/10.1097/NEN.0000000000000214 PMID: 26115190

11. Gudi V, Gingele S, Skripuletz T, Stangel M. Glial response during cuprizone-induced de- and remyelination in the CNS: Lessons learned. Frontiers in Cellular Neuroscience. 2014. https://doi.org/10.3389/fncel.2014.00073 PMID: 24659953

12. Denic A, Johnson AJ, Bieber AJ, Warrington AE, Rodriguez M, Pirko I. The relevance of animal models in multiple sclerosis research. Pathophysiology. 2011; 18: 21–29. https://doi.org/10.1016/j.pathophys.2010.04.004 PMID: 20537877

13. Brockschnieder D, Sabanay H, Riethmacher D, Peles E. Ermin, A Myelinating Oligodendrocyte-Specific Protein That Regulates Cell Morphology. J Neurosci. 2006; 26: 757–762. https://doi.org/10.1523/JNEUROSCI.4317-05.2006 PMID: 16421295

14. Wang T, Jia L, Yang G, Ji S, Yao L, Zhang B. Identification of Juxtanodin promoter and its transcriptional regulation during the ATRA-induced differentiation of C6 cells. Mol Cell Biochem. 2011; 350: 177–183. https://doi.org/10.1007/s11010-010-0696-y PMID: 21221725

15. Wang T, Jia L, Lv B, Liu B, Wang W, Wang F, et al. Human Ermin (hErmin), a new oligodendrocyte-specific cytoskeletal protein related to epileptic seizure. Brain Res. 2010/10/12. Department of Biochemistry and Molecular Biology, Fourth Military Medical University, Xi'an 710032, China.; 2011; 1367: 77–84. https://doi.org/10.1016/j.brainres.2010.10.003 PMID: 20934411

16. Zhang B, Cao Q, Guo A, Chu H, Chan YG, Buschdorf JP, et al. Juxtanodin: An oligodendroglial protein that promotes cellular arborization and 2′,3′-cyclic nucleotide-3′-phosphodiesterase trafficking. Proc Natl Acad Sci U S A. 2005; 102: 11527–11532. https://doi.org/10.1073/pnas.0500952102 PMID: 16051705

17. Ruskamo S, Chukhlieb M, Vahokoski J, Bhargav SP, Liang F, Kursula I, et al. Juxtanodin is an intrinsically disordered F-actin-binding protein. Sci Rep. 2012; 2. https://doi.org/10.1038/srep00899 PMID: 23198089

18. Jahn O, Tenzer S, Bartsch N, Patzig J, Werner HB. Myelin proteome analysis: Methods and implications for the myelin cytoskeleton. Neuromethods. 2013; 79. https://doi.org/10.1007/978-1-62703-266-7_15

19. Wang S, Wang T, Liu T, Xie RG, Zhao XH, Wang L, et al. Ermin is a p116RIP-interacting protein promoting oligodendroglial differentiation and myelin maintenance. Glia. 2020; 68. https://doi.org/10.1002/glia.23838 PMID: 32530539

20. Kuhlmann T, Remington L, Maruschak B, Owens T, Brück W. Nogo-A is a reliable oligodendroglial marker in adult human and mouse CNS and in demyelinated lesions. J Neuropathol Exp Neurol. 2007; 66: 238–246. https://doi.org/10.1097/01.jnen.0000248559.83573.71 PMID: 17356385

21. Neman J, de Vellis J. Myelinating Cells in the Central Nervous System—Development, Aging, and Disease. In: Lajtha A, Perez-Polo JR, Rossner S, editors. Handbook of Neurochemistry and Molecular Neurobiology: Development and Aging Changes in the Nervous System. Boston, MA: Springer US; 2008. pp. 61–75. https://doi.org/10.1007/978-0-387-32671-9_3

22. Wergeland S, Torkildsen Ø, Myhr KM, Mørk SJ, Bø L. The cuprizone model: Regional heterogeneity of pathology. APMIS. 2012; 120: 648–657. https://doi.org/10.1111/j.1600-0463.2012.02882.x PMID: 22779688

23. Vincze A, Mázló M, Seress L, Komoly S, Ábrahám H. A correlative light and electron microscopic study of postnatal myelination in the murine corpus callosum. Int J Dev Neurosci. 2008; 26. https://doi.org/10.1016/j.ijdevneu.2008.05.003 PMID: 18556167

24. Pernet V, Schwab ME. The role of Nogo-A in axonal plasticity, regrowth and repair. Cell and Tissue Research. 2012. https://doi.org/10.1007/s00441-012-1432-6 PMID: 22588543

25. Ternaux JP, Portalier P. Nogo-A expression in mature oligodendrocytes of rat spinal cord in association with specific molecules. Neurosci Lett. 2002; 332. https://doi.org/10.1016/S0304-3940(02)00910-2

26. Montani L, Gerrits B, Gehrig P, Kempf A, Dimou L, Wollscheid B, et al. Neuronal Nogo-A modulates growth cone motility via Rho-GTP/LIMK1/cofilin in the unlesioned adult nervous system. J Biol Chem. 2009; 284. https://doi.org/10.1074/jbc.M808297200 PMID: 19208621

27. Thomason EJ, Escalante M, Osterhout DJ, Fuss B. The oligodendrocyte growth cone and its actin cytoskeleton: A fundamental element for progenitor cell migration and CNS myelination. GLIA. 2020. https://doi.org/10.1002/glia.23735 PMID: 31696982

28. Back SA, Luo NL, Borenstein NS, Levine JM, Volpe JJ, Kinney HC. Late oligodendrocyte progenitors coincide with the developmental window of vulnerability for human perinatal white matter injury. J Neurosci. 2001; 21. https://doi.org/10.1523/JNEUROSCI.21-04-01302.2001 PMID: 11160401

29. Bénardais K, Kotsiari A, Škuljec J, Koutsoudaki PN, Gudi V, Singh V, et al. Cuprizone [bis(cyclohexylidenehydrazide)] is selectively toxic for mature oligodendrocytes. Neurotox Res. 2013; 24: 244–250. https://doi.org/10.1007/s12640-013-9380-9 PMID: 23392957

30. Bø L. The histopathology of grey matter demyelination in multiple sclerosis. Acta Neurologica Scandinavica. 2009. https://doi.org/10.1111/j.1600-0404.2009.01216.x PMID: 19566500

31. Hohlfeld R. Does inflammation stimulate remyelination? Journal of Neurology. 2007. https://doi.org/10.1007/s00415-007-1009-6

32. Salek Esfahani B, Gharesouran J, Ghafouri-Fard S, Talebian S, Arsang-Jang S, Omrani MD, et al. Down-regulation of ERMN expression in relapsing remitting multiple sclerosis. Metab Brain Dis. 2019/05/23. United States; 2019; 34: 1261–1266. https://doi.org/10.1007/s11011-019-00429-w PMID: 31123898

33. Albert M, Antel J, Brück W, Stadelmann C. Extensive cortical remyelination in patients with chronic multiple sclerosis. Brain Pathol. 2007; 17: 129–138. https://doi.org/10.1111/j.1750-3639.2006.00043.x PMID: 17388943

Supplementary figure 1.

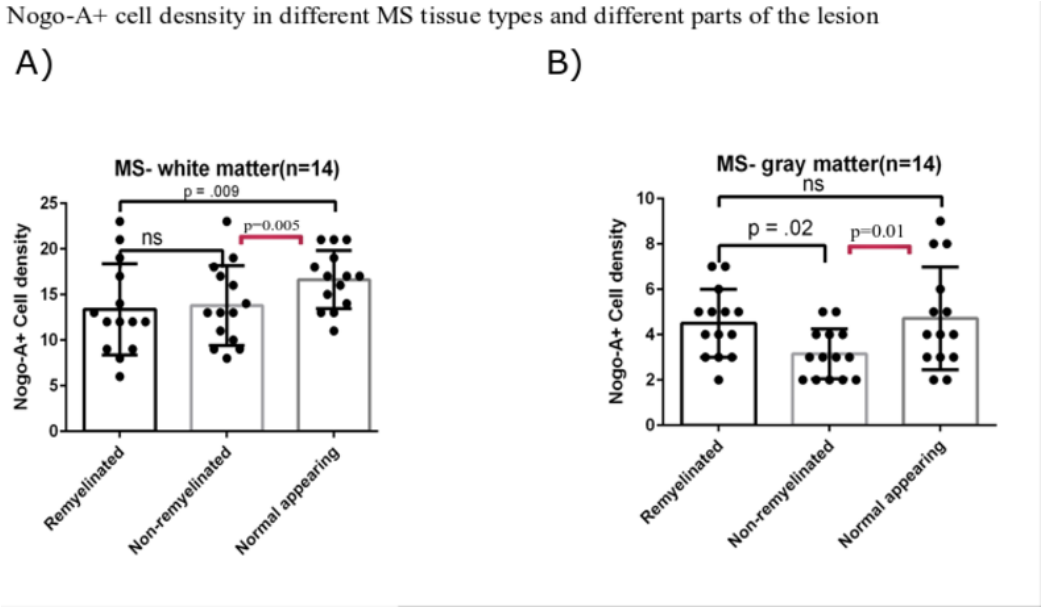

The ARRIVE Essential 10: Compliance Questionnaire

Use this questionnaire to evaluate how well a manuscript complies with the ARRIVE Essential 10. It can be applied to any manuscript describing comparative experiments in living animals, by assessors such as journal staff, editors, or peer reviewers.

	Item	Question(s)	Answers
1	Study Design	Are all experimental and control groups clearly identified?	☐ Yes, for at least one experiment ☐ No
		Is the experimental unit (e.g. an animal, litter or cage of animals) clearly identified?	☐ Yes, for at least one experiment ☐ No
2	Sample Size	Is the exact number of experimental units in each group at the start of the study provided (e.g. in the format '*n*=')?	☐ Yes, for at least one experiment ☐ No
		Is the method by which the sample size was chosen explained?	☐ Yes, for at least one experiment ☐ No
3	Inclusion & Exclusion Criteria	Are the criteria used for including and excluding animals, experimental units, or data points provided?	☐ Yes, for at least one experiment ☐ No
		Are any exclusions of animals, experimental units, or data points reported, or is there a statement indicating that there were no exclusions?	☐ Yes, for at least one analysis ☐ No
4	Randomisation	Is the method by which experimental units were allocated to control and treatment groups described?	☐ Yes, for at least one experiment ☐ No
5	Blinding	Is it clear whether researchers were aware of, or blinded to, the group allocation at any stage of the experiment or data analysis?	☐ Yes, for at least one experiment ☐ No
6	Outcome Measures	For all experimental outcomes presented, are details provided of exactly what parameter was measured?	☐ Yes, for at least one experiment ☐ No
7	Statistical Methods	Is the statistical approach used to analyse each outcome detailed?	☐ Yes, for at least one analysis ☐ No
		Is there a description of any methods used to assess whether data met statistical assumptions?	☐ Yes, for at least one analysis ☐ No ☐ Not applicable
8	Experimental Animals	Are all species of animal used specified?	☐ Yes, for at least one experiment ☐ No
		Is the sex of the animals specified?	☐ Yes, for at least one experiment ☐ No ☐ Not applicable to species
		Is at least one of age, weight or developmental stage of the animals specified?	☐ Yes, for at least one experiment ☐ No
9	Experimental Procedures	Are both the timing and frequency with which procedures took place specified?	☐ Yes, for at least one experiment ☐ No
		Are details of acclimatisation periods to experimental locations provided?	☐ Yes, for at least one experiment ☐ No
10	Results	Are descriptive statistics for each experimental group provided, with a measure of variability (e.g. mean and SD, or median and range)?	☐ Yes, for at least one experiment ☐ No ☐ Not applicable to the type of data collected
		Is the effect size and confidence interval provided?	☐ Yes, for at least one experiment ☐ No ☐ Not applicable to the type of analysis used

Notes on questionnaire design

The ARRIVE guidelines are a useful resource for authors preparing manuscripts describing animal research, and also provide a framework to evaluate the transparency of those manuscripts. To assess reporting quality, numerous studies have in the past sought to operationalise reporting guidelines (including ARRIVE). Typically, this involves scoring a manuscript's degree of compliance with guideline items in a binary fashion (e.g. an item is either not reported or reported) [1-3], a graded fashion (e.g. not, partially, or completely reported) [4,5], or a combination of the two [6].

This questionnaire has been designed to be as concise and user-friendly as possible. The number of questions used to assess a manuscript's compliance has been kept to a minimum, and in most cases each question is designed to be answered in a binary fashion. Compliance with some Essential 10 sub-items is inherently impossible to judge in this way, instead requiring a subjective judgement on the level of detail provided. For this reason, not all sub-items are represented by a question in this questionnaire.

To facilitate binary answers, it has been necessary to identify the minimum information in a manuscript sufficient to comply with each question. The strengths of this approach include the relatively short length of the questionnaire (and the correspondingly low time burden of using it), and the avoidance of ambiguity that would arise from a graded answering system, in which an intermediate score (e.g. 'partially/insufficiently reported') could denote a number of distinct deficiencies in compliance with an item (e.g. either only part of the item was complied with, or only the reporting of some experiments in the manuscript complied with the item.)

Limitations of this approach centre on the necessity to identify the minimum information sufficient to comply with each question. In some cases, this has resulted in questions that require a guideline sub-item's criteria to have been fulfilled in the reporting of only one experiment in a manuscript. As a result, not all experiments in a manuscript may be described in a way that fulfils that criterion, despite the manuscript being considered to comply with the guidelines overall.

References

1. Hair *et al* (2020). *Res Integ Peer Rev*. doi: 10.1186/s41073-019-0069-3
2. Tihanyi *et al* (2019). *J Surg Res*. doi: 10.1016/j.jss.2018.10.038
3. Zhao *et al* (2020). *BMC Vet Res*. doi: 10.1186/s12917-020-02664-1
4. Han *et al* (2017). *Plos One*. doi: 10.1371/journal.pone.0183591
5. Chatzimanouil *et al* (2019). *J Am Soc Nephrol*. doi: 10.1681/ASN.2018050515
6. Leung *et al* (2018). *Plos One*. doi: 10.1371/journal.pone.0197882

Paper-3

ASN Neuro

An association of Chitinase-3 like-protein-1 with neuronal deterioration in multiple sclerosis.

Journal:	*ASN Neuro*
Manuscript ID	ASN-23-0037
Manuscript Type:	Original Papers
Knowledge Environments:	NEURO Immunity, NEURO Degeneration
Keywords:	demyelination < NEURO Degeneration, neuroinflammatory disorders < NEURO Immunity, neurotoxicity < NEURO Degeneration

Abstract: Elevated levels of Chitinase-3-like protein-1 (CHI3L1) in cerebrospinal fluid (CSF) have previously been linked to inflammatory activity and disease progression in multiple sclerosis (MS) patients. This study aimed to investigate the presence of CHI3L1 in the brains of MS patients and in the cuprizone model in mice (CPZ), a model of toxic/metabolic demyelination and remyelination in different brain areas. In MS grey matter (GM), CHI3L1 was expressed primarily in astrocytes and in a subset of pyramidal neurons. In neurons, CHI3L1 immunopositivity was associated with lipofuscin-like substance accumulation, a sign of cellular ageing that can lead to cell death. The density of CHI3L1-positive neurons was found to be significantly higher in normal-appearing MS grey matter tissue compared to that of control subjects ($p = 0.014$). In MS white matter (WM), CHI3L1 was detected in astrocytes located within lesion areas, as well as in perivascular normal-appearing areas, and in phagocytic cells from the initial phases of lesion development. In the CPZ model, the density of CHI3L1-positive cells was strongly associated with microglial activation in the WM and choroid plexus inflammation. Compared to controls, CHI3L1-immunopositivity in WM was increased from an early phase of CPZ exposure. In the GM, CHI3L1 immunopositivity increased later in the CPZ exposure phase, particularly in the deep grey matter region. These results indicate that CHI3L1 is associated with neuronal deterioration, pre-lesion pathology, along with inflammation in MS.

Original Manuscript

An association of Chitinase-3 like-protein-1 with neuronal deterioration in multiple sclerosis.

Intakhar Ahmad[1,2], Stig Wergeland[2], Eystein Oveland[3,4], Lars Bø[1,2]

[1] Department of Clinical Medicine, University of Bergen, Norway

[2] Norwegian Multiple Sclerosis Competence Centre, Department of Neurology, Haukeland University Hospital, Bergen, Norway

[3] Proteomics Unit at the University of Bergen (PROBE), Department of Biomedicine, University of Bergen, Norway.

[4] Institute of Marine Research, IMR, Postboks 1870 Nordnes, 5817 Bergen, Norway

Corresponding author: Lars Bø, Norwegian Multiple Sclerosis Competence Centre, Haukeland University Hospital, PO Box 1400, 5010 Bergen, Norway, E-mail: lars.bo@helse-bergen.no Tel: (47) 97432421

Running title: Chitinase-3-like protein 1 in MS and Cuprizone model.

Keywords: Chitinase-3-like protein 1 (CHI3L1); Multiple sclerosis; Cuprizone model; Inflammation; Demyelination; Neurodegeneration.

Abstract

Elevated levels of Chitinase-3-like protein-1 (CHI3L1) in cerebrospinal fluid (CSF) have previously been linked to inflammatory activity and disease progression in multiple sclerosis (MS) patients. This study aimed to investigate the presence of CHI3L1 in the brains of MS patients and in the cuprizone model in mice (CPZ), a model of toxic/metabolic demyelination and remyelination in different brain areas. In MS grey matter (GM), CHI3L1 was expressed primarily in astrocytes and in a subset of pyramidal neurons. In neurons, CHI3L1 immunopositivity was associated with lipofuscin-like substance accumulation, a sign of cellular aging that can lead to cell death. The density of CHI3L1-positive neurons was found to be significantly higher in normal-appearing MS grey matter tissue compared to that of control subjects ($p = 0.014$). In MS white matter (WM), CHI3L1 was detected in astrocytes located within lesion areas, as well as in perivascular normal-appearing areas and in phagocytic cells from the initial phases of lesion development. In the CPZ model, the density of CHI3L1-positive cells was strongly associated with microglial activation in the WM and choroid plexus inflammation. Compared to controls, CHI3L1-immunopositivity in WM was increased from an early phase of CPZ exposure. In the GM, CHI3L1 immunopositivity increased later in the CPZ exposure phase, particularly in the deep grey matter region. These results indicate that CHI3L1 is associated with neuronal deterioration, pre-lesion pathology, along with inflammation in MS.

Introduction

Chitinase-3-like protein-1 (CHI3L1), also known as YKL-40, is a glycoprotein primarily expressed in various tissues and cells, including macrophages, neutrophils, chondrocytes, and endothelial cells (Bonneh-Barkay et al., 2010; Recklies et al., 2002). This protein has garnered significant attention in the field of neuroscience due to its involvement in various physiological and pathological processes in the central nervous system (CNS) (Pinteac et al., 2021). CHI3L1 plays a role in multiple sclerosis (MS) pathogenesis, both clinically and experimentally. It has been implicated in functions such as inflammation, tissue injury, repair, and remodeling across different tissues (Lee et al., 2011; Zhao et al., 2020).

In the clinical context, CHI3L1 has emerged as an important biomarker in MS. Increased expression levels of CHI3L1 have been observed in the cerebrospinal fluid (CSF) of individuals with MS. It has been reported that elevated CSF levels of CHI3L1 are associated with an increased risk of conversion from clinically isolated syndrome (CIS-MS) to clinically definite MS (Roslind & Johansen, 2009). Furthermore, the extent of disability in patients with MS has been shown to be correlated with increased levels of CHI3L1 in CSF (Comabella et al., 2010). Pérez-Miralles et al. (2020) demonstrated that elevated CSF levels of CHI3L1 are predictive of further disability development in primary progressive MS patients. Gil-Perotin et al. (2019) suggested that combined measurement of CHI3L1 and neurofilament light chain protein (NFL) can help differentiate MS phenotypes and predict clinical progression. Additionally, Floro et al. (2022) conducted a meta-analysis indicating that relative increases in CSF levels of CHI3L1 may distinguish primary progressive MS (PPMS) from relapsing-remitting MS (RRMS) and secondary progressive MS (SPMS). In a recent study, CHI3L1 has been suggested as a potentially useful biomarker for treatment decision-making in MS patients (Lucchini et al., 2023). In the study by Lucchini et al., multiple neuroinflammatory markers in the cerebrospinal fluid (CSF) were assessed in a large cohort of RRMS patients. The findings demonstrated that the group with high concentrations of both CXCL13 and CHI3L1 had a significantly higher risk of relapse, increased MRI activity, and evidence of disease activity during follow-up. Hence, the authors concluded that CSF levels of CXCL13 and CHI3L1 serve as strong prognostic markers in RRMS patients.

Experimental studies have provided insights into the functioning of CHI3L1 in the CNS. *In vitro* experiments have demonstrated that CHI3L1 exhibits a neuron-specific cytotoxic effect, leading to neurite retraction and reduced neuronal survival (Huang et al., 2014; Matute-Blanch et al., 2020). Furthermore, Jiang et al. (2019) reported that CHI3L1 promotes the proliferation of oligodendrocyte precursor cells (OPCs).

The cellular origin of CHI3L1 within the CNS remains an area of interest. Immunohistochemical studies have identified CHI3L1 immunopositivity in astrocytes and macrophages/microglia in MS brain tissue, particularly in active and chronic active white matter lesions (Cubas-Núñez et al., 2021; Hinsinger et al., 2015). However, a systematic assessment of CHI3L1 distribution in grey matter lesions (GMLs) and normal-appearing grey matter (NAGM) in MS has not been conducted to date.

Studies on the role of CHI3L1 in demyelination have been reported in the experimental autoimmune encephalomyelitis (EAE) mouse model. Mouse breast regression protein 39 (BRP-39) is homologous to the human CHI3L1 protein (Cantó et al., 2015). In one study, BRP-39 knockout female mice with EAE showed increased clinical scores and immunopathological markers of central nervous system (CNS) inflammation compared to controls (Bonneh-Barkay et al., 2012). However, another study using a combination of male and female mice and a different dose of antigen peptide found no difference in the clinical course of EAE between wild-type and BRP-39 knockout mice of the same mouse strain (Cantó et al., 2015). Although the EAE model provides insights into immune-mediated mechanisms and therapeutic interventions for MS, it primarily mimics the relapsing-remitting form of MS and does not fully capture the progressive aspects and long-term neurodegeneration seen in the disease (Giovannoni et al., 2017). On the other hand, the cuprizone (CPZ) model involves the administration of cuprizone, a copper chelator that induces demyelination in a toxicological manner (Skripuletz et al., 2011). The CPZ model exhibits features resembling the progressive forms of MS, making it suitable for studying progressive disease processes (Matsushima & Morell, 2001). To our knowledge, there are no studies published on the involvement of CHI3L1 in the pathogenesis of demyelination/neurodegeneration in the cuprizone (CPZ) model.

Therefore, the purpose of our study is to investigate the distribution of CHI3L1-expressing cells in both the MS brain and a mouse model of toxin-induced de- and remyelination known as the cuprizone (CPZ) model. By examining CHI3L1 expression patterns in MS lesions, including grey matter lesions, we aim to further elucidate the role of CHI3L1 in MS pathogenesis. Additionally, this study aims to contribute to the current knowledge by providing a comprehensive assessment of CHI3L1 distribution in the CNS. The novelty of our study lies in the systematic evaluation of CHI3L1 immunopositivity in grey matter lesions (GMLs) and normal-appearing grey matter (NAGM) in MS by expanding the assessment beyond white matter lesions.

Materials and methods

Human brain tissue samples

In this study, we have included autopsy material from 9 MS cases, along with 5 controls with no known CNS disease and no histopathological signs of infection, inflammation, or neurodegeneration. Demographic and clinical data were collected retrospectively (**Table 1**). The brain tissue samples were obtained from The Norwegian MS Registry and Biobank in the Department of Pathology, Haukeland University Hospital, Bergen, Norway. The study was approved by the institutional review board for medical research ethics of Western Norway (permit No: 2013-560). Consent to use tissue for research was taken in writing, either by the patient or after death by the nearest living relative. The medical records tagged with personal information were anonymized before those were used for research.

Particular attention was given to select brain samples from MS patients who were not too old to prevent the confounding effects of age-related CNS pathology. The median age of MS patients was 45 (min 34, max 52), while that of controls was 40 (min 30, max 53). However, the MS patients had a minimum disease duration of 7 years, which is sufficient to investigate disease progression.

Human brain histopathology

For human brain histopathology, sections (5-6 µm) from paraffin-embedded blocks were immunohistochemically stained for target proteins. For immunohistochemistry, the sections were dewaxed with xylene and then rehydrated through gradients of ethanol and into water. For antigen retrieval, sections were incubated in the Diva Decloaker antigen retrieval solution (DV2004LX, Biocare Medical, CA, USA) at pH 6.2; 120°C; at 15 psi for 15 min. Primary antibodies used for immunohistochemistry were myelin proteolipid protein, PLP (1:1000, Rabbit monoclonal, Abcam, RRID: AB_2915963; overnight at 4°C), HLA-DR (1:20, mouse monoclonal, DAKO, RRID:AB_2262753; 2h at RT) and CHI3L1 (1:200, Rabbit polyclonal, Abcam, RRID: AB_2891040; 24h at 4°C). The sections were blocked with a blocking solution (EnVision FLEX Peroxidase-Blocking Reagent, Dako, Glostrup) and visualized with EnVision+ System (Dako, Glostrup) following the manufacturer's guideline (EnVision Systems: EnVision+ Dual Link, Single Reagents; HRP. Rabbit/Mouse). The tissue sections were finally counterstained with hematoxylin before mounting permanently in Dibutylphthalate Polystyrene Xylene (DPX). The omission of the primary antibody acted as a negative control. The Sudan Black B (Sigma-Aldrich®) lipid staining, widely used to react against lipofuscin aggregates in cells, was applied to tissue sections from controls and MS patients containing cerebral cortex (Evangelou & Gorgoulis, 2017). Multiplex staining was performed using both immuno-enzymatic and immuno-fluorescence techniques, depending on the visual distinction required. Using the same primary antibodies immuno-enzymatic double labelling was carried out with the EnVision+ Dual Link System-HRP (Agilent Technologies Inc.) according to the manufacturer's instructions. In the immunofluorescence procedure, the sections were first deparaffinized and then blocked using PBS and 5% BSA before being stained in a humidified chamber at RT. The primary antibodies used were identical to single stainings. To label the primary antibodies, the VectaFluor™ Duet Immunofluorescence Double Labeling Kit was utilized, and DAPI (Invitrogen™) was applied for nuclear counterstaining. In our study, we identified neurons in the cortex based on their well-known distinct morphological features, which have also been highlighted by García-Cabezas et al. (2016).

Lesion identification, categorization, and quantification of CHI3L1+ cell density in human brain

Grey and white matter lesions were analyzed separately (n = 57). GMLs were initially categorized according to the Bø-Trapp classification system (Bø et al., 2003b, 2003a). Since mixed WM-GM lesions (type I) have immune cell infiltrates (Bø et al., 2003b), GM lesions have been grouped into mixed WM-GM lesions (n = 6) and purely intracortical lesions, types II, III, and IV (n= 19). For white matter lesions, lesions were classified according to inflammatory activity (Bö et al., 1994). In the WM part, HLA-DR staining was the basis for categorizing lesions (n= 32) as either active, chronic active, or inactive, and corresponding PLP staining was used to identify MS lesion areas (Ahmad et al., 2021; Oveland et al., 2021). Early active, active, and chronic active white matter lesions were put in the active lesion group (n =15). Immunopositivity was counted as a cumulative value of positive cell profiles in three random visual field fields of 0.0625 mm^2 each in regions of interest (ROI) by light microscopy (Zeiss Axio Imager A2, Wetzlar, Germany) using an ocular morphometric grid. Since cortical neurons in the controls were very weakly immunopositive for CHI3L1, careful thresholding was applied compared with neighbouring neurons.

Cuprizone (CPZ) experiment

For the cuprizone experiment, 48 female C57BL/6 mice were obtained from Taconic Biosciences (Tornbjerg, Denmark) at the age of 7 weeks. It has been reported that there is no significant difference in the demyelination severity induced by Cuprizone in male and female C57BL/6 mice (Vega-Riquer et al., 2019). During the acclimatization and experimental periods, they were housed in six per cage in Macrolon IVC-II cages (Scanbur, Karlslunde, Denmark). After one week of adaptation to the laboratory environment, 8-week-old mice were randomized to eight groups of six mice and exposed to 0.2% (w/w) CPZ (bis-cyclohexanone-oxaldihydrazone, Sigma-Aldrich, St. Louis, MO) in mouse diet for up to six weeks. Food and tap water were provided ad libitum throughout the experimental period. Mice were sacrificed weekly (6 per week) during CPZ exposure, and the remaining group (n=6) was sacrificed two weeks after ending CPZ exposure. Control mice (n=6) were sacrificed at the onset of the experiment. To minimize suffering and distress for the animals, their cages were provided with bedding, nesting material, shelters, and chewing implements. Pain relief and, thus a need for analgesics was not expected in this study. In one experiment group, one mouse out of a group of six died after three weeks of cuprizone exposure, and that mouse was excluded from the analysis. The experiment was conducted

following the recommendations of the Federation of European Laboratory Animal Science Associations and the ARRIVE guidelines (du Sert et al., 2020). The Norwegian Animal Research Authority approved the experimental protocol.

Mouse brain histopathology

Mice were euthanized by CO2 asphyxiation, and collected brains were post-fixed in 4% neutral buffered formalin (NBF) for 7 days, then embedded in paraffin. All analyses were performed on 5 µm coronal sections from the bregma +1 mm. The CPZ sections were incubated with primary antibodies against myelin proteolipid protein, PLP (1:1000, Rabbit monoclonal, Abcam, RRID: AB_2915963; overnight at 4°C), MAC3 (1:200, Rat monoclonal, BD Biosciences, RRID: AB_394780; 24h at 4°C), CHI3L1(Brp39) (1:200, Rabbit polyclonal, Abcam, RRID: AB_2891040; 24h at 4°C). The sections were blocked with peroxidase blocking solution (Dako, Glostrup) and visualized with the EnVision+ System (Dako, Glostrup, DK). The tissue sections were counterstained with hematoxylin. The omission of the primary antibody was used as a negative control for the secondary antibody following the same immunohistochemical methods used for human samples.

Quantification of CHI3L1+, MAC3+ cell density, and myelin content in CPZ mouse brain

In the CPZ model, the density of CHI3L1 and MAC3 immunopositive cells in grey matter (cerebral cortex), in white matter (corpus callosum), and in a mixed tissue area (deep grey matter) were examined by light microscopy (Zeiss Axio Imager A2, Wetzlar, Germany) using an ocular morphometric grid on three random areas. Study areas are marked in the **Figure. 5A** and the study design is schematically explained in the **Figure. 5B**. The ocular morphometric grid covered an area of 0.0625 mm^2. For the cortex, systematically randomized areas in the primary somatosensory cortex within layers 2-5 were quantified. Cell densities were the nearest whole number of the average of three randomly selected areas in the cortex and the deep grey matter. For the corpus callosum, a single count from each of the two lateral and the medial part. Counts were averaged to a single integer value.

Statistical analysis

Due to the non-normal distribution pattern of the data, statistical analysis was performed using the Wilcoxon sign rank test to evaluate pairwise differences between different lesion groups within the same tissue samples in human specimens. The Kruskal-Wallis test was utilized to determine the overall difference between the control and MS tissue samples. For CPZ samples, the temporal changes in CHI3L1+ cell density in different brain tissue regions during demyelination were analyzed using one-way analysis of variance (ANOVA) with Tukey's HSD test. An independent-samples t-test was applied to determine the statistical significance of the differences between the sample group and the control group. The Pearson Correlation Coefficient (r) was calculated to assess the relationship between cell densities and various immunostainings across the entire experimental period in different tissue regions. All analyses were performed using GraphPad Prism version 9.0 (GraphPad Software Inc., San Diego, CA). Results were considered significant at $p < 0.05$.

Results

CHI3L1 expression pattern in human grey matter tissue

In MS brains, CHI3L1 immunopositivity was not restricted to the grey matter lesion areas; diffuse immunopositivity was observed throughout the cerebral cortex (**Figure. 1)**. The frequency and extent of CHI3L1 immunopositivity were increased in and around GM lesions (**Figure. 1A, 1D)**. Strong CHI3L1 immunopositivity was frequently detected in cells with reactive astrocyte morphology and in astrocyte-like cell processes in the extracellular matrix areas around the clusters of strongly CHI3L1-positive reactive astrocyte looking cells (**Figure. 1A-B**). It is already established through hybridisation studies that, *in vivo*, the transcription of CHI3L1 is primarily connected with astrocytes (Bonneh-Barkay et al., 2010). Additionally, we found that a minor subset of pyramidal neurons and a small minority of cells having the morphology of non-activated astrocytes were less intensely immunopositive for CHI3L1 (**Figure. 1A, 1C**). The extracellular matrix adjacent to neurons or non-activated astrocytes was not immunopositive for CHI3L1 (**Figure. 1A, 1C, 1E**). In neurons, in and around GM lesions, granular CHI3L1+ vesicles were

observed in the cell body cytoplasm around the nucleus (**Figure. 1D-E**). Rarely, axons were weakly immunopositive for CHI3L1 (**Figure. 1E**).

Normal-appearing MS cortex and control cortex also contained CHI3L1 immunopositive neurons (**Figure. 2A-B**). Though, the control cortex was very weakly positive for neurons (**Figure. 2B).** The density of CHI3L1 immunopositive neurons was significantly higher ($p = 0.014$) in normal-appearing MS tissue when compared to controls (**Figure. 2C**). The density of CHI3L1 immunopositive cells was significantly higher in the grey matter part of mixed GM/WM lesions (type I) than in pure GM lesions and normal appearing cortex (**Figure. 2D**).

Features of CHI3L1+ cells

The CHI3L1+ granular structures have an association in pyramidal neurons having lipid-containing residues (lipofuscins), as identified by relating CHI3L1 and Sudan black staining pattern of the same region of the same tissue blocks with the help of morphological details at subcellular level (**Figure. 3A-B**). Negligible or absent Sudan black staining was evident in the control grey matter samples (**Figure. 3C**). The co-labeling of CHI3L1 and lipofuscin was not feasible due to incompatible methodologies. It is noteworthy that only a subset of neuronal cells had lipofuscin vesicles stained by Sudan black, and no Sudan black-positive glial or infiltrating cells were observed in the cortex.

Colocalization of CHI3L1 was detected on GFAP+ cells (astrocytes), primarily in cellular processes (**Figure. 3D**). HLA-DR+ cells were also positive for CHI3L1 (**Figure. 3E**). It was evident that CHI3L1 positivity was predominant in reactive astrocytes; however not all reactive astrocytes were CHI3L1 positive (**Figure. 3D**).

CHI3L1 expression pattern in human white matter tissue

In MS normal-appearing white matter (NAWM), cellular and extracellular CHI3L1 immunopositivity was frequently observed both in the lining and immediately outside of the perivascular space (**Figure. 4A-B**). Not all blood vessels were positive for CHI3L1+ cells, however, most of the CHI3L1+ cells in the vicinity of blood vessels had an activated astrocyte morphology (**Figure. 4A).** Like in grey matter areas, extracellular matrix areas around clusters of

strongly positive astrocytes were immunopositive for CHI3L1, morphologically consistent with astrocyte processes (**Figure. 4B**). In MS spinal cord, the density of CHI3L1 positive astrocytes was increased in subpial WM areas (**Figure. 4C**). In early-stage WM MS lesions, cells with the morphology of foamy macrophages (containing abundant intracellular myelin remnants, identified by PLP positivity) were immunopositive for CHI3L1 (**Figure. 4D-E**). Foamy macrophages were accompanied by CHI3L1 astrocytes (**Figure. 4F**). In control brains, only very few cells were immunopositive for CHI3L1 compared to MS-WM **(Supplementary Figure. 1)**. Since the borders of active/chronic active white matter lesions were densely infiltrated by CHI3L1+ phagocytic macrophages, the density of CHI3L1+ cells were significantly higher in active/chronic active WM lesions compared to inactive lesions, NAWM areas, and control WM (**Figure. 4G**).

Temporal variation and distribution of CHI3L1 expression during and after cuprizone exposure in mice

The majority of CHI3L1-immunopositive cells in the white matter of the CPZ mice had microglial morphology. However, in the WM of control mice, almost no CHI3L1-immunopositivity was present, except for some immunopositivity within blood vessels (**Figure. 5C**). The increase in CHI3L1 immunopositivity was more pronounced and occurred earlier in the corpus callosum than in deep grey matter or cerebral cortex, yet a gradual increase of CHI3L1 immunopositivity was also observed in the deep grey matter during the entire experimental period (**Figure. 5C-D**). White and grey matter parts showed profound differences in the pattern of CHI3L1 positivity. In the cortex, the increase of immunopositivity was slower and less pronounced, and went back almost to pre-exposure levels after ending the CPZ exposure (**Figure. 5C-D**). The density of CHI3L1+ cells declined sharply in the corpus callosum ($p=0.002$). Unlike in the cortex, the WM (corpus callosum) decline did not reach the pre-exposure level.

The density of Mac-3+ cells in the corpus callosum increased during CPZ exposure and waned quickly after completing the exposure, which follows the pattern of CHI3L1 distribution. In deep grey matter, CHI3L1+ cells appeared earlier in white matter tracts, where microglia activation was observed (**Figure. 6A-B**). On the contrary, CHI3L1+ neurons were detected at a later stage of CPZ exposure (**Figure. 6C**), which follows the pattern in the cortex area (**Figure. 6D**). The increase in density of Mac-3+ cells during CPZ exposure was less pronounced in the cortex **(Figure. 6E)**. Combination of white and grey matter tissue parts made the increase in Mac-

3 positivity moderate in the deep grey matter, and Mac-3 immunopositivity was mostly confined to white matter patches in the deep grey matter **(Figure. 6B, 6E).** The density of CHI3L1+ cells and Mac-3+ cells were significantly correlated in the corpus callosum of the CPZ mice ($r= 0.76$, $p<0.05$). CHI3L1 immunopositivity also showed a strong association with choroid plexus inflammation identified by Mac-3 immunopositivity **(Supplementary Figure. 2)**

Discussion

This study investigates the presence of CHI3L1 in the brains of MS (mostly PMS) patients and in the cuprizone model in mice to characterize further the role of CHI3L1 in the pathogenesis of MS. The findings are consistent with prior results indicating that the molecule plays a role in modulating the inflammatory response within the CNS. Furthermore, this study also discovered increased CHI3L1 immunopositivity in the cortex of individuals with MS.

While the role of CHI3L1 in the pathogenesis of MS is unknown, most studies on CSF samples from MS patients indicate that CHI3L1 may be a marker of CNS inflammation (Burman et al., 2016). Expression and/or secretion of CHI3L1 may be neurotoxic, as CHI3L1 concentrations similar to those measured in the CSF from active MS patients, were mildly neurotoxic to primary cultured neurons in vitro (Matute-Blanch et al., 2020). The CSF level of CHI3L1 was correlated to cognitive impairment in the early stages of MS (Quintana et al., 2018). Clinically isolated syndrome (CIS) patients with high CSF levels of CHI3L1 have been reported to have a four times higher risk for the development of neurological disability, compared to CIS subjects with low CSF CHI3L1 levels (Canto 2015). The observations above indicate an association of CHI3L1 with neuronal degeneration and/or decreased neuronal function in MS. This is supported by data from other neurodegenerative diseases. Elevated CHI3L1 level in CSF is a biomarker for Alzheimer's Disease development (Wennström et al., 2015). CHI3L1 expression levels are significantly upregulated in the motor cortex of patients with motor neuron disease in sporadic amyotrophic lateral sclerosis (Sanfilippo et al., 2017).

In this study, in grey matter, extensive CHI3L1 immunopositivity was observed in astrocytes in lesion- and near-lesion areas, and in granular cytoplasmic structures in pyramidal

neurons (**Figure. 1**). This is a similar pattern to what has recently been reported in Alzheimer's disease cortex (Hok-A-Hin et al., 2022). Although very faintly CHI3L1+ neurons were detected in control brains, they were significantly more frequent in the MS brains, in the lesions, in near-lesion- and normal-appearing areas, compared to the control brains **(Figure. 2C).**

In neurons, CHI3L1 immunopositivity was mainly confined in the subcellular areas that that exhibit positivity for lipid vesicles (lipofuscin) **(Figure. 3A-B)**. Lipofuscin accumulation in the CNS is associated with ageing (Gray & Woulfe, 2005), interpreted to be a product of defective cellular metabolism, including mitochondrial dysfunction, incomplete mitophagy, altered proteostasis, protein misfolding and aggregation, and endolysosomal dysfunction(Moreno-García et al., 2018). The macroautophagy-lysosomal pathway is essential for maintaining protein and energy homeostasis (Lamark & Johansen, 2012). Dysfunctions of the lysosomal system have been implicated in neurodegenerative diseases with protein aggregation and mitochondrial dysfunction. The asparaginyl endopeptidase legumain is upregulated in neurons in Alzheimer's disease and in posttraumatic neurodegeneration. This molecule is considered as a biomarker and a potential therapeutic target for Alzheimer's disease (Song, 2022). Legumain is also activated in lysosomes and is also present in aggregates in the frontal cortex neurons of the MS brain (Oveland et al., 2021). Lipofuscin is a cytoplasmic accumulation of lipid and protein debris (Gray & Woulfe, 2005) . Endocytosis and endosomal sorting can bring extracellular macromolecules to lysosomes (Ferguson, 2019). Chitinase-like proteins can bind extracellular matrix components (Kognole & Payne, 2017), and membrane-associated proteins can be endocytosed within the neuron by several possible routes (Henaff & Salinas, 2010; Parton & Dotti, 1993). However, this study did not explore the source or the entry mechanism of CHI3L1 into neuronal cells.

In early active white matter lesions, foamy phagocytic cells (macrophages) were positive for CHI3L1 (**Figure. 4D-E**). CHI3L1 immunopositivity in macrophages was tightly associated with inflammation, as the inflammatory regions of active/chronic active WM lesions and the mixed GM/WM lesions had the highest density of CHI3L1+ cells (**Figure. 2D, 4G**).

In perivascular areas of normal-appearing white matter in MS, astrocytes in perivascular areas were frequently immunopositive for CHI3L1 (**Figure. 4A-B**). CHI3L1 immunopositivity may thus be associated with blood-brain barrier (BBB) integrity in the early stages of white matter

lesion development, as plasma protein leakage is a white matter phenomenon, whereas plasma protein leakage is frequently absent in grey matter lesions (Van Horssen et al., 2007).

In the CPZ model, CHI3L1 immunopositivity was closely related to the inflammatory response, and mostly detected in cells with microglial morphology (**Figure. 5C**). During the CPZ exposure phase, the spontaneous remyelination process starts around week three (Ahmad et al., 2021). Interestingly, the increase of CHI3L1 immunopositivity started to rise from that time point, even in grey matter parts (**Figure. 5D**). This indicates that CHI3L1 might be associated with remyelination processes, as inflammatory cells participate in the early signaling of remyelination events (Skihar et al., 2009). The correlation of CHI3L1 with remyelination is supported by an observation indicating that molecules of the CHI3L1 family can induce oligodendrogenesis in the EAE model (Starossom et al., 2019).

CHI3L1+ microglial cells appeared early in the WM fibre tracts embedded in the deep grey matter during the CPZ exposure period. This was followed by the appearance of CHI3L1+ neurons in deep grey matter (**Figure. 6A-6C**). In the late stage of CPZ exposure, a few cortical neurons were also found immunopositive (**Figure. 6D**). These data support an association of CHI3L1 neuronal immunopositivity with inflammation-related insults in neuronal cells.

The present study has limitations. Most autopsy MS samples were from the progressive MS phenotype, and the observed pattern of CHI3L1 immunopositivity needs to be verified in earlier stages of MS or RRMS. The median age for the control patients was 5 years lower than for the MS patients. The variation could introduce a higher degree of association between CHI3L1 and the degeneration of lipofuscin-positive neurons, given that elevated levels of neuronal lipofuscin are a common characteristic of ageing. However, the data from the CPZ model supports the appearance of CHI3L1+ neurons being associated with inflammation-related neuronal stress in the brain. Our study discerned the association between lipofuscins and CHI3L1+ neurons by comparing the CHI3L1 and Sudan Black staining in the same regions of identical tissue blocks. The study encountered a methodological constraint due to our inability to perform double staining of CHI3L1 and lipofuscin, resulting from the incompatibility between the immunostaining and chemical staining techniques applied to each. Despite an extensive literature search, we couldn't find any verified protocols for performing double staining with Sudan Black-B and an antibody.

Remarkably, Sudan Black B (Sigma-Aldrich®), a unique lipid staining method for Lipofuscin, enables the identification of senescent cells (Evangelou & Gorgoulis, 2017). Our study identified cortex neurons based on distinct morphological features. Colocalization analysis confirmed the astrocyte identity of CHI3L1+ cells with an astrocyte morphology. The study also found that antigen-presenting cells with a microglia/macrophage morphology were CHI3L1 positive. The microglial/macrophage identity of these cells was confirmed by the colocalization of CHI3L1 with HLA-DR. Several previous studies by us and others have found that HLA-DR+ cells in MS-lesions are macrophage/microglia (Bø et al., 1994). Future studies could focus on exploring colocalization patterns of CHI3L1+ neurons using various neuronal markers.

In addition to the known role of CHI3L1 in neuroinflammation, this study highlights some previously unidentified roles of CHI3L1 in MS pathology, by identifying its association with neurodegeneration in GM and BBB abnormalities in the WM. These findings are further strengthened by the observed association of CHI3L1 positivity with the inflammation of the choroid plexus in the cuprizone mouse (**Supplementary Figure. 2**), since choroid plexus inflammation is correlated to neurodegeneration and malfunction of BBB (Čarna et al., 2023; Wolburg & Paulus, 2010).

Conclusions

This research elucidates further roles of CHI3L1 in the pathogenesis of MS, particularly its progressive form. The central findings predominantly underscore CHI3L1's association with neuronal deterioration, pre-lesion pathology, and inflammatory changes in MS, thereby affirming its contribution to the disease's progression. While the study corroborates earlier findings linking CHI3L1 with macrophage infiltration and glial activation, it expands our understanding by demonstrating a higher level of CHI3L1 immunopositivity in the cortex of MS patients. Broadly, this investigation has revealed new aspects of CHI3L1's role in MS pathology. It highlights its correlation with neuronal degradation in grey matter, abnormalities in the blood-brain barrier, and the occurrence of CHI3L1 positivity tied to inflammation of the choroid plexus in a cuprizone mouse model.

References

Ahmad, I., Wergeland, S., Oveland, E., & Bø, L. (2021). A higher proportion of ermin-immunopositive oligodendrocytes in areas of remyelination. *PLOS ONE*, *16*(8), e0256155. https://doi.org/10.1371/journal.pone.0256155

Bö, L., Mörk, S., Kong, P. A., Nyland, H., Pardo, C. A., Trapp, B. D., Bo, L., Mork, S., Kong, P. A., Nyland, H., Pardo, C. A., & Trapp, B. D. (1994). Detection of MHC class II-antigens on macrophages and microglia, but not on astrocytes and endothelia in active multiple sclerosis lesions. *J Neuroimmunol*, *51*(2), 135–146. https://doi.org/10.1016/0165-5728(94)90075-2

Bø, L., Vedeler, C. a, Nyland, H. I., Trapp, B. D., & Mørk, S. J. (2003a). Subpial demyelination in the cerebral cortex of multiple sclerosis patients. *Journal of Neuropathology and Experimental Neurology*, *62*(7), 723–732. https://doi.org/10.1093/jnen/62.7.723

Bø, L., Vedeler, C. A., Nyland, H., Trapp, B. D., & Mørk, S. J. (2003b). Intracortical multiple sclerosis lesions are not associated with increased lymphocyte infiltration. *Multiple Sclerosis*, *9*(4), 323–331. https://doi.org/10.1191/1352458503ms917oa

Bonneh-Barkay, D., Wang, G., LaFramboise, W. A., Wiley, C. A., & Bissel, S. J. (2012). Exacerbation of experimental autoimmune encephalomyelitis in the absence of breast regression protein 39/chitinase 3-like 1. *Journal of Neuropathology and Experimental Neurology*, *71*(11). https://doi.org/10.1097/NEN.0b013e31826eaee7

Bonneh-Barkay, D., Wang, G., Starkey, A., Hamilton, R. L., & Wiley, C. A. (2010). *In vivo* CHI3L1 (YKL-40) expression in astrocytes in acute and chronic neurological diseases. *Journal of Neuroinflammation*, *7*. https://doi.org/10.1186/1742-2094-7-34

Burman, J., Raininko, R., Blennow, K., Zetterberg, H., Axelsson, M., & Malmeström, C. (2016). YKL-40 is a CSF biomarker of intrathecal inflammation in secondary progressive multiple sclerosis. *Journal of Neuroimmunology*, *292*, 52–57. https://doi.org/10.1016/j.jneuroim.2016.01.013

Cantó, E., Espejo, C., Costa, C., Montalban, X., & Comabella, M. (2015). Breast regression protein-39 is not required for experimental autoimmune encephalomyelitis induction. *Clinical Immunology*, *160*(2), 133–141. https://doi.org/10.1016/j.clim.2015.06.004

Čarna, M., Onyango, I. G., Katina, S., Holub, D., Novotny, J. S., Nezvedova, M., Jha, D., Nedelska, Z., Lacovich, V., Vyvere, T. Vande, Houbrechts, R., Garcia-Mansfield, K., Sharma, R., David-Dirgo, V., Vyhnalek, M., Texlova, K., Chaves, H., Bakkar, N., Pertierra, L., … Stokin, G. B. (2023). Pathogenesis of Alzheimer's disease: Involvement of the choroid plexus. *Alzheimer's and Dementia*. https://doi.org/10.1002/alz.12970

Comabella, M., Fernández, M., Martin, R., Rivera-Vallvé, S., Borrás, E., Chiva, C., Juli, E., Rovira, A., Cantó, E., Alvarez-Cermeño, J. C., Villar, L. M., Tintoré, M., & Montalban, X. (2010). Cerebrospinal fluid chitinase 3-like 1 levels are associated with conversion to multiple sclerosis. *Brain*, *133*(4), 1082–1093. https://doi.org/10.1093/brain/awq035

Cubas-Núñez, L., Gil-Perotín, S., Castillo-Villalba, J., López, V., Solís Tarazona, L., Gasqué-Rubio, R., Carratalá-Boscá, S., Alcalá-Vicente, C., Pérez-Miralles, F., Lassmann, H., & Casanova, B. (2021). Potential Role of CHI3L1+ Astrocytes in Progression in MS. *Neurology(R) Neuroimmunology & Neuroinflammation*, *8*(3). https://doi.org/10.1212/NXI.0000000000000972

du Sert, N. P., Hurst, V., Ahluwalia, A., Alam, S., Avey, M. T., Baker, M., Browne, W. J., Clark, A., Cuthill, I. C., Dirnagl, U., Emerson, M., Garner, P., Holgate, S. T., Howells, D. W., Karp, N. A., Lazic, S. E., Lidster, K., MacCallum, C. J., Macleod, M., … Würbel, H. (2020). The arrive guidelines 2.0: Updated guidelines for reporting animal research. *PLoS Biology*, *18*(7). https://doi.org/10.1371/journal.pbio.3000410

Evangelou, K., & Gorgoulis, V. G. (2017). Sudan black B, the specific histochemical stain for lipofuscin: A novel method to detect senescent cells. *Methods in Molecular Biology*, *1534*. https://doi.org/10.1007/978-1-4939-6670-7_10

Ferguson, S. M. (2019). Neuronal lysosomes. In *Neuroscience Letters* (Vol. 697). https://doi.org/10.1016/j.neulet.2018.04.005

Floro, S., Carandini, T., Pietroboni, A. M., De Riz, M. A., Scarpini, E., & Galimberti, D. (2022). Role of Chitinase 3-like 1 as a Biomarker in Multiple Sclerosis: A Systematic Review and Meta-analysis. *Neurology(R) Neuroimmunology & Neuroinflammation*, *9*(4), 1–14. https://doi.org/10.1212/NXI.0000000000001164

García-Cabezas, M. Á., John, Y. J., Barbas, H., & Zikopoulos, B. (2016). Distinction of neurons, glia and endothelial cells in the cerebral cortex: an algorithm based on cytological features. *Frontiers in Neuroanatomy*, 10. https://doi.org/10.3389/fnana.2016.00107

Gil-Perotin, S., Castillo-Villalba, J., Cubas-Nuñez, L., Gasque, R., Hervas, D., Gomez-Mateu, J., Alcala, C., Perez-Miralles, F., Gascon, F., Dominguez, J. A., & Casanova, B. (2019). Combined Cerebrospinal Fluid Neurofilament Light Chain Protein and Chitinase-3 Like-1 Levels in Defining Disease Course and Prognosis in Multiple Sclerosis. *Frontiers in Neurology*, *10*. https://doi.org/10.3389/fneur.2019.01008

Giovannoni, G., Cutter, G., Pia-Sormani, M., Belachew, S., Hyde, R., Koendgen, H., Knappertz, V., Tomic, D., Leppert, D., Herndon, R., Wheeler-Kingshott, C. A. M., Ciccarelli, O., Selwood, D., di Cantogno, E. V., Ben-Amor, A. F., Matthews, P., Carassiti, D., Baker, D., & Schmierer, K. (2017). Is multiple sclerosis a length-dependent central axonopathy? The case for therapeutic lag and the asynchronous progressive MS hypotheses. In *Multiple Sclerosis and Related Disorders* (Vol. 12). https://doi.org/10.1016/j.msard.2017.01.007

Gray, D. A., & Woulfe, J. (2005). Lipofuscin and aging: a matter of toxic waste. In *Science of aging knowledge environment : SAGE KE* (Vol. 2005, Issue 5). https://doi.org/10.1126/sageke.2005.5.re1

Henaff, D., & Salinas, S. (2010). An endocytic CARriage tale: Adenoviruses internalization and trafficking in neurons. *Virulence*, *1*(3). https://doi.org/10.4161/viru.1.3.11379

Hinsinger, G., Galéotti, N., Nabholz, N., Urbach, S., Rigau, V., Demattei, C., Lehmann, S., Camu, W., Labauge, P., Castelnovo, G., Brassat, D., Loussouarn, D., Salou, M., Laplaud, D., Casez, O., Bockaert, J., Marin, P., & Thouvenot, E. (2015). Chitinase 3-like proteins as diagnostic and prognostic biomarkers of multiple sclerosis. *Multiple Sclerosis*, *21*(10). https://doi.org/10.1177/1352458514561906

Hok-A-Hin, Y. S., Hoozemans, J. J. M., Hu, W. T., Wouters, D., Howell, J. C., Rábano, A., van der Flier, W. M., Pijnenburg, Y. A. L., Teunissen, C. E., & del Campo, M. (2022). YKL-40 changes are not detected in post-mortem brain of patients with Alzheimer's disease and frontotemporal lobar degeneration. *Alzheimer's Research and Therapy*, *14*(1). https://doi.org/10.1186/s13195-022-01039-y

Huang, C., Huang, B., Bi, F., Yan, L. H., Tong, J., Huang, J., Xia, X. G., & Zhou, H. (2014). Profiling the genes affected by pathogenic TDP-43 in astrocytes. *Journal of Neurochemistry*, *129*(6). https://doi.org/10.1111/jnc.12660

Jiang, L., Xu, D., Zhang, W. J., Tang, Y., & Peng, Y. (2019). Astrocytes induce proliferation of oligodendrocyte progenitor cells via connexin 47-mediated activation of Chi3l1 expression. *European Review for Medical and Pharmacological Sciences*, *23*(7). https://doi.org/10.26355/eurrev_201904_17583

Kognole, A. A., & Payne, C. M. (2017). Inhibition of Mammalian Glycoprotein YKL-40. *Journal of Biological Chemistry*, *292*(7). https://doi.org/10.1074/jbc.m116.764985

Lamark, T., & Johansen, T. (2012). Aggrephagy: Selective disposal of protein aggregates by macroautophagy. In *International Journal of Cell Biology*. https://doi.org/10.1155/2012/736905

Lee, C. G., Da Silva, C. A., Dela Cruz, C. S., Ahangari, F., Ma, B., Kang, M. J., He, C. H., Takyar, S., & Elias, J. A. (2011). Role of chitin and chitinase/chitinase-like proteins in inflammation, tissue remodeling, and injury. *Annual Review of Physiology*, *73*. https://doi.org/10.1146/annurev-physiol-012110-142250

Lucchini, M., De Arcangelis, V., Piro, G., Nociti, V., Bianco, A., De Fino, C., Di Sante, G., Ria, F., Calabresi, P., & Mirabella, M. (2023). CSF CXCL13 and Chitinase 3-like-1 Levels Predict Disease Course in Relapsing Multiple Sclerosis. *Molecular Neurobiology*, *60*(1). https://doi.org/10.1007/s12035-022-03060-6

Matsushima, G. K., & Morell, P. (2001). The neurotoxicant, cuprizone, as a model to study demyelination and remyelination in the central nervous system. *Brain Pathology*, *11*(1), 107–116. https://doi.org/10.1111/j.1750-3639.2001.tb00385.x

Matute-Blanch, C., Calvo-Barreiro, L., Carballo-Carbajal, I., Gonzalo, R., Sanchez, A., Vila, M., Montalban, X., & Comabella, M. (2020). Chitinase 3-like 1 is neurotoxic in primary cultured neurons. *Scientific Reports*, *10*(1). https://doi.org/10.1038/s41598-020-64093-2

Moreno-García, A., Kun, A., Calero, O., Medina, M., & Calero, M. (2018). An overview of the role of lipofuscin in age-related neurodegeneration. In *Frontiers in Neuroscience* (Vol. 12, Issue JUL). https://doi.org/10.3389/fnins.2018.00464

Oveland, E., Ahmad, I., Lereim, R. R., Kroksveen, A. C., Barsnes, H., Guldbrandsen, A., Myhr, K. M., Bø, L., Berven, F. S., & Wergeland, S. (2021). Cuprizone and EAE mouse frontal cortex proteomics revealed proteins altered in multiple sclerosis. *Scientific Reports*, *11*(1). https://doi.org/10.1038/s41598-021-86191-5

Parton, R. G., & Dotti, C. G. (1993). Cell biology of neuronal endocytosis. In *Journal of Neuroscience Research* (Vol. 36, Issue 1). https://doi.org/10.1002/jnr.490360102

Pérez-Miralles, F., Prefasi, D., García-Merino, A., Gascón-Giménez, F., Medrano, N., Castillo-Villalba, J., Cubas, L., Alcalá, C., Gil-Perotín, S., Gómez-Ballesteros, R., Maurino, J., Álvarez-García, E., & Casanova, B. (2020). CSF chitinase 3-like-1 association with disability of primary progressive MS. *Neurology(R) Neuroimmunology & Neuroinflammation*, *7*(5). https://doi.org/10.1212/NXI.0000000000000815

Pinteac, R., Montalban, X., & Comabella, M. (2021). Chitinases and chitinase-like proteins as biomarkers in neurologic disorders. In *Neurology(R) neuroimmunology & neuroinflammation* (Vol. 8, Issue 1). https://doi.org/10.1212/NXI.0000000000000921

Quintana, E., Coll, C., Salavedra-Pont, J., Muñoz-San Martín, M., Robles-Cedeño, R., Tomàs-Roig, J., Buxó, M., Matute-Blanch, C., Villar, L. M., Montalban, X., Comabella, M., Perkal, H., Gich, J., & Ramió-Torrentà, L. (2018). Cognitive impairment in early stages of multiple sclerosis is associated with high cerebrospinal fluid levels of chitinase 3-like 1 and neurofilament light chain. *European Journal of Neurology*, *25*(9). https://doi.org/10.1111/ene.13687

Recklies, A. D., White, C., & Ling, H. (2002). The chitinase 3-like protein human cartilage glycoprotein 39 (HC-gp39) stimulates proliferation of human connective-tissue cells and activates both extracellular signal-regulated kinase- and protein kinase B-mediated signalling pathways. *Biochemical Journal*, *365*(1). https://doi.org/10.1042/BJ20020075

Roslind, A., & Johansen, J. S. (2009). YKL-40: a novel marker shared by chronic inflammation and oncogenic transformation. *Methods in Molecular Biology (Clifton, N.J.)*, *511*, 159–184. https://doi.org/10.1007/978-1-59745-447-6_7

Sanfilippo, C., Longo, A., Lazzara, F., Cambria, D., Distefano, G., Palumbo, M., Cantarella, A., Malaguarnera, L., & Di Rosa, M. (2017). CHI3L1 and CHI3L2 overexpression in motor cortex and spinal cord of sALS patients. *Molecular and Cellular Neuroscience*, *85*. https://doi.org/10.1016/j.mcn.2017.10.001

Skihar, V., Silva, C., Chojnacki, A., Döring, A., Stallcup, W. B., Weiss, S., & Yong, V. W. (2009). Promoting oligodendrogenesis and myelin repair using the multiple sclerosis medication glatiramer acetate. *Proceedings of the National Academy of Sciences of the United States of America*, *106*(42). https://doi.org/10.1073/pnas.0909607106

Skripuletz, T., Gudi, V., Hackstette, D., & Stangel, M. (2011). De- and remyelination in the CNS white and grey matter induced by cuprizone: The old, the new, and the unexpected. In *Histology and Histopathology* (Vol. 26, Issue 12). https://doi.org/10.14670/HH-26.1585

Song, M. (2022). The Asparaginyl Endopeptidase Legumain: An Emerging Therapeutic Target and Potential Biomarker for Alzheimer's Disease. In *International Journal of Molecular Sciences* (Vol. 23, Issue 18). MDPI. https://doi.org/10.3390/ijms231810223

Starossom, S. C., Campo Garcia, J., Woelfle, T., Romero-Suarez, S., Olah, M., Watanabe, F., Cao, L., Yeste, A., Tukker, J. J., Quintana, F. J., Imitola, J., Witzel, F., Schmitz, D., Morkel, M., Paul, F., Infante-Duarte, C., & Khoury, S. J. (2019). Chi3l3 induces oligodendrogenesis in an experimental model of autoimmune neuroinflammation. *Nature Communications*, *10*(1). https://doi.org/10.1038/s41467-018-08140-7

Van Horssen, J., Brink, B. P., De Vries, H. E., Van Der Valk, P., & Bø, L. (2007). The blood-brain barrier in cortical multiple sclerosis lesions. *Journal of Neuropathology and Experimental Neurology*, *66*(4), 321–328. https://doi.org/10.1097/nen.0b013e318040b2de

Vega-Riquer, J. M., Mendez-Victoriano, G., Morales-Luckie, R. A., & Gonzalez-Perez, O. (2019). Five Decades of Cuprizone, an Updated Model to Replicate Demyelinating Diseases. *Current Neuropharmacology*, *17*(2). https://doi.org/10.2174/1570159x15666170717120343

Wennström, M., Surova, Y., Hall, S., Nilsson, C., Minthon, L., Hansson, O., & Nielsen, H. M. (2015). The inflammatory marker YKL-40 is elevated in cerebrospinal fluid from patients with Alzheimer's but not Parkinson's disease or dementia with Lewy bodies. *PLoS ONE*, *10*(8). https://doi.org/10.1371/journal.pone.0135458

Wolburg, H., & Paulus, W. (2010). Choroid plexus: Biology and pathology. In *Acta Neuropathologica* (Vol. 119, Issue 1). https://doi.org/10.1007/s00401-009-0627-8

Zhao, T., Su, Z., Li, Y., Zhang, X., & You, Q. (2020). Chitinase-3 like-protein-1 function and its role in diseases. In *Signal Transduction and Targeted Therapy* (Vol. 5, Issue 1). https://doi.org/10.1038/s41392-020-00303-7

Tables

Table 1. Clinical and demographic description of MS brain autopsies and control cases

MS	MS Phenotype	Gender	Age at autopsy (years)	Disease duration (years)	Cause of death
1	Progressive	Male	43	7	Bronchopneumonia
2	Progressive	Male	34	13	Bronchopneumonia
3	Progressive	Male	43	7	Bronchopneumonia
4	Progressive	Male	46	12	Suicide
5	Relapsing-remitting	Female	52	20	Bronchopneumonia
6	Progressive	Female	45	8	Acute pyelonephritis with sepsis
7	Progressive	Male	52	8	Acute pyelonephritis
8	Progressive	Male	50	20	Bronchopneumonia
9	Progressive	Female	45	8	Acute pyelonephritis with sepsis
Control					
1		Female	37		Epilepsy*
2		Male	53		Diabetes mellitus
3		Female	47		Heart disease (HSCRT)
4		Male	40		Endocarditis
5		Female	30		Lymphangioleiomyomatosis (LAM)

** MS patients may have exhibited higher EDSS values.

*The epilepsy patient had no prior history of CNS disease, indicating that the seizure occurred without any identifiable pre-existing structural or functional abnormalities in the brain, classifying it as cryptogenic epilepsy. Furthermore, in terms of CHI3L1+ cell distribution, the epilepsy sample did not exhibit a significant difference compared to the distribution observed in the four other control samples.

**The available information on the disease course of the MS cases included in the study is limited, as many patients with progressive disease of long duration are not followed regularly at the department of neurology but are being treated by the nursing home physician. Infection as a cause of death indicates that the patients were likely to be severely disabled.

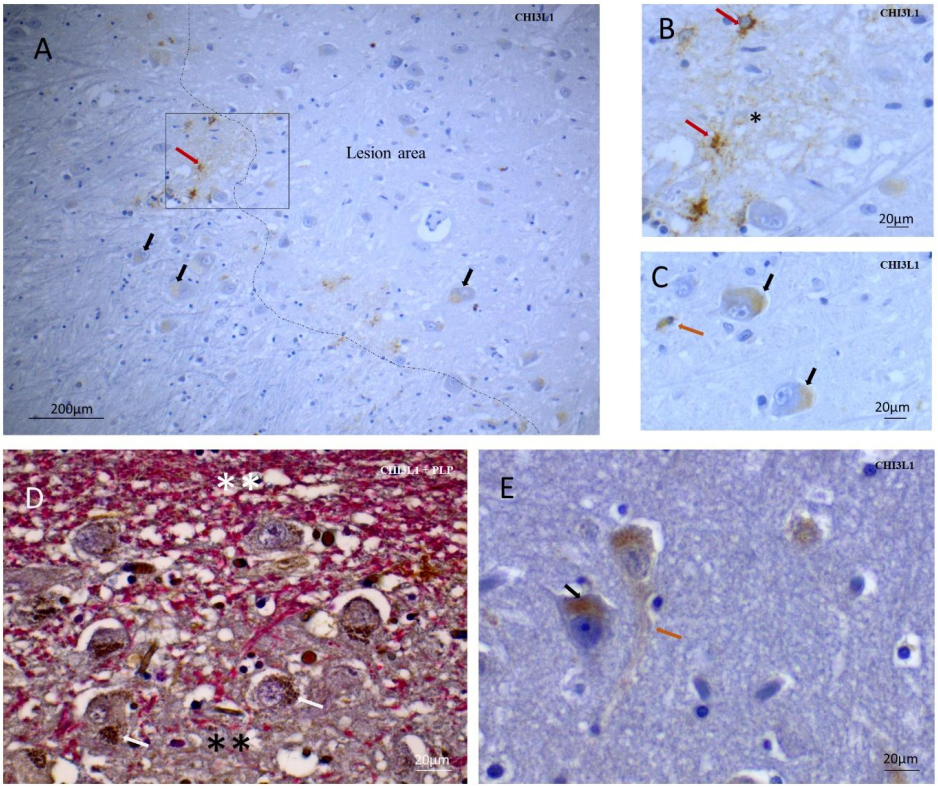

Figure. 1. Pattern of CHI3L1 positivity in MS grey matter (GM) tissue part

A) GM area stained with CHI3L1 antibody. Immunopositivity is observed in the lesion area and near the lesion area with shadows of myelin fibres (marked with a dashed line), and strongly CHI3L1+ reactive astrocytes (red arrow). Cytoplasmic material in neurons is faintly positive for CHI3L1(black arrow). **B)** The rectangular box in 1A is presented in higher magnification. There are strongly CHI3L1+ reactive astrocytes (red arrow), and (*) represents a positive extracellular matrix for CHI3L1. **C)** CHI3L1 positive cytoplasm in neurons (black arrow) and a cell with the morphology of a resting astrocyte (yellow arrow). **D)** Double stained, Myelin protein-PLP (red) and CHI3L1(brown), CHI3L1+ aggregates in neuronal soma (white arrow) on a GM lesion border (black ** represents the demyelinated area and white ** represents normal-appearing myelination) **E)** CHI3L1+ neuronal soma (black arrow) and axon (yellow arrow) in a normal-appearing cortex area.

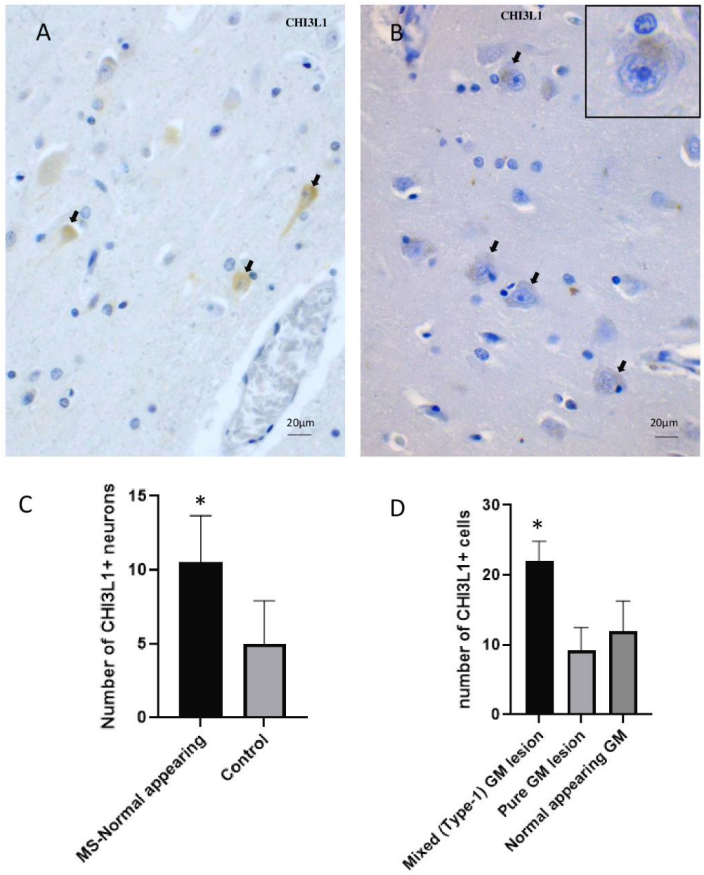

Figure. 2. Differential distribution of CHI3L1+ cells in non-lesional MS grey matter and control grey matter

A) A normal-appearing GM area immunostained for CHI3L1, some positive neurons (back arrow). **B)** A control grey matter area stained with CHI3L1, some faintly positive neuronal soma (black arrow); inset highlights the pattern of positivity in higher magnification **C)** Distribution of CHI3L1 positive neurons in normal-appearing GM parts in MS and in controls (mean, SEM). **D)** Density of CHI3L1 positive cells in different types of grey matter lesions and normal-appearing tissue parts (mean, SEM). The Kruskal-Wallis test assessed overall differences between control and MS tissue samples. The Wilcoxon sign rank test compared pairwise differences within lesion groups Abbreviations: * = significantly different from other group/groups at $p<0.05$.

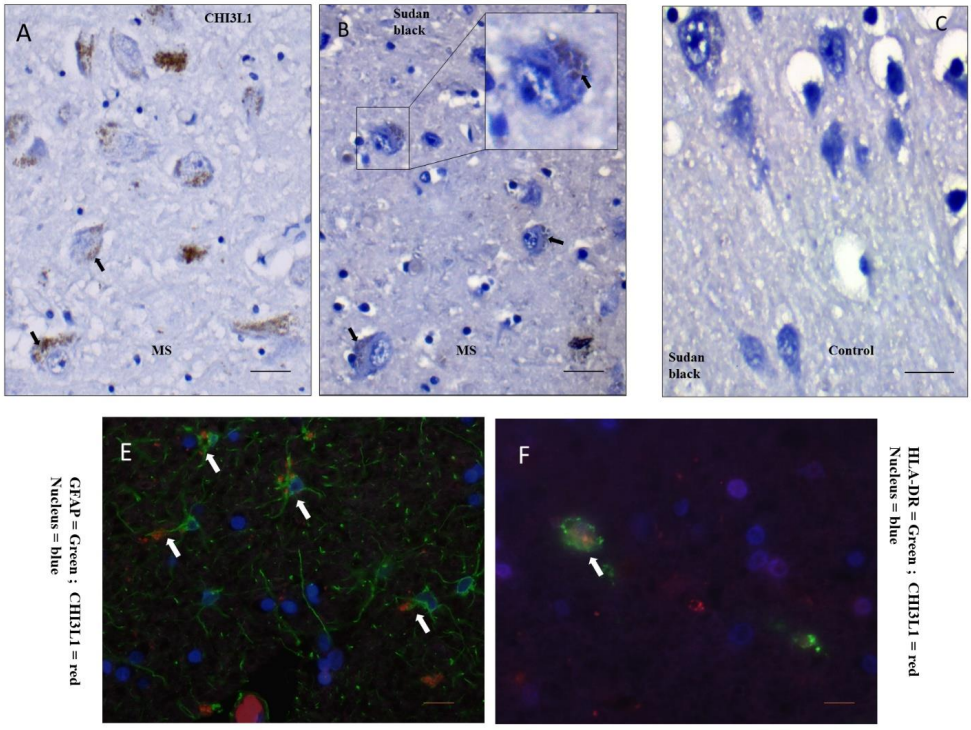

644

645

646 **Figure. 3. Cells having CHI3L1 positivity and their features.**

647 **A)** In a GM (cortex), near lesion area with CHI3L1 staining, large pyramidal neurons contain
648 granules positive for CHI3L1 (black arrow). **B)** In the matching area on the same tissue block,
649 Sudan Black positive neurons (black arrow) that confirm the presence of lipofuscin vesicles in
650 cellular location of CHI3L1 positivity **C)** Sudan Black staining of control grey matter shows
651 negligible amount of positivity **D)** immunofluorescent staining to observe colocalisation of the cell
652 type marker, GFAP for astrocytes (green) and chitinase (red) **E**) immunofluorescent staining to
653 observe colocalisation of the cell type marker, HLA-DR for antigen-presenting
654 microglia/macrophages (green) and chitinase (red). Scale bar = 20 μm.

655

656

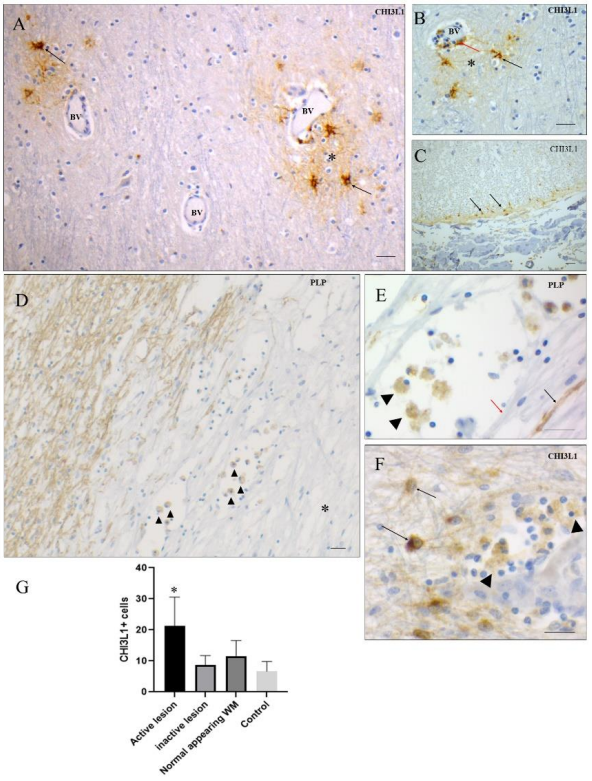

Figure. 4. CHI3L1+ cell density and distribution pattern in different white matter tissue parts.

A) In a white matter normal appearing area, a population of CHI3L1+ astrocytes (black arrow) around blood vessels (BV), CHI3L1 positive extracellular matrix (* mark). **B**) A closer view of the blood vessel (BV) area, where there are CHI3L1+ astrocytes (black arrow), positive extracellular matrix (* mark), and positive cells in the perivascular area (red arrow). **C)** Cells of astrocyte morphology in the subpial layer of the spinal cord are positive for CHI3L1 (black arrow). **D)** PLP staining shows active lesion areas where positive phagocytic cells contain myelin remnants (black arrowhead) which is a feature of an early stage of lesion formation. **E**) PLP staining shows teaming of phagocytic cells (arrowhead) having a mixture of myelinated (black arrow) and demyelinated (red arrow) fibres of axons. **F)** Reactive astrocytes (black arrow) expressing CHI3L1 were found alongside foamy macrophages (arrowhead). **G)** Density of CHI3L1+ cells in different types of white matter lesions and normal-appearing tissue parts and WM of controls (mean, SEM). Given the non-normal data distribution, the Wilcoxon sign rank test compared pairwise differences within lesion groups in human tissue samples. Scale bar = 20 µm. Abbreviations: * = significantly different from other groups at $p<0.05$.

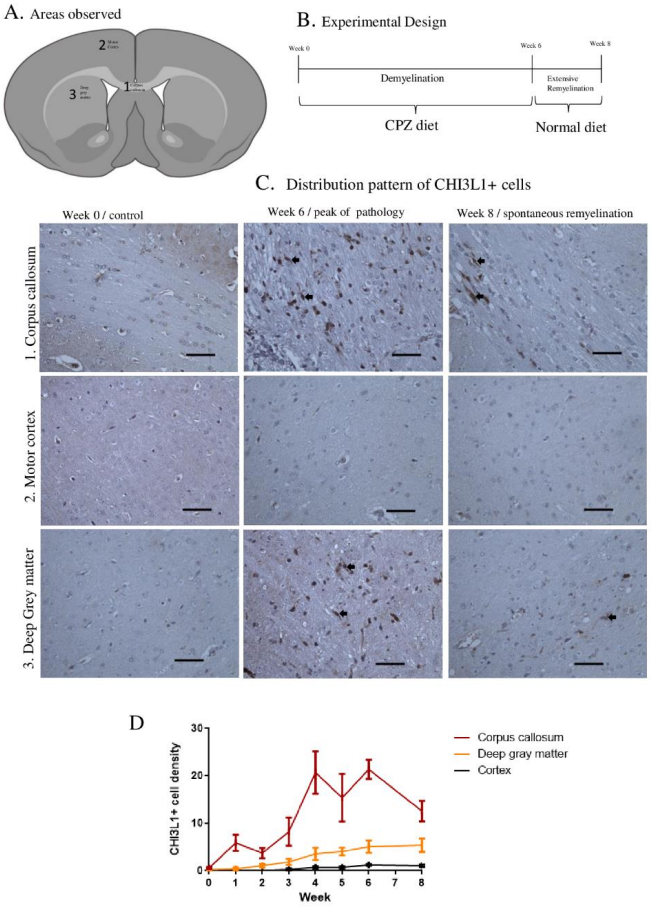

674

675 **Figure. 5. Spatio-temporal CHI3L1+ cell densities in the cuprizone experiment**

676 **A**) Areas of the mouse brain taken into analysis, the corpus callosum, motor cortex, and deep grey
677 matter (mixed tissue type) **B**) Schematics of the cuprizone experiment, the beginning (week 0),
678 disease peak (week 6) and 2 weeks after CPZ exposure (Week 8). **C**) Distribution pattern of
679 CHI3L1+ cells in the areas of interest at different time points, the corpus callosum represents white
680 matter, The motor cortex signifies purely grey matter tissue, while deep grey matter demonstrates
681 a mixture of white matter and grey matter tissue **D**) Graphs show the dynamics of CHI3L1+ cells
682 throughout the CPZ experimental period (mean, SEM). Scale bar = 20 μm.

683

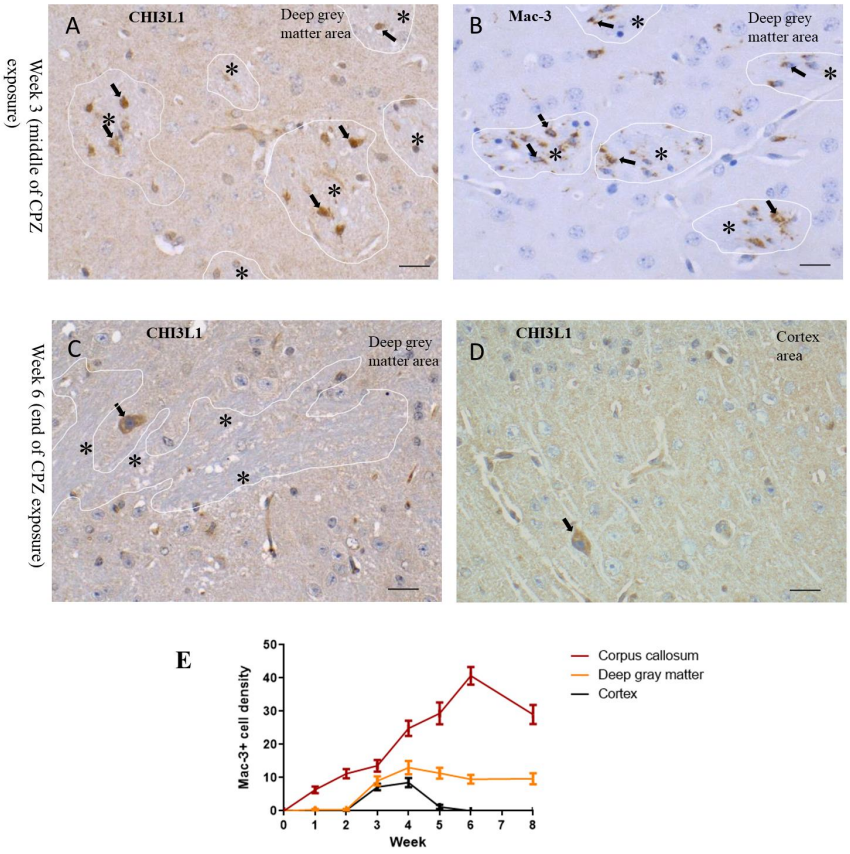

Figure. 6: Distribution of CHI3L1+ cells in relation to inflammatory marker Mac-3+ cells in the CPZ experiment

A) In the deep grey matter area (mixed white and grey matter) at week 3, CHI3L1+ cells (black arrow) appeared only in the white matter (WM) patches (marked with a white line and a *). **B**) In the deep grey matter area at week 3, Mac3+ cells (black arrow) showing microglia infiltration in WM patches (marked with a white line and a *). **C)** In the deep grey matter area at week 6, CHI3L1+ neurons (black arrow) appeared in the grey matter part, white matter area is marked with a white line, and *s **D)** At week 6, CHI3L1-positive neurons appeared sporadically in the deeper layer of the cortex (a positive neuron is marked with a black arrow). **E)** Graphs show the dynamics of Mac-3+ cells throughout the CPZ experimental period (mean, SEM). Scale bar = 20 µm.

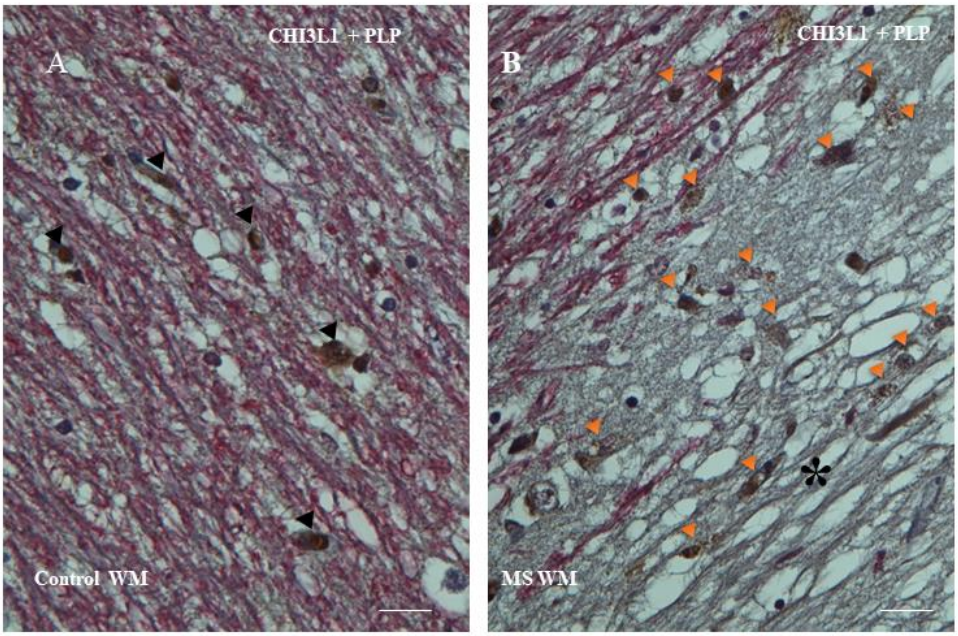

Supplementary figure. 1: Density of CHI3L1+ cells in white matter tissue

Both images are stained for CHI3L1 (brown) and myelin proteolipid protein, PLP (pink). **A)** Control white matter (WM) shows very few CHI3L1+ cells; positive says are marked with black arrowheads **B**) Higher density of CHI3L1+ cells is observed in MS-WM; positive says are marked with yellow arrowheads, and the lesion area is marked with a *****. Scale bar = 20 μm.

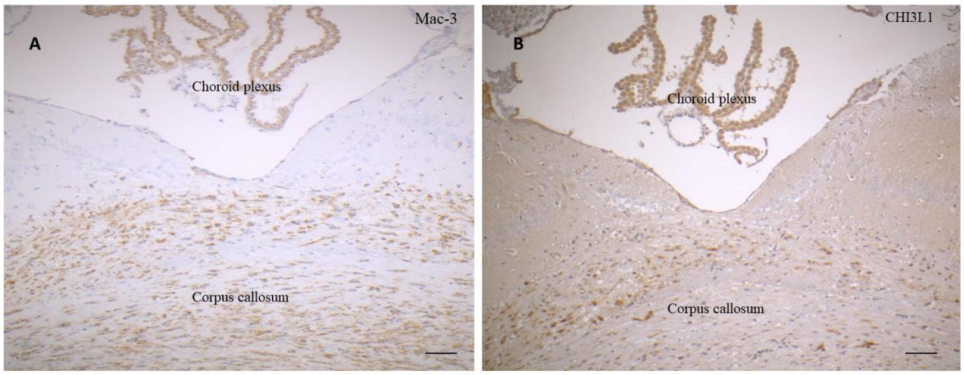

Supplementary figure. 2: Inflammation of choroid plexus and its association with CHI3L1

The images show DAB-stained (brown) slides from analogous regions in the mouse brain for two separate target molecules. **A)** Mac-3 immunopositivity indicates the level of inflammation in the choroid plexus and in the corpus callosum. **B**) Expression of CHI3L1 in the inflamed area in the brain matching the area in A. Scale bar = 20 µm.

Graphic design: Communication Division, UiB / Print: Skipnes Kommunikasjon AS

uib.no

ISBN: 9788230851029 (print)
9788230861202 (PDF)